Université de Toulouse

# THÈSE

En vue de l'obtention du

## DOCTORAT DE L'UNIVERSITÉ DE TOULOUSE

**Délivré par** l'Université Toulouse III – Paul Sabatier
**Discipline ou spécialité** : Génétique – Biologie cellulaire

---

**Présentée et soutenue par** Mlle Jacqueline BUTTERWORTH
**Le** 22 avril 2011

**Titre** :

Les troubles visuels : De la génétique à la biologie cellulaire

---

**JURY**
Docteur Yves Courtois : Rapporteur
Professeur John Conrath : Rapporteur
Professeur Philippe Gain : Rapporteur
Professeur Gérard Bouche : Président du jury

---

**Ecole doctorale** : Biologie-Santé-Biotechnologies
**Unité de recherche** : INSERM U563, CHU Purpan, 31024 TOULOUSE
**Directeur(s) de Thèse** : Professeur Patrick Calvas/Professeur François Malecaze
**Rapporteurs** : Professeur Patrick Calvas/Professeur François Malecaze

Je vous remercie tous d’avoir accepté d’évaluer ce travail. Je vous prie de recevoir toute ma reconnaissance.

A Monsieur le Docteur Yves Courtois,
Qui m’a fait l’honneur de participer en tant que membre du jury de cette thèse.

A Monsieur Professeur John Conrath,
Qui m’a fait le plaisir de prendre part au jury de cette thèse.

A Monsieur Professeur Philippe Gain,
Qui a accepté le rôle de rapporteur de cette thèse.

A Monsieur Professeur Gerard Bouche,
Qui m’a apporté son aide et accepté de prendre part au jury de cette thèse. Je vous prie de recevoir mes sincères remerciements pour votre aide.

## Merci à… (Thank you to…)


- **Ma famille** qui m'a soutenue et encouragée tous les jours pendant ma thèse. (My parents and my family for supporting me everyday throughout my PhD).
- Tous les membres de l'équipe FM/PC (ma co-thésarde **Dawiyat Massoudi,** *le kick-ass paillasse GM tueuse de souris*, **Angélqiue Erraud** *la rousse*, **Matthias Macé**, **Christine Peres** *la reine des westerns*, **Nicolas Chassaing**, **Weihua Meng**) pour les cinétiques trépanés, pour des journées aux westerns, pour des cours d'informatique, pour la découverte des dissections d'embryons humains, et surtout pour me supporter dans mon petit coin bruyant du bureau (le vendredi !). **Stephane Galiacy** de m'avoir accordé le projet sur la cornée.
- Les membres de l'équipe qui sont partis :

  **Sandrine Paget** : Pour tes connaissances fortes dans le monde de la myopie, et des bons moments partagés au labo.

  **Heather Etchevers** : Pour l'aide à la rédaction de tous et conseils bien efficaces. Toujours très positive, un modèle à suivre.
- **Dr Michèle Allouche** pour les corrections de l'article et la rédaction de ma thèse.
- **La Fédération des Aveugles Français** (FAF) pour le financement de 7 mois de plus, qui m'a permis d'envoyer mon article et clôturer le travail (avec ça aussi mes beaux-parents, pour la correction de mon dossier de candidature pour le FAF !)
- **Hélène Coppin** pour ses connaissances en qPCR et son aide dans la rédaction de ma thèse, et pour ses conseils de carrière.
- **Sophie Allart** pour son aide au confocale, de l'acquisition des photos (**Daniel Sapède** là pareil !) jusqu'à l'envoie de l'article.
- **Florence Capilla** et **Delphine Lestrade** pour des milliers de lames HE.
- Les ingénieurs chez MPR, **Chloé Latour et Céline Besson**, merci pour les cassettes de western, parmi d'autres produits que je n'avais pas dans notre labo, ou qui marchaient mieux que les miens ! Merci Chloé pour la correction des sections françaises.
- **L'école doctorale** notamment Abdel Saoudi et Justin Teissie.
- **L'équipe Jean-Philippe Girard à l'IPBS,** notamment dieu le père **gégé** et **Steph Roga** pour ma première expérience dans la recherche, pour m'avoir donné l'envie et la motivation. Christine Moussion et Nathalie Ortega pour ses idées intelligentes.
- Merci aux **collaborateurs CHU** pour leur motivation dans le recrutement des patients.
- Merci aux **patients** eux-mêmes pour leur aide bénévole.
- **Mes amis** pour le muscat quand il le fallait ! On va en voir plus de ça !
- Le meilleur pour la fin, spécialement ***my sunshine***, parce qu'il a vécu la thèse pareil (des nuits dans photoshop, corrections de speech, logiciels de statistiques…) sans rien demander, et toujours était là !

# Index

Sections translated into French are indicated by (#) after the title


| Section | Title | Page |
|---|---|---|
| **Publications/Scientific communications** | | 6 |
| **Abbreviations** | | 7 |
| **Definitions** (indicated in the text by *) | | 9 |
| **General Introduction (#)** | | 11 |
| **Project 1:Genetics** | | 13 |
| **The Genes Underlying the High Myopia Phenotype in the French Caucasian Population** | | |
| **I** | **Introduction The Eye: A Visual System** | 14-42 |
| 1 | The Eye: Structure, Function and Development | 14 |
| 2 | Myopia: Changes in Visual Refraction | 18 |
| 3 | Epidemiology | 21 |
| 4 | The Use of Animal Models to Determine the Mechanisms Underlying Myopia | 22 |
| 5 | The Human Myope: Genetics versus the Environment | 27 |
| 5.1 | Environmental Effects | 27 |
| 5.2 | Human Myopia Genetics | 28 |
| 5.3 | High Myopia Genetic Mapping | 30 |
| 6 | **Revision: Human High Myopia Genetics (#)** | 42 |
| **II** | **Aims (#)** | 43-45 |
| **III** | **Materials and Methods** | 47-63 |
| 1 | Axial length as the High Myopic Sujbect Phenotype Criterion | 47 |
| 2 | Genetic Heterogeneity Limitation | 49 |
| 3 | Subject Recruitment | 51 |
| 4 | Power Calculation Estimations | 53 |
| 5 | Multi-step Association Study Design | 56 |
| 6 | DNA and Phenotype Bank | 58 |
| 7 | Genotyping Technology | 59 |
| 8 | **Revision: Methods (#)** | 61 |
| **IV** | **Results** | 64-69 |
| 1 | Recruitment Outcomes | 64 |
| 2 | Genotyping of the First 192 Extreme High Myopes | 67 |
| **V** | **Perspectives** | 70-72 |
| 1 | Completion of All GWAS Stages | 70 |
| 2 | Confirmation of a Role for GWAS Candidate Genes in Human Myopia Developement | 71 |
| 3 | **Conclusion: Project 1 (#)** | 72 |

| | | |
|---|---|---|
| **VI** | **Myopia and Corneal Refractive Surgery** | 73-76 |
| 1 | Different Corneal Refractive Surgery Techniques | 73 |
| 2 | Secondary Complications | 75 |
| 3 | Current Research on Opacity Formation | 76 |

**Project 2: Cell Biology** 77
**Identification of Stromal Cells Expressing Stem Cell markers Throughout *in vivo* Adult Murine Corneal Wound Healing**

| | | |
|---|---|---|
| **I** | **Introduction The Cornea: A Transparent Window** | 77-122 |
| 1 | The Cornea: Structure, Function and Development | 78 |
| 2 | Normal Adult Corneal Renewal | 83 |
| 3 | The Corneal Wound Healing Response | 88 |
| 4 | **Revision: Corneal Stromal wound Healing (#)** | 100 |
| 5 | Identification of Corneal stromal cells Expressing Stem Cell Markers | 102 |
| 6 | Stem Cell Injection Studies; Taking it One Step Further | 113 |
| 7 | Implications of the Expression of Embryonic Stem Cell Markers by Corneal Stromal Progenitor Cells | 116 |
| 8 | **Revision: Corneal Stromal Progenitor Cells (#)** | 121 |
| **II** | **Aims (#)** | 123-125 |
| **III** | **Materials and Methods** | 126-140 |
| 1 | *In vivo* Animal Corneal Wound Healing Models | 126 |
| 2 | Our *In vivo* Mouse Corneal Wound Healing Model | 127 |
| 3 | Quantitative RT-PCR | 131 |
| 4 | *Sox2* RT-PCR | 133 |
| 5 | Quantitative Telomerase Activity Analysis | 134 |
| 6 | Immunohistochemistry | 136 |
| 7 | Immunoblotting | 139 |
| **IV** | **Results and Discussion** | 141-167 |
| 1 | Increased Expression of Keratocyte Progenitor Cell Markers During *in vivo* Corneal Wound Repair | 142 |
| 2 | Reexpression of Embryonic Cell Markers in the Wounded Stroma Corresponds to an Activated Adult Keratocyte Phenotype | 150 |
| 3 | A Neural Crest-derived Repair Pathway Replenishes Lost Wound Zone Keratocyte Cells | 158 |
| 4 | Different Interpretations of the Upregulation of Progenitor Cell and Undifferentiated Keratocyte Cell Markers in the Wounded Stroma | 159 |
| 5 | Conclusion (#) | 165 |
| 6 | **Article Manuscript (Submitted)** | 168-204 |
| **V** | **General Discussion** | 205-216 |
| 1 | Different Adult Tissue Regeneration Models | 205 |
| 2 | Functions and Origins of the Corneal Stromal Progenitor Cell Subpopulation(s) | 207 |
| 3 | Roles of the New Activated Keratocyte Phenotype | 208 |

| | | |
|---|---|---|
| 4 | The Wounded Stromal Response; A Complex Network of Cell Repair Signals | 209 |
| **VI** | **Perspectives** | 217-221 |
| 1 | Short Term Experimentation Currently Underway | 217 |
| 2 | Long Term Experimentation to Develop | 219 |
| 3 | Therapeutic Implications for Corneal Opacity Treatments | 220 |
| 4 | **Conclusion: Project 2 (#)** | 222 |
| **Summary (#)** | | 224 |
| **Annex 1** | **Published Review 1** entitled "Axial length: An underestimated endophenotype of myopia" | 2226 |
| **Annex 2** | **Published Review 2** entitled "Axial length of Myopia: A Review of Current Research" | 228 |
| **Annex 3** | Project 1 : Recruitment Protocol | 236 |
| **Annex 4** | Project 1 : Patient Recruitment File | 240 |
| **Annex 5** | Project 1 : Volonteer Recruitment Press Articles | 243 |
| **Bibliography** Project 1 and 2 | | 244-274 |
| **Index**: Internet Image Bibliography Project 1 and 2 | | 275 |
| **Cover page summaries (#)** | | 276-277 |

# Publications

### Articles/Reviews Published in Peer-reviewed Journals/Reviews

- W. Meng, **J. Butterworth**, F. Malecaze, P. Calvas (2010). Axial Length of Myopia: a Review of Current Research. *Ophthalmologica*. 225(3):127-134 (Annex 1 page 230). (2nd Author PhD).
- W. Meng, **J. Butterworth**, F. Malecaze, P. Calvas. (2009). Axial length: An underestimated endophenotype of myopia. *Med Hypotheses*. 74 (2): 252-253 (Annex 2 page 232). (2nd Author PhD).
- A. Fenwick, R.J. Richardson, **J. Butterworth**, M.J. Barron, and M.J. Dixon. (2008) Novel Mutations in *GJA1* Cause Oculodentodigital syndrome**.** *J Dent Res.* 87: 1021-1026. (2nd Author Master degree).

### Articles Submitted in Peer-reviewed Journals

- **J. Butterworth**, D. Massoudi, A. Erraud, P. Fournié, E. Ancele, C. Peres, M. Macé, F. Malecaze, M. Allouche P. Calvas, S. Galiacy. *In vivo* reexpression of stem cell markers in adult stromal cells during murine corneal wound repair. *Cell Research*. Submitted 3rd March 2011. (Article Manuscript page 172). (1st Author PhD).
- D. Massoudi, **J. Butterworth**, A. Erraud, P. Fournié, F.Malecaze, S.D. Galiacy (2011). Differential spatio-temporal expression of FACIT type XII collagen splice variants during mouse corneal wound healing. *Matrix Biology.* Submitted late January 2011. (2nd Author PhD).

# Scientific Communications

### Scientific Conference Presentations

Marie Curie Collaboration (MyEuropia Research Training Network) Projet Progression Presentations:

- Spain, Murcia, Espinardo Campus, Optical Laboratory: January 2010.
- Italy, Venice: January 2009 (mid-term review for the justification of our collaboration and contribution).
- Germany, Tuebingen, Institute for Ophthalmic Research, Section of Neurobiology of the Eye: February and June 2008.
- UK, London, King's College London, Department of Twin Research and Genetic Epidemiology: September 2007.

### General Public Presentations

- Fédération des Aveugles et Handicapés Visuels de France**:** Final year PhD grant award ceremony, Paris.
- Human subject recruitment protocol presentations and set-up in public CHU ophthalmology services:
    - Bordeaux, CHU Pellegrin: April 2008.
    - Toulouse, CHU Purpan and Rangueil February 2008.

### Poster

- European Marie Curie Conference, Barcelona, Spain, June 2008: The high myopia gene hunt.

### Written Reports and Succesful Grant Proposals

- Marie Curie Collaboration 6-month interval progress reports (2007-2010).
- Fédération des Aveugles et Handicapés Visuels de France final year PhD grant award (2010).
- Mastr degree report (2007).

# Abbreviations

| | |
|---|---|
| **α** | alpha |
| **β** | beta |
| **γ** | gamma |
| **-** | Negative/Decrease |
| **+** | Positive/Increase |
| **χ** | Chi-square test |
| **ALDH3** | Aldehyde dehydrogenase 3A1 |
| **ALK** | Automated lamellar keratoplasty |
| **ASP** | Affected sibpair |
| **BBC** | British Broadcasting Corporation |
| **bp** | Basepairs |
| **BSA** | Bovine Serum Albumin |
| **CIC** | Centre d'Investigation Clinique |
| **CNG** | Centre national de Génotypage |
| **CNS** | central nervous system |
| **CNV** | Copy number variation |
| **COPs** | Neural-crest derived corneal stroma precursors (short; corneal precursors) |
| **CPD** | Cumulative population doublings |
| **Ct** | Cycle threshold |
| **c-Ten** | Customized transepithelial non-contact ablation |
| **D** | Day/Dioptries |
| **DAF** | Disease allele frequancy |
| **DAPI** | 4,6-Diamidino-2-phenylindole |
| **E** | Embryonic day/Efficiency |
| **ECM** | Extracellular matrix |
| **EDTA** | Ethylenediaminetetraacetic acid |
| **EGF** | Epidermal growth factor |
| **EMT** | Epithelial-to-mesenchymal transition |
| **EnMT** | Endothelial to mesenchymal transition |
| **FACS** | Fluorescent-activated cell sorting |
| **FBS** | Fetal bovine serum |
| **FGF** | Fibroblast growth factor |
| **FGFR** | Fibroblast growth factor recepetor |
| **GABA** | gamma aminobutyric acid |
| **GFP** | Green fluorescent protein |
| **GRR** | Genotype relative risk |
| **GWAS** | Genome wide association analysis |
| **HE** | Hematoxylin and eosin staining |
| **HGF** | Hepatocyte growth factor |
| **HNK-1** | Human Natural Killer-1 carbohydrate (Neural crest cell marker) |
| **HWE** | Hardy Weinberg equilibrium |
| **IBS** | Identity by state |
| **IL** | Interleukin |
| **Kb** | Kilobase |
| **KGF** | Keratinocyte growth factor |
| **LASEK** | Laser Assisted Sub-Epithelium Keratomileusis |

| | |
|---|---|
| **LASIK** | Laser Assisted In-Situ Keratomileusis |
| **LD** | Linkage disequilibrium |
| **LOD** | Logarithm of the odds' |
| **LUM** | Human lumican gene |
| **M** | Molar |
| **Mb** | Megabases |
| **MDS** | Multidimensional-scaling |
| **MMC** | Mitomycin C |
| **MMPs** | Matrix Metalloproteinases |
| **MYOC** | Myocilin |
| **MYP** | Myopia loci |
| **NCBI** | National Centre for Biotechnology Information |
| **NCDSCs** | Neural crest-derived stem cell-like cells |
| **NPVF** | Neuropeptide VF precursor |
| **OD** | Absorbance (optical density) |
| **OR** | Odds ratio |
| **PCR** | Polymerase chain reaction |
| **PDGF** | Platelet-derived growth factor |
| **PLA** | Processed lipoaspirate |
| **PPG** | Preproglucagon |
| **PRK** | Photorefractive keratectomy |
| **PTK** | phototherapeutic keratectomy |
| **QCPN** | Quail nucleus-specific antibody |
| **RAF** | Risk allele frequency |
| **RK** | Radial keratotomy |
| **RPE** | Retinal pigment epithelium |
| **RT-qPCR** | Reverse transcriptase quantitative polymerase chain reaction |
| **SEM** | Standard error of the mean |
| **Shh** | Sonic hedgehog |
| **SMA** | Smooth muscle actin |
| **SNP** | Single nucleotide polymorphism |
| **SSEA-4** | Stage-specific embryonic antigen-4 |
| **SCMs** | Stem cell markers |
| **SVZ** | Subventricular zone (SVZ) of the lateral ventricles in the forebrain |
| **TDT** | transmission disequilibrium test |
| **TE** | Tris, EDTA buffer |
| **Tert** | Telomerase reverse transcriptase |
| **TGF** | Transforming growth factor |
| **TGIF** | Transforming factor β-induced factor |
| **TIMP** | Tissue inhibitor matrix metalloproteases |
| **TNF** | Tumor necrosis factor |
| **UMSCs/UHSCs** | Umbilical mesenchymal stem cells/Umbilical hematopoietic stem cells |
| **UTR** | Untranslated region |
| **VEGF** | Vascular endothelial growth factor |

# Definitions

| * | **Definition** |
|---|---|
| **Additive model** | When combined effects of disease alleles at different loci are equal to the sum of their individual effects |
| **Agonist** | A false ligind that binds to a cell receptor to mimic the action of the natural ligind |
| **Aneuploidy** | Miss-segregation of chromosomes resulting in extra or missing chromosomal numbers |
| **Antagonist** | A false ligand that binds to a cell receptor to inhibit normal ligand-binding actions and responses |
| **Apoptosis** | A programmed form of cell death with minimal debris release due to absence of cell lysis and lysozomal enzyme release |
| **Autocrine** | Intra-cellular |
| **Autologous** | Derived from the self same individual |
| **Blastocyst** | Inner cell mass that subsequently forms the embryo |
| **Cell fate** | Self-renewal and expansion versus differentiation properties |
| **Cerebral cortex** | Sheet of outermost neural tissue to the cerebrum of the mammalian brain |
| **Chemokine** | Cytokine molecules with immune trafficking roles |
| **Chemotaxis** | Cell movement in response to a chemical substance |
| **Chimeric graft** | Donor cells/tissue are grafted into a host of a different species |
| **Cytokine** | Small secreted cell-signaling protein molecules |
| **Dendritic processes** | Cell body branching-out-like structures |
| **Dry-eye syndrome** | Tear film disorder resulting in chronically dry eyes |
| **Ganglia** | Encapsulated neural cell bodies |
| **Gap junction** | Cell-cell structures that allow inter-cytoplasm connections |
| **Genomic imprinting** | A subset of alleles expressed according to either inheritance fom the mother or from the father |
| **Glial cells** | Nonc-neuronal cells that serve as support cells in the nervous system |
| **Heritability** | Mesure of the variation of a phenotype due to genetic factors |
| **HMG-box** | Sex-determining region on the Y chromosome |
| **Homeobox** | Transcription factors that switch on other gene networks, typically in embryonic development |
| **Immunologic privilege** | The toleration of the introduction of a foreign antigen without eliciting an inflammatory immune response |
| **Indian** | American Indian race (Amerindians, Amerinds, or Red Indians) |
| **Inuit** | Culturally similar indigenous people inhabiting |

| | |
|---|---|
| | the Arctic regions of Canada |
| **IQ** | Score derived from a standardised test designed to assess intelligence |
| **Keratectasia** | Abnormal bulging/protrusion of the cornea of the eye |
| **Keratoconus** | Abnormal cone-shaped protrusion of the cornea of the eye |
| **Keratoplasty** | A cornea transplant to replace damaged or defected corneas, also referred to as a corneal transplant, penetrating keratoplasty or corneal graft |
| **Lymphangioblast** | Lymph vessels that arise from mesenchymal stem cells |
| **Microkeratome** | A precise surgical instrument with an oscillating blade designed for creating a corneal incision flap |
| **Monomorphic SNPs** | SNP for which a single allele (homozygous) can be identified in a population of interest |
| **Neural tube** | Compartment of the developing brain and spinal cord comprising neural precursor cells |
| **Overt** | An observable disease phenotype |
| **Pannus** | Fibrotic vascular membrane that covers the corneal surface |
| **Paracrine** | Inter-cellular |
| **Penetrance** | The proportion of individuals carrying the particular real risk allele that also express the associated phenotype |
| **Phototherapeutic keratectomy** | Laser ablation procedure to remove stromal opacities or irregularities |
| **Pterygium** | A wing-shaped, fibrovascular conjunctival outgrowth that centripetally invades the clear cornea |
| **Retina proper** | Photoreceptor layer |
| **Retinoic acid receptors** | Nuclear receptors that function as ligand-dependent transcription factors |
| **Sherpa** | Ethnic group from the high mountainous Himalaya region of Nepal |
| **Slit lamp** | A high-intensity light source that can be focused to shine a thin sheet of light into the eye. It is used in conjunction with a microscope. |
| **Support cell** | Play a role in the maintenance of hair cell function and structure |
| **Vimentin** | Intermediate filament important for eukaryote cytoskeleton structure |

# General Introduction

This PhD thesis is composed of **two projects**. The first project is a genetic study on high myopia, the second project is a cell biology study on the corneal stroma.

High myopia can lead to severe impairment of vision, and in extreme cases to blindness, making it a serious public health concern. The first project is a **genetic study** designed to better define the **genes underlying the high myopia phenotype in the French Caucasian population.** It is based on a **new genome-wide scan method designed** to capture all underlying genetic variants of the high myopic phenotype within this population. The identification of genes involved in high myopia development is not only crucial for the understanding of the physiopathology of the disease, but also for the development of alternative treatments that today rely on the correction of refractive error by wearing glasses or contact lenses.

Myopia can be corrected by refractive error surgery. This requires the removal of corneal stromal tissue to reshape the cornea. In the majority of cases, this corneal wound heals and does not leave a scar. However, in an average of 1.75% of operated patients the wound healing response is impaired, leading to corneal stromal scarring, known as “opacities”. These reduce corneal transparency and impede clear vision. It is important to analyse the cellular mechanisms that cause this abnormal wound response in order to improve the current surgical treatments of myopia.

The second part of this PhD thesis is a **cell biology** project. It is a phenotypic study of **corneal stromal cells throughout *in vivo* adult murine corneal wound healing.** Our results demonstrate for the **first time *in vivo*** that following corneal injury, corneal stromal cells can express a range of stem cell markers during wound repair. These new *in vivo* findings may provide targets for the prevention or treatment of corneal opacities.

**The projects can be read independently. The most important chapters and all conclusions are translated into French** (indicated by $^{(\#)}$ following the titles in the index).

# Introduction générale

Ce manuscrit de thèse est composé de **deux projets**. Le premier projet est une étude génétique sur la myopie forte, et le second une étude de biologie cellulaire sur la cornée stromale.

La myopie forte peut gravement altérer la vision. Dans des cas extrêmes, elle peut causer une cécité, posant un problème de santé publique sérieux. Le premier projet est une **étude génétique** visant à mieux **identifier les gènes impliqués dans la myopie forte chez une population française caucasienne**. Cette étude est basée sur une **nouvelle méthode de criblage de l'ensemble du génome** pour capturer toutes les variations génétiques causantes. L'identification des gènes impliqués dans le développement de la myopie forte est non seulement essentielle pour la compréhension de la physiopathologie de la maladie, mais également pour le développement de nouveaux traitements, qui aujourd'hui, reposent sur une correction de la réfraction à l'aide de lunettes ou de lentilles.

La myopie peut être corrigée par la chirurgie réfractive. Cette chirurgie consiste à l'ablation du tissu cornéen stromal pour remodeler la cornée. Dans la plupart des cas, la blessure ne laisse pas de cicatrice. Cependant, en moyenne 1,75 % des patients opérés ont une réponse cicatricielle stromale anormale qui mène à la formation d' « opacités » dans le stroma de la cornée qui réduisent la transparence cornéenne et nuisent à la vision. Il est important d'analyser les mécanismes cellulaires causant cette cicatrisation anormale en vue d'améliorer les traitements actuels de la myopie.

Le second projet de cette thèse porte sur la **biologie cellulaire**. C'est une étude phénotypique des **cellules cornéennes stromales lors de la cicatrisation cornéenne chez la souris adulte**. Pour la première fois, nous mettons en évidence la localisation *in vivo*, de cellules cornéennes stromales exprimant des marqueurs de cellules souches lors de la réparation stromale. Ces nouvelles données *in vivo* pourraient fournir des cibles pour la prévention et le traitement des opacités cornéennes.

**Les deux projets peuvent être lus séparément. Les chapitres les plus importants sont traduits en français ainsi que les conclusions** (indiqué dans l'index derrière le titre par $^{(\#)}$).

**The Genes Underlying the High Myopia Phenotype in the French Caucasian Population**

# I Introduction

## The Eye: A Visual System

Humans are highly visual species. Most of our information about the world comes to us through our eyes, from which most of our cultural and intellectual heritage is stored and transmitted as words and images to which our vision gives access and meaning [1].

### 1 The Eye: Structure, Function and Development

### 1.1 Global Structure and Function of the Eye

Light enters the eye through the pupil and is focused on the retina. The cornea and the lens focus images from different distances onto the retina. The colored ring of the eye, the iris, controls the amount of light entering the eye by controlling pupil size upon contraction and expansion. It closes when light is bright, and opens when light is dim. The tough white sclera covers the outside of the eye. Towards the most anterior part of the eye the sclera gives rise to a transparent structure in order to allow the light to enter; the cornea. Ciliary muscles automatically control the focusing action of the lens. Images formed on the retina are transmitted to the brain by the optic nerve. The choroid forms the vascular layer of the eye supplying nutrition to the eye structures. A “jelly-like” substance called the vitreous humor fills the space between the lens and the retina. The lens, iris and cornea are nourished by a clear fluid, the aqueous humor, formed by the ciliary body that fills the space between the lens and the cornea. This space is known as the anterior chamber. The fluid flows from the ciliary body to the pupil and is absorbed through the channels in the anterior chamber. The delicate balance of aqueous production and absorption controls the pressure within the eye (Fig.1) [1].

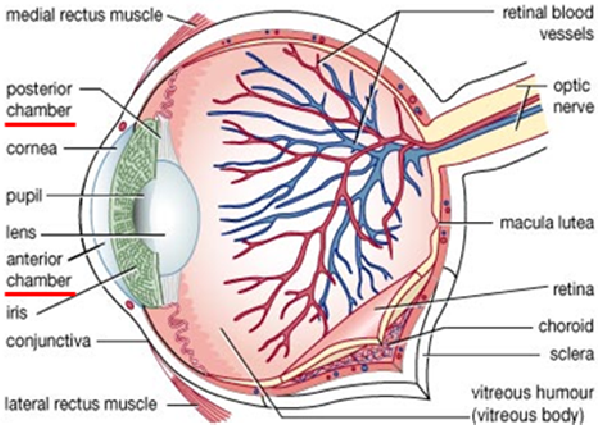


**Fig.1. The Anatomical Structure of the Eye.** The anterior and posterior chambers relate to two spaces divided-up by the lens and iris (adapted from Index A).

## 1.2 Embryonic Eye Development

Human eye development is throughout the early development stage. Within a month a miniature adult eye is almost formed and development is complete by the end of embryonic week 8. The eyes of all vertebrates develop in a pattern which produces an "inverted" retina in an invaginated cup-like structure. The eye is derived from three types of embryonic tissue: 1. Essentially the neural tube* (**neuroectoderm**), from which arises the retina proper* and its associated pigment cell layer. 2. The **mesectoderm (neural plate)** of the head region, which produces the choroid, ciliary body, iris and corneosclera. The mesectoderm is of neural crest cell origin; cells that are actually of neural plaque origin but detach and migrate into the mesoderm during neurulation. This is an epithelial-to-mesenchymal transition (EMT). 3. The **surface ectoderm**, from which derives the lens [1].

The earliest stage of eye development is the formation of the paired optic vesicles on either side of the forebrain. These growing diverticula expand laterally into the mesectoderm of the head and develop a stalk-like connection to the main portion of the rudimentary central nervous system. In humans, this process begins at about embryonic day 22 (E22). The vesicles continue to grow; their connection to the brain becomes progressively narrower and more stalk-like. The forming stalks will eventually become the rudiments of the optic nerves (Fig.2.A) [1].

Simultaneously to formation of the optic vesicles, the surface ectoderm thickens to form a lens placode. This is a region visible on the surface of the embryo. This transformation is triggered by the proximity of the optic vesicles. Once the formation of the lens placode has begun, the expanding optic vesicles begin to invaginate to form a cup-shaped structure, and also to fold along their centerline, enclosing a small amount of angiogenic mesenchymal tissue as they do so (Fig.2.B). The mesenchyme forms the hyaloid artery and vein, which supply the forming lens. Later, in the fully formed stage this will derive the central artery and vein of the retina [1].

The optic cup then invaginates and folds, forming two distinct layers. The inner layer forms the neurosensory retina. The outer layer forms the pigment epithelium layer, which lies outside the sensitive portion. The space between these two layers (intraretinal space) is obliterated when the two layers fuse. The uveal and corneoscleral tunics differentiate from the surrounding mesectoderm. Meanwhile, the surface ectoderm of the lens placode thickens and begins to differentiate into the lens vesicle. As the lens rudiment detaches and drops into position, a space forms external to it that becomes the anterior chamber of the mature eye.

The surface ectoderm and the mesectoderm above it differentiate into the eyelids and the cornea respectively [1].

By approximately E40, the retina begins to develop as the intraretinal space is eventually obliterated. Neuro-sensory photoreceptor retinal cells (rods and cones) are developed (Fig.2.C). The remaining template ectoderm serves as a template for the organisation of corneal keratocytes (a detailed description of corneal development is in *Project 2 section 1.5 page 83*). Tissue maturation continues from here until birth. At birth the only remaining requirement is the concentration of cone cells in the retina macula. The postnatal human eye structure then continues to grow until around the age of 3 years old [1].

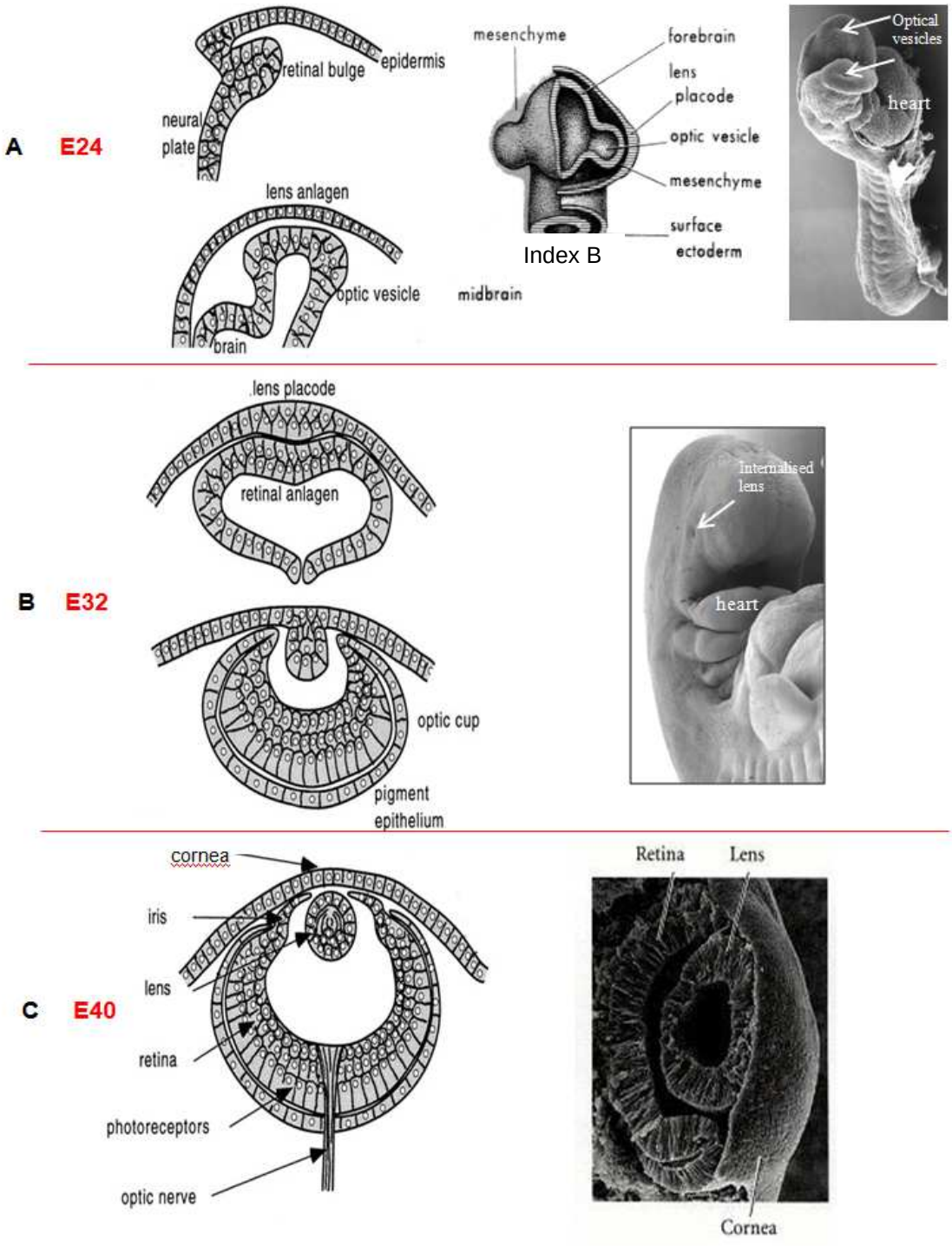


**Fig.2. Schematic Representation of Vertebrate Embryonic Eye Development.** A: Formation of the paired optic vesicles on either side of the forebrain. B: The surface ectoderm thickens to form a lens placode, a region visible on the surface of the embryo. The expanding optic vesicles begin to invaginate to form cup-shaped structures. C: The retina begins to develop as the intraretinal space is obliterated. The lens detaches from the surface and the cornea begins to form from the thickened ectoderm. Photos of human embryos in A and B were kindly donated by Dr Heather Etchevers (INSERM UMR910, La Timone, Marseille). Left panel images [2]. Bottom right image [3].

## 2 Myopia: Changes in Visual Refraction

### 2.1 The Normal Eye and Refraction

In the normal eye, entering light rays are focused and intersect on the retina by a succession of transparent components; the cornea, lens, aqueous and vitreous humors. This creates a sharp image that is transmitted to the brain by the optic nerve. This is normal emmetropic refraction. The ciliary muscles adjust lens shape to properly focus images on the retina depending on the distances of the images; this is known as accomodation (Fig.3.A).

Emmetropisation is acquired by coordinated growth of eye structures and it is considered for an emmetrope that there are no further refractive changes after the age of 16 years old [4, 5]. Refraction depends on the refractive index of the cornea, lens, vitreous and aqueous humor, as well as the anterior chamber depth and the axial length of the eye (**refractive components**) [6]. Anomalies in these components result in refractive error defects and a failure of the eye to focus images sharply on the retina, causing blurred vision.

### 2.2 Myopia, High myopia and Hyperopia

#### 2.2.1 Myopia

Myopic eyes relate to blurred far vision due to image formation in front of the retina (Fig.3.B). However, close objects appear clear without the eye's accommodation effect, thus myopia is also called shortsightedness. The extent of myopia is clinically measured by the correction necessary to reestablish clear vision in dioptries (D). Different types of myopia can be distinguished by their origins [7, 8]:

- Pseudo-myopia: This is a false myopia due to consecutive spasms in accommodation.
- Excessive corneal curvature: This is frequent in patients suffering from Keratoconus (a degenerative disorder involving structural changes within the cornea. It becomes thinner and adopts a more conical shape than its normal gradual curve).
- Increased lens refractive indice: Due to cataract, the size and shape of the lens.

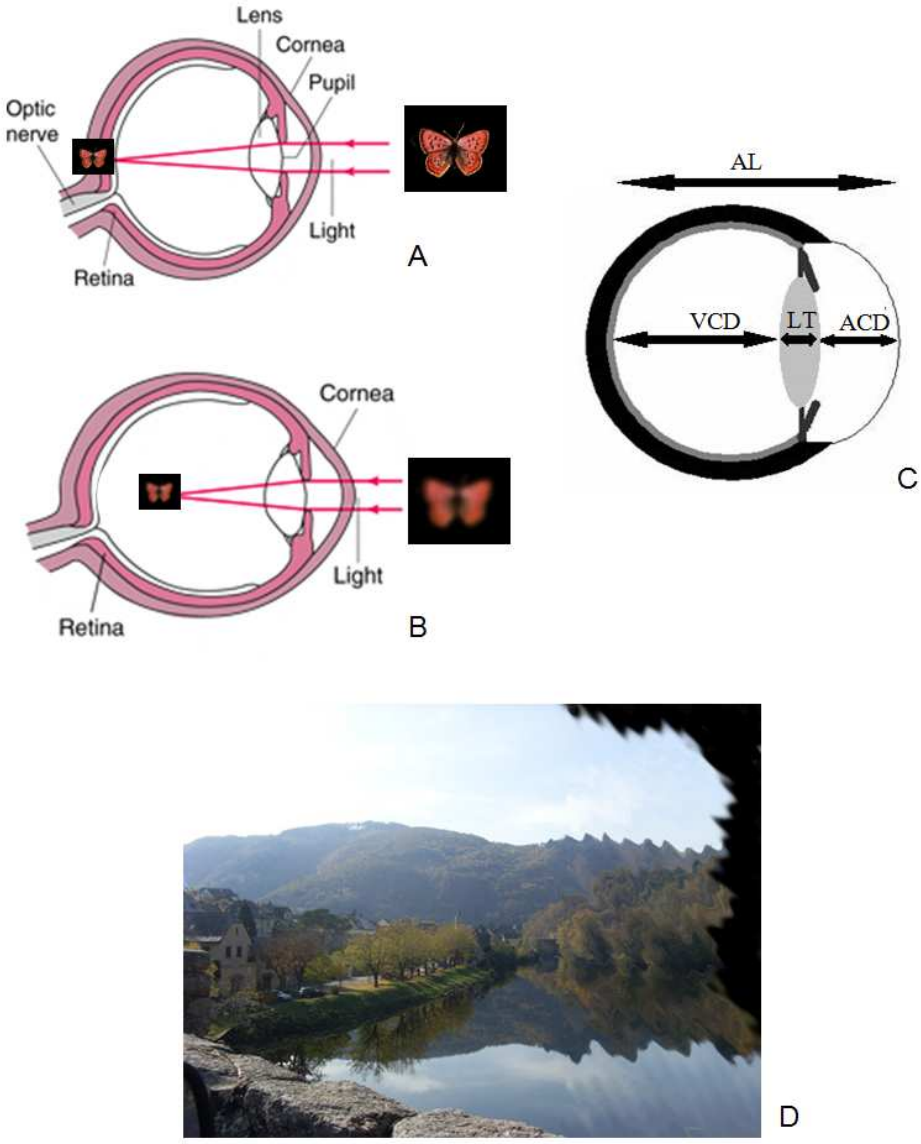


**Fig.3. Emmetropic and Myopic refraction.** A: A normal emmetropic eye; a clear image focused directly on the retina. B: A myopic eye; image focused in front of the retina and note the inceased axial length of the eye. C: The combination of anterior chamber depth (ACD), lens thickness (LT) and posterior chamber depth (VCD) = axial length (AL) [9]. D: Representation of the visual defect of a high myopic patient suffering from retinal detachment. Photo effect kindly designed by Remy Pillot (ActenGo, Toulouse).

- Increased **axial length**: Axial length is a combination of anterior chamber depth, lens thickness and posterior chamber depth (Fig.3.C). Axial length myopia is the most common form of myopia [6]. The normal eye measures approximately 24 mm. Axial length myopia can be separated into three forms by artificial clinical definition of corresponding refractive error values [6, 10]:

1. **Weak myopia**: Corresponding to an error of refraction between -0.5 D and -3 D.
2. **Moderate myopia**: Corresponding to between -3 D and -6 D.
3. **High myopia**: Corresponding to an error of refraction ≤-6 D [6, 10, 11]. Some genetic definitions of high myopia are not in agreement with this clinical definition. Geneticists sometimes study only phenotypes with higher errors of refraction (-8 to -12 D) in order to be certain of exclusion of milder forms of myopia [12, 13]. High myopia usually develops by a rapid refractive error decrease between the ages of 10 and 12 years during education [6, 14]. High myopia is accompanied in almost all cases by an increase in axial length due to accelerated post natal eye growth [15]. Clinically, high myopia corresponds to an axial length increase to at least 26mm [11]. A 1 mm axial length elongation corresponds to a 2-2.5 D refractive error shift [16]. Some high myopes with extensively increased axial lengths have refractive errors beyond -20 D. It is well confirmed that there is a negative relationship between axial length and myopia, the more severe (negative) the myopia, the longer the axial length [17, 18]. High myopia can lead to blinding secondary complications, such as retinal detachment (Fig.3.D), retinal hemorrhage and glaucoma, making high myopia one of the principal causes of adult visual defects and blindness in the world [19-26].
4. As well as appearing as an isolated pathology, high myopia can also appear as part of **a rare disease syndrome**. The majority of these syndromes are associated with collagen defaults, such as Type I Stickler (type 2 alpha (α) 1 collagen) and Type II Stickler (type II collagen mutations).

### 2.2.2 Hyperopia

This can be considered as the opposite to myopia, or farsightedness. The point of focus is behind the retina because the cornea is too flatly curved, the axial length is too short, or both. In adults, both near and distant objects are blurred. Children and young adults with mild hyperopia may be able to see clearly due to their ability to accommodate.

### 2.2.3 Distribution of Refractive Errors in the General Population

Upon removal of highly myopic and hyperopic subjects from the general population, refractive errors demonstrate a normal distribution. The same observation is made for each of the refractive components in the general population (Fig.4) [27]. This led to the hypothesis

that there is a relationship between all the refractive components that contribute to the overall refractive status. Conversely, analysis of the refractive components including the highly myopic and hyperopic subjects in the general adult population results in loss of a normal distribution, and a deviation towards an accumulation of myopes (Fig.4). This has been regarded as a ***compensatory correlation between refractive components***; one component is out of line, so the others adjust to compensate [28]. In other words, the refractive components excessively try to emmetropise.

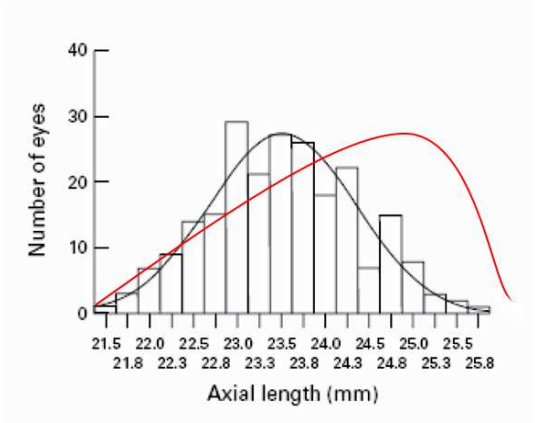


**Fig.4. Distribution of Axial Lengths in the General Population.** Black line: Normal distribution of axial length in a population of 114 twins 20-45 years old (excluding severely high myopic and hyperopic subjects). Red line: Estimation of graph curve deviation towards an accumulation of myopes when all axial length data in the general population is accounted for (adapted from [29]).

## 3 Epidemiology

Human myopia and high myopia prevalence varies depending on the age group concerned and the country and region under study. Due to variable inter-study criteria it is also difficult to make accurate conclusions from the different population studies that have been carried out. In general, myopia is the most common refractive disorder world-wide and is thought to affect approximately 20% of the western (industrialised) population aged between 40 and 80 years old (16% in Australia, 18% in Holland, 25% in America) [30]. However, in Asian countries myopia prevalence is higher; approximately 80% in some urban populations in Honk Kong, Taiwan and Singapore [31-34]. In 2004, average high myopia prevalence in the western population of adults aged over 40 years old was estimated to be 4.5% [30]. The rate in Asian populations is higher, manifesting 8 to 9% of high myopes [30, 35, 36]. Multiple studies, as well as national and international government statistics have found an increase in the prevalence of myopia over the last few decades [37, 38].

## 4. The Use of Animal Models to Determine the Mechanisms Underlying Myopia Development

The majority of animal models used to investigate the physiopathological mechanisms at play in myopia development are induced myopic forms in rodents that are simple to manipulate in laboratory conditions. Species used include primates (Marmoset and Rhesus monkeys), cats, tree-shrews, especially small rodents (mouse and guinea pig), and in most cases chicks. Myopia development is achieved by both eye lens **defocalisation** and complete eye light deprivation (**form deprivation**). Animal models have been developed on young animals before completion of adult eye development.

### 4.1 Animal Visual Defocalisation Models

Lenses can be fixed to the exterior of animal eyes (Fig.5.A). A negative lens provokes an artificial myopia so the image is focused behind the retina, thus the animal eye reacts by increasing the axial length [39-42]. Conversely, a positive lens provokes eye globe length to decrease as the image is focused in front of the retina [39]. As soon as the eye retains clear vision, growth or retraction ceases. Also, if the lenses are removed soon enough (before the adult eye is formed), the eye can restore emmetropia and a normal axial length is restored [42].

### 4.2 Animal Visual Deprivation Models

Complete monocular light deprivation can be achieved by suturing the eyelids, using an opaque cover or translucid diffuser, allowing no, or a small amount of light to pass (Fig.5.B). Results obtained show that under these conditions the axial length continues to grow, and only slows down growing when the eye is reexposed to normal light. This is explained by a lack of image focus on the retina, leading to the complete lack of a signal to stop ocular growth [40, 43-49]. Once the cover is removed the eye returns to emmetropy and a normal axial length is restored, but again, only if the developing eye does not reach full adult size [40, 50, 51]. If so, the myopia can persist.

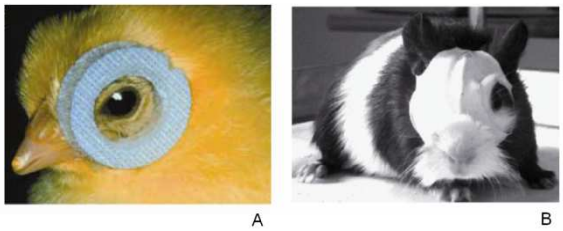


**Fig.5. Animal Models of Myopia.** A: A defocalisation lens fixed to a chick [51]. B: Guinea pig monocular form deprivation using a facemask [52].

On the whole, animal studies use environmental factors to provoke ocular growth, influencing axial length growth to mimick the human myopic phenotype. From here, comparisons between normal and myopic animal eye tissue structures and molecular gene expression levels have allowed the identification of mechanisms that could underly the human myopic disease phenotype. Animal models are generally moderate myopic forms; results being equally considered as potential players in the development of high myopia. Below are the some most important examples.

### 4.3 Scleral Thinning

The sclera is an external rigid connective tissue of collagen fibrils and proteoglycans that are responsible for the highly organised scleral structure. Human high myopia is often associated with posterior staphyloma. This is scleral thinning and weakening, often leading to a scleral tissue protrusion [53-55]. The proteoglycans decorin and biglycan regulate collagen fibril assembly and spacing in the sclera. Aggrecan is composed of elastic laminin and fibrilin, responsible for the hydration of the sclera. The sclera is constantly remodelling throughout eye growth, but in the case of high myopic eyes, the sclera is excessively remodeled. Animal defocalisation and deprivation models confirm this, showing increased scleral remodelling and thinning with increased axial length [43, 56]. Two different hypothesises have been put forward; 1. The sclera ***undergoes*** remodelling caused by axial length increase and/or 2. Scleral properties are ***pre-modified*** (more elastic) and well adapted for axial length increase, thus being a *cause* of scleral remodelling. In both cases, collagen fibril diameters decrease and proteoglycan quantity is reduced [15, 57-59], contributing to the weakened biomechanical properties of the sclera.

Hypotheses have looked into a role of the factors involved in scleral remodelling in the development of myopia. Notably matrix metalloprotease (MMP) family members 1, 2, 3, 9 and 14 regulated by tissue inhibitor matrix metalloproteases (TIMP) are present, but not active in the normal human sclera [60-64]. It was discovered in myopic scleral tissue that MMP2 activity is increased [62], in parallel to reduced TIMP3 or unchanged TIMP1 and 2 activities [59, 65]. MMP2 is involved in collagen fibril degradation, implying a reduced scleral structural organisation in myopic eyes [65, 66].

### 4.4 Local Emmetropisation Defects

We know that the process of emmetropisation is regulated by image formation on the retina. This induces sclera remodelling and a compensatory axial length elongation in order for retinal positioning to be altered to focalise images [59]. However, deprivation of a specific and small retinal area in animal models resulted in only this specific area elongating axially [67]. Similarly, blocking transmission of image signals via the optic nerve to the brain did not prevent myopia [68]. Finally, the retina exerts Go/Grow and Stop signals for eye growth depending on the permanence of visual messages received. Go/Grow signals correspond to those elicited during childhood hypermetropy, and Stop signals are elicited when emmetropy is gained. Chick models have shown that changing negative lenses for positive lenses for even just a few minutes each day prevents myopia development, indicating the existence of *counteracting* Go/Grow and Stop retinal signals [69]. These studies favor the idea that myopia development is deregulation of the eye's own local emmetropisation mechanisms.

### 4.5 Identification of Molecules in Retinal Signaling with Implications in Myoia Development (*Molecular Candidates*)

It is generally believed that the pathways involved in the control of eye growth involve signal cascades initiated in the retina which send signals through the retinal pigment epithelium (RPE) and choroid to control the growth of the sclera. However, the identities of the retinal molecules and pathways involved are still unclear. Recent work has investigated global changes in retinal gene expression during the development of animal myopia, giving some insights into molecules involved in the regulation of ocular growth. Below are some major examples.

#### 4.5.1 Retinal Neurotransmitters

##### A Gamma Aminobutyric Acid (GABA)

GABA is a human neurotransmitter that mediates neurotransmitter inhibition throughout the retina and central nervous system (CNS). Three main classes of GABA receptors exist; $GABA_A$, $GABA_B$, and $GABA_C$ receptors [70, 71]. $GABA_A$ retinal neurotransmission has no effect on pre-induced myopia in animal models, yet $GABA_A$ antagonists* limit form-deprivation myopia development [72]. The same effect is observed by $GABA_C$ [73]. Both $GABA_B$ agonists* and antagonists decrease eye growth [72]. This implies

both Go/Grow and Stop roles for these molecules in retinal signaling and myopia development.

#### B Glucagon

Glucagon is a 29-amino-acid long peptide produced by the proteolytic cleavage of the precursor molecule preproglucagon (PPG) [74]. Glucagon is part of a superfamily of secretin-glucagon peptides that act through G-protein coupled receptors, and has increasingly been identified as a possible neurotransmitter in the CNS [75, 76]. At the RNA transcript level, it has been reported that *PPG* levels were initially upregulated following 2 h of negative-lens treatment, before showing significant down-regulation after 24 h of lens wear [77]. It has also been demonstrated that glucagon agonists can prevent experimentally induced myopia, while glucagon antagonists can prevent compensation for positive lens wear [78]. This suggests a Stop signal role for glucagon in the modulation of eye growth through direct and rapid action on retinal circuits to enhance sensitivity early-on in the signaling process [79].

### 4.5.2 Growth Factors

#### A Transforming Growth Factor-β (TGF-β)

TGF-β is a protein involved in the stimulation and inhibition of diverse cellular signaling events depending on the 'cellular context', from proliferation and cellular differentiation to programmed cell death. The TGF-β signalling system is highly conserved throughout the animal kingdom [80]. Of primary importance to myopia development, TGF-β regulates extracellular matrix (ECM) turnover, and the three mammalian isoforms of TGF-β (TGF-β1, TGF-β2 and TGF-β3) have been shown to regulate collagen production by scleral cells. Furthermore, decreased TGF-β expression, which occurs within 24 h of the initiation of myopia development, has been linked to the altered regulation of ECM production found in the sclera of eyes developing myopia [81]. Recent *in vivo* mammalian work suggests the presence of a constant myofibroblast cell population in the sclera [82]. These cells exhibited a contractile phenotype which could be modulated by all TGF-β isoforms. The increase in TGF-β pathway mediated changes in myofibroblast numbers in the sclera was found to increase myopia development, and vice versa; reduced TGF-β pathway mediated changes in myofibroblast numbers resulted in myopia recovery. On the other hand, when scleral cells were exposed to both reduced TGF-β levels and increased static stress, a larger population of scleral myofibroblast cells were found to be present. Thus, although TGF-β is a major

contributor to the remodelling of the sclera during changes in eye growth, it is matrix stress that is the major determinant of the scleral cell phenotype.

### B Fibroblast Growth Factor-2 (FGF-2)

FGFs with their receptors (FGFRs) and signaling cascades are involved in a diverse range of cellular processes including proliferation, apoptosis*, cell survival, chemotaxis*, cell adhesion, motility and differentiation. FGF-2 is a potent mitogen for fibroblasts and myofibroblasts [83], and has also been shown to be involved in the control of ECM turnover, specifically regulating collagen and proteoglycan production, and mediating tissue degradation through controlling synthesis of MMPs and their regulators [84]. Importantly, FGF-2-mediated signaling is regulated through its capacity to bind proteoglycans [85]. Studies have shown that exogenous delivery of FGF-2 can prevent the development of myopia in the chick [86], reducing the excessive axial elongation and retinal neuronal apoptosis in chronic form-deprivation myopia [87]. Both FGF-2 and FGFR-1, are expressed ubiquitously in the retina and sclera of chicks [88], so evidence as a whole indicates that FGF-2 is a potential regulator of retinoscleral signaling, controlling sclera remodelling and ocular growth in myopia development.

## 4.6 Contribution to the Understanding of the Mechnanisms Underlying Human Myopia Development

Animal models show that myopia can be reversed by a local active emmetropisation effect and suggest that human myopia is the result of default in the emmetropisation response. Unfortunately today we cannot precise whether an accommodation default is the cause or the consequence of myopia. Similarly, in some human subjects an defect in emmetropisation has been observed before [89, 90] and others after [91] myopia development. Thus, human myopia development is due to a **genetic** defect resulting in a default in the emmetropisation program, and an **environmental** emmetropisation defect that results in eye growth in search of visual input. Both of these cases result in axial length elongation. Moreover, **multiple molecular changes in myopic animal tissues imply that human myopic and high myopic disease phenotypes are polygenic.** From here, genetic studies are required to confirm an underlying genetic defect, and consequently which of these molecular candidates could underly the genetic defects causing this defect in human emmetropisation.

## 5 The Human Myope: Genetics versus the Environment

A disease phenotype can vary depending on the variation in response to environmental factors as a function of the underlying genetic makeup, a phenomenon known as **gene-environment interaction** [92]. Myopia is a complex trait affected by both genetic and environmental factors, and their interactions [93]. The increase in myopia rates over the last few decades shows that genetics cannot account fully for the myopic phenotype. Many active studies involving large human cohorts have been carried out to try and quantify such environmental-gene interactions. Note that such studies are limited for high myopia due to greater difficultly in human cohort collection compared to the more prevalent moderate myopia phenotype.

### 5.1 Environmental Effects

A number of studies have shown that the incidence of myopia increases with level of education [94, 95]. Many studies have shown a correlation between myopia and IQ* [96], likely due to the confounding factor of formal education. Other personal characteristics, such as school achievement, time spent reading for pleasure, language abilities and time spent in sport activities correlates to the increasing occurrence of myopia [97, 98].

#### 5.1.1 Education and Near-work

Former studies investigating education levels and refractive error prevalences discovered that upon introduction of an education system among young Alaskan Eskimos, the rate of myopia increased compared to older Eskimos that did not have a high level of education [99]. Similar studies carried out on Indian*, Inuit* and Sherpa* ethnic populations with former low education levels gave similar results [100-102]. Note that high myopia rates were very rare in these studies. Higher levels of myopia are mentioned in studies carried out on highly educated western populations [37, 95, 103]. In Singapore young adults with 3-5 years of university study show a 40% rate of high myopia [104].

Level of education is often used as a surrogate measure for near work with more myopia among the more educated [95, 105, 106]. Several clinical studies have documented an association between myopia and higher levels of children's near work [107-110]. Support for an important role for near work also comes from animal studies that have demonstrated the plasticity of refractive error in response to environmental stimuli. Neonatal chicks, tree-shrews and monkeys experience increased ocular growth and become myopic or less

hyperopic after wearing minus lenses, presumably to compensate for the hyperopic defocus produced by these lenses [111-114]. The current environmental model derived from these studies is that exposure to hyperopic defocus from accommodative lag during prolonged near work leads to excessive growth of the eye and a myopic refractive error.

### 5.1.2 Urban versus Rural Lifestyles

A handful of studies have shown that myopia prevalence is higher in urban compared to rural populations. For example, the myopia rate in school children aged 6-7 years old in Singapore city was found to be higher than in Xiamen city (a countryside Chinese city); the lowest rates were found in Xiamen countryside [115]. As these Chinese populations were of similar genetic backgroubd (predominantly from Southern China), it was postulated that the differences in myopia rates in these three localities may be related to environmental factors. Children closer to or living in the countryside may spend more time doing outdoor activities, thus increased greater distance accommodation, and less near-work accommodation. The same correlation is observed with myopia rates and the amount of time children spend doing outdoor sport activities, notably in more rural country regions [98, 116]. Modern food habits in industrialised countries have also shown a favorable link between increased sugar levels, hyper-insulination and interaction with retinoic acid receptors* in the retina of developing children, resulting in increased axial elongation [117]. This suggests hormonal interaction and regulation of vitreous chamber growth.

## 5.2 Human Myopia Genetics

Myopia and high myopia appear as complex traits. Complex traits do not show typical Mendelian inheritance patterns [118]. The majority of high myopia is caused by increased axial elongation [119], caused by multiple gene effects (polygeneity). Myopia and high myopia can be compared to the continuous and complex height trait, which is also controlled by both different genetic and environmental factors [118]. The simultaneous involvement of several different genes makes the study of complex disease phenotypes difficult as individuals suffering from myopia or high myopia can have the same or different underlying gene mutations or even different mutations in the same gene(s). This is known as genetic **heterogeneity**. In addition, individuals with a causative genetic variation may not express the phenotype, while others do. Despite this complexity, myopia and high myopia have shown genetic inheritance in the following genetic studies.

**Myopia and high myopia phenotypes coexist in the same families as myopia is a continuous trait that is difficult to separate into two separate diseases. Thus, note that many references to studies on the myopia phenotype (including molecular candidates indentified in animal myopia models) are extrapolated to the high myopia phenotype.**

### 5.2.1 Heredity

#### A Twin Studies

Twin studies have presented the strongest evidence for genetic inheritance in the control of eye size and refractive errors. Monozygotic twins have much higher (83-97%) concordance of myopia and related ocular components, such as axial length, anterior chamber depth and corneal curvature, compared to dizygotic twins (47-50%) [29, 120-124]. Considering that monozygotic twins share the totality of their genetic patrimony and dizygotic twins share only half, these differences in concordance can only be genetic. This is assuming that more often twins are brought up together, implying that differences in concordance are genetic more than environmental [125].

#### B Family Studies

Family studies indicate that if at least one of two parents is myopic, then the children are more likely to develop myopia and have longer anterior and vitreous chambers, even before the onset of myopia development [126-130]. It was also shown that having 2 myopic parents instead of no myopic parents significantly increases the risk of developing myopia [131].

#### C Segregation Analysis

Despite the heterogeneity of myopia, a handful of studies have tempted to test the segregation of myopia in family studies. It was found that high myopia in the majority of cases favours an autosomal dominantly transmitted disease model [132-134]. Only one case of autosomal recessive transmission of high myopia in a consanguineous Chinese family has been suggested [135].

### 5.3 High Myopia Genetic Mapping

Despite the complexities in the myopia and high myopia phenotype and different environmental effects, many researchers have made attempts to localise candidate genes with

genetic susceptibility to myopia and high myopia. Many different genetic mapping techniques and analyses have been tested to try and trace myopia and high myopia susceptibility genes in family-based and population-based studies using different ethnic-originated cohorts. It is important to understand genetic mapping techniques in order to evaluate the importance of the different candidate chromosomal and candidiate genes put forward for high myopia susceptibility**.**

### 5.3.1 Microsatellites versus Single Nucleotide Polymorphisms

#### A Microsatellites

Microsatellites, also called short tandem repeats or sequence length polymorphisms, are assays of short repeated sequences. They are usually di-, tri- and tetra-nucleotide repeats that display different length variations with different alleles carrying different numbers of repeat units. They are multi-allelic and there are 5-10 for each allele at each locus (Fig.6.A) [118]. Differences in DNA length can be detected using automated DNA sequencers via capillary gel electrophoresis. This separates microsatellite containing fragments that are amplified by polymerase chain reaction (PCR). Microsatellite genetic maps show known positions of microsatellites, thus indicate the location of a DNA variation in relation to the genes in the chromosomal region. This information is also readily available in NCBI (National Centre for Biotechnology Information) databases. Concerning myopia, microsatellites have been successfully used for linkage analysis, linking myopia genes of interest to large chromosomal regions [136-152]. These regions can extend into a few thousand kilobases (Kb) segments.

#### B **Single Nucleotide Polymorphisms** (SNP)

An SNP is a DNA variation of a single base. Approximately 99.9% of the human genomes between unrelated individuals are identical. The remaining 0.1% is accounted for by 80% by SNP variation. SNPs are bi-allelic and thus simple to detect (Fig.6.B). There are different classes of SNP variations:

- Coding SNPs: Single base variations in the exon sequence, thus present at protein level.
- Non-synonymous SNPs: Variations that result in coding of a different amino acid.
- Synonymous SNPs: Variations that do not encode a different amino acid.

- Non-coding SNPs: Variations found only in DNA introns, thus not present at protein level. These can have functional consequences if the variation occurs in a gene promoter region or 5'/3' untranslated region (UTR). These variations can effect gene transcription, mRNA splicing or mRNA stability.

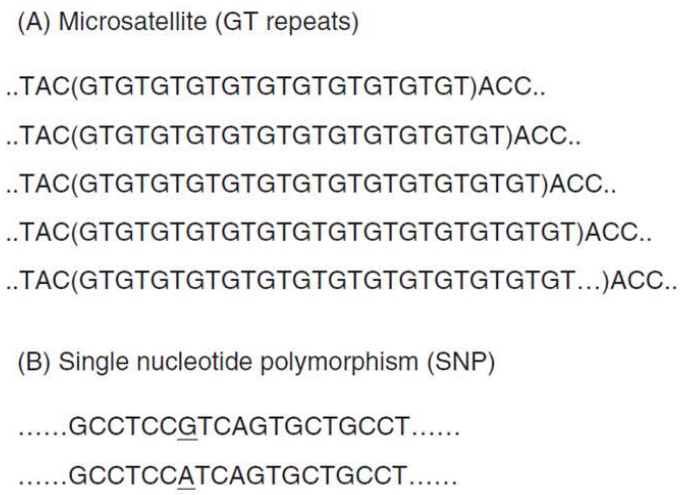


**Fig.6. Microsatellite and SNP Markers.** A: A multi-allelic microsatellite with each allele carrying at least 11 GT di-nucleotide repeats (placed within brackets for the sake of clarity). B: A di-allelic SNP with a G allele and A allele (underlined) [118].

### C **Linkage Disequilibrium** (LD)

LD is a theory that describes a non-random association of SNPs markers at two or more loci, not necessarily on the same chromosome. Two SNPs that are in strong LD may serve as proxies for one another. That is, if the correlation between the two SNPs, measured by an $r^2$ value, is high (Fig.7). If this is the case, genotyping one of the SNPs gives nearly complete information regarding the genotype of the other SNP. Therefore, a SNP array that genotypes 1 million SNPs effectively assays a larger proportion of human genetic variation than represented on the array. Taking advantage of this principle, genotyping array manufacturers have been specifically designing arrays to query SNPs that correlate with, or 'tag', a large number of other SNPs in the human genome [153]. The requisite knowledge of the LD structure in the genome was largely facilitated by the International HapMap Project [154]. HapMap data is an online database with free access to SNP allele frequencies and LD data of human control populations including Nigeria, America (CEU; Northern and Western European ancestry), Japan and China.

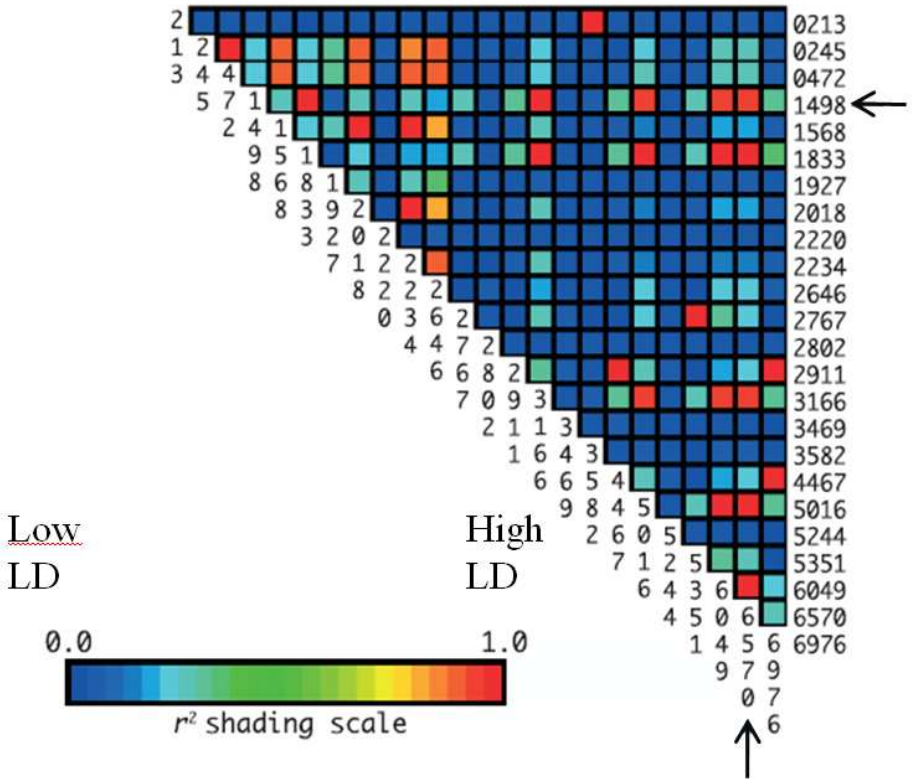


**Fig.7. *IL10* Gene Common SNPs in a Visual LD Block** (CEU population). $r^2$ between SNPs is shown (VG2 program; http://pga.gs.washington.edu/VG2.html). The important point is that even in a 7-kb non-recombinant region (sometimes referred to as a 'haplotype block'), if we genotyped SNPs 1498 and 6570 (indicated by arrows), we would observe strong LD between several markers ($r^2$ = 1; shown in red). But there are clearly a number of SNPs (for example, 2767, 2911, 3582 and 4467) that are weakly associated with either of these two marker, therefore not all variation would be detected (adapted from [155]).

Microsatellites allow zoom in analyses into chromosomal regions containing susceptibility genes. Large-scale studies require between 400 and 800 microsatellites evenly spaced throughout the genome, meaning strong systematic searching. This is expensive and time consuming [118]. SNPs give a vague genetic marker "hot spot" requiring further genotyping studies on huge chromosomal regions. However, SNPs can undergo modern high-throughput genotyping analyses meaning genetic mapping is a faster process. SNPs are also more stable, especially synonymous SNPs as they are considered to be protected from natural selection processes. This means SNPs are easier to trace across different population generations [118].

### 5.3.2 **Copy Number Variation** (CNV)

CNVs are segments of DNA ranging from 1 kb to several megabases (Mb), for which copy-number differences have been revealed by comparison of two or more genomes [156]. Inter-human variation in CNV is approximately 0.7% [157]. These quantitative structural variants often encompass one or more genes [158]. They can be CNV gains (duplications or insertional transpositions), losses (deletions), gains or losses of the same locus, or multi allelic or complex rearrangements [158]. CNVs can affect gene function in several ways. Deletion or disruption of one or more genes can cause functional loss, with CNVs functioning as dominant or recessive alleles according to the cellular function of the affected gene product(s). Alternatively, CNVs may disrupt a regulatory element, generate novel fusion products, or act by causing genomic imprinting* and differential allelic expression [156, 159]. Conversely, some large CNVs involving dozens of genes have shown no overt* phenotype [156, 158, 160, 161]. To date variations in CNV have not yet been reported to underly the myopia or high myopia phenotypes.

### 5.3.3 Qualitative versus Quantitative Analysis

A **qualitative trait** is a discontinuous trait with two or more distinct categories where each category can be separated from the other categories and qualitative disease traits are shown by phenotypic deviations from the norm. For example, the ABO blood group system.

A **quantitative trait** is a continuous trait and exhibits a wide range of possible phenotypes in a constant spectrum. It does not follow Mendelian inheritance and quantitative trait diseases are usually complex. In genetic studies myopia and high myopia phenotypes of refractive error and axial length phenotypes have been converted into qualitative traits upon fixation of a specific phenotype threshold. High myopia has often been classed as an error of refraction of at least -6 D [6, 10, 11]. Different threshold have however been set depending on different studies, leading to difficulties in comparison of results [118].

### 5.3.4 Linkage Analysis; Parametric versus Non-parametric

Genetic mapping uses both qualitative and quantitative traits in linkage studies. Briefly, linkage analysis is a method used for detecting if there is significant evidence for co-segregation of disease alleles at a marker locus in family pedigrees (more powerful with multi-generation pedigrees). The linkage of markers to a disease mutation is quantified by a logarithm of the odds' (LOD) score. A LOD score of $\geq 3$ is considered to be significant

evidence of linkage. **Parametric** linkage analysis requires a certainty of the correct disease model, the frequency of disease allele(s) and the penetrance* for each genotype. **Non-parametric** linkage analysis does not take into account these factors. This is because either the disease model is unknown, or as in the case of myopia and high myopia, the disease does not follow normal Mendelian inheritance. If an incorrect model is specified for parametric analysis, linkage analysis could not only miss true linkage, but moreover perhaps result in false significant linkages. Non-parametric analysis can be carried out on smaller nuclear families, but power is lost. The affected sibpair (ASP) analysis is the simplest type of allele-sharing method commonly used to map genes in complex eye diseases [137, 138, 144-146]. Both parametric and non-parametric linkage analyses have been used to identify myopia and high myopia genetic loci, parametric linkage analysis assuming an autosomal dominant inheritance in most cases [136, 139-142, 149-152, 162, 163]. Note two X-linked myopia localisations have been identified [143, 150, 151].

### 5.3.5 Association Analysis

Association analysis is considered a more powerful method for detecting multiple small gene effects in complex diseases (Fig.8) [164]. Association analysis is based on significantly increased or decreased frequency of an SNP marker allele in a disease phenotype compared to a control phenotype. Association analysis takes into account tagSNP LD, thus associated SNPs can actually be located in DNA sequences far from the original associated SNP marker. There are two different cohort-based association analyses that can be carried out:

#### A Population-based Case Control Analysis

This is the most widely used method for common complex trait genetic studies. SNP frequencies are compared between a set of disease affected subjects and a set of unaffected control subjects. Both cases and controls must be unrelated, but come from the same population (similar age, gender repartition, ethnic and geographical background). A greater or reduced % of SNP frequency in the cases compared to controls is considered to be an association of the SNP marker allele with the disease phenotype. The chi-square ($\chi^2$) test is used to measure statistical significance of this association. Human subject recruitment for this method is easier and quicker as family pedigrees are not required. However, inappropriate matching between case and control populations can result in false positive associations due to

different allele frequencies between different populations (population stratification). This method has been widely used recently in myopia and high myopia candidate gene analyses.

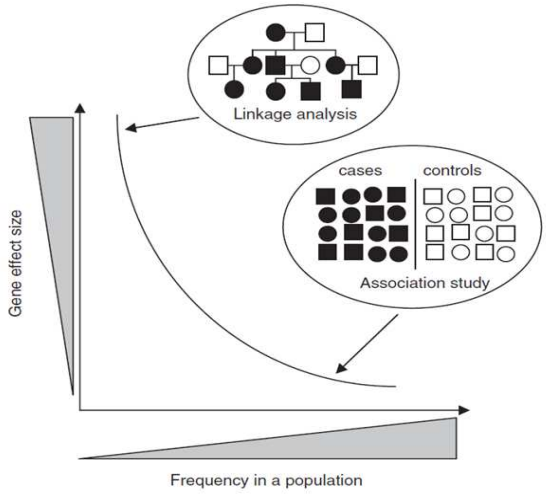


**Fig.8. Gene Mapping Strategies for Diseases with Different Gene Effect Sizes.** Genes involved in rare Mendelian diseases show large effects and are best mapped by parametric linkage analysis in large families. Genes involved in common complex diseases exhibit small effects and are best identified by genetic association studies using cases and controls [118].

### B Family-based Association Analysis

This can be used to overcome population stratification issues sometimes encountered in population-based association analysis as this method requires small nuclear families, with both affected parents and offspring. The parents provide internal control data, assuming that non-transmitted alleles to offspring are not associated to the disease phenotype. The transmission disequilibrium test (TDT) is the most widely used version of this method, testing for distortion in the transmission of alleles from a heterozygous parent to an affected child. The frequency of the transmitted allele is compared to that of the non-transmitted allele [165]. Again, this method has been used as a myopia candidate gene search approach.

### 5.3.6 Candidate Gene Approach

Candidate genes are selected according to prior known biological function and expression in tissues associated to the disease phenotype [166]. Myopia and high myopia candidate gene analyses have predicted mutations in genes expressed in eye tissues, in many cases having previously shown a potential role in myopia development in animal experimentation models as previously described in *section 4 page 22.*

It does appear more logic to start by a whole genome search to identify chromosomal regions with a potential collection of human myopia susceptibility genes in order to then conduct grouped candidate gene scans. However, genome scans are very expensive and time consuming in human subject recruitment, resulting in replacement by simple candidate gene scans in smaller cohorts. This has similarly been carried out for complex diseases such as diabetes and hypertension [118]. The most common analysis method for this candidate gene method is case-control association analysis. *TGFβ1* [167] and Lumican (*LUM*) [168] were identified as myopia susceptibility genes by this method. These candidates were initially considered interesting candidiates from previous animal models, demonstrating a potential role of TGFβ signaling in retinal growth signals [81], and LUM proteoglycan, as the myopic sclera shows a reduction in proteoglycan quantity [57].

Candidate gene analyses have also been carried out on potential genes identified in chromosomal regions localised by intital whole genome scans [167, 169-173]. These studies can be considered as follow-up, or **replication studies**. For example, genes in the MYP2 locus underwent a replication study, but disagreed with previous significant association shown between the high myopia phenotype and the Transforming factor β-induced factor (TGIF) gene [169, 171]. To date only 3 candidate regions/genes have survived a total of approximately twelve high myopia gene replication studies [174-179].

### 5.3.7 Genome-wide Association Analysis (GWAS)

#### A The Principle of GWAS

The goal of GWAS is to find the variants that are statistically more prevalent in individuals with a disease than in individuals free of the disease. A study typically entails collecting large numbers of affected (cases) and unaffected (controls) individuals, and running the DNA of all individuals on SNP arrays. Genotyping data is then mined for statistically significant differences in allele frequencies between the two groups. The associated variant is then either a disease predisposition allele, or in LD with such an allele. In recent years, GWAS has been facilitaed in majority by both the Affymetrix (Dr Stephen P.A. Fodor, Ph.D, Santa Clara, California, USA) and Illumina (CW Group, Larry Bock, San Diego, California, USA) genotyping platforms. A considerable factor for doing GWAS is the cost of genotyping enormous numbers of cases and controls. Large numbers of subjects are necessary due to the high density of the arrays, meaning hundreds of thousands of variants need to be tested, resulting in hundreds of thousands of significancy tests. In order to avert huge numbers of

false positive associations, the p-value threshold for statistical significance must be very stringent to accommodate this huge multiple testing burden; typically lower than $10^{-6}$. This problem was exemplified by the study performed by the *Wellcome Trust Case Control Consortium* [180]. Here, the authors performed GWAS on seven different diseases, 2000 cases for each different disease. Rather than having separate panels of control individuals for each disease, the study shared 3000 unaffected controls across all the diseases. All 17 000 individuals were genotyped using the Affymetrix 500K SNP array. The density of the array allowed the researchers to test an enormous number of SNPs, but the multiple tests meant that only associations with p-values less than $5 \times 10^{-7}$ were reported as significant. The large sample sizes were therefore necessary for power sufficient to obtain such low p-values. A collaborative GWAS was also carried out on the quantitative trait of height among human adult subjects. This localised 20 different candidate loci, implying that a wide range of developmental and signaling molecules underly the height trait [181]. However, again cohort sizes were extensive, reaching 16 482 cases, and p-values were set to the $10^{-7}$ to $10^{-10}$ range.

### B GWAS on <u>all</u> Refractive Error Phenotypes

Two major successful GWAS were published in late 2010 based on global refractive errors, thus a range of hyperopic to myopic phenotypes [177, 178]. The Hysi et al., (2010) [177] study that made BBC (British Broadcasting Coproation) news headlines initially scanned the genomes of 4270 individuals from a UK-based twin cohort and found a consistency of SNPs localised in the 15q25 chromosomal region (low p-values of $10^{-8}$). A replication study in combined European cohorts meant a total of 13 414 individuals were scanned for the same SNP variations in this region. This resulted in identification of one particular associated SNP in the region with a $10^{-9}$ p-value threshold. This SNP fell in the transcriptional initiation site of the *RASGFR1* gene, a gene known to be highly expressed in mouse neurons and the retina [182]. RASGFR1 protein was then found to be expressed in human retinas [177]. Mouse *RASGFR1* knockout mice showed heavier crystalline lens, and mouse *RASGFR1* knockdown mice imply that RASGFR1 is required for normal retinal function. Thus, could the *RASGFR1* gene disrupt the human lens contribution to ocular refraction, or play a role in defect retinal signaling pathways that could lead to myopia? [177].

Similarly, Solouki et al., 2010 [178] carried out an initial genome scan on 5328 Dutch individuals, followed by replication studies in 4 independent cohorts (total of 10 280 individuals). This identified an SNP in the 15q14 chromosomal region (p-value of $10^{-14}$),

adjacent to the SNP localised by Hysi et al., (2010) [177] on 15q25. The associated SNP fell between the genes *ACTC1* and *GJD2*, also found to be expressed in the human retina [178]. A role for ACTC1 in ECM remodelling, and a role for GJD2 in retinal transmission have been put forward, but not proven. Will future high myopia GWAS show association to these same genes suggested to underlie general refractive error phenotypes?

### C GWAS on the High Myopia Phenotype

Collecting thousands of high myopic subjects is much more demanding than individuals with general refractive error pehnotypes from the general population. To date there has only been one GWAS study carried out on the *high* myopia phenotype using a Japanese population-based case-control cohort [183]. This study was split into a 3-step association analysis:

- **Step 1**: Genome scan of 297 cases with a high myopic phenotype (axial length ≥28mm) and 934 controls from a Japanese SNP database. This identified 29 SNPs with a set p-value ≤10-4 (less stringent than GWAS previously mentioned) (Fig.9).
- **Step 2**: Replication genotyping step with 533 cases with a less severe high myopic phenotype (≥26 mm) and 977 matched Japanese controls recruited by the authors themselves. 22 SNPs from the first stage in strong LD were genotyped using custom SNP TaqMan genotyping (Cetus Corporation, Emeryville, USA). Again less stringent p-values of $10^{-3}$ were set.
- **Step 3**: Analysis of both steps combined (Joint analysis): 1 SNP with a more stringent p-value of $2.22 \times 10^{-7}$ was identified in chromosome 11q24. This SNP fell within 200 kb of two uncharacterised genes (Fig.10). Their expression in the human retina was however consequently confirmed.

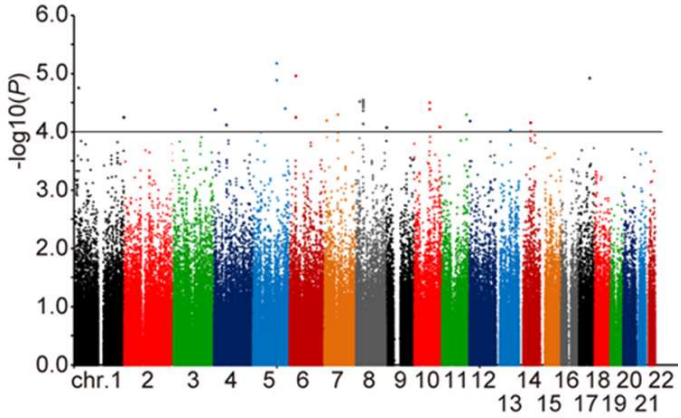


**Fig.9. Manhattan Plot of 1st Stage Results**. Chart of adjusted p-values obtained by the trend $\chi^2$-test plotted in 2log10 scale according to their chromosome location. The dots above the line correspond to the 22 SNPs with a p-value $\leq 10^{-4}$ [183].

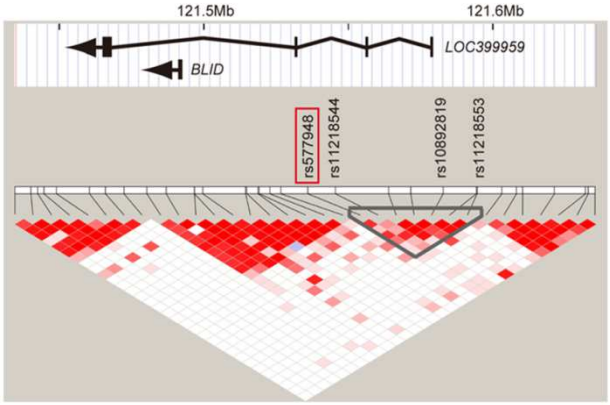


**Fig.10. Joint Analysis (3rd stage) Results.** The 11q24.1 locus is in proximity to the *BLID* and *LOC399959* genes. Structures, orientations and locations of the *BLID* and *LOC399959* genes on NCBI Reference Sequence Build 36.1, together with pair-wise LD estimates of the SNP markers located within a 200-kb region encompassing the associated rs577948 marker (red box) (adapted from [183]).

As required for all candidate genes identified by GWAS, the next step in this study is to deduce the true functionality of the SNP variation in the underlying high myopia disease phenotype. Consequently, replication studies in cohorts of different ethnic origins, and then grouped cohorts of multiple ethnic origins (meta-analyses) should be carried out to test for candidate gene extrapolation between different populations [118].

### 5.3.8 High Myopia Genetic Loci

Linkage and association studies have identified to date 18 myopia (MYP) loci that have been approved by HUGO Gene Nomenclature Committee in 15 different chromosomes, although some of these remain to be confirmed [184] (*summarised in table 1 page 41*). Approximately 16 chromosomal localisations have been described for high myopia from studies based on a range of different ethno-geographic populations. Note that loci 7p15 [162], 14q22.1-q24.2 (MYP18) [135], 11q24 [183], and adjacent loci 5p15.33-p15.2 [185] and 5p13.3-p15.1 [176] have also been identified for high myopia. The MYP1 high myopia locus is the only locus to have been replicated in an independent significant linkage study [186], and the 5p15 region replicated in an independent population-based association analysis [179]. In some cases moderate myopia mapping has been found to coincide with high myopia mapping localisations; a strongest linkage signal for moderate myopic subjects was localised within the MYP12 high myopia locus by two different groups [174, 187]. It would seem that chromosome 2 could harbor both myopia and high myopia susceptibility genes.

Only a handful of these genome wide studies have been able to localise specific gene variations associated with the high myopic phenotype; Han et al., (2006) [12] localised a polymorphism in the hepatocyte growth factor (*HGF)* gene, Wang et al., (2006) [168] a polymorphism in LD in *LUM*, and Tang et al., (2007) [188] identified an association with the myocilin gene (*MYOC*) [189-191].

Replication studies have in majority been frustrating, resulting in contradictory reports published for specific loci and genes, even among studies carried out on the same population. First identifications are often greeted with enthusiasm and then disappointment as follow-on studies fail to replicate results. Attention to the interpretation of multiple and conflicting findings of association studies is required.

**Table.1. Myopia and High Myopia (indicated by arrows) Loci** mapped by linkage and association analysis (adapted from [118]). The missing MYP18 locus (14q22.1-q24.2) corresponds to the recently identified autosomal recessively transmissed locus of high myopia [135]. Note that some statitstical significance levels are not always attained (right-side column: LOD/p-values), meaning replication studies are required for confirmation.

| Myopia locus[†] | Authors (years) | Inheritance/ QTL[‡] | Location | Ethnicity of subjects | Types of families | Linkage analysis (PL or NPL)[§] | Affected status[¶] | Max LOD[††] |
|---|---|---|---|---|---|---|---|---|
| *MYP1* | Schwartz *et al* (1990)[41] | XR | Xq28 | Danish | Large pedigrees | PL | — | 4.80 |
| *MYP2* | Young *et al* (1998)[42] | AD | 18p11.31 | American and Chinese | Moderate to large multigenerational families | PL | ≤ -6.00 D SE | 9.59 |
| *MYP2* | Lam *et al* (2002)[43] | AD | 18p11.31 | Hong Kong Chinese | Moderate pedigrees | PL | ≤ -6.00 D | 2.10 |
| *MYP3* | Young *et al* (1998)[44] | AD | 12q21-23 | German/Italian | A large pedigree | PL | ≤ -6.00 D SE | 3.85 |
| *MYP3* | Farbrother *et al* (2004)[45] | AD | 12q21-23 | UK population | Nuclear families | PL, NPL | ≤ -6.00 D in the least negative meridian of both eyes | 2.54 |
| *MYP4* | Naiglin *et al* (2002)[46] | AD | 7q36 | French and Algerian | Large to moderate pedigrees | PL, NPL | ≤ -6.00 D both eyes | 2.81 |
| *MYP5* | Paluru *et al* (2003)[47] | AD | 17q21-22 | English/Canadian | A large pedigree | PL | ≤ -6.00 D SE | 3.17 |
| *MYP6* | Stambolian *et al* (2004)[48] | AD | 22q12 | American families of Ashkenazi Jewish descent | Large pedigrees | PL, NPL | ≤ -1.00 D in each meridian for both eyes | 3.54 |
| *MYP6* | Stambolian *et al* (2006)[49] | AD | 22q12 | Additional Jewish descent | Pedigrees | PL, NPL | ≤ -1.00 D in each meridian for both eyes | 4.73 |
| *MYP6* | Klein *et al* (2007)[50] | QTL | 22q12 | Americans of Northern European and/or German ancestry | Sib-pairs | NPL | Mean +0.44 D SE; range: -12.12 to +8.38 D | *P* value = 0.00330 |
| *MYP7* | Hammond *et al* (2004)[51] | QTL | 11p13 | UK population | Dizygotic twin pairs | NPL | Mean SE < 0 D | 6.10 |
| *MYP8* | Hammond *et al* (2004)[51] | QTL | 3q26 | UK population | Dizygotic twin pairs | NPL | Mean SE < 0 D | 3.70 |
| *MYP9* | Hammond *et al* (2004)[51] | QTL | 4q12 | UK population | Dizygotic twin pairs | NPL | Mean SE < 0 D | 3.30 |
| *MYP10* | Hammond *et al* (2004)[51] | QTL | 8p23 | UK population | Dizygotic twin pairs | NPL | Mean SE < 0 D | 4.10 |
| *MYP10* | Stambolian *et al* (2005)[52] | AD | 8p23 | Old Order Amish | Families with affected sibs | PL, NPL | ≤ -1.00 D in each meridian for both eyes | 2.03 |
| *MYP11* | Zhang *et al* (2005)[53] | AD | 4q22-27 | Han Chinese in a small village of central China | A large pedigree | PL | Range: -5.00 to -20.00 D | 3.11 |
| *MYP12* | Paluru *et al* (2005)[54] | AD | 2q37.1 | US family of northern Europe | A large pedigree | PL | ≤ -6.00 D SE; range: -7.25 to -27.00 D | 4.75 |
| *MYP13* | Zhang *et al* (2006)[55] | XR | Xq23-25 | Chinese | A large pedigree | PL | ≤ -6.00 D SE; range: -6.00 to -20.00 D | 2.75 |
| *MYP13* | Zhang *et al* (2007)[56] | XR | Xq23-27.2 | Chinese | A large pedigree | PL | ≤ -6.00 D SE; range: -7.00 to -16.00 D | 2.79 |
| *MYP14* | Wojciechowski *et al* (2006)[57] | QTL | 1q36 | Ashkenazi Jewish | Moderate to large multigenerational families | PL | Mean -3.46 D SE; ≤ -1.00 D in each meridian for both eyes | 9.54 |
| *MYP15* | Klein *et al* (2007)[50] | QTL | 1q41 | Americans of Northern European and/or German ancestry | Sib-pairs | NPL | Mean +0.44 D SE; range: -12.12 to +8.38 D | *P* value = 0.00019 |
| *MYP16* | Klein *et al* (2007)[50] | QTL | 7p21 | Americans of Northern European and/or German ancestry | Sib-pairs | NPL | Mean +0.44 D SE; range: -12.12 to +8.38 D | *P* value = 0.0023 |
| *MYP17* | Nallasamy *et al* (2007)[58] | AD | 10q21.2 | Hutterite population from South Dakota | A large pedigree | PL | Mean -7.04 D; range -3.75 to -13.25 D | 3.22 |

[†] Myopia loci are shown in standard gene symbols approved by Human Gene Nomenclature Committee but *MYP15*, *MYP16* and *MYP17* are newly identified and the gene symbols are still tentative
[‡] Inheritance is indicated as X-linked recessive (XR), autosomal dominant (AD). QTL represents quantitative trait locus.
[§] PL represents parametric linkage analyses whereas NPL represents non-parametric linkage analyses, usually affected sibpair analysis
[¶] SE represents spherical equivalent in dioptres (D)
[††] Max. LOD stands for maximum 'logarithm of the odds' score. Only *P* values are given for *MPY6*, *MYP15* and *MYP16* in Klein's study.

## 6 Revision: Human High Myopia Genetics

High myopia is due to image focalisation in front of the retina and in most cases a significant increase in the axial length of the eye. For analysis in genetics studies the high myopia phenotype has been clinically defined as an error of refraction ≤-6 D or by an axial length ≥26mm. High myopia is due to both a combination of multiple genetic defects and multiple environmental factors, and their interactions between them. This makes high myopia a complex, polygenic and hetergenous disease, thus difficult to analyse in terms of searching for its multiple small gene effects. Several genomic regions have however now been identified as harbouring potential high myopia candidate genes, but the same genes have been rarely identified in different high myopic populations. More up-to-date population genotyping genome scans with increased speed of analysis and increased coverage of genetic variation using SNP markers are making the analysis of complex diseases more feasible. However, these studies require large cohorts, with the requirement of replication and functional-variant studies before confirmation of the identification of genuine high myopia genes.

## 6 Récapitulatif: La génétique de la myopie forte humaine

La myopie forte est caractérisée par la focalisation des images devant la rétine et dans la plupart des cas, par une augmentation importante de la longueur axiale du globe oculaire. Pour des analyses génétiques, le phénotype de la myopie forte est classé par une erreur de réfraction ≤-6 D ou par une longueur axiale ≥26mm. La myopie forte est due à des anomalies génétiques, aux facteurs environnementaux, mais ainsi aux interactions environnementales-génétiques. Par conséquent la myopie forte est une maladie complexe et polygénique dont la recherche des multiples gènes causants modestes est laborieuse. A ce jour, plusieurs régions chromosomiques ont été identifiées comme comportant des gènes responsables de la myopie forte. En revanche, les mêmes régions ou gènes ont été rarement identifiés dans des études de réplication sur d'autres populations de myopes forts. Les techniques de génotypage modernes, plus rapides, prennent en compte l'augmentation de la couverture des variations génomiques à l'aide des marqueurs SNPs, rendant l'analyse des maladies complexes plus accessible. Ces analyses nécessitent tout de même de grandes cohortes, avec l'obligation de poursuivre des études de réplication et des études fonctionnelles des variations potentielles.

# II Aims

## 1 Previous Work on High Myopia Genetics in the French Caucasian Population

The laboratory began the recruitment of a human high myopic cohort in 1998 following the identification of two different chromosomal localisations for high myopia on 18p11.31 and 12q21.23 in American and German/Italian cohorts resepectively [148, 163]. From here, a flow of studies have led to the conclusion of the intervention of multiple genes in the high myopia phenotype in the French Caucasian population:

A. The very first study was a segregation analysis on a cohort of 32 French families showing that 58.4% of the high myopic subjects favoured an autosomal dominant transmission with weak penetrance [134].
B. The laboratory's first localisation on chromosome 7q36 for high myopia gave only *suggestive linkage* upon assumption of autosomal dominant transmission with weak penetrance (parametric LOD score=2.81) [139]. This study incorporated 23 multigeneration high myopic French families, a total of 140 participants. The subject inclusion phenotype was ≤-5 D. Not only did this study include 2 Algerian families, only one suggestive localisation was identified, suggesting that a larger cohort was required for such analysis.
C. The cohort was extended between 2003 and 2004 by new subject recruitment of pre-existing multigeneration families and recruitment of new families that harboured at least 2 high myopic subjects. This resulted in a total of 26 multigeneration families, a total of 445 subjects, of which 136 were high myopes. The same high myopic phenotype of ≤-5D was used for the high myopia phenotype threshold. This cohort was then used for two studies:

### 1. A Candidate Gene Search

337 autosomal microsatellite markers were used from the ABI PRISM linkage mapping set for genotyping. Parametric linkage analysis again showed suggestive linkage to several chromosomal localisations (genome hot spots). This confirmed **multiple gene intervention** in the French population, and the

requirement of larger cohorts for multiple but small gene effects. Only non-parametric linkage analysis retained a significant linkage on chromosome 7p15 (LOD score=4.07) (Fig.11.) [162].

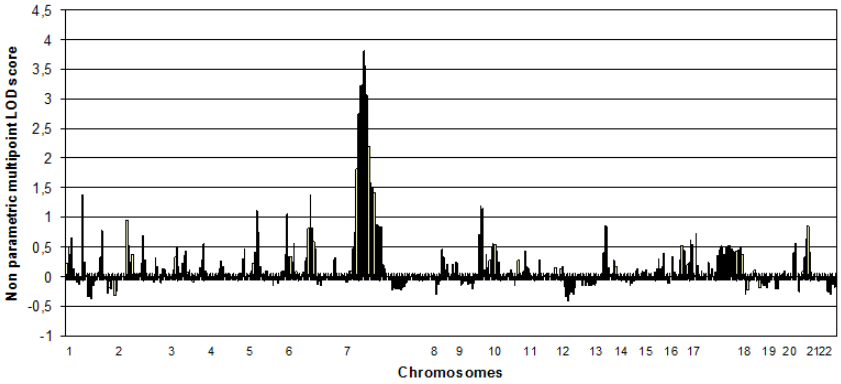


**Fig. 11**. Non Parametric Multipoint Linkage Analysis Results [162]: Significant linkage to 7p15, but also suggestive linkage (several smaller peaks).

The 7p15 region was a 6.65 Mb segment harboring 67 genes. Several "top genes" were considered to potentially play a role in eye structure, function and/or development, one of them being Neuropeptide VF Precursor (*NPVF*). NPVF is a neurotransmitter expressed in the CNS and retina [192, 193]. It has shown a capacity to inhibit GABA neurotransmission [192]. As previously mentioned (*section 4 page 24*) agonists and antagonists of GABA have previously demonstrated retinal go/stop growth signals during animal experimental myopia development [72], making *NPVF* mutations an interesting candidate for high myopia.

2. **Determination of the Genetic Heratibility of High Myopia**

As parametric linkage analysis did not give significant results, analysis of the genetic influences on ocular refraction and axial length was carried out assuming a polygenic inheritance of high myopia. Estimates for both refractive error (20%) and axial length (20%) showed equally mildly to moderate inheritance in this French cohort [194]. This confirmed again that multiple genes with small effects underlie the phenotype, as well as considerable environmental influences.

D. The whole high myopic and control family cohort participated in Terri Young's multinational linkage analysis that led to confirming the *COL2A1* gene as a myopia susceptibility [195]. However, the French families were not linked to this locus, excluding this as a candidate gene in the French population, and further demonstrating heterogeneity in the myopia phenotype between different ethnic populations.

## 2 New Aims for the Study of High Myopia Genetics in the French Caucasian Population

The identification of the 7p15 region left the laboratory with two different possibilities for the next step upon my arrival in the laboratory; a replication genotyping study in the 7p15 linked region in order to either narrow down the selection of candidate genes, or exclude the region, or; try to overcome the problem of low power of detection of multiple small gene effects to capture all genome hot spots.

### 2.1 Management versus Scientific Decisions

Initial views were to progress in further confirming or excluding the 7p15 chromosomal localisation in the French population using custom tagSNP genotyping in a population based case-control association analysis. This was supported by a newly suggested linked region in to the moderate myopia phenotype in an African American cohort [196] that overlapped with the 7p15 region identified by Paget and Julia., 2008 (Fig.12). This further suggested an implication of this chromosomal region in the myopia and high myopia phenotypes.

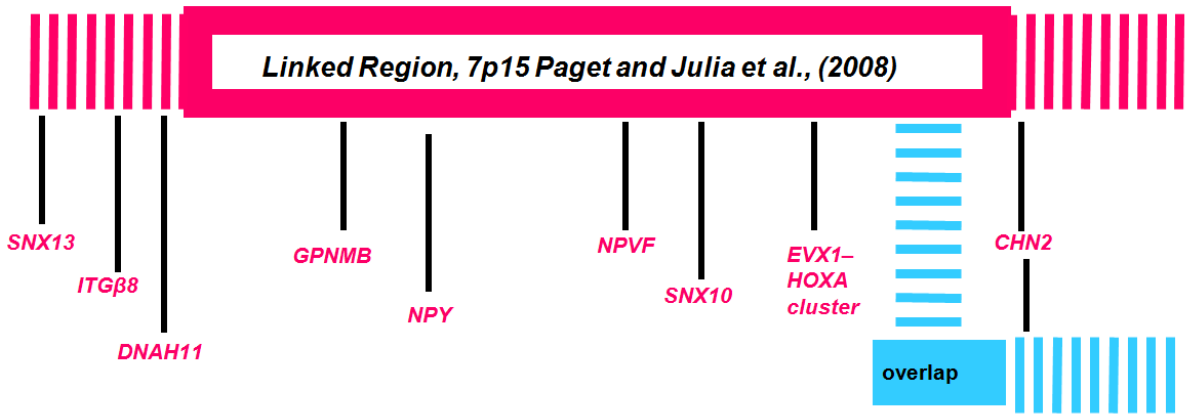


**Fig.12**. **Schematic Representation of the 7p15 Region Overlap.** Blue overlap: The suggestively linked region to the moderate myopia phenotype in the African American population [196] overlaps in part with the region identified by Paget and Julia., 2008 [162].

Confliction with my initial progress made on the 7p15 replication approach was the requirement to once again launch a recruitment scheme to create unrelated case and control cohorts. Recruitment of human subjects is a time-consuming and exerting process. A special offer fom Affymetrix whole genome high-throughput SNP genotyping ensured my final decision to reconduct a genome-wide scan with a new population. This time by means of a population-based case-control SNP association analysis to:

1. Increase the power in the detection of multiple small gene effects, meaning more chance this time of localising all gene effects that could have been only suggestively linked in the previous study. As SNP association analyses take into account LD, they are considered the most powerful method to date for detecting multiple gene effects [164].
2. Eliminate family recruitment constraints by recruiting unrelated subjects.

### 2.3 Aims of Project 1

The aim of Project 1 was to carry out a new genome scan in order to localise candidate genes associated to the French Caucasian high myopic phenotype using a population-based case-control SNP association analysis. The study required a design based on increasing the power of the analysis, while taking into consideration realistic time and financial limiting factors. Thus, we analysed the advantages of using axial length as a less complex phenotype inclusion criterion, we determined an approach to limit cohort admixture and we launched a new subject recruitment scheme to establish a new DNA and phenotype data bank.

### 2.3 Résumé des objectifs

Les objectifs du premier projet étaient de répliquer un génotypage pangénomique afin de localiser de gènes de susceptibilité à la myopie forte par une analyse d'association cas-témoin à l'aide de marqueurs SNP dans une nouvelle population française caucasienne non-apparentée. Cette étude à été conçue pour améliorer la puissance statistique de l'analyse, tout en respectant les contraintes de temps et l'aspect financier. Nous avons employé la longueur axiale comme critère d'inclusion phénotypique moins complexe, recherché une approche pour limiter la stratification de la cohorte et lancé un nouveau système de recrutement clinique pour établir une nouvelle banque d'ADN et de phénotypes.

# III Material and Methods

## 1 Axial length as the High Myopic Sujbect Phenotype Criterion

Axial length is the largest determinant for non-syndromic myopia [6] as a negative relationship is observed between axial length and refractive error [17, 18]. As axial length increases, the more negative the refractive error is. To date the majority of myopia and high myopia genome scans have used refractive error data to create artificial phenotype boundaries for high myopic subjects [118]. Only one GWAS study has used axial length regardless of refractive error data to include subjects in their study [183]. We analysed the benefits of using the axial length phenotype as the deciding factor for the inclusion of high myopic subjects in our GWAS.

The most important point to make is that **heritability*** of axial length is more consistent among different ethnic and geographical populations than refractive error [129, 197, 198]. Twin studies demonstrated that axial length is highly heritable and genetic effects can explain up to 88% of this parameter [199, 200]. Nuclear family studies also showed higher concordance of the heritability of axial length than refractive error [130]. Heritability of axial length versus refractive error is *summarised in table 2 below*. In the minority, the French cohort was the only study showing exactly the same heritability of axial length and refractive error in multigeneration families including high myopic subjects [194]. However, this cohort was small.

| Country or region | Study type | Heritability of AL | Heritability of RE |
|---|---|---|---|
| Sardinia Italy Male | Family | 60% | 18%-27% |
| Female[A] | | 31% | |
| Taiwan[B] | Twin | 67% | 33% |
| | Twin | 94% | 89%-91% |
| USA[C] | Population | 67% | 58% |
| France[D] | Family | 20% | 20% |

A

| | Heritability | | |
|---|---|---|---|
| Trait | Twins | Sibs | Nuclear families |
| Axial length[E] | 0.88 | 0.73 | 0.75 |
| Refractive error[F] | 0.82 | 0.50 | 0.21 |

B

**Table 2. Heritability of Axial Length (AL) versus Refractive Error (RE)** in A: Different geographic and ethnic cohorts. B: Different family-based analyses (A: [129]; B: [198]; C: [197]; D: [194]; E: [201]; F: [130]).

Secondly, segregation analyses suggested that AL is under polygenic control [194]. However, the idea that the axial length heritability remains more stable across populations suggests that axial length may have less underlying genes encoding for the phenotype than refractive error does. Polygenic traits with less encoding genes are easier to analyse in terms of searching for their underlying genes [194]. On the other hand, the heritability of myopia was found to be vary significantly among twin, sibling and nuclear family studies as manifested by Table 2.B. [202]. The more distant the samples were, the less heritability they possessed. Even though case-control studies using unrelated subjects obviously do not share inherited myopia genes, on the whole the fact that there is a correlation between myopia and axial length suggests that both phenotypes share some common gene effects across subjects [201], meaning that we would not be searching for different genes using either of the two phenotypes in unrelated subjects.

Furthermore, a litterature review on the trait variance of axial length caused by environmental factors has been found to be only around 6%, different from that of refractive error ranging from 14%-33% [130, 201]. As myopia is a complex trait influenced by both genetic and environmental factors and their interactions [109, 203, 204], limiting the environmental influences as much as possible is beneficial in GWAS aimed solely at localising gene effects associated to the phenotype.

Nowadays, modern ultrasound velocity reading machinery allows ophthalmologists to use optical partial coherence interferometry to determine the axial length of their patients to clarify the severity of axial length myopia. These machines are now widely present in most hospital ophthalmology services, meaning recording axial length data of recruited subjects is not an over demanding criterion and can be easily integrated into a clinical protocol.

Overall, using axial length as the subject phenotype inclusion criterion should help reduce the number of genes underlying the phenotype and reduce the environmental influences, thus minimising bias caused by the more complex refractive error trait. We can say that axial length can be used as an **endophenotype** for the myopia phenotype [205]. This means axial length can be used as a concept to distinguish the more complex myopia trait with a more simple genetic connection. Clinically defined high myopia corresponds to an axial length of at least 26 mm [11]. Thus, **we set a minimum axial length of 26 mm for the new recruitment criterion of high myopic patients in the new GWAS.** Please refer to Annex 1 (*page 226*) and Annex 2 (*page 228*) for our published reviews on the use of axial length myopia as a GWAS subject phenotype inclusion criterion.

## 2 Genetic Heterogeneity Limitation

An important factor to take into account when designing a population-based case-control GWAS is the propensity for population substructure, known as population stratification [206]. Systematic differences in allele frequencies occur between different populations due to different ancestry. The problem for GWAS is stratification can lead to spurious claims of association to an SNP variant that in fact arises from case and control genetic background admixture, and not an association to a real disease-causing SNP variation [207, 208]. Consequently, it is widely appreciated that successful GWAS requires case and control subjects to be well matched for their ethnic and geographic backgrounds (*Wellcome Trust Case Control Consortium* [180]).

Several studies have been carried out using recent SNP genotyping arrays to specifically compare allele frequencies between different ethnic populations and to test for the possibility that false claims of association can arise due to population admixture [209-215]. Significant differences in allele frequencies were more manifest between populations with increasing numbers of SNP markers used to scan the genomes [211, 212]. Grouping of population allele frequencies was found to form clusters depending on geographic location of the subjects. In Europe, the population clusters were said to mirror identically distinct geographical regions in the continent (Fig.13).

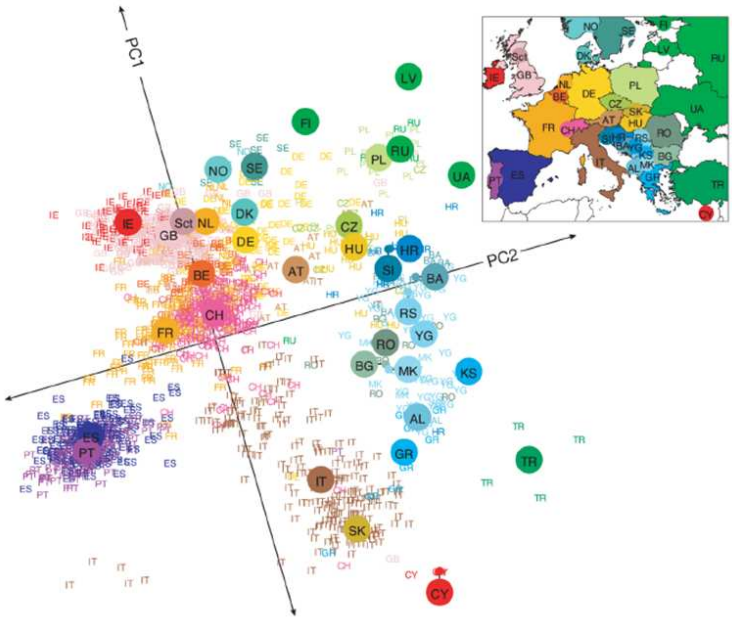


**Fig.13. Population Admixture in Europe.** Statistical summary of genetic data from 1 387 Europeans genotyped using the Affymetrix 500K array. PC1 and PC2 refer to principal component analyses used to produce a 2D visual summary of genetic variation, corresponding to a schematic representation of the map of Europe. AL, Albania; AT, Austria; BA, Bosnia-Herzegovina; BE, Belgium; BG, Bulgaria; CH, Switzerland; CY, Cyprus; CZ, Czech Republic; DE, Germany; DK, Denmark; ES, Spain; FI, Finland; FR, France; GB, United Kingdom; GR, Greece; HR, Croatia; HU, Hungary; IE, Ireland; IT, Italy; KS, Kosovo; LV, Latvia; MK, Macedonia; NO, Norway; NL, Netherlands; PL, Poland; PT, Portugal; RO, Romania; RS, Serbia and Montenegro; RU, Russia, Sct, Scotland; SE, Sweden; SI, Slovenia; SK, Slovakia; TR, Turkey; UA, Ukraine; YG, Yugoslavia (adapted from [213]).

Admixture can be found within the French population [216]. The best method for eliminating this effect would be to use the French Basque population isolate that has shown very limited population admixture (Fig.14) [211, 216]. However, recruiting subjects from this population from Toulouse would have been complicated. Instead we aimed to firstly **limit population admixture by recruiting only subjects "claiming" to be of European French ancestry**. This was monitored by recruiting only subjects that could precise that both their maternal and paternal grandparents were of European French origin. I put emphasis on the "claiming" as we can never be certain, we have to assume that subjects recruited are accurate regarding their family history. As shown by Fig.13. there is some overlap between Spanish, Belgian and Swiss population allele frequencies with those of the French population, but we decided to eliminate subjects with these origins in order to retain the most homogeneic population as possible.

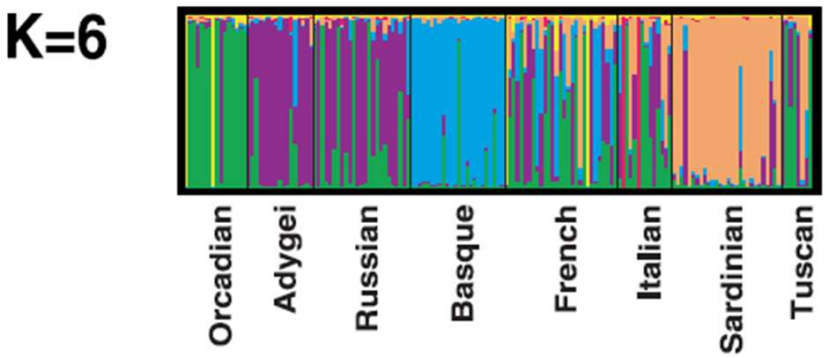


**Fig.14. Estimated Population Structures within Europe**. K represents a model population clustering system for the partition of means of allele frequencies. K1>K6:Increasing population clustering resulting in coverage of the means represented by the appearance of different colours. At K=6 the French population shows several mixed population ancestries, whereas the Basque population shows next to no admixture (adapted from [216]).

Secondly, we decided to check the extent of population stratification in our new French Caucasian cohort using multidimensional-scaling (MDS) on our final genotyping data. This method uses identity by state (IBS); calculation of the sharing of alleles between unrelated individuals without prior knowledge of pedigree structure [175, 217]. MDS then represents IBS as a position with a pre-specified dimension. The genetic background of other subjects is represented as a distance from other subjects in relation to both sharing and differences in alleles [218]. MDS plots allow visualisation of clusters of individuals with similar allele frequencies, and dispersed individual points correspond to subjects with distinct differences in

allele frequencies. This allowed us to remove individuals with outlier genetic admixture from our genotyping data analysis, reducing false positive associations.

## 3 Subject Recruitment

A part-time research assistant was responsible for the recruitment of high myopic patients 2.5 days per week from the general flow of patients in the Ophthalmology Service, CHU Purpan, Toulouse. Recruitment entailed subject agreement to participate upon signing of a consent form, a brief ophthalmology examination, completion of a personal and medical questionnaire, and finally a venous blood sample donation was taken. A new recruitment protocol based on axial length phenotypes was carefully designed in order to maximise the simplicity of the recruitment procedure for both clinicians and patients.

### 3.1 The Recruitment Protocol

A simple protocol (Annex 3 *page 236*) was established among ophthalmologists working in the service to make them familiar with the study underway and to explain their role in the selection of high myopic and control subjects for the research assistant. Patients corresponding to the criteria were then fully examined by the research assistant. 3 x 10 ml EDTA tubes of venous blood were collected from each subject once the recruitment procedure was complete.

#### 3.1.1 The Recruited Phenotypes

##### A High Myopic Subjects

Firstly, patients claiming not to have maternal and paternal grandparents of European French origin were not recruited. If the patient was not fully certain of a European French origin, it was clearly stated in the patient file (Annex 4 *page 240*) and the patient preceded the recruitment procedure.

Secondly, a medical questionnaire was completed and excluded patients that were aware of any affection by diabetes, syndromic myopia or other eye diseases including retinitis pigmentosa, retinopathy of prematurity, corneal dystrophy, keratoconus, congenital and closed-angle glaucoma and Wagner's disease. Severely anisometropic and strabismic amblyopic patients were also excluded. Only patients having undergone cataract surgery for whom we had access to pre-operative refractive values and axial length measurements were recruited.

Thirdly, it was also checked that the myopia development started before or around the age of 12 years old. Briefly the ophthalmology examination entailed measurement of refractive values using standard autorefractometry after dilation with cyclopentolate 10% (age ≤16 years) or tropicamide (≥16 years). Patients with astigmatism ≤-2 D were excluded from recruitment. Visual acuity, intraocular pressure and eye fundus examination was performed to be certain of no syndromic forms of high myopia. Axial length was evaluated by A-scan ultrasonography. A total of 3 readings were taken for each eye and the average value was recorded. **Only patients with a bilateral axial length of ≥26mm proceeded to blood sample donation and inclusion in the cohort.**

Finally, a genealogical tree including as much detail as the patient could provide on family history of myopia and high myopia was noted in the patient file, along with the patient contact details and ophthalmology information.

#### B Control Subjects

Control subjects were often ***unrelated*** friends accompanying patients being examined in the Ophthalmology Service. In addition to the exclusion criteria mentioned in *section 3.1.1 page 51*, any known first, second and third degree family history of high myopia resulted in exclusion of the subject. Subjects underwent exactly the same ophthalmology examination as high myopic patients. Subjects with **bilateral axial lengths ≥24 mm were excluded from the study. A second inclusion criteria was added of an error of refraction between $^{-}$0.5D and $^{+}$0.5D to prevent recruitment of weak-moderate hyperopic and myopic patients.**

### 3.2 Recruitment Constraints

Recruitment capacity of CHU Purpan Toulouse was overestimated. An average of only 4 high myopes was recruited per week, meaning only small cohort sizes were attained between 2007 and mid-2009. Several steps were thus required to accelerate recruitment:

1. We extended the recruitment procedure by collaborating with public hospital Ophthalmology Services throughout France (CHU Rangueil (Toulouse), Bordeaux, Montpellier, Marseille, Nice, Strasbourg, Lille, Amiens). A simple protocol and simplified version of the patient file was presented, along with a supply of blood sample equipment to each service. Afterwards, blood samples and

patient files were sent to our laboratory. Telephone conversations with the patients allowed completion of the phenotype database.

2. A press campaign was launched to incite general public volunteer high myopic and control subjects in Toulouse. This included a hospital internet page, public journal articles, radio and television edits (Annex 5 *page 243*). Volunteer phenotypes were initially analysed by telephone conversation. Corresponding volunteer phenotypes to the inclusion criteria led to a private appointment with the research assistant for collection of the full patient profile and blood donation. Volunteers were not rewarded.
3. Collaboration with the Centre National de Génotypage (CNG) in Paris was accepted to provide us with Affymetrix Array 6.0 genotyping data for 500 French control subjects (unpublished data) in the near future. Private ophthalmology services did not wish to collaborate.
4. By the beginning of 2010 a Centre d'Investigation Clinique (CIC) protocol was well established for the recruitment of high myopic and control patients in concert with the CHU Purpan Ophthalmology Service. Anonymous patient files could be obtained from the CIC to maintain our laboratory phenotype database.

## 4 Power Calculation Estimations

The power is the probability of successfully detecting a gene effect of a particular size upon elimination of type I (false-positive association) and type II (false-negative association) error rates [219]. In other words, the number of samples required to avoid claims of spurious association and to avoid neglecting true association. The statistical power to detect association between genetic variation and a phenotype is a function of several factors including [220]:

- The frequency of the risk allele (RAF).
- The Odds ratio (OR); a descriptive statistic for the effect size of the associated allele or genotype.
- Penetrance; the proportion of individuals carrying the particular real risk allele that also express the associated phenotype.
- Sample size.
- Genetic heterogeneity of the study population.

Obviously, statistical power is enhanced when RAF is higher (the risk allele has a relatively strong effect) and a large sample size from the same ethnic and geographical background is available (Fig.15.A). P-values for GWAS have to be stringent to adjust for multiple testing [164, 221, 222]. However, associations that are not statistically overwhelming ($p<0.05$) can be taken into account considering that type I error rates would be high, and that a replication step would be necessary before confirming an association [223]. An example of such a study is the GWAS on the high myopia phenotype by Nakanishi et al., 2009 [183] (*Introduction section 5.3.7 page 38*).

In common complex diseases, such as myopia, most susceptibility variants have modest effect sizes with ORs of 1.1 to 1.5 [224]. Power calculations can be implemented to give us estimates of the number of subjects required for a case-control association analysis with a reasonably high statistical significance, usually set at least 80% [225]. Free accessible on-line calculator softwares are readily used (examples, Genetic Power Calculator and CaTS; [219, 226]). Typically, it was calculated that sample sizes of approximately 1000 cases and controls were required to detect ORs of approximately 1.5 with at least 80% power using a additive model* (Fig.15.B). This was also assuming a non-stringent p-value <0.01. Thus these results, along with limited subject recruitment, suggested the requirement of an alternative to very large cohort sizes in order to increase the power of the GWAS study.

It is known that more penetrant alleles with larger effects require smaller samples [220]. Thus, **we aimed to include only the most severe axial length myopia phenotypes for the GWAS**. This was an attempt to increase the power of the study by increasing the OR, penetrance and RAF. On the other hand it was estimated that a severe high myopic phenotype inclusion would further limit subject inclusion, increasing the time taken to reach sufficient cohort sizes. Thus, in addition we also opted for a multi-step association analysis to overcome small cohort effects.

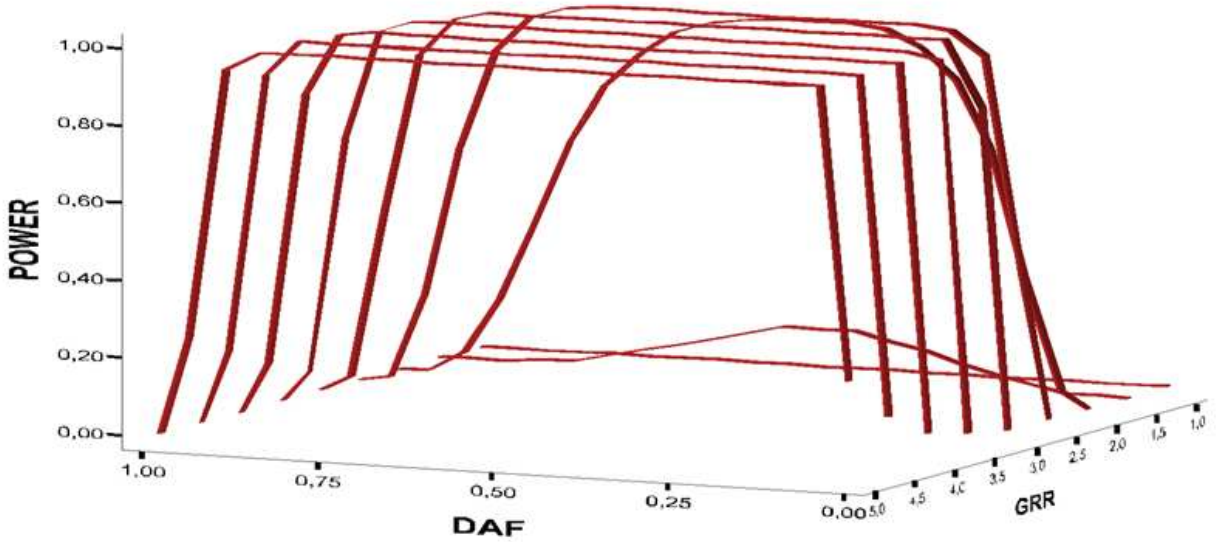


A

| Number of cases and controls (equal) | Power (%) | p-value |
|---|---|---|
| 478 | 97.45 | 0.1 |
| 607 | 94.9 | 0.05 |
| 903 | 84.61 | 0.01 |

B

**Fig.15. Power Calculations.** A: Graphical representation of how statistical power is enhanced when disease allele frequency (DAF; RAF) is higher and Genotype Relative Risk (GRR; odds ratio) has a stronger effect (calculated using Genetic Power Calculator [219]). B: Calculation of estimations of sample sizes required to detect ORs of approximately 1.5 with at least 80% power *depending on the p-value*. High myopia prevalence of 0.03 (approximately 3%) and an estimated DAF of 0.05 were taken into account in the calculations. Lowering the p-value redues the overall power of the study to detect an association, but reduces type I error rates (Genetic Power Calculator; [219]).

## 5 Multi-step Association Study Design

Well constructed multi-stage design GWAS maintain the same power as a single step GWAS, but reduce genotyping requirements [227-229]. Moreover, while genotyping and analysis of earlier recruited subjects is underway, recruitment of new subjects can continue simultaneously for the following step(s). In order to retain the power of the study, care is needed in the division of subjects between each stage and the number of markers analysed in each stage, as well as consideration into how testing for significant association between the different steps should be carried out [226, 230].

Two-stage GWAS, as introduced by Satagopan et al., 2002 [227], is based on genotyping part of the samples using a commercial high-density panel (in most cases 300 000 to a million SNPs), followed by genotyping the most significant SNPs using a customised SNP panel on the remainder of the samples. The remainder of the samples must be from a new cohort, but of same ethnic origin. A final analysis combining the information from both steps (joint analysis) is more powerful than treating the design as independent replication steps [226]. This is because joint analysis exploits the additional information about how significant the first stage associations are combined, not just the fact that they exceed independent p-value thresholds [230].

Two-stage design GWAS can be extended to multi-stage designs, with successively smaller proportions of significant SNPs being tested in new samples at each subsequent stage. Indeed, earlier studies have been conducted in this manner [231]. Hirschhorn and Daly (2005) [231] implemented the idea that a more modest threshold for 'passing' markers as significant can be used during the evaluation of the initial scan of the genome [232-234]. This requires bearing in mind that a large, but reasonably controlled number of false-positive results also pass this threshold. All markers that pass the first threshold must then be tested in a second, independent population sample. Hirschhorn and Daly (2005) declare that the second population must be similar in size, or larger than the initial population.

The second stage is carried out for only a small fraction of the markers that were contained in the initial screen, and it is also suggested that marker genotyping should be carried out using a different method, as different technologies are better suited for SNP sets of different sizes. A third stage can also be used for even greater stringency. This once again requires a new cohort for genotyping of candidate regions or genes (Fig.16).

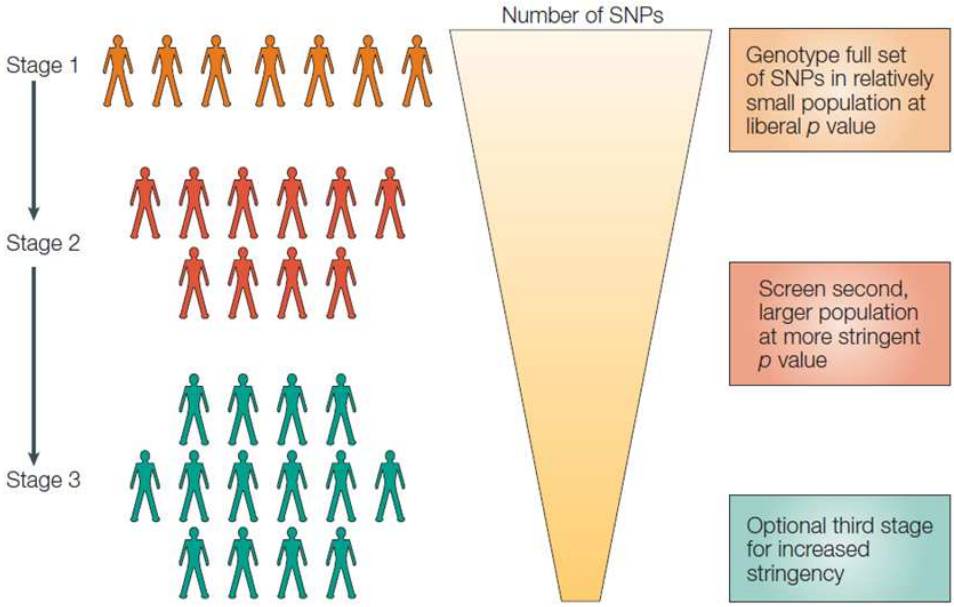


**Fig.16. Mulit-step GWAS Design** minimises sample sizes at each stage, thus genotyping costs [231].

The third step of a GWAS can be carried out by deep sequencing of genome hot spots identified in a second replication stage [230]. Due to the high cost of sequencing it is advisable to do the fine mapping first to narrow down the region or groups of genes of interest. On the other hand, next generation sequencing DNA "bar coding" and DNA pooling method costs are at the moment reducing rapidly. We may soon want to soon proceed directly to sequencing with larger chromosomal candidate regions [235].

Taking these points into consideration we opted for a **multi-step three stage design**. The first scan being a whole genome scan with a modest p-value cut-off using 192 cases and 3000 controls from the United Kingdom in the *Wellcome Trust Case Control Consortium* [180]. Cases included in this stage corresponded to the extreme axial length high myopia phenotype. The second stage will entail a customised SNP replication stage of regions identified in the first scan on a similar size cohort with either the same inclusion phenotype, or less severe high myopic phenotype (depending on recruitment progression). A more stringent p-value would be required in this step to eliminate type I and type II error rates before the final step. Finally, in the third stage we aim to deep sequence smaller candidate regions or candidate genes directly identified by: 1. The second stage hot spot regions and/or 2. Joint analysis of both the first and second stages. Candidate genes will be prioritised according to

known or potential roles in structure, development and/or function of the eye, thus myopia and high myopia development. I have summarised the stages of our current GWAS in Fig.17.

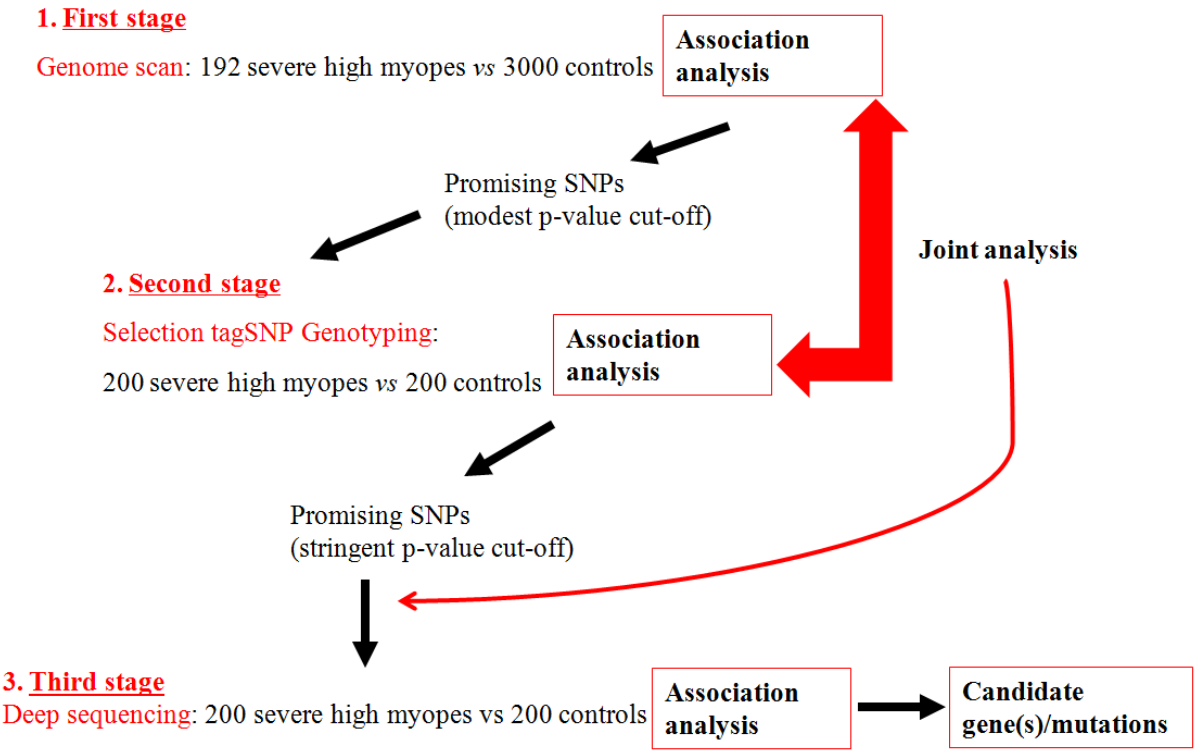


**Fig.17. Our Multi-step High Myopia GWAS Design**

## 6 DNA and Phenotype Bank

### 6.1 Blood DNA Extraction

Double stranded DNA was extracted from the venous blood samples within 72 hours following standard proteinase K and Salting out methods. Briefly, cells were lysed using 2.5% Nonident P40 (Roche, UK). Nuclei were pelleted and resuspended in 20% sodium lauroyl sarcosinate (Sigma, France) and proteinase K (Eurobio, France). This was to lyse the nuclear membranes and digest proteins. DNA released into solution was precipitated from the aqueous layer by the addition of 95% ethanol and 7.5 M ammonium acetate. DNA was then resuspended in 15mM NaCl, and finally re-precipitated by washing with 70% ethanol. DNA was resuspended and dissolved in 10 mM Tris HCl and 1 mM EDTA (TE) buffer at $^{+}4$°C. DNA concentration was only determined prior to genotyping sample preparation due to ongoing dissolving of DNA. DNA concentration was determined by measuring absorbance (OD) at 260nm in a cuvette spectrophotometer. A separate DNA sample for each patient was

also stored at ¯20°C in 95% ethanol. Patient files were transformed into anonymous database phenotypes in the laboratory.

### 6.2 Failed Blood DNA Extraction

Failure of DNA extraction from blood samples was overcome by using Oragene® saliva buccal cell DNA extraction kits (DNA Genotek, Canada). These were sent as individual kits with instructions to the subject households and returned by post (nonhazardous). The commercial DNA extraction protocol was followed. Buccal cell-extracted DNA quantity and quality was analysed by:

1. Comparing 260nm OD absorbencies to an internal blood-extracted DNA control.
2. Comparing human RNA polymerase 2 (RNA Pol II) primer PCR amplification products to an internal blood-extracted DNA control by agarose gel electrophoresis.
3. Visually checking for DNA degradation by migration of genomic DNA on 1% agarose gels.

## 7 Genotyping Technology

### 7.1 Affymetrix Array 6.0

Affymetrix® Genome-wide Human SNP Array 6.0 is a probe array containing in total approximately 1.8 million genetic variation detectors. These are split into 906 000 SNP and 946 000 CNV probes. Together, this makes this genotyping array high-throughput in terms of physical coverage of the genome, with an inter-marker spacing of 680 bp (basepairs). Approximately 482 000 SNPs are derived from the previous 500K mapping array (Affymetrix® SNP 5.0). The remaining 424 000 SNPs include new tagSNP markers derived from the International HapMap Project, better representation of SNPs on chromosomes X and Y, mitochondrial SNPs, SNPs in recombination hotspots and new SNPs added to the SNP database after completion of the Mapping 500K Array. For this project I was fortunate to negotiate a special offer for batches of genotyping to be progressively carried out (giving time for subject recruitment) by Affymetrix® at Atlas BioLabs GmbH, Berlin, Germany.

## 7.2 The Protocol

### A Preparation of DNA Samples

Genotyping required pre-preparation in the laboratory of total double-stranded genomic DNA (50 ng/µl) dissolved in TE buffer (0,1 mM EDTA, 10 mM Tris HCl, pH 8,0). In order for the acception of DNA sample genotyping, Atlas BioLabs GmbH Microarray Service Unit requested confirmation for each DNA sample that:

- An approximate 10-20 kb major genomic DNA band was observed on 1% agarose gels.
- OD 260/280 nm purity ratio was between 1.8 and 2.

This was a test for high quality non-degraded DNA. 30 µl of pre-selected DNA samples were then anonymously numbered in 96 well microtiter plates (BIORAD, Cat no. MLP9601) according to Atlas BioLab service instructions and delivered at ¯20°C.

### B The Affymetrix® Technology Protocol

The principal steps of the genotyping protocol included DNA sample preparation (fragmentation and labeling), DNA hybridisation to the chip, followed by washing and staining, and finally chip scanning (Fig.18).

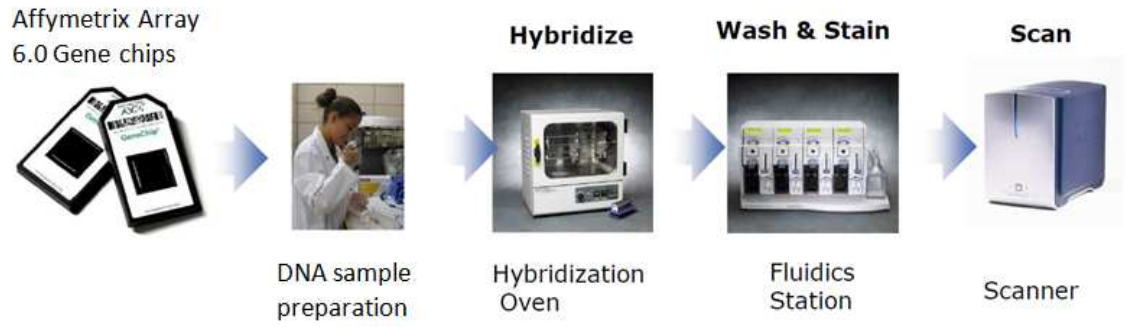


**Fig.18. Affymetrix® Array 6.0 Gene Chip Work Flow** with adapted equipment.

Briefly, the Affymetrix® Genome-Wide Human SNP Nsp/Sty 6.0 Assay Kit contained reagents for the critical steps in the assay. Atlas BioLabs GmbH Microarray Service Unit carried out 3 negative controls (water) per plate. The genomic DNA was digested with Nsp I and Sty I restriction enzymes and ligated to adaptors that recognised cohesive 4 bp overhangs.

All fragments resulting from restriction enzyme digestion, regardless of size, were substrates for adaptor ligation. A generic primer that recognised the adaptor sequence was used to amplify adaptor-ligated DNA fragments. PCR conditions have been optimised to preferentially amplify fragments in the 200 to 1 100 bp size range. PCR amplification products for each restriction enzyme digest were combined and purified using polystyrene beads. The amplified DNA was then fragmented, labeled and hybridised to the array chips for scanning. Washing steps eliminated subject DNA that did not bind to specific SNP/CNV probes. Simplified versions of the protocol are represented in Fig.19.

### C Data Handling

The Genome-Wide Human SNP Array 6.0 was used in conjunction with Affymetrix® Genotyping Console, which implements a novel genotype calling algorithm called Birdseed. Birdseed performed a multiple-chip analysis to estimate signal intensity for each allele of each SNP. Genotyping Console is designed to streamline genotyping calling and genotyping quality control. In addition to the algorithm, features include automated quality-control that sorts samples by quality-control call rate, visualisation of quality-control metrics across samples and SNP cluster visualisation. Atlas BioLabs GmbH provided us directly with quality-control call rates for all DNA samples, SNPs and CNVs.

*I attended a 4 day training scheme at the Génopole Biopuce plateforme, Rangueil, Toulouse. I genotyped 3 spurious DNA samples using Affymetrix® Array 6.0 assay protocol and adapted Affymetrix® equipment. I also learnt the global data handling methods required for data handling of raw data chip scan reads.*

## 8 Revision: Methods

For GWAS analysis we opted for a design to increase power by recruiting subjects based on their axial length phenotype, considered to be a less complex trait than the more commonly used refractive error phenotype. We also aimed to limit case-control population admixture by excluding subjects not of European French ethno-geographical origin. Inadequate recruitment, meaning smaller cohorts than anticipated, implied the requirement of using a more severe axial length phenotype and a multi-step association analysis approach to increase the power.

## 8 Récapitulatif: Les Méthodes

Pour améliorer la puissance de l'étude pangénomique, nous avons opté pour un recrutement des patients selon leur phénotype de longueur axiale, considéré comme un trait phénotypique moins complexe que celui de l'erreur de réfraction. Nous avons aussi limité la stratification de notre cohorte cas-témoin en excluant des sujets n'étant pas d'origine française européenne. Un recrutement insuffisant de myopes a imposé l'utilisation d'un phénotype de longueur axial extrême et une analyse d'association multi-étape pour augmenter la puissance de l'étude.

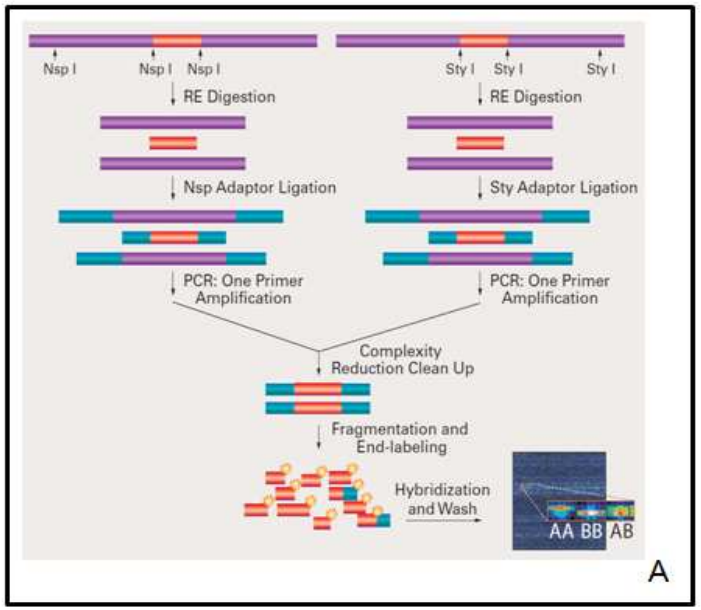


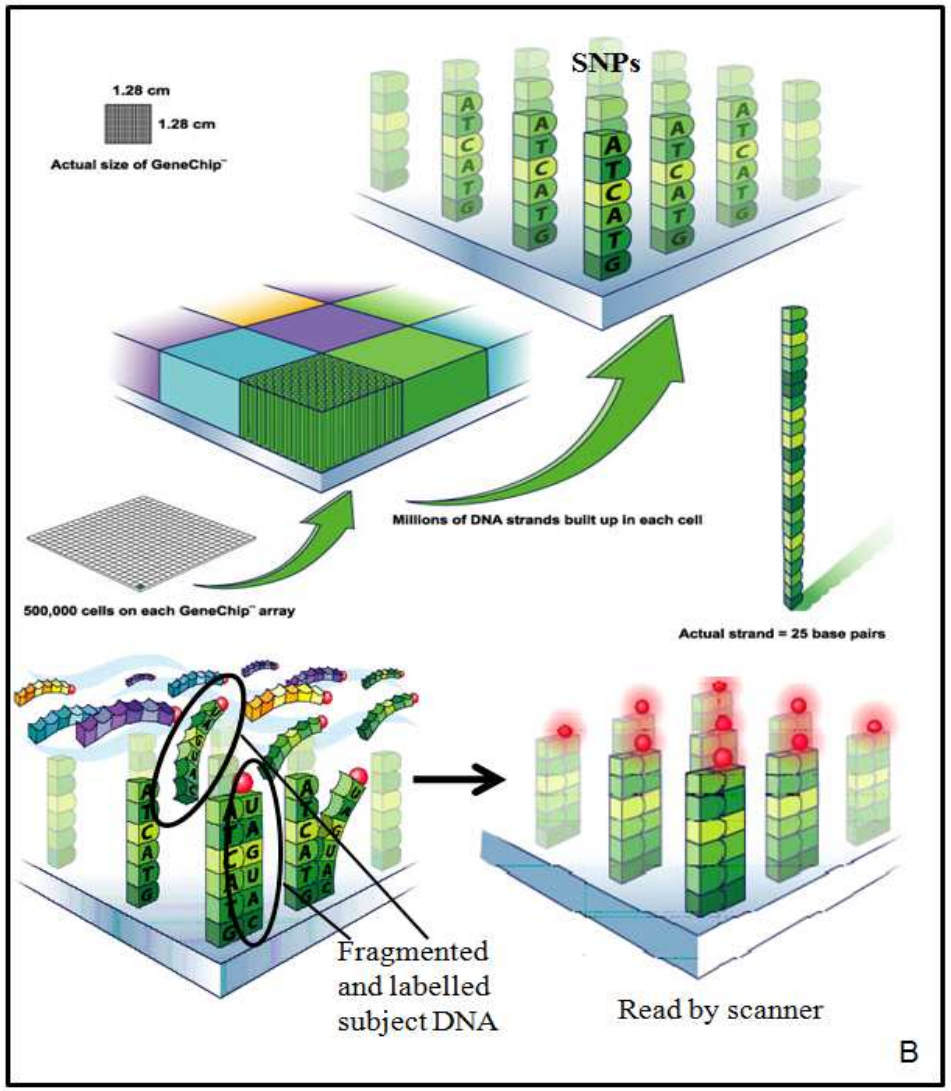


**Fig.19. Affymetix Array 6.0 Genotyping at the Molecular Level**.

A: DNA sample preparation (Index C)

B: Diagramatic representation of fragmented and labelled subject DNA specifically binding to known SNP/CNV variations, or being washed away, before scanning of the hybridised DNA fragments and transformation of signal intensity into allele frequency data. (Adapted from Index D).

# IV Results

## 1 Recruitment Outcomes

### 1.1 High Myopic Cohort

To date a total of 406 European French high myopes with an axial length ≥26mm have been recruited. *All data is represented as the average of right and left eye measurements*. Axial length ranged from 26mm to 37mm within this cohort. The mean axial length was 29.05mm. The majority of recruited subjects had an axial length between 26-27mm.

Refractive error ranged between -5D and -31D. A few (n = 7) myopes with ≥-6 D refractive errors were recruited using this axial length phenotype inclusion criteria, meaning a total of 98.3% recruited phenotypes were included in the final cohort. The mean refractive value was -12.1D. Cohort axial length and refractive error phenotypes are *summarised in Fig.20.*

The age range of the cohort was from 18 to 86 years old, but subject inclusion was based on the age of onset of myopia development, not the current subject age in order to eliminate subjects with age-related high myopic development.

The female to male ratio was 61% to 39% respectively (Fig. 20.C).

The majority (84.5%) of the cohort was recruited at Purpan Hospital, Toulouse. Subjects from the other ophthalmology services in collaboration accounted for: Rangueil (0.7%), Bordeaux (1.5%), Montpellier (1.7%), Marseille (2.5%), Nice (2.5%), Strasbourg (3.7%), Amiens (1.2%) and Lille (1.7%) of the total recruited subjects.

### 1.2 Control Cohort

Unfortunately to date only 90 control subjects have been recruited by CHU Purpan, Toulouse. Cohort axial length and refractive error data is *summarised in Fig.20*. The mean axial length was 23.07mm and mean refractive error was -0.006D. This corresponds to an emmetropic phenotype. The female to male ratio is approximately equal, 52% to 48% respectively (Fig.20.D) and the age range was similar to that of the high myopic cohort.

**Fig.20. Distribution of Axial Length and Refractive Error Phenotypes in the High Myopic and Control Cohorts**. A: Axial length. B: Refractive error. Data is an average of subject right and left eye measurements. C: Female to male ratio in the high myopic cohort; 0.61:0.39 respectively. D: Female to male ratio in the control cohort; 0.52:0.48 respectively.

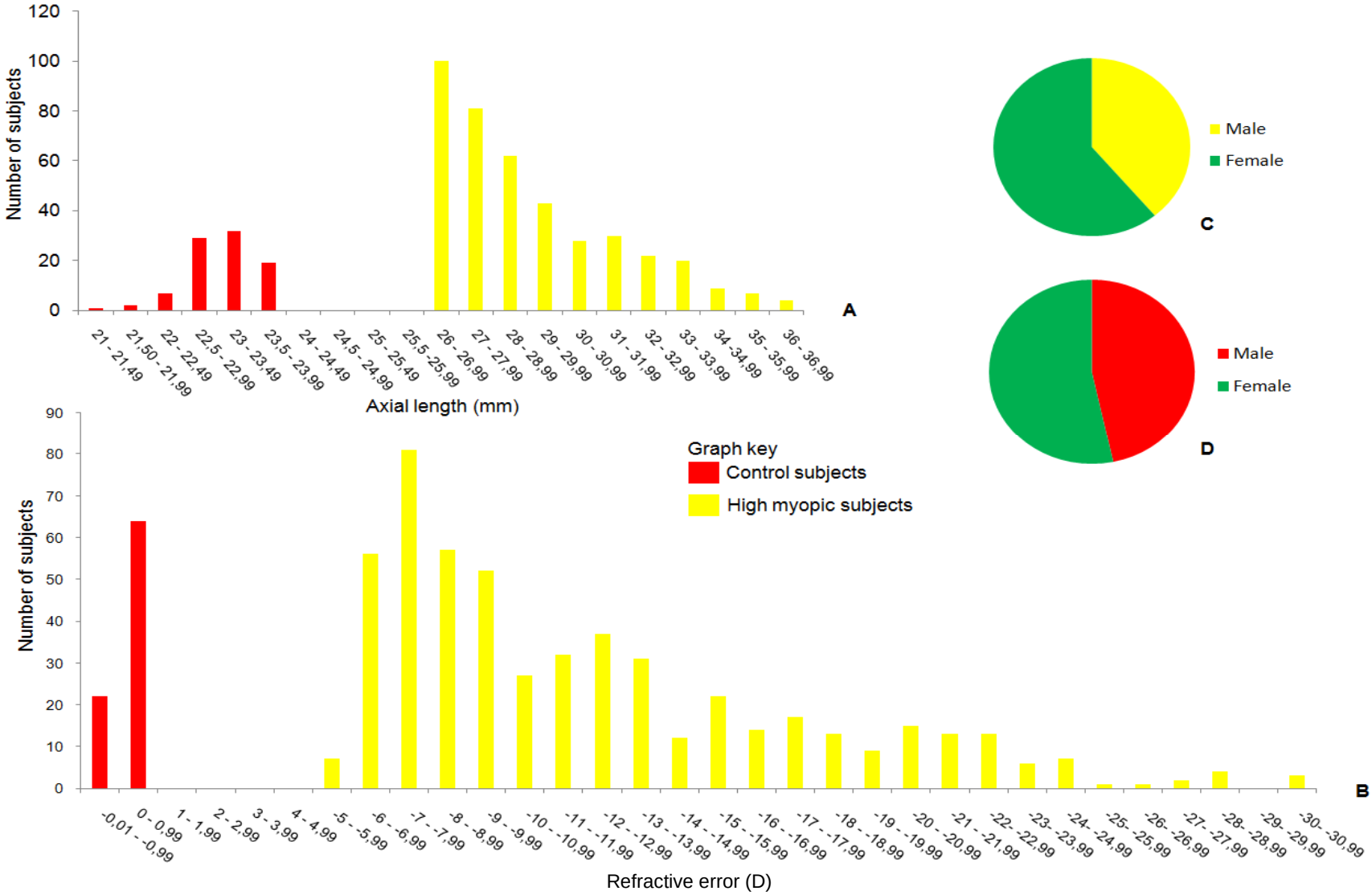

### 1.3 DNA Bank

The laboratory owns genomic DNA for all subjects in these cohorts. Only 0.6% of high myopic subject DNA was extracted using saliva kits, the remainder by blood. An average final DNA concentration of 300ng/µl was extracted from blood samples. Final DNA concentration from saliva kits was found to be approximately 3-fold lower (~100ng/µl) than DNA extracted from blood. This concentration is still largely adequate for genotyping methods. UV visualisation of human RNA Pol II PCR amplification products and genomic DNA migration on 1% agarose gel showed both efficient PCR amplification and little degradation of saliva-extracted DNA (data not shown). On the other hand, external work has shown subject-specific DNA degradation by DNA extracted from saliva buccal cells, resulting in the suggestion of DNA degradation screening before use in high-throughput genotyping methods [236]. Furthermore, buccal cell aneuploidy* related to age and lifestyle environmental factors [230, 237] could influence CNV genotyping results (no observation). To date, our saliva-extracted DNA samples haven not been genotyped, and will only be genotyped in the future if the cohort is lacking in blood- extracted DNA.

### 1.4 Extreme Axial Length High Myopic Cohort

Within our high myopic cohort, 190 subjects had an axial length exceeding 28.5mm, and 280 subjects with a refractive error below -10D. Thus, a first set of subjects were genotyped (1st stage) based on the inclusion criteria set at an axial length ≥27.5 mm and refractive error ≤-10D. The corresponsing axial length and refractive error phenotypes of this extreme high myopic cohort are *summarised in table 3*. Female to male partition was however not equal (64% and 36% respectively). Only extreme cases recruited at CHU Purpan, Toulouse, were genotyped in this group. Control genotypes will be supplied later by the CNG to perform the association analysis.

| Phenotype | Mean | Standard deviation |
|---|---|---|
| Axial length (mm) | 30.17 | 2.32 |
| Refractive error (D) | -15.43 | 5.05 |

**Table 3. Axial Length and Refractive Error Phenotypes of the First 192 Extreme High Myopes Genotyped**. Data represents the mean of subject right and left eye measurements.

## 2 Genotyping of the First 192 Extreme High Myopes

The first 192 subjects with the most extreme axial length phenotypes have been genotyped. This is stage 1 of our GWAS.

### 2.1 Genotype Filtering Procedures

Raw genotyping data underwent a series of SNP, CNV and DNA sample filtering procedures carried out by Dr Meng and Dr Macé (biostatisticians) in the laboratory. This resulted in elimination of SNPs, CNVs and subject samples at several stages.

#### A SNPs, CNVs and DNA Sample Quality-Control

Three of the 192 DNA samples were below the Birdseed quality-control call rate threshold of ≥86% and were thus excluded from further analysis. Otherwise, the remaining samples had a mean call rate of 99.65%. SNPs and CNVs with a quality-control call rate threshold of ≤97% were eliminated.

#### B DNA Sample Filtering

A sample DNA gender check tested that subject DNA sex was in agreement between genotyping results and initial gender phenotype status. A Kinship examination eliminated closely shared extended LD blocks between individuals that suggested subjects were related. One subject was found to be a sibling of another, resulting in elimination of one of these subjects.

#### C SNP Filtering

The following SNPs were removed from analysis:

- Monomorphic SNPs[*].
- X and Y chromosome SNPs.
- SNPs with extreme minor allele frequencies of (<0.01).
- SNPs with Hardy Weinberg equilibrium (HWE) $p<1 \times 10^{-4}$. The HWE principle considers that in large randomly mating populations, allele genotype frequencies should remain constant [238]. Thus, SNP allele frequencies that showed deviation

from HWE were removed. This could be regarded as an internal control test [239]. HWE was calculated using the Fisher's exact test.

### D CNV Filtering:

Quanti-SNP software assigned allele frequencies to SNPs within CNVs. Afterwards the following CNVs were removed from analysis:

- CNVs that overlapped chromosome centromeres.
- Different CNVs that overlapped (forming clusters) by 70% with each other were considered as one CNV.
- DNA samples with more than 20 CNVs.

## 2.2 Population Stratification

Preliminary population stratification was analysed among the 192 extreme subjects using the MDS method by Dr Meng in the laboratory (Fig.21). This resulted in elimination of a further 6 individuals in order to maintain a homogenic population, limiting admixture but unfortunately reducing the total number of subjects analysed. Unsurprisingly, one outlier was found to originate from the Basque population isolate.

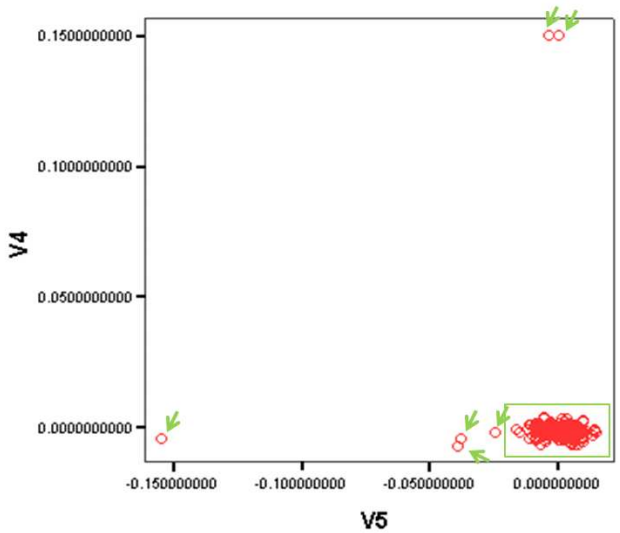


**Fig.21. MDS Plot of Extreme High Myopic Cohort** (192 subjects). A cluster of subjects with similar genetic background (allele frequencies) can be visualised (green box). These individuals are from the same population. Green arrows represent outlier subjects with different allele frequencies to subjects in the cluster. These subjects are from different population admixture and were eliminated from the study. V4 and V5 correspond to the two main dimensions used to form a presentable visualisation of the cluster and outliers.

## 2.3 Overall Genotyping Outcomes

Filtering resulted in genotype data for a totoal of 182 extreme high myopes with 704, 325 SNPs. This represents 95% of total initial subject DNA samples and 77% of total inititial SNPs that were genotyped. 937 CNVs were identified within the 182 extreme high myopes, of which 62 have not been annotated by Affymetrix®, implying these could be *de novo* CNVs. 10% of the extreme high myopic subjects harbored these CNVs.

# V Perspectives

## 1 Completion of All GWAS Stages

A second replication stage will be carried out to genotype the "top" SNPs from this first stage. Custom SNP genotyping using Illumina BeadXpress® Veracode technology at Génopole, Toulouse, will be used on cohorts of approximately 200 high myopes (axial length ≥26mm) and 200 controls. To increase coverage of candidate regions/genes, tagSNPs will be selected in LD blocks. A case-control association analysis for stage 2 genotyping data alone, as well as a joint association analysis of stages 1 and 2 data, will be performed; both with a more stringent p-value to select associated SNPs. Associated SNPs should indicate specific candidate region(s) and/or will be located within or in proximity to associated genes. Candidate regions and/or genes will then proceed to a final deep sequencing stage. Sequencing will also be carried out at Génopole, Toulouse, using the Roche 454 GS Flx sequencer. We aim to sequence 200 high myopes (axial length ≥26mm) and 200 controls. Cohort sizes will however depend on recruitment progression. Dr Meng (biostatistician) in the laboratory will work on the statistical association analyses.

Given the possibility that candidate gene expression in human eye tissues could be unknown, this experimental data would be required to confirm that the candidate gene could play a structural and/or functional role(s) in the eye, thus a role in human myopia development [177, 178]. Candidate regions and/or candidate genes identified will also be compared to candidate genes already identified in previous genome scans for myopia and high myopia, and genes identified as potentially playing a role in the development of myopia in animal models. Finally, candidate gene interacting partners will be elucidated in order to decipher the gene networks at play. This is known as data mining and is based on the use of free on-line software that combines all literature observations, for example Ensembl, Gene Ontology [240] and Human Interactome [241]. From here, we could predict roles for candidate gene(s) identified in our GWAS in myopia development.

## 2 Confirmation of a Role for GWAS Candidate Genes in Human Myopia Development

Firstly, our genotype data will be included in other myopia and high myopia GWAS in collaboration with other laboratories that posses human cohorts recruited in terms of their refractive error phenotypes. Meta-analyses will confirm or reject the implication of the same gene(s) in myopia development in different populations, indicating the same or different molecular mechanisms underlying refractive error phenotypes.

Secondly, after confirmed replication studies an animal gene knock-out or knock-in model of the candidate gene(s) could be developed. Likewise, analysis of the changes in expression of the candidate gene(s) identified in our study in eye tissues of form-deprived or defocused myopic animal models could be carried out. On the whole, such animal models would allow the comparison of structural eye phenotypes (axial length, sclera thickness…) and gene expression changes (upregulation, downregulation) with normal eye tissues in an attempt to determine a mechanistic role of the candidate gene(s) in myopia development.

## 3 Conclusion: Project 1

To overcome the problem of difficult familial subject recruitment and the high heterogeneity underlying the high myopic phenotype, previous genome scans were replaced by a new whole genome SNP population-based case-control association analysis. This study design takes into account LD, a more powerful method for detecting multiple small effects in complex diseases. A new recruitment scheme was launched to include unrelated subjects based on axial length phenotypes, potentially reducing the number of genes underlying the phenotype and reducing the environmental influences compared to the more complex refractive error trait. Genetic admixture of the population was limited by excluding subjects not of French Caucasian origin. Unfortunately we overestimated subject recruitment capacity, thus to overcome the problem of a small cohort effect power calculations indicated the requirement to carry out a multi-step study. The first step was based on an initial whole genome scan of subjects with a severe axial length phenotype and with a modest p-value threshold. Today subject recruitment is ongoing to complete the next two stages in order to identify candidate chromosomal regions and/or genes. Replication of the associated candidate gene(s) and or mutation(s) will be required in different ethno-geographic populations to

confirm a role in myopia development. The identification of genes involved in myopia development is the first step in the comprehension of the physiopathology of the disease, and also in the development of new therapeutic treatments for severe vision threatening myopias that today can only be improved by wearing spectacles, contact lenses and intra-ocular lens implant surgery.

## 1 Conclusion: Projet 1

Pour surmonter les problèmes de recrutement des cas familiaux apparentés et l'hétérogénéité élevée du phénotype de la myopie forte, les anciennes analyses de criblage génomique ont été remplacées par une nouvelle étude d'association pangénomique sur une population cas-témoin non-apparenté en utilisant des marqueurs SNP. Ceci prend en compte le LD, une méthode plus puissante pour détecter plusieurs effets modestes dans des maladies complexes. Un nouveau recrutement basé sur le phénotype de la longueur axiale à été constitué en comparaison au phénotype plus complexe d'erreur de réfraction, **permettant** de réduire potentiellement le nombre de gènes causants et les influences environnementales. La stratification de la cohorte a été limitée en excluant des sujets n'étant pas d'origine caucasienne. Malheureusement, nous avons surestimé les capacités de recrutement. Les résultats de calculs de puissance ont donc indiqué le besoin d'effectuer une analyse d'association multi-étape pour contrer la problématique posé par une petite cohorte. Ceci implique un premier scan pangénomique dans une cohorte avec un phénotype de longueur d'axial extrême, ainsi qu'un seuil de valeur de p modeste. A ce jour un recrutement est en cours pour compléter toutes les étapes de l'étude. Finalement, une réplication d'un ou plusieurs gènes ou d'une ou plusieurs mutations associées serait nécessaire dans d'autres populations d'origines différentes afin de confirmer un rôle dans le développement de la myopie forte. L'identification des gènes impliqués dans le développement de la myopie est un premier pas pour comprendre la physiopathologie de la maladie, mais également pour le développement de traitements thérapeutiques pour les myopies extrêmes menaçant la vision, qui sont à ce jour corrigées par le port de lunettes, lentilles ou par des implants intraoculaires.

# VI Myopia and Corneal Refractive Surgery

Nowadays refractive errors can be improved by refractive error surgeries. Corneal refractive surgery increases the quality of life of patients without actually curing the axial length defect. However, this requires altering the corneal shape which damages the corneal stromal and epithelial tissues. This can is some cases lead to corneal stromal opacities, known as ‘haze”, that reduce clear vision.

## 1 Different Corneal Refractive Surgery Techniques

All techniques function by flattening the corneal curvature, thus modifying the refractive index of the cornea, and in turn improving the overall refractive error. Nowadays surgical techniques are often based on the use of excimer lasers (focused beams of ultraviolet radiation) to ablate corneal stromal tissue.

### 1.1 Flap Procedures

A flap in the corneal surface creates a hinged door effect so that corneal stromal tissue can be exposed. Stromal tissue can then be removed using either a microkeratome* (more traditional surgery known as automated lamellar keratoplasty (ALK)) or by using an excimer laser (surgery known as laser assisted in-situ keratomileusis (LASIK)) (Fig.22.A). Laser-assisted sub-epithelial keratectomy (LASEK) functions by alcohol solution weakening of some of the outer epithelial cells in order to create an outer epithelial cell flap, followed by excimer laser stromal ablation. Afterwards, the flap can then be repositioned in its original place for wound healing.

### 1.2 Incision Procedure

This technique is based on the use of spoke-shaped incisions made into the cornea (Radial keratotomy (RK)) (Fig.22.B). This method has now been largely replaced by excimer laser methods.

### 1.3 Surface Procedures

Unlike the other techniques that require physical contact with the corneal tissue, this method consists of direct ablation of anterior stromal segments without any direct contact with the cornea. An example is photorefractive keratectomy (PRK) that functions by excimer laser removal of some of the outer epithelial cells so that small amounts of stromal tissue can then be ablated. C-Ten (customized transepithelial non-contact ablation) is a refinement of LASEK and PRK. It is the newest and the fastest laser treatment. “C” for “customised” refers to the individualisation of the treatment for each patient, conforming to each individual’s requirements determined by the topography of the corneal surface, the extent of the correction, pupillary size and the patient’s lifestyle requirements. “Ten” for transepithelial non-contact. This refers to the non-contact ablation of the epithelial layer (Fig.22.C). After the laser treatment the epithelium regenerates within a few days, all the while being protected by a contact lens.

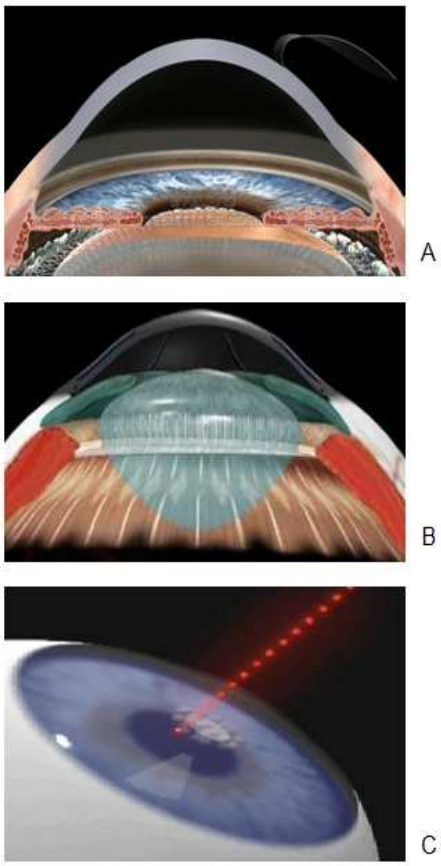


**Fig.22. The Different Techniques of Corneal Refractive Surgery.** A: The flap procedure. B: The incision procedure; creation of radial incisions in the cornea. C: The surface procedure; direct ablation of anterior stromal segments without any eye contact (A: Index E. B: Index F. C: Index G).

## 2 Secondary Complications

Based on a worldwide literature review on the quality of life and patient satisfaction following myopia LASIK surgery, an average of 95.4% of patients are satisfied with their outcome [242]. Although the risk of complications is decreasing compared to earlier days, there is still a small chance for serious patient-specific problems following corneal refractive surgery. The ability to anticipate confounding biological responses at the level of the individual patient remains limited. In some cases, a predisposition to mechanical instability or abnormal regulation of corneal healing can lead to serious complications such as keratectasia* or loss of corneal transparency, known as **haze** or **opacity** (Fig.23.B) [243]. Nowadays a minorority of myopic patients, less than 3.5% (average 1.75%) undergoing PRK develop significant late-onset clinical corneal opacities that result in permanent visual defects [244, 245]. Other symptoms, such as corneal starbursts (Fig.23.C), double-vision, cornea neovascularisation and dry-eye syndrome* can develop following corneal refractive surgery.

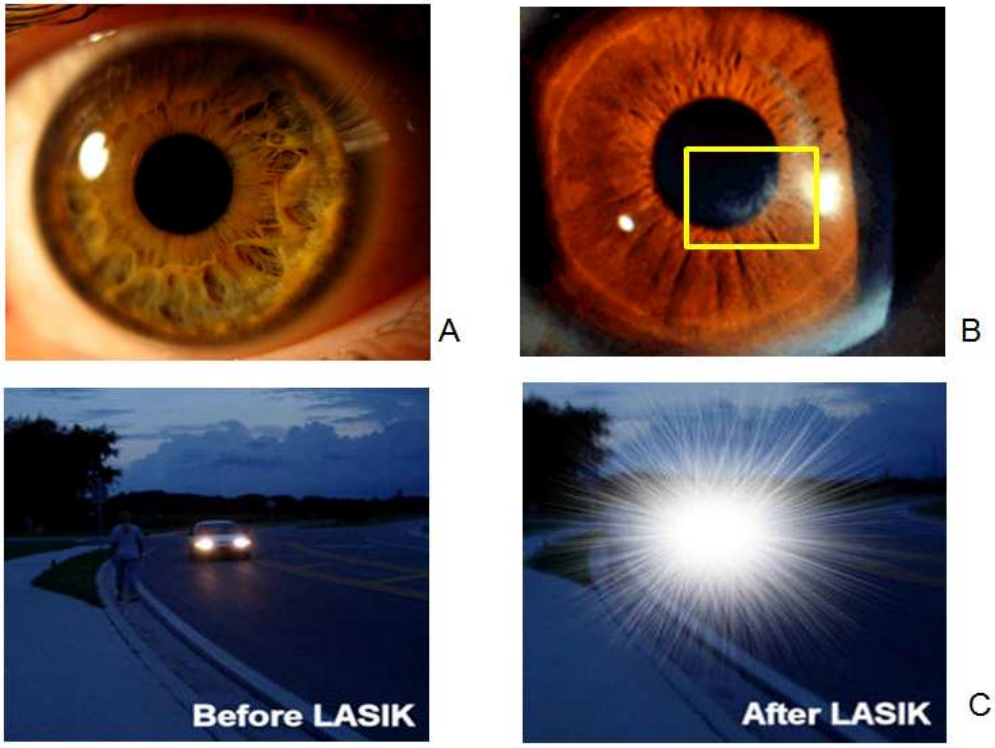


**Fig.23. Secondary Complications following Corneal Refractive Surgery.** A: Normal cornea. B: Corneal opacity formation (Index H)**. C:** Corneal starburst effect: blurred vision and patterns around lights in dim light following LASIK (Index I).

## 3 Current Research on Corneal Opacity Formation

Animal models have been largely based on the capacity of haze formation following corneal refractive surgery. It has been shown that higher rates of haze formation is manifested by rabbits having undergone PRK compared to LASIK for equivalent high myopia [243, 246]. This is due to highly invasive PRK damage to the epithelium and stromal layers, whereas LASIK leaves these structures relatively undisturbed apart from at the flap margin. Refractive surgery nowadays is rarely used to treat high myopic patients as the required corneal remodelling amplifies the stromal damage, and thus the wound healing response, accounting for higher rates of haze [244].

There is also a research area based on haze formation following epithelial scraping/rubing and more severe alkali burns, traumas (lacerations), and bacterial, viral or fungal infections (Kerititis). These injuries result in more acute corneal wound responses and hypertrophic scarring (Fig.24). Tissue scarring, which in some cases can lead to blindness, remains a major challenge for both clinicians and researchers at the cellular level. A worrying consequence is the lack of efficient therapies to treat and to prevent the condition. Once a corneal scar develops, surgical management remains the only option for visual rehabilitation, the definitive treatment being corneal transplantation. As our understanding of corneal wound healing and haze formation improves, so will our ability to offer interventions for preventing and restoring corneal haze. The main goal of research in this area is to improve the understanding of the biomechanical and wound healing pathways at play in the corneal wound response [243].

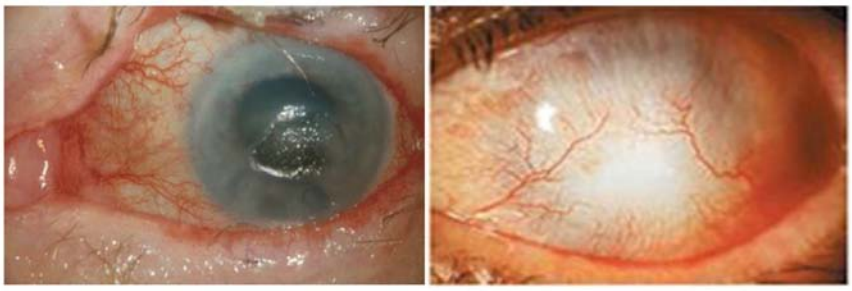

**Fig.24. Corneal Scarring** due to A: Herpes zoster keratitis viral infection (Index J). B: Alkali burning (Index K).

# The Identification of Stromal Cells Expressing Stem Cell Markers throughout *in vivo* Adult Murine Corneal Wound Healing

# I Introduction

## The Cornea: A Transparent Window

In all species the cornea is a highly specialised transparent structure located at the anterior most surface of the eye giving a window to the outer world.

### 1 The Cornea: Structure, Function and Development

#### 1.1 Gross Anatomy

The cornea is an external transparent dome-shaped projection from the spherical scleral eyeball tissue (Fig.1.A). The thickness of the central human cornea is 0.52mm and increases toward the periphery. The diameter of the adult cornea is about 11mm, being slightly larger horizontally than vertically. In contrast, many animal corneas have a similar thickness over a considerable area (i.e. the mouse). The relative size of the cornea varies among animal species depending on the animal size (increase size, increase corneal size) and environmental conditions, being generally larger in nocturnal animals than those active in daylight (i.e. the mouse; note the similar eye ball:corneal size ratio) (Table 1) [247]. The cornea receives nutrients and oxygen via diffusion from the tear fluid on the outside, and from the aqueous humour on the inside [248].

| **Species** | **Diameter** (mm) | | **Corneal thickness** (mm) |
|---|---|---|---|
| | **Eye ball** | **Cornea** | |
| Man | 24 | 11 | 0.52 |
| Cynomolgus monkey | 18 | 9 | 0.4 |
| Rabbit | 17 | 12 | 0.4 |
| Rat | 6 | 5.5 | 0.2 |
| **Mouse** | **3.5** | **3** | **0.15** |

**Table 1**. Relative ocular and corneal dimensions of different speices (adapted from [247]).

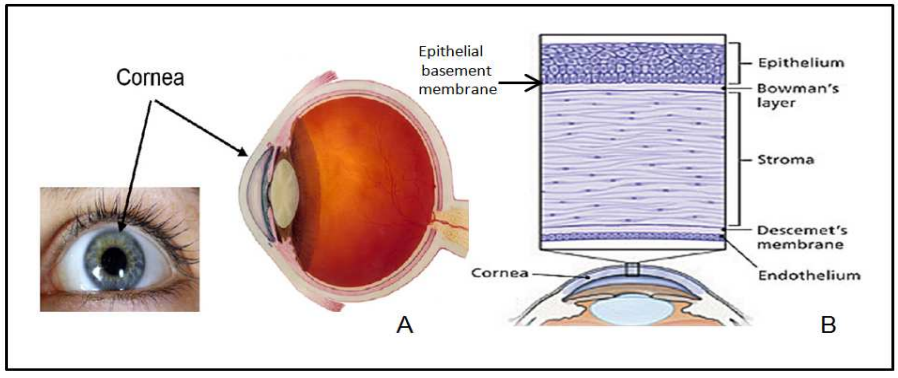


**Fig.1.**A: **The Transparent Corneal Structure** located at the most anterior surface of the eye (index A). B: A zoom on the epithelial, stromal and endothelial cell layers of the human cornea.

Functional and mechanical structural aspects of the human cornea have been studied in animal corneas and findings can be extended to all other species [247]. Otherwise, known differences are stated.

### 1.2 The Function of the Cornea

The cornea provides two-thirds of the optical power of the eye [249]. The lack of blood elements in the central corneal tissue allows light to pass through, be refracted and inverted upon accompanying action of the lens, and focused on the retina to form clear vision. The cornea also has a protective role by acting as an external barrier to infectious agents. Thin nerve leashes are present in the corneal epithelial layer that contain nociceptors that are sensitive to touch, temperature and chemicals; touching the cornea causes an involuntary reflex to close the eyelid. The cornea is one of the most densely innervated organs of the human body [250], and is considered to have 3–400 times more nerve endings than the skin epidermis (outer skin cell layer). Together the transparency, avascularity and the presence of resident immune cells [251] that promote immunologic privilege* [252] makes the cornea an original and well-adapted tissue for clear vision.

### 1.3 Mechanical Structure of the Cornea

The cornea is a simple, but good model example of an organ composed of multiple cell types that are required to cooperatively maintain corneal structural integrity, transparency and prevent invasion from outside pathogens. The cornea is composed of three main cell layers (Fig.1.B):

1. An outermost squamous tight stratified **epithelium** which is in contact with the tear film. This is composed of 3-7 cell layers depending on the species [253]. The mouse corneal epithelium is 3-6 cells in thickness [254], wheras it is is 5-7 cells in thickness in humans [255]. The epithelium provides the external barrier to the outside.
2. The innermost layer is a mono-**endothelial** cell layer. This is required for fluid transport pumping out of the stroma and into the aqueous humour. Note that these are non-vascular endothelial cells.
3. The intermediate layer is the corneal **stroma**. This accounts for 90% of the total corneal thickness [247]. The corneas combination of strength and transparency is due

to the highly organised micro- and nano-scale structure of the stroma [253, 256]. On the micro-scale, the stroma is comprised of chiral 250-400 lamellae of heterodimeric collagen fibrils in majority of type I, V and VI collagens [257-259]. These lamellae bundles are arranged in parallel and tightly packed. Nano-scale hydrophilic proteoglycans surround the collagen fibrils. These impose a uniform spacing of collagen fibres, giving the cornea the capacity to reduce light scatter and promote corneal transparency [260]. Keratoan sulphate and dermatan sulphate proteoglycans are the predominant proteoglycans in the human stroma. These belong to the family of small leucine-rich repeats and contain core proteins lumican, keratocan, mimican and decorin [259]. Nerves innverate the peripheral stroma from the cornea-scleral border, and then extend into the central stroma in decreasing branch sizes, where the majority then penetrate into the corneal epithelium [261]. Finally, **adult keratocyte cells** are sandwiched between the stromal lamellae, completing the molecular source of what we call the corneal stromal ECM [262] (Fig.2.A). The biochemical stromal structure and function is considered very similar across different species [263].

**The Bowman's layer** is a smooth collagen adhesion layer found below the epithelial basement membrane in the superficial stroma. It is considered important for additional structural support of the outer epithelial cell layer via attachment of basal epithelial cells through cell-matrix adhesion structures called hemidesmosomes [264]. More recent debates imply more important roles for this layer in epithelial-stromal cell interactions [265]. In humans the Bowman's layer is composed of condensely packed type V collagen fibres. This layer is not to be mistaken as a thicker epithelial basement membrane; even though collagen compositions and functions appear similar between the two structures, it is a separate and additional layer to the basement membrane. It is absent from tadpole and carnivore corneas. It is thicker in higher mammals (cat, cattle, human) and thinner in lower mammals (rat, guinea pig, mouse,rabbit) [266].

**The Descemet's membrane** is named after the French physician Jean Descemet (1732-1810) and can be considered as an exaggerated basement membrane of the corneal endothelium that retains endothelial cell structure and organisation [267]. The Descemet's membrane is composed of a different collagen type to the normal stroma, notably type III

collagen [268].

### 1.4 The Adult Keratocyte Cell

Adult keratocytes are cranial neural crest mesenchymal-derived fibroblast cells that are flattened and sparsely arranged in the normal adult corneal stroma [262]. They form an interconnected cellular network with one another through dendritic processes* that form gap junctions* (Fig.2.B) [269]. Cell activity coordination is via these communications. It is even said that keratocyte cells form a syncytium (a large cytoplasmic structure with many nuclei) [270]. Keratocyte cells are poorly supplied with organelles and have small elongated nuclei, but contain rough endoplasmic reticulum and golgi apparatus, characterising a slow turnover (**quiescent**) with an active protein synthesis function [269]. Lumican, keratocan and mimican mRNA has been localised in keratocytes, giving these cells the role of stromal ECM collagen and proteoglycan synthesis and maintenance [271]. Keratocyte cells also show high expression of water-soluble crystalline proteins which are fundamental for the transparency of the cornea [272]. In the mammalian cornea, these proteins include aldehyde dehydrogenase isozymes [273], the prominent isoforms being ALDH1A1 and ALDH3A1 [274]. These enzymes eliminate insoluble protein aldehyde groups, minimising fluctuations in refractive indexes within keratocyte cell cytoplasms so that they match the refractive index of the surrounding ECM, thus rendering the cornea transparent [272].

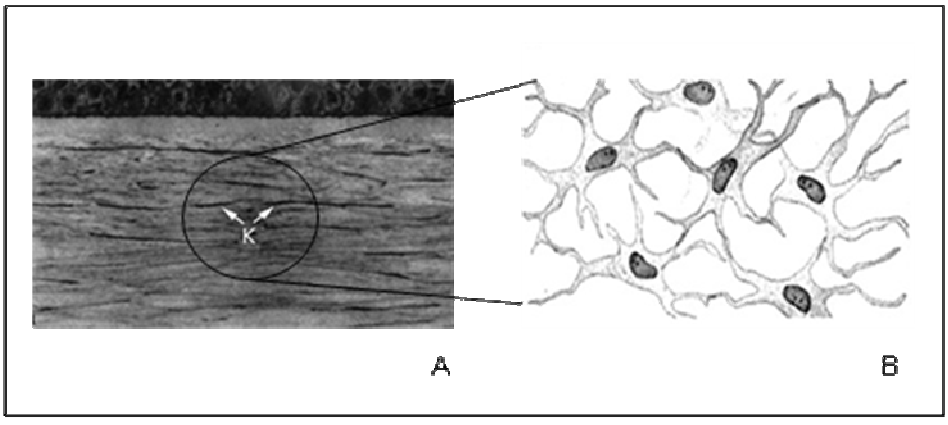


**Fig.2.**A: *In vivo* confocal microscopy of a section of a human cornea (arrowheads: keratocyte cells) (adapted from [275]). B: Schematic representation of the human keratocyte network (adapted from [275]).

### 1.5 Embryonic Development of the Cornea

Embryonic eye development is throughout early developmental stages, with corneal

development also starting within these early stages of development. I have summarised vertebrate corneal development with references to the different stages of chick corneal development as this is the most studied embryonic corneal development model [262].

Initally, the cornea is comprised of a surface ectoderm overlying the lens vesicle. Subsequently, at embryonic day 3 (E3) in the chick, separation of the surface ectoderm from the lens gives rise to a primitive epithelial cell layer that synthesises a primary stroma (loosely arranged collagen fibrils) [276, 277]. This is followed by two mesectoderm neural crest-derived mesenchymal cell migration waves between the ectoderm and the lens. The first wave forms the endothelial cell layer, and the second wave at E4 gives rise to the stromal keratocyte cell population. **Note that both endothelial and stromal keratocyte cells are neural crest-derived mesenchymal cells, whereas epithelial cells are of surface ectoderm origin, thus two different cell lineages** [278, 279].

By E6 in chick embryos, keratocyte stromal cells begin to secrete ECM components of collagen and proteoglycans [262, 280-283]. Between this stage and eyelid opening, the stroma dehydrates, thus becoming thinner and transparent. Keratcoyte cell density declines and they resume their adult flattened cell morphology, and form an interconnected keratocyte cell network. They enter a quiescent state, residing in $G_0$ phase. However, note that keratocyte cells *do not complete* terminal differentiation. Finally, the eyelids fuse in front of the eye, cutting off the epithelial cornea surface's amniotic fluid supply before birth [284, 285]. This final development stage is the same for all species. Vertebrate cornea development is schematically summarised *in Fig.3 page 83*.

In humans, corneal development starts as early as the $6^{th}$ week of early-stage embryonic development, with the neural crest-derived mesenchymal cell waves occurring in the $7^{th}$ embryonic week of development [262]. In rodents however, there is only a single neural crest-derived mesenchymal cell migration influx that forms the endothelial and stromal cells, but the structural and cellular outcomes are identical [286]. Human stromal cells begin to secrete ECM components in the $8^{th}$ week in human embryonic development, with eyelid fusion between 3-6 months, meaning that the corneal stroma is completely developed pre-natally [284, 285].

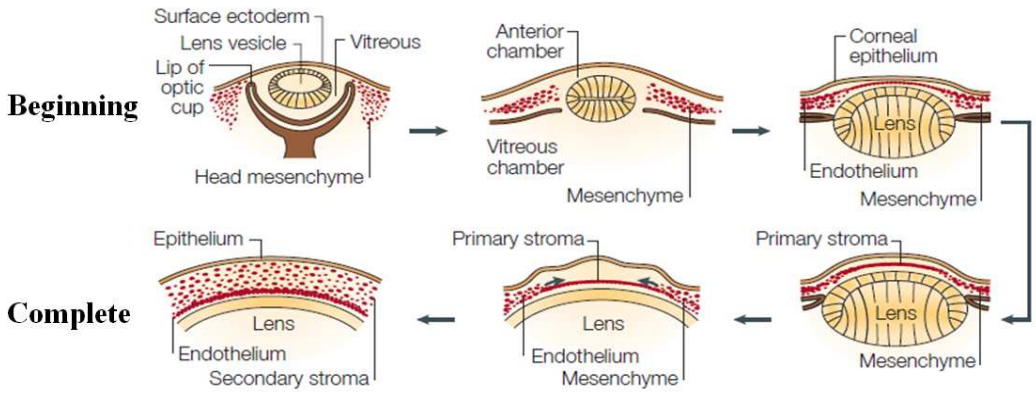


**Fig.3. Development of the Vertebrate Cornea**. The cornea begins to develop when the surface ectoderm closes and after lens vesicle detachment from the surface ectoderm. Afterwards, neural crest mesenchymal cells invade the provisional stromal ECM and form the corneal stroma (adapted from [287]).

## 2 Normal Adult Corneal Renewal

Tissue-derived stem cell populations have now been characterised in many adult tissues. They are able to maintain and regenerate a given tissue for the organism's lifetime. However, before we start discussing adult corneal tissue renewal, we need a set of properties so we can distinguish stem cells from normal somatic cells (definitions reviewed in [288, 289]).

### 2.1 Stem Cell Definitions

- **Stem cell:** Can be viewed as a cell that can self-renew many times without executing certain gene programs associated with a special function.
- **Self-renewal**: At least one daughter cell remains a stem cell.
- **Slow cell cycle:** Most of the time stem cells are in the $G_0$ growth arrested state but can easily resume the cell cycle in demand to give rise to differentiating and highly proliferative progeny.
- **Stem cell niche:** Stem cells usually require a specific micro-environment that provides external factors required for maintaining "stemness".
- **Stem cell markers:** A combination of negative expression of known differentiated stem cell markers and positive expression of known undifferentiated markers is used to experimentally identify stem cells. For examples see *table 2 page 87*.

- **Multipotent**: The ability to differentiate into different cells of the same tissue of embryonic origin. These can be judged as pre-determined cell types.
- **Pluripotent**: Ability to differentiate into any cell type, not just those of their tissue of origin.
- **Progenitor cells:** Similar to stem cells, but their progeny in most cases does not renew and the cell population becomes terminally differentiated after a limited number of cell divisions. In terms of stem and progenitor cells, both can be expanded under correct circumstances.

## 2.2 Corneal Epithelium Turnover

A high rate of adult epithelial cell renewal is required to maintain a stable and continuous contact of the corneal outer layer with the tear film layer to assure a smooth refractive surface. Renewal is also required to sustain a tight barrier integrity, necessary for preventing infiltration by pathogens and fluid loss [254]. Like the skin, corneal epithelium turnover is sustained upon a fine balance between cell loss by desquamation at the outer most surface, and cell replacement by migration and proliferation of epithelial stem cells [290-292]. It is assumed that all mammalian species normal epithelial surface turnover is completed within 7 to 14 days [291].

### 2.2.1 Corneal Epithelial Stem Cells

#### A Populations and Localisations

The limbal region is the tissue in the cornea-scleral transition zone (Fig.4.A.B). In the limbus the epithelial tissue thickness increases (approximately 10-12 cell layers in humans), and the endothelial cells are larger and flatter and connect with the trabecular meshwork (mesh-like drainage canals). The Bowman's layer and Descemet's membrane are no longer present. The epithelial basement membrane lies directly on the stroma, and the stromal collagen structure is less organised with decreased keratocyte abundance. This overall structure forms unique ridge-like constructions, named the limbal palisades of Vogt [293]. The limbal region is also vascularised, providing nutrients and support factors for cells [293-296]. Limbal basal epithelial stem cells are thought to reside in this protected limbal niche (Fig. 4.C) [297, 298]. Here these cells cycle slowly throughout life, maintaining a small but highly proliferative characteristic [294, 297, 299-301]. Their daughter cells, known as

transient amplifying cells, migrate centripetally into the basal layer of the corneal epithelium (Y component), where they then differentiate into the upper layers of the corneal epithelium (X component), with desquamation of outer epithelial layers occuring in order to replace the outer surface layer (Z component). This maintains the balance between cell production and cell loss [302], and is known as the X, Y, Z hypothesis (Fig.5.A).

The limbal niche was the only known epithelial stem cell niche until 2008 when new findings showed evidence of epithelial stem cells throughout the epithelial surface itself [291, 303]. Moreover, Chang et al., (2008) [303] found that epithelial surface stem cell proliferation and migration in the corneal centre was as vigorous as stem cells from the limbus in an *ex vivo* human donut limbal ablation model (removal of the limbal epithelium). This indicates that the limbus may not be the only region enriched in stem cells (Fig.5.B).

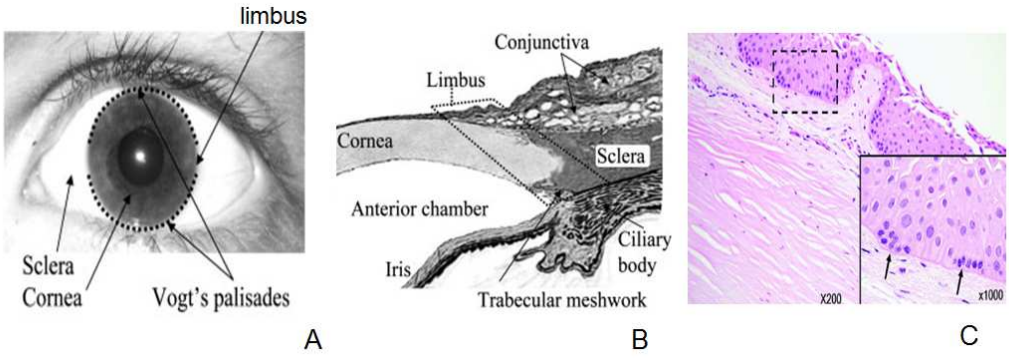


**Fig.4**. **The Corneal Limbus**. A: The corneal limbus is localised to the corneoscleral border. The upper and lower regions most protected by the eyelids contain the Vogt's palisades [304]. B: Cross-section of the corneoscleral transition. The corneal epithelium is contiguous with the conjuctiva, the corneal stroma transits into the sclera, whereas the corneal endothelium links with the trabecular meshwork [304]. C: Hematoxylin and eosin staining (HE) of a normal human corneal limbus demonstrating the palisades of Vogt with small putative residing stem cells (arrows in indent). Small nuclear:cytoplasm represents stem cells [305].

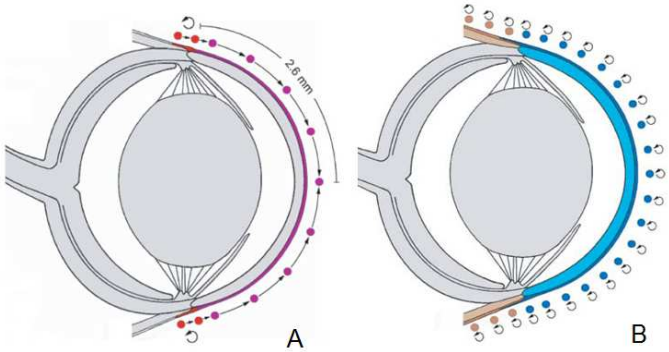


**Fig.5. Epithelial Stem Cells**. A: X, Y, Z hypothesis of limbal basal epithelial stem cell epithelial renewal. Limbal basal epithelail stem cells (red) generate transient amplyfing cells (purple) that migrate into the epithelium and differentiate into outer surface epithelial cells [291]. B: Epithelail surface stem cells are distributed throughout the whole ocular surface [291].

## B Molecular Markers of Limbal Basal Epithelial Stem Cells

For three decades now work has been progressing on the identification of stem cell markers for limbal basal epithelial and transient amplifying stem cells. Markers recognised are briefly *summarised in table 2 page 87. Please note* that in studies aimed to determine epithelial stem cell marker profiles, known markers of stem cells from other ectoderm-derived tissues (such as the epidermis) are good candidates as tissues from the same embryonic origin generally give rise to stem cells with at least partially overlapping marker profiles [306]. This idea of comparative study is now starting to be successfully applied to identify different stem cell populations from the same embryonic origins even across different species [307].

| Molecule | Expression + / - | Brief description/role |
|---|---|---|
| ΔN**p63**α | + | Cell maintenance |
| ABCG2 | + | Universal stem cell marker, cell membrane transport protein |
| C/EBPδ/Bmi-1 | + | Self-renewal |
| Calizzarin | + | Cell growth |
| Catenin α2 | + | Linking protein between cadherins |
| Collagen VI, α1 and α2 chains | + | Structural |
| Connexin 43 | - | Keratin-containing intermediate filament |
| Cytokeratin 12 | - | Keratin-containing intermediate filament |
| Cytokeratin 14 | + | Keratin-containing intermediate filament |
| Cytokeratin 15 | + | Keratin-containing intermediate filament |
| Cytokeratin 3 | - | Keratin-containing intermediate filament |
| Disabled 2 | + | Integrin binding molecule |
| Epiregulin | + | Member of the epidermal growth factor family |
| Glial cell-derived neurotrophic factor (GDNF) and their corresponding receptors TrkA and GDNF family receptor alpha (GFRα)-1 | + | Inflammatory mediators |
| Heat shock protein 70 | + | Heat shock response |
| Hes1 | + | Major Notch target |
| Inhibitor of DNA binding molecule 4 | + | Inhibit/promote DNA binding |
| Integrin α9 | + | Cell membrane receptor |
| Integrins α2, α6 and β4 | - | Cell membrane receptor |
| Involucrin | - | Structural component of mature squamous epithelial cells |
| Musashi-1 | + | Cell differentiation |
| N-cadherin | + | Cell adhesion |
| Notch 1 | + | Progenitor cell maintenance |
| P-cadherin | + | Cell adhesion |
| Spondin-1 | + | Intestinal growth factor |
| Superoxide dismutase 2 | + | Enzyme; dismutation of superoxide |
| Tissue inhibitor of metalloproteinase 2 | + | Stem cell regulator |
| Transglutaminase 2 | + | Regulates protein cross linking |
| Wnt-4 | + | Progenitor cell maintenance |
| Importin 13 | + | Nuclear transport |

Adheshion

**Table 2. Limbal Basal Epithelial Stem Cell Markers:** p63 is considered a reliable marker for both active and resting epithelial stem cells (adapted from [304]).

### 2.3 Corneal Endothelium Turnover

It is considered that human corneal endothelial cells no longer divide beyond an adult age of approximately 20 years old, the endothelium thus being a stable structure [308]. The potential existence of endothelial precursor cells has only been investigated in corneal endothelial wound healing (*section 3.4 page 96*).

### 2.4 Corneal Stroma Turnover

Stromal ECM maintenance is required to retain corneal transparency. However, keratocyte turnover is very, very low (2-3 years) and mitosis cannot be traced. Remodelling of a normal, healthy stromal ECM is not even detectable over time [309], with early experiments using radioactive markers estimating a 2-3 month turnover time for the production of sulphated polysaccharides, and even longer for collagen [310]. Only following corneal injury do keratocyte cells become mitotically active.

## 3 The Corneal Wound Healing Response

The idea of a tissue repair mechanism replacing normal homeostatic tissue regeneration events in mammalian wound healing initially derives from the idea of selective pressure and evolution. In most wounded organs, fast fibrotic repair of the damaged tissue saves lifes, but results in at least partial loss of the original fucntion of the tissue. This is not always the case for the cornea. Clear vision is crucial for survival in most species. In animals the corneal repair events are more self-regenerative than fibrotic, restoring clear vision. However, wether regenerative versus fibrotic corneal repair events occur is dependent on the species, the extent of the corneal wounding and regulation of the keratocyte phenotype throughout the wound healing process [311].

### 3.1 The Cascade of Cellular Events in Corneal Wound Healing

Following corneal injury cells in the epithelium and stroma, as well as nerves and the ocular surface tear film participate in a cooperative orchestrated response to restore corneal structure and function. Many different cytokines*, growth factors, chemokines* and their receptors that are involved in cell-cell regulatory interactions and immune cell functions that are required to not only heal the wound, but to eliminate debris and microbes that must not gain entry into the stromal layer. Many of these responses occur simultaneously or at least

overlap. In this section I focus on the keratocyte cell wound responses (as do many review authors on this subject) in respect to findings using mammalian corneal injury models. We do however need to consider the totality of the contribution from the different components of the wound healing pathway to appreciate the efficiency of the overall wound response.

The most recent overview of the corneal stromal wound response was made by Dupps and Wilson., (2006) [243] (Fig.6). Briefly, outer corneal epithelial injury is the initial trigger of the corneal wound response. This is followed by almost instantaneous apoptosis* of keratocyte cells in proximal stromal tissue underlying the wounded epithelial zone. Shortly afterwards keratocyte cells in the stroma neighbouring the wound zone begin to migrate and proliferate into the wound zone devoid of keratocyte cells. These are known as activated keratocytes, and consequently adopt a repair fibroblast cell phenotype. These cells are responsible for the synthesis and deposition of the new stromal ECM, thus stroma repair (also known as stroma remodelling). Bone marrow-derived magrophage cells also migrate into the cornea to elicit phagocytosis of apoptotic and necrotic debris. (I will not focus on the roles of these cells in this project). Depending on the extent of the injury, activated keratocyte cells can also differentiate into myofibroblast cells. These cells are associated with corneal opacity formation.

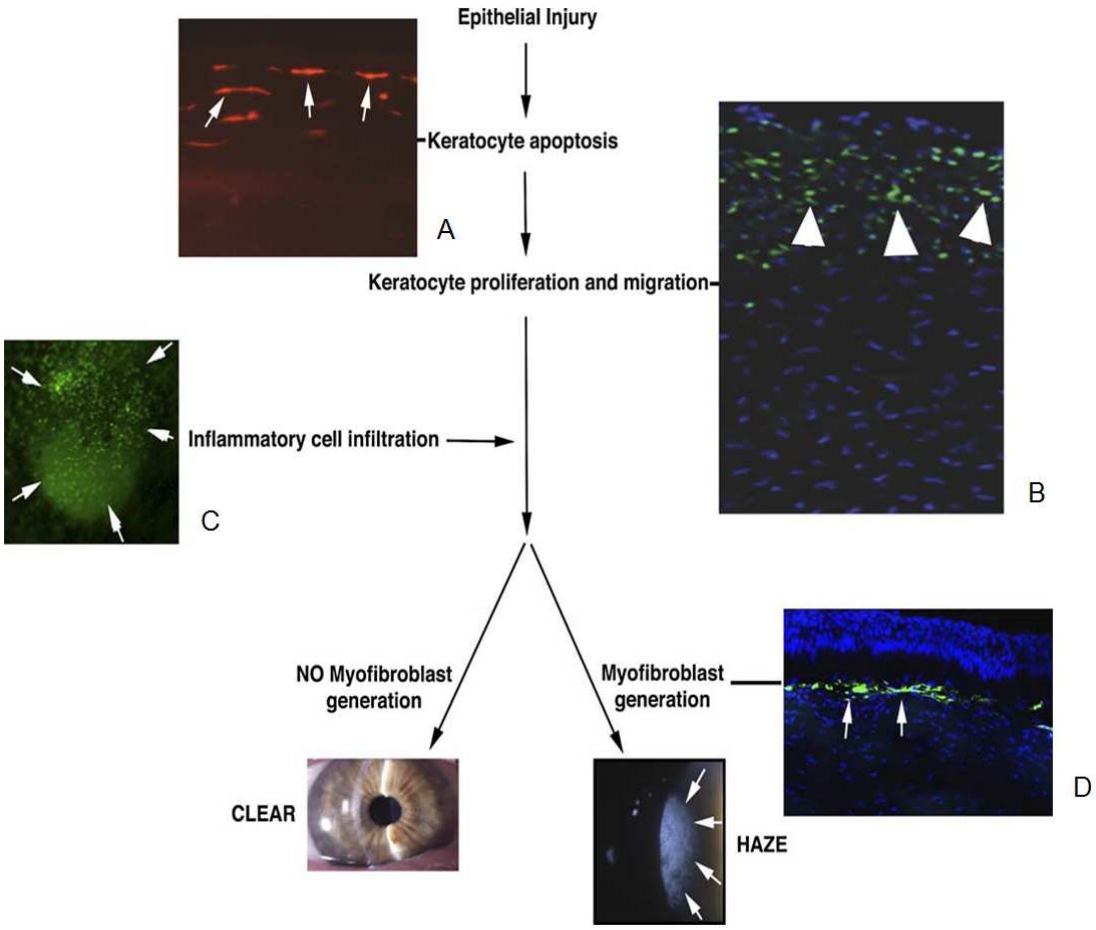


**Fig.6. Schematic Events of Corneal Wound Healing** put forward by Dupps and Wilson. (2006) [243]. A: Human corneal section having undergone epithelial scrape prior to enucleation for choroidal melanoma. Arrows: TUNEL staining assay reveals keratocytes undergoing apoptosis. X500. B: Immunostaining carried out with Ki67 marker for mitosis in the peripheral and posterior cornea of a rabbit cornea epithelial scrape injury model. Arrows: Cells undergoing mitosis 24h following injury. X400. C: GFP-positive bone marrow-derived cells can be seen migrating into the cornea at 24h after injury in a chimeric mouse (whole flat-mount). D: Myofibroblast development in the stroma near the injured surface epithelium in a rabbit cornea at one month after PRK. Arrows: Myofibroblasts detected by alpha-smooth muscle actin (α-SMA) immunostaining. The slit lamp photos of a clear cornea and a cornea with haze are both from humans (X5).

### 3.2 The Epithelial Wound Response

The epithelium being the outermost corneal layer is subject to insult from abrasions, scrapes and chemical exposures [243]. Epithelial wound repair is the same regardless of the extent and type of the injury (excluding complete epithelial removal) and can be separated into three phases. These phases are considered to be the same events as those in normal corneal epithelial homeostasis previously described in *section 2.2,1 page 85,* and can be separated into a latent phase, a cell migration phase and a cell proliferation phase [312, 313].

The latent phase refers to the direct movement, sometimes referred to as a sliding effect, of basal epithelial cells next to the wounded zone that cover the denuded area. In rabbit and monkeys this occurs as early as 4-6 hours following injury [314]. This forms a monolayer of epithelial cells over the wound zone, also referred to as the "fibrin plug". It has been proven that desmosome cell adhesion proteins between the basement membrane and epithelial basal cells are completely lost in proximity to the wound zone in order to diminish the normal tight stratified epithelial structure and to promote this basal cell sliding effect [314-317].

The migration phase involves migration of epithelial cells across the whole wound zone before mitosis commences, producing a linear arrangement of cells across the wound zone. The migration of cells is mediated by formation and contraction of their actin filaments [318, 319]. Upon completion of cell migration and complete covering of the wound zone by serial epithelial cell layers, it is important to regenerate tight adhesion between the epithelium and underlying stroma layer to begin stroma remodelling. Synthesis of new desmosomes and gap junctions* accomplish this [320].

In the proliferation phase, we return to the X, Y, Z function of limbal basal epithelial stem cells localised in the limbus. Once these cells migrate into the wound zone, they proliferate until normal thickness of the epithelium layer is regenerated (re-epithelialisation). Reports using animal models show that this is generally complete within 1-7 days, depending on the species and the extent of the injury [311, 321].

Damage to the epithelium, and essentially damaging the epithelial basement membrane and Bowman's layer, results in changes in epithelial-epithelial cell and epithelial-stroma cell signaling via changes in release of cytokines*, growth factors and chemokines* compared to release under normal homeostatic conditions [322]. An example is the Interleukin (IL)-1 cytokine regulator. This cytokine comes into play in normal epithelium homeostatic regeneration, but does not enter the normal stromal layer due to epithelial

basemement membrane and Bowman's layer integrity [323]. In the wounded stroma, not only does IL-1 activate keratocyte apoptosis, but IL-1 is also capable of regulating other growth hormones (Keratinocyte growth factor (KGF), HGF) [324] that themselves regulate keratocyte migration and proliferation [325]. Similarly, expression of cytokines* [323] and growth factors [326] in tear fluid have also been reported to increase shortly following corneal injury [322]. In the case of incision wounding, these factors would penetrate into the corneal stroma to trigger a variety of keratocyte cell proliferation, migration, and differentiation responses [327].

## 3.3 The Stromal Wound Response

### 3.3.1 Keratocyte Apoptosis

Earlier work shown by animal corneal incision models (that penetrate into the stroma) showed that keratocyte cells neighbouring wound zone edges disappeared after only a few hours post-wounding [328-332]. Similarly, Wilson et al., 1996 [332] demonstrated that keratocyte cells in proximity to animal epithelial surface scrape injuries involving damage to the epithelial basement membrane also disappeared. This group was the then first to prove that keratocyte cells disappear by apoptosis, and that this is the first event in the stromal wound healing cascade [333]. Apoptosis of keratocyte cells prevents further corneal inflammation and subsequent loss of clear vision. Afterwards, experimentation carried out on animal models implied that stromal keratocyte apoptosis is ongoing in the stromal wound zone for approximately 1 week [334, 335]. This suggests that earlier keratocyte cells that migrate and proliferate into the direct wound zone could also apoptose once [323]. Additonally it was found that stromal cells also begin to undergo necrosis after a first wave of cell apoptosis [323]. Necrosis has been characterised as a passive, accidental cell death resulting from environmental perturbations with uncontrolled release of inflammatory cellular components [336].

Up to 25-50% of stromal keratocyte cells can apoptose following corneal injury, depending on the extent of the injury, the species and indeed if the epithelial basement membrane and stromal layer itself are also directly injured [337]. Epithelial scraping, mechanical epithelial pressure and epithelial viral infection have shown to only cause superficial keratocyte apoptosis and necrosis. Differently, incision wounding has unsurprisingly shown more anterior keratocyte apoptosis and necrosis, posterior to the

incision made. This was believed to be due to increased diffusion of pro-apoptotic cytokines* into the central stroma [323].

### 3.3.2 Keratocyte Activation, Migration and Proliferation: Stroma Remodelling

Following keratocyte apoptosis, the corneal stroma is left with a stromal "gap" which is relatively devoid of keratocyte cells [323]. The process of repair begins with the **activation of keratocyte** cells adjacent to this cellular-emptiness. These cells are detectable as early as 6 hours following injury in humans. An activated keratocyte cell phenotype can be distinguished by an increase in size and an increase in the number of nucleoli. The morphology of the cells at this stage resembles that of fibroblast cells with a fusiform shape [311]. Furthemore, the cell cytoskeleton is found to be similar to that found in skin fibroblasts in repair tissue [338]. Zieske and coworkers [339] demonstrated that these cells **migrate** into the direct wound zone devoid of cells. Repair fibroblast cells show also synthesis of α5 integrin chain which results in the formation of α5$\beta$ (beta) 1 integrin heterodimers, known as the classic fibronectin receptor that mediates cell-ECM attachments. This occurs at the same time as fibrin plug deposition in the stromal wound zone [340], suggesting that this receptor may be responsible for the formation of repair fibroblast focal adhesion that enable these cells to migrate on the fibronectin "provisional" matrix into the wound zone [338].

**Prolifeartion** of repair fibroblasts occurs approximately 3 days following injury at the wound zone periphery. Mitosis in rodent corneal incision models peaks after about 6 days following injury. These accumulated cells invade the fribrin plug in the wound zone [311]. Proliferation continues for several days [335, 339].

An active synthesis function of repair fibroblast is implied as they exhibit an enlarged cytoplasm and contain many organelles; rough endoplasmic reticulum, mitochondria, free ribosomes, golgi complexes. They are also capable of incorporating radiolabelled (with sulphate) macromolecular structures [341]. Active synthesis at this point is involved in **production of repair ECM** [342]. This new ECM is not only deposited in a disorganised manner, it is of a different composition to the normal corneal stromal ECM as the ratios of collagen types differ [343, 344]. With this, an increased compaction and alignment of collagen fibrils has been observed (Fig.7) [345]. This contributes to a reduction in corneal transparency.

ECM degradation enzymes are also switched on in wounded corneal stromas. Enzymes involved are principally MMPs, a family of zinc-containing endopeptidases known to be active in corneal stromal wound healing [346, 347]. MMP-1, MMP-3 and MMP-9 are not present in the normal corneal stroma, but synthesis is activated in repair fibroblasts [348-351]. Similarly, synthesis of MMP-2 (the only MMP found in the normal corneal stroma) is upregulated and the majority is converted into functional protein in repair fibroblasts [348, 350, 351]. These proteinases may play a role in the degradation of damaged or provisional ECM, but their expression patterns correlate with the stroma remodelling process, suggesting they may also play a role in the deposition of new ECM [258].

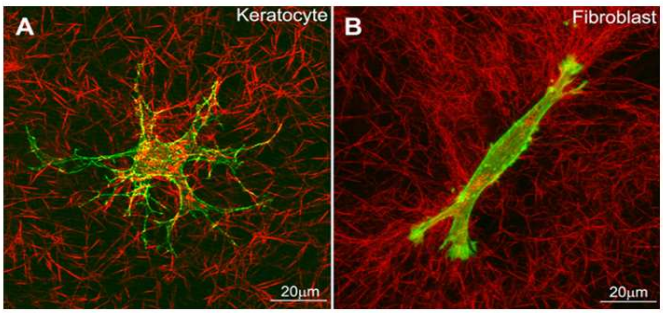


**Fig.7. Corneal Keratocyte (A) and Repair Fibroblast (B) Cells.** 3D matrice cell culture of primary rabbit keratocyte cells in serum-free medium (A) and in 10% FBS (B). Immunostaining with f-actin (green) and collagen fibrils (red). Keratocytes harbour a stellate morphology with numerous cell processes that run a tortuous path between and along collagen fibrils without any apparent impact on their alignment. Repair fibroblasts typically have a bipolar morphology with thin pseudopodial processes and increased compaction and alignment of collagen fibrils parallel to the pseudopodial tips (adapted from [345]).

Beyond approximately day 10 post-wounding (again depending on the species and extent of injury), a more quiescent repair fibroblast cell state is restored, even though new ECM repair tissue is continuously synthesised over many months in order to restore a normal ECM for correct vision. Firstly, collagen is deposited in a lamellar pattern [352], followed by graduly interweaving of collagen lamellae into the wound edge [309]. The collagen fibril sizes become more regular and organised, clearing the opaque repair ECM tissue and regenerating normal corneal transparency [353, 354]. This is a normal repair pathway, but afterwards, **what cell phenotype is derived from the repair fibroblast cells?**

### 3.3.3 Myofibroblast Formation: Regeneration versus Fibrosis

There is a delicate balance between stromal regeneration (repair fibroblast cells) and fibrosis (myofibroblast cells). Stromal repair that restores a transparent stroma is based on the hypothesis that repair fibroblast cells could revert back to thier normal quiescent keratocyte phenotype, but this has not yet been confirmed [323, 355]. Alternatively, fibrosis can occur when repair fibroblasts differentiate into myofibroblast cells. This usually occurs in response to more acute corneal injuries that cause damage to the epithelial basement membrane, resulting in increased signal release into the stroma. A role for TGF signaling in myofibroblast formation is well established [344], giving TGFβ siganling a key role in corneal opacity formation. Note that there are significant species-related differences in the tendency to generate myofibroblast cells [243].

α-Smooth Muscle Actin (SMA) is a an intracellular structural intermediate filament in myofibroblast cells [356, 357], allowing us to distinguish these cells from active fibroblast and keratocyte cells. Between one and two weeks following such injuries, stromal cells can stain positive for α-SMA in the stroma below the wound zone [358]. Expression of α-SMA also mirrors the invasion of stromal wound zones by repair fibroblasts (*see Fig.20 page 128*), but expression continues in each cell over the weeks, even years, of wound contraction [356]. α-SMA can also be used as a marker of partially committed embryonic progenitor cells [359], implying that myofibroblast cells are undifferentiated cells.

Comparison of *ex vivo* keratocyte and myofibroblast cells has deduced that myofibroblast cells produce additional growth factors [324] and collagen [337, 360, 361], as well as glycosaminoglycans (also known as mucopolysaccharides), collagenases and gelitinases, indicating a crucial role for these cells in the stroma remodelling process [362-367]. On the other hand, myofibroblast cells have reduced transparency due to reduced water-soluble corneal protein crystalline production compared to normal keratocyte cells, resulting in less transparent cell properties [272]. Large numbers of myofibroblasts reduces corneal transparency [344, 358].

In most cases myofibroblast cells disappear once stroma remodelling is complete. Spontaneous disappearance of myofibroblasts has been observed even years following injury and corneal transparency can de regenerated. Again, this is a normal repair pathway but it is still unclear how the myofibroblast cell phenotype disappears from the remodelled stroma. Some reports claim that myofibroblasts gradually disappear by apoptosis [358]. This is

thought to be post-stroma remodelling myofibroblast apoptosis and resorption of the disordered matrix is thought to be carried out by the repopulating keratocyte cells [368]. Supporting this idea was very recent work reporting that inflammatroy cells, and even adult keratocyte cells, may produce IL-1α and/or IL-1β cytokines* that could act in a paracrine* fashion to regulate myofibroblast apoptosis in regions of corneal haze [369]. Moreover, myofibroblasts were shown to produce themselves IL-1α and/or IL-1β , suggesting modulation of apoptosis via autocrine* suicide [369].

On the other hand, it has been reported that myofibroblasts are not terminally differentiated and possess the ability to restore keratocyte phenotypes [355]. However, further work is still required to verify if myofibroblasts directly regenerate keratocyte cells in stromal wound healing. It also remains unclear if all activated keratocyte cells transform into myofibroblast cells, or if there is a subpopulation of original keratocyte cells that possess this transformation capacity [311, 333].

In some cases, myofibroblast cells remain permanently in the corneal stroma following injury, causing a constant reduced vision, or in the worst cases blindness. The cellular events and mechanisms that underly this myofibroblast persistance are not characterised. This is a pathological, fibrotic repair pathway.

### 3.4 The Endothelial Wound Response

Earlier work attributed a non-self regenerative characteristic to adult corneal endothelial cells and it was considered a stable structure with no known stem cells. Observation of corneal endothelial wound healing indicated a morphological cell enlargement and migration function, which were considered the major means of endothelial repair [370, 371]. These theories are now under debate considering that several *in vitro* and *ex vivo* studies have shown endothelial cell mitotic changes and proliferation in response to stimulation by growth promoting agents, such as serum [372-374], EGF (Epidermal growth factor) [370, 372, 375] or a combination of the two [373]. Moreover, *in vitro* human endothelial cells from both young and old donors have shown the capacity to proliferate in response to growth-promoting agents [376]. Consequently, in 2005 the potential presence of multipotent endothelial precursor cells was suggested by a handful of groups. It was discovered that *ex vivo* human endothelial cell colonies expressed both mesenchymal and neuronal markers. Differentiated progeny showed corneal endothelial cell-like morphology and pump functions

[377]. These cells however were considered only progenitor cells as they were no longer capable of growing clonally beyond passage 3. Interestingly, McGowan et al., (2007) [378] showed that exposed damaged endothelial cells from human corneal graft beds demonstrate increased expression of a range of adult progenitor and undifferentiated embryonic stem cell markers. This supports the idea of an endothelial progenitor cell population required for adult endothelial cell regeneration, residing in the posterior limbus as hypothesised by the authors [378]. This correlates with former work claiming the migration of endothelial cells from the wounded peripheral into wounded endothelial areas to afflict a repair role [374, 379, 380].

### 3.5 The Wounded Corneal Stromal Inflammatory Response

Rodent corneal wound healing models show that within the first 24 hours following corneal injury an influx of inflammatory cells migrate into the stroma [381]. These originate from the limbal blood vessels and aqueous tears [382]. This is due to epithelial and keratocyte cell responses to elevated cytokine* levels, triggering infiltration in majority by macrophages/monocytes and T cells [243]. The function of inflammatory cells in the wound healing response is a scavenger effect for release of keratocyte cellular components following necrosis and invasion of pathogens from the injury. These are phagocytosed by inflammatory cells [243]. Exploration into inflammatory cell types and signaling pathways involved in the stromal inflammatory response is still at the beginning of research experimentation and there still remains a lot to unravel.

### 3.6 Corneal Wounding and Angiogenesis

Angiogesis is the process by which new blood vessels derive from endothelial cells of pre-existing blood vessels (hemangiogenesis) [383, 384]. Lymph vessel formation (lymphangiogenesis) is also an angiogenic process where new lymph vessels arise from endothelail cells from primitive veins, local lymphangioblasts* or bone marrow-derived cells [385]. Both processes are regulated by pro-angiogenic and anti-angiogenic factors [386]. Examples of pro-angiogenic factors previously identified in the cornea are FGF-2 and Vascular endothelial growth factor family members (VEGF). Examples of anti-angiogenic factors include Angiostatin (recognised as endothelial cell migration and proliferation inhibitor) [387] and Pigment epithelium-derived factor (PEDF) [386]. The maintenance of corneal avascularity is an active process of production of anti-angiogenic factors that

counterbalance the pro-angiogenic factors. However, pro-angiogenic factros are upregulated following more severe corneal injuries from trauma, infection and inflammatory or degenerative disorders [388, 389]. This can cause in *a minority of cases* the dual invasion of the cornea by both blood and lymph vessels [386].

### 3.6.1 Hemangiogenesis in the Wounded Cornea

Blood vessels in humans and animal corneal wound healing models are usually visible to the naked eye (Fig.8). The blood vessels normally grow inferiorly into the central cornea from the limbus, sclera or conjunctiva, and then usually extend between the stromal collagen lamellae and the corneal epithelium and Bowman's layer [390]. The idea of a circular ring-like system around the cornea to promote communication has been put forward [391]. To date, work on animal model hemangiogenesis is in majority based on elucidating mechanisms aimed at understanding the growth factor signaling pathways that promote this response [386].

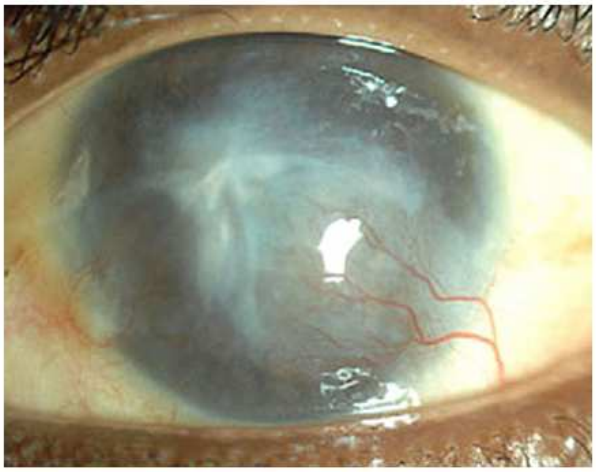

**Fig.8**. **Clinical Appearance of Human Corneal Hemangiogenesis** in corneal infection Acanthamoeba Keratitis. Corneal vessel growth inferiorly into the central cornea from the sclera [392]. (Acanthamoeba Keratitis is a rare disease in which amoebae invade the cornea).

### 3.6.2 Lymphangiogenesis in the Wounded Cornea

Unlike blood vessels, lymph vessels cannot be observed by the naked eye in the cornea. Recent studies have developed experimental models to analyse lymph vessels separately from blood vessels. This is using Lyve-1, a lymphatic vessel endothelial cell-

specific hyaluronan receptor antibody that has been successfully used by immunostaining techniques to localise lymph vessel ultrastructural features in corneal wound healing animal models and human corneas exhibiting neovascularisation (secondary to keratitis, transplant rejection, trauma, and limbal stem cell insufficiency). Results indicate that lymph vessel outgrowth into the stroma towards the central corneal wound from the limbal region can occur within 2 days following mouse corneal suturing (corneal incisions with nylon/silk sutures). Moreover, lymph vessel formation has been found to be correlated with the degree of hemangiogenesis in both wounded mouse and human corneas (Fig.9.) [393, 394]. Lymph vessels however were found to regenerate earlier than blood vessels, at approximately 14 days following suturing injury, whereas blood vessels were still observed 6 months post-wounding [393].

Interestingly, a handful of reports claim that lymphangiogenesis in wounded mouse corneas can occur in the absence of hemangiogenesis, depending on the inflammatory stimuli used [395, 396]. Chimeric mouse models have shown that corneal stroma bone marrow-derived cells can incorporate to form lymphatic vessels following suturing injury. It was suggested that these lymphatic endothelial precursors may be macrophages that transdifferentiate into lymphatic endothelial cells [385, 397].

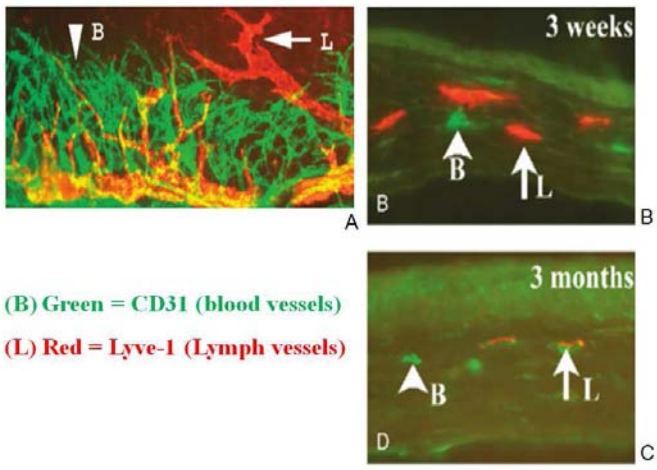


**Fig.9. Parallel Outgrowth of Blood Vessels** ($CD31^{+++}/Lyve\text{-}1^{-}$) **and Lymphatic Vessels** ($CD31^{+}/Lyve\text{-}1^{+++}$) from the mouse limbus to the central corneal inflammatory stimulus (suture–incision). A: Whole cornea flat mount 3 days after injury. X100. B: Frozen sections 3 weeks following injury. X40. C: Frozen sections 3 months following injury. X40 (Adapted from [393]). CD31 is expressed by bone marrow-derived and endothelial cells [398, 399].

Experimentation aimed at determining a role for lymph vessels in the wounded cornea is just emmerging. Ideas are particularly focused on a role of antigen-presenting cell trafficking from the the cornea into lymph nodes [400]. Co-localisation of blood and lymphatic vessels could be based on their complementing functions of tissue fluid and protein balance, as well as this immune cell trafficking in wound repair [400].

Very recent work has proven differences in the extent of lymph vessel formation following injury between different mouse strains [401]. Moreover, different patterns of corneal hemagngiogenesis and lymphangiogenesis were identified using different wound models on the same mouse species [402], indicating high variation in corneal lymph vessel formation which is species and wound-nature dependent.

## 4 Revision: Corneal Stromal wound Healing

Across different species corneal stromal wound healing follows the same flow of events (*summarised in Fig.10 page 101*). Keratocyte cells apoptose in the wound zone, then neighbouring keratocyte cells migrate and proliferate into the stromal cell gap, where they adopt a repair fibroblast cell phenotype for stroma remodelling. Increasing wound size and depth, damaging the epithelial basement membrane and Bowman's layer, increases the extent of keratocyte apoptosis and leads to more fibrotic stromal wound healing responses. Keratocyte cells differentiate into myofibroblast cells, leading to reduced corneal transparency and corneal opacities. Further work is required to deduce if repair fibroblast cells and myofibroblast cells regenerate normal keratocyte cells, or apoptose following stroma remodelling to restore normal stromal transparency. It is unclear why in some cases myofibroblast cells can persist in the corneal stroma once stroma remodelling is complete.

## 4 Récapitulatif: La cicatrisation cornéenne stromale

Parmi les différentes espèces, l'enchainement des événements de la cicatrisation cornéenne stromale est identique (*résumés dans Fig.10 page 101*). Les kératocytes entrent en apoptose dans la zone blessée, puis les kératocytes voisins migrent et prolifèrent dans la zone de blessure stromale, où ils adoptent un phénotype de fibroblastes réparateurs pour le remodelage du stroma. En augmentant la taille et la profondeur de la blessure, et en blessant essentiellement la lame basale épithéliale et la couche de Bowmann, cela provoque la différenciation des kératocytes en myofibroblastes, conduisant au

développement des opacités cornéennes et à une réduction de la transparence de la cornée. D'autres travaux sont nécessaires pour déterminer si les cellules fibroblastiques réparatrices et myofibroblastiques se transforment en kératocytes normaux, ou s'ils entrent en apoptose après le remodelage du stroma pour restaurer la transparence de la cornée. Dans une minorité des cas, une fois le remodelage achevé, des myofibroblastes persistent dans le stroma par un mécanisme inconnu, provoquant alors une réponse cicatricielle anormale, plutôt fibrotique que réparatrice.

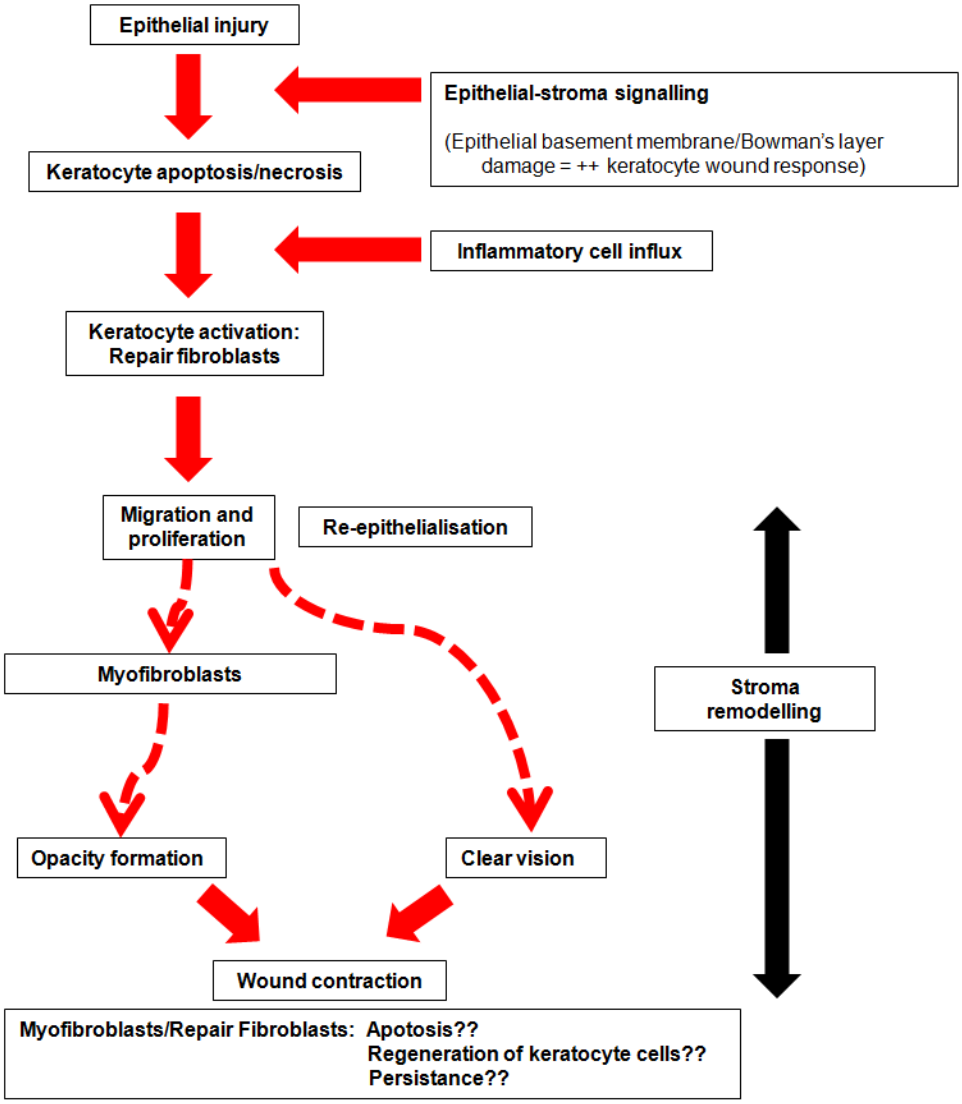


**Fig.10. Schematic Representation of the Corneal Stromal Wound Response**, taking into account both normal repair and fibrotic pathways (intermittent arrows).

## 5 Identification of Corneal Stromal Cells Expressing Stem Cell Markers

Much more attention has been placed on the definition and behavior of corneal epithelial stem cells for their self-regenerative ability in corneal wound healing than stromal cells. However, more recently several studies have indicated the localisation of a corneal stroma cell subpopulation that can grow clonally, express known adult and embryonic stem cell markers, exhibit multipotent characteristics and then switch phenotype to a functional keratocyte-like cell. This is not characteristic of the quiescent adult keratcoyte cell phenotype, thought to be the cell population that exclusively preoccupied the stroma. This suggests for the first time the localisation of a novel population of cells in the normal corneal stroma with stem cell characteristics.

### 5.1 *In vitro* and *ex vivo* Corneal Stromal Cell Studies

The first reports raising the question concerning the existence of corneal stromal stem cells were made in 2005. These theories were discovered upon the use of modified versions of previously developed cell culture models for culture medium-free stem cell "spheroid" formation with normally adherent corneal stromal cells [403-405]. Spheroids refer to grouped cells that expand in cell aggregates [406-410]. Funderburgh et al., (2005) [404] were the first to report that cloned stromal cells formed cell aggregates that continued to grow as free-floating spheroids (Fig.11). It was then found that spheroids could be *in vitro* amplified and maintained multipotency even after several passages. Changes in cell morphology, mRNA and protein expression were analysed in spheroids compared to primary stromal cell cultures in order to deduce the potential existence of stem cell characteristics and deduce where these cell might originate from.

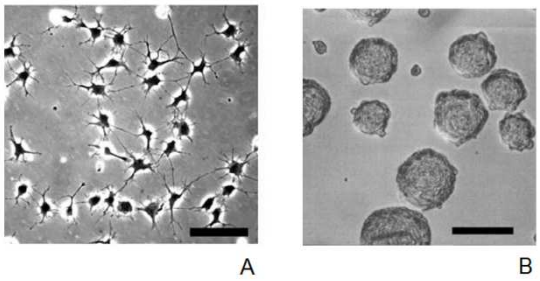


**Fig.11. Spheroid Formation by Corneal Stromal Cells**. A: Primary keratocytes in mitogen-free medium exhibiting a dendritic morphology. B: Aggregates become spherical and could be readily separated from individual cells following culture in supplemented medium (FGF, insulin, transferrin, selenous acid). Scale bars represent 100 µm (adapted from [404]).

## 5.2 The First Report of Corneal Stromal Stem-like Cells by Funderburgh et al., (2005)

### A Localisation of a Clonal Stromal Progenitor Subpopulation

Funderburgh et al., (2005) [404] showed that approximately 3% of freshly isolated bovine stromal cells were able to grow clonally for 65-70 population doublings under spheroid culturing conditions. Selected spheroid clones displayed a keratocyte-like dendritic morphology and expressed high levels of keratocyte-specific markers keratocan, keratocan sulphate and ALDH3A1 throughout their life spans. Similar to *in vivo* keratocyte cells, cloned cells were thought to secrete keratocan sulphate as immunostaining found protein expression localised to peripheral cell structures. Generally, adult tissue stem cells show a replicative life span of 200-300 cumulative population doublings (CPD). This gave the idea that clonal bovine stromal cells were more likely to be progenitor cells rather than stem cells [411].

### B Upregulation of Stem Cell Markers

This group showed that cloned stromal cells demonstrated an upregualted expression of several genes known to be expressed by multiple adult tissue restricted stem cell lineages and by embryonic stem cells derived from neural crest tissues (Fig.12). Among **adult tissue stem cell** gene markers were genes ***Bmi1***, ***SCF***, ***FHL1***, ***Abcg2***, ***CD73***, ***CD90*** and ***CD166***:

**Bmi1** is a member of a polycomb group of transcription factor repressors that regulate chromatin modification for gene silencing [412, 413]. Bmi1 is necessary for efficient self-renewal and division of adult hematopoietic stem cells, as well as adult peripheral and CNS neural stem cells. Alternatively it is also crucial for the differentiation of progeny cells [414, 415].

**SCF** ligand**,** also known as Kit-ligand, binds to a transmembrane growth factor known as kit (or CD117). Kit contains an intracellular kinase domain. Upon SCF binding, both SCF and Kit domains can be cleaved proteolytically. Depending on the resulting isoform, SCF can either activate or inhibit self-renewal of hematopoietic stem cells [416-418]. SCF has also been shown to be produced by *in vitro* mesenchymal stem cells when differentiated toward stromal and osteogneic lineages [419].

**Fhl1 is** Four and a half LIM1, a transcription factor identified as being upregulated in both adult and embryonic neural, hematopoietic and dermal stem cells [420, 421].

**Abcg2 (**ATP-binding cassette sub-family G member 2) is a member of a family of multidrug transporter proteins already known to be expressed by many kinds of stem cells such as hematopoietic [422-424], mesenchymal [424], muscular[424], neural [425, 426], cardiac [427], pancreatic islet [428], skin [428-430] and corneal limbal epithelial stem cells [297]. Isolation of rich stem cell side populations from adult tissues can be yielded after Hoechst 33342 dye incubation and isolation according to cell surface expression of Abcg2 by flow cytometry. This side population was attributed an Abcg2 transporter protein function (also known as BCRP1) [424, 431-433]. Cells expressing Abcg2 show high clonogenic potential [434].

**CD90** and **CD166** are cluster of differentiation cell surface molecules used for cell-sorting of bone marrow-derived mesenchymal stem cells [435, 436].

Among the genes expressed by corneal stromal clonal cells were also **embryonic stem cell markers** expressed throughout neural crest and/or ocular tissue development. These were genes ***Notch1***, ***Pax6***, ***Six2***, ***Six3***:

**Notch1** protein is a Notch homologue (Notch 1-4). Notch interacts with a number of cell surface-bound ligands (Delta-like 1, 3, 4 and Jagged 1 and 2). Upon Notch binding to its receptor, a downstream cascade of cleavage events are activated, resulting in nuclear translocation of Notch. Here, Notch acts on downstream targets to regulate cell fate* decisions, meaning Notch plays a role in stem and progenitor cell self-renewal and expansion, as well as differentiation [437, 438]. Notch1 is primarily expressed during neural and hematopoietic development, but has also now been identified in regenerating adult tissues [439].

**Pax6** is a highly conserved homeobox* transcription factor expressed widely throughout nervous system development, and essentially throughout development of the eye; the lens, corneal epithelium, iris, ciliary body, all neural retinal layers and the retinal pigment epithelium [440, 441]. In $Pax6^{-/-}$ mice, eye and olfactory system development stops at an early stage [440, 442, 443]. *Pax6* misexpresison shows ectopic eye formation (not in usual tissue locations) in drosophila and vertebrates [444, 445]. Pax6 is thus known as the “master regulator of eye development” and was not considered to be expressed in adult tissues until more recently. Later work has now shown a role for Pax6 in adult regenerating tissues, for

example in neural and retinal progenitor cells, mirroring its cell fate* roles found as in embryonic tissues [446-448].

**Six2** and **Six3** also code for homeobox proteins essential for eye development [449]. Six2, Six3 and Pax6, along with Bmi1 and Notch1, are expressed in the neural plate of early vertebrate embryos. After migration of neural crest cells, Six2 transcripts are found in a variety of non-neuronal connective tissues, including the eye [450]. Afterwards, Six2 expression was considered to be localised only in the adult retina [451]. In the same developmental stages, Six3 expression is limited to the retina, lens, hypothalamus, and pituitary [452]. Six3 expression diminishes, or is absent in most adult ocular tissues, except for the retina [451].

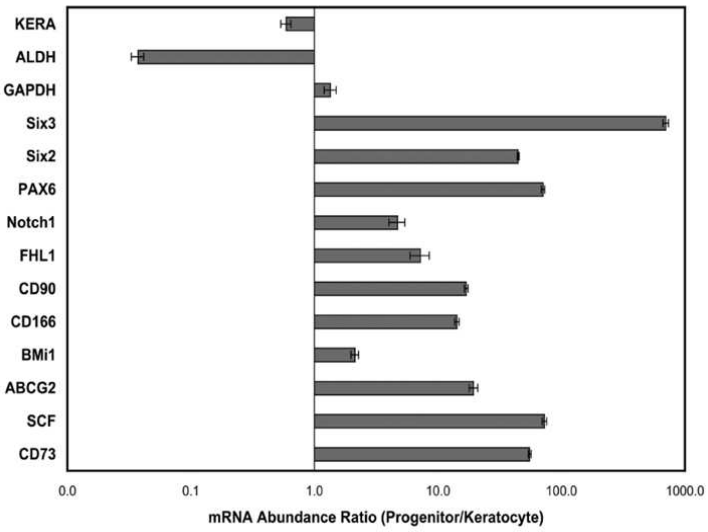


**Fig.12. Relative mRNA Upregulation of Stem Cell Markers by Corneal Stromal Progenitor Cells** normalised to primary keratocyte cells. Expression of known keratocyte markers is reduced (*Kera* and *Aldh*) [404].

### C Pax6 and Corneal Stromal Progenitor Cells

Finally, this same group demonstrated by flow cytometry that 4% of adult bovine corneal stromal cells express Pax6 protein. Immunostaining of primary stromal cells confirmed this by showing that rare corneal stromal cells expressed Pax6 protein, whereas cloned progenitor cells however showed high levels of nuclear-localised Pax6 protein. This indicated the presence of a previously unrecognised population of Pax6-positive cells in the adult corneal stroma.

**This study gave first suggsestions for the existence an adult corneal stromal progenitor cell subpopulation expressing both adult tissue and embryonic stem cell markers, thus a distinct population from adult keratocytes, with a possible keratocyte replenishment function.**

### 5.3 Corneal Stromal Progenitor Cells show Multipotentency

Du et al., (2005) [403] found expression of ABCG2 protein by a few cells in the peripheral (adjacent to the corneal limbus) and central corneal stroma of human cadaver corneas. Moreover, ABCG2-positive stromal cells coexpressed PAX6 protein (Fig.13).

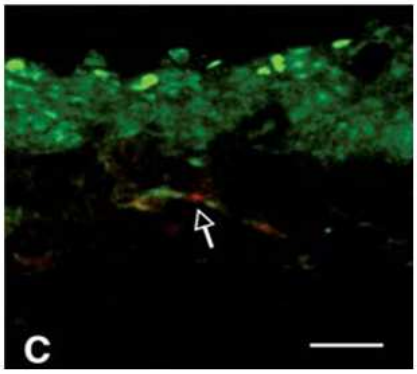


**Fig13. Stromal Cell ABCG2 (red) and PAX6 (green) coexpression** in central human cornea. Scale bar represents 30 μM. X40 (adapted from [403]).

From here, cadaver human corneal stromal cells were expanded in conditions to promote cell proliferation and not differentiation, and were then isolated as a side population of ABCG2-expressing cells. Further cloning of this cell side population resulted in loss of AGBCG2 and PAX6 expression, but upregulation of keratocyte-specific markers (including KERA, keratocan sulphate and ALDH3A1). Moreover, under different cell culture conditions the cloned cell side population differentiated into different cell lineages. Under chondrogenic conditions, cells expressed cartilage specific markers; collagen type II, cartilage oligomatrix protein and aggrecan. Cartilage oligomatrix protein in humans produces a noncollagenous structural ECM protein found in cartilage [453]. Aggrecan is a large aggregating dermatan sulphate proteoglycan that forms a major structural component of cartilage [454]. Under neurogenic cell culture conditions, neural cell-specific mRNA and protein expression was found for neurofilament protein and β-tubulin II. Neurofilament proteins are comprised of cytoskeletal elements that preserve the neuronal structure [455]. β-tubulin III is the protein component of neuronal microtubules [456].

Simultaneous to this work carried out by the Du et al., (2005) group [403], the Yoshida et al., (2005) group [457] discovered that addition of serum and stimulation with TGF-β resulted in α-SMA expression by mouse corneal stromal progenitor cells spheres. This suggested that stromal progenitor cells could differentiate into myofibroblast-like cells, further implying a possible repair function of these cells in the stroma.

**Together these results imply that stromal progenitor cells exhibit a multipotent differentiation potential under correct conditions, characteristic of mesenchymal stem cells in other adult tissues required for somatic cell regeneration.**

### 5.4 *In vitro* ECM Production by Corneal Stromal Progenitor Cells

Du et al., (2007) [458] demonstrated for the first time that isolated human stromal progenitor cells were capable of forming an *in vitro* matrix containing keratocan, keratocan sulphate, collagen type V and collagen type VI. The secretion of ECM components by stromal progenitor cells was found to be denser than secretion by stromal fibroblasts, and isolated regions of the matrix showed parallel alignment of collagen fibrils, characteristic of the normal corneal stromal lamellar organisation. **This indicated that *in vitro* stromal progenitor cells have the ability to secrete an organised ECM.**

Secondly, cadherin 11 cell-cell adhesion proteins and connexin 43-containing gap junctions* were more abundant in stromal proegnitor cell populations compared to corneal stromal fibroblast cell populations. This suggests not only a role for cell-cell interaction in directing ECM secretion between wounded stromal cells, but also that stromal ECM secretion could depend on stromal progenitor cell activity, and not just that of repair fibroblast cells.

Finally, loss of expression of both adult tissue stem cell and embryonic stem cell markers was found progressively throughout spheroid culture passaging, followed by an upregulation of keratocyte-specific markers. **This indicates that stromal progenitor cells caould switch phenotype to functional keratocyte-like cells, again implying a keratocyte regeneration role of progenitor cells.**

### 5.5 Attempts to Identify Neural Crest-derived Stromal Progenitor Cells

In order to test for the presence of progenitor cells that could originate from a permament corneal stromal cell population, Yoshida et al., (2006) [457] isolated a spheroid

side population of neural-crest derived mouse corneal stromal precursors (corneal precursors; COPs). These were isolated from primary stromal cells according to cell surface expression of stem cells markers **Abcg2** and **Notch1**, but also **Nestin** and **Musashi-1** (described below):

**Nestin** is a type VI intermediate filament protein expressed in rapidly dividing cells of the embryonic developing cerebral cortex* [459], CNS and peripheral nervous system stem, and some myogenic tissues [460-462]. Nestin is found abundantly expressed in neuroepithelial progenitor cells and reflects an undifferentiated cell state [463]. The loss of Nestin expression is linked to differentiation [463]. It has been suggested that Nestin plays a role in distribution of vimentin* filaments to daughter cells during progenitor cell division [460, 464]. It is also worth mentioning that it has been reported that Nestin expression is transiently induced in regenerating adult tissues, essentially in the same tissues Nestin is expressed throughout embryonic development [465, 466]. Nestin is not expressed by adult keratocyte cells and is best known as a marker of neural stem cells [467].

**Musashi-1 (**Msi-1) was first reported to be required for correct neural sensory organ development in Drosophila [468]. Now in adult mammals it is commonly considered a specific marker for stem/progenitor cells of neural origin [469, 470]. Msi-1 is a translational suppressor of specific mRNA targets within the Notch signaling cascade, maintaining neural stem cell proliferation [471].

Yoshida et al., (2006) [457] validated these results using a transgenic mouse carrying a Nestin-GFP enhancer, considered to act selectively in neural stem/progenitor cells [472]. GFP expression was observed in the mouse corneal stromas. Isolation of these cells found expression of both **adult tissue neural stem cell** (**Sca-1$^+$/CD34$^+$/<u>CD45$^-$</u>/<u>c-kit$^-$</u>**) and **embryonic neural stem cell** (**Twist$^+$/Snail$^+$/Slug$^+$/Sox9$^+$**) marker profiles. These markers are described below in this respective order:

**Sca-1** is a cell surface-anchored protein of the lymphocyte antigen family found in the majority of cases on hematopoietic stem cells in the mouse [473-476]. Sca-1 has been proven necessary for hematopoietic stem cell self-renewal [477]. Reports indicate a role of Sca-1 in progenitor/stem cell lineage fates. Sca-1 expression by mesenchymal-derived corneal stromal cells is unsurprising, and a precise role remains unclear.

**CD34** is a cell surface glycosylated transmembrane protein used for isolating hematopoietic stem cells [478, 479]. Interestingly, CD34 was first reported to be found on all keratocyte cell surfaces of normal human corneal stromas. Then, this stromal CD34 expression was found to be lost in several types of corneal diseases [480, 481]. CD34 expression is constant upon expansion of human keratocytes, but CD34 expression is lost when keratocytes differentiate into myofibroblasts [482]. Thus, CD34 has since been considered a specific *in vivo* and *in vitro* normal keratocyte marker. This implies that COPs retain some keratocyte-like phenotype characteritics.

**CD45** is a type 1 transmembrane protein tyrosine phosphatase enzyme and was first identified as a major surface protein on hematopoietic cells, making up approximately 10% of the total cell surface area of B and T cells [483]. CD45 has been found to not only regulate activation and proliferation of lymphocytes, but it also plays a role in regulation of immature, undifferentiated hematopoietic stem cells and their progeny [484]. This implies a non-hematopoietic origin of COPs.

**C-kit** is the receptor for the SCF ligand (*section 5.2 page 103*), again implying that COPs are not likely to be bone marrow-derived progenitor cells.

**Twist** transcription factor family is best known as a regulator of proliferation and differentiation of mesenchymal cells in mesodermic embryonic tissues, but expression in adult tissues has been identified [485-493]. Twist2 regulates stromal mesenchymal cell proliferation [494] and differentiation upon downstream transcriptional repression [485, 488]. Loss of Twist2 activity in the normal adult mouse corneal stroma leads to corneal thinning due to keratocyte cell loss, confirming the need for Twist2 in adult keratocyte turnover [495].

**Sox9** is a member of the HMG-box* transcription factor family [496]. Sox9 belongs to the subgroup E of the Sox protein family that are essential involved in many aspects of nervous system development in vertebrates [497, 498]. However, more recent reports show expression of *Sox9* mRNA during human adult neurogenesis. Inhibition of Sox9 function leads to increased neurogenesis and simultaneous loss of dividing precursors, showing Sox9 protein levels are a prerequisite for regulating adult neuronal differentiation [497]. Similarly, reports made by Poché et al., (2008) [499] showed that Sox9 was also essential for post natal mouse survival and differentiation of retinal Müller glial cells.

**Snail** and **Slug** belong to the same family of transcription factors that are best known as transcriptional repressors. Their functions are involved in both embryonic and adult cell

events, ranging from apoptosis to cell division. They are known to control the more general epithelial-mesenchymal transitions (EMT), during which epithelial cells lose their cell-cell junctions and acquire mesenchymal cell characteristics. This leads to cell migration. These transcription factors have been well studied in human cancers where EMT is promoted [500]. Their role in the corneal stroma remains undetermined.

**In summary, at least a proportion of corneal stromal progenitor cells could be *in situ* neural crest-derived progenitor cells that express an intriguing array of adult tissue and embryonic stem cell.**

### 5.6 The Corneal Stroma Harbours Bone Marrow-derived Progenitor Cells

Bone marrow stroma contains mesenchymal and hematopoietic stem cells. These cells are multipotent stem cells that can differentiate into a variety of cell types, notably blood cells, but also osteoblasts, chondrocytes, myocytes, adipocytes, and β-pancreatic islet cells. They can also transdifferentiate into neuronal cells. New roles in adult tissue repair for these stem cell populations are emerging, considering their ability to enter the blood circulation, followed by homing to injured tissues [501, 502].

#### 5.6.1 Bone Marrow-derived Hematopietic Progenitor Cells

Bone marrow-derived cells have been identified in the normal mouse corneal stroma, particularly macrophages and $CD11c^+$ dendritic cells [503-505]. Dendritic cells refers to stellate-shaped cells that recognise foreign antigens and control T-cell activation [506, 507]. CD11c belongs to the β2 integrin family of receptors that mediate cell-cell interactions [508]. It has been found at high levels on most human dendritic cells, but also on monocytes, macrophages, neutrophils and some B cells [509]. Nakamura et al., (2005) [510] transplanted wild-type C75BL/6 mice with bone-marrow derived and bone marrow-derived hematopoietic stem/progenitor cells from enhanced GFP transgenic mice. It was found that GFP-positive cells migrated into both peripheral and central corneal stromas (Fig.14). Immunohistochemistry analyses showed that GFP-positive cells were in fact $CD11c^+/CD11b^+$ or $CD11^-/CD11b^-$ bone marrow-derived cells (Fig.15). $CD11c^+/CD11b^+$ cells were likely to account for bone marrow-derived antigen-presenting cells or macrophages. On the other hand, $CD11c^-/CD11b^-$ cells could have been progenitor cells that migrated into the corneal stroma.

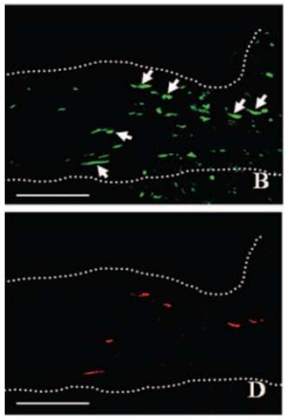


**Fig.15. CD11b Staining (red) of GFP-positive Bone-marrow Derived Hematopoietic Progenitor/Stem Cells (green) in Host Mouse Corneas.** Only some GFP cells immunostained with CD11b (arrows), giving rise to the possibility of migration of progenitor cells into the corneal stroma. A similar result was obtained for staining with CD11c. Dotted lines: corneal tissue outline. Scale bars represent 100 µm [510].

Sosnova et al., (2005) [511] took these findings further and identified a major population of $CD34^+/CD11b^+$ bone marrow-derived cells cells, and a minority population of $CD45^+/CD34^+$ bone marrow-derived cells in normal mouse and rat corneal stromas. A small proportion of these latter cells were also Sca-$1^+$. This gives evidence for the possibility of the localisation of two distinct bone-marrow derived cell populations in the normal corneal stroma; not only $CD11b^+$ macrophages, but also progenitor/stem cells that express bone marrow-derived stem cell markers. More recently a proportion of stroma myofibroblast cells generated following epithelium scraping in C57BL/6J-GFP chimeric mice were found to be bone marrow-derived cells that migrate into the wounded cornea [512].

### 5.6.2 CD133-positive Stromal Cells

Thill et al., (2007) [513] found that 5.3% of normal human cadaver corneal stromal cells isolated by flow cytometry express CD133. CD133 is a transmembrane glycoprotein which was initially considered to be localised exclusively to cellular protrusions of immature hematopoietic stem cells [514, 515]. In humans CD133 expression has now been detected in endothelial progenitors, and stem cells from other epithelia, glia, glioblastomas and neurons. CD133 is also regarded for the moment as a general marker of undifferentiated adult cancer cells [515-518]. At the transcript level several different CD133 isoforms exist, of

which isoform CD133-2 has been found expressed in a variety of adult tissues [519, 520], including the human corneal epithelium [521].

Thill et al., (2007) [513] found that *in vitro* CD133-positive normal stromal cell-derived colonies demonstrated a uniform morphology. This morphologic phenotype is said to be typical of macrophage/monocyte lineage cells, giving rise to a possible source of resident CD133-positive cell-mediated immunity during corneal infection or injury. Furthermore, under clonogenic conditions this macrophage lineage differentiated into lumican-expressing keratocyte cells. Afterwards, further surface marker expression analyses revealed different CD133 marker profiles of normal stromal cells:

- **CD133/ABCG2-positive**: CD133-positive cells costained positive for ABCG2 protein in the normal central cornea, reinforcing the idea that CD133-positive cells have clonogenic potential.
- **CD133/CD34-positive**: 3.6% of CD133-positive cells coexpressed keratoycte-specific CD34 marker, and co-protein expression was found in the normal central cornea (Fig.16). This subpopulation could be keratocyte precursor cells.

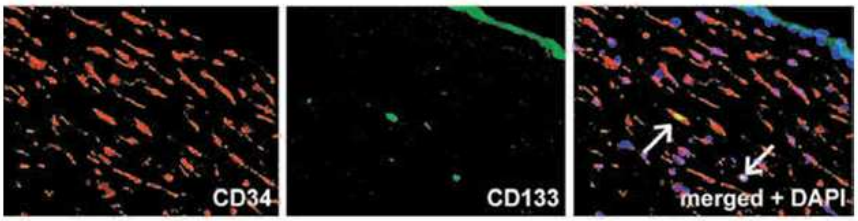


**Fig. 16**. **Normal Human Central Cornea Coimmunostaining with CD34 (red) and CD133 (green)**. The right column photograph shows the merged images of red and green fluorescence, and nuclear staining with DAPI. Triple-positive cells are indicated by arrows. X20 (adapted from [513]).

- **CD133/CD45/CD14-positive**: 20-80% of CD133-positive normal stromal cells coexpressed CD45 and CD14. Different research findings has shown that peripheral blood CD14-positive monocyte cells possess the potential to differentiate into endothelial-like cells [522, 523]. This suggests this stromal cell population could be an undifferentiated repair cell population.
- **CD133/CD14-positive, CD45-negative**: A small $CD133^{+}/CD14^{+}/CD45^{-}$ normal stromal cell population was also isolated.

Stromas from diseased human corneas were removed from patients receiving keratoplasty* surgery due to herpes keratitis infection, keratoconus* or graft failure. It was found that CD133-positive cells accounted for up to an average of 26.8% of these corneal stromal cells, and virtually all these cells were CD14-positive, but CD45-negative. Thus, this $CD133^{+}/CD14^{+}/CD45^{-}$ cell population was suggested to be an intermediate stage of differentiation into the final $CD133^{+}/CD45^{+}/CD14^{+}$ repair cell phenotype, and that these cells would eventually differentiate into keratocyte cells. On the whole, even though corneal stromal CD133 expression colocalised with expression of other known hematopietic stem cell markers, given the known wide adult tissue-derived stem cell expression of CD133, the origins and functions of the stromal cells that express CD133 in human corneas remains unclear.

**This collection of studies shows that corneal stromal progenitor cells may not be only recruited locally, but also from external bone marrow-derived cell lineages that migrate into and reside in the normal corneal stroma for a potential keratocyte cell regeneration fucntion. This would explain the identification of different, and in some cases overlapping, bone marrow-derived and neural stem cell marker expression profiles for stromal progenitor cells.**

## 6 Stem Cell Injection Studies; Taking it One Step Further

Due to the shortage of cornea donors for cornea keratoplasty* and high immune rejection rates, stem cell-based therapy to correct exclusively the defected corneal stromal layer (harbouring myofibroblast cells) became of great interest after the discovery of potential corneal stromal progenitor cell populations. Animal models so far have been based on the outcomes of directly injectecting corneal stromal progenitor and bone marrow-derived mesenchymal stem cells into the corneal stroma, and the effect this has on stroma remodelling of mice harbouring disorganised corneal stromal structures. Mesenchymal stem cells can be obtained in large quantities from plentiful tissues sources, often autologous* tissue sources, such as adipose and new born umbilical stem cells. This avoids the requirement of stem cell subculturing of normal corneal stromal progenitor cells. Corneal stromal disorganised mice are generated by lumican null ($Lum^{-/-}$) mice. $Lum^{-/-}$ mice corneal stromas show loss of

specialised corneal keratin sulphate proteoglycans, notably lumican, resulting in largre and altered collagen fibril diameters and organization [524, 525]. This increases light scattering in the cornea, resulting in corneal opacities [526], similar to those caused by trauma, inflammation and infection in humans via differentiation of keratocyte cells into myofibroblasts, and altered secretion of ECM components. $Lum^{-/-}$ mice are therefore a good animal model for testing the restoration of corneal transparency via cell injection.

### 6.1 Corneal Stromal Progenitor Cell Injection

Normal human corneal stromal progenitor cells were isolated, cloned and tagged with membrane dye before direct injection into the corneal stromas of $Lum^{-/-}$ mice [527]. The cells were rapidly distributed throughout the murine stromas within 48 hours following injection, and were still stable in the corneas for up to 10 weeks. Human (not mouse) KERA protein expression was localised in the stromas of injected mice, showing survival and correct functioning of the injected human stromal cells in the murine corneas. The absence of an immune response is consistent with reports that adult stem cells induce immune suppression [528]. Finally, the $Lum^{-/-}$ mice injected corneas regained a stromal ECM indistinguishable from that of wild type mice, demonstrating restoration of corneal transparency. These results imply firstly that adult human corneal stromal stem cells are suitable for and survive xenograft transplantation. Secondly, these findings further imply that *in vivo* corneal stromal wound healing could harbour a stroma remodelling contribution from stromal progenitor cells that differentiate into functional keratocyte-like cells.

### 6.2 Different Tissue-derived Bone Marrow-derived Stem Cell Injections

Human processed lipoaspirate derived (PLA) cells possess stem cell characteristics; they show extensive proliferative capacity and give rise to differentiated progeny [529]. Several *in vivo* studies have shown PLA cells to be suitable for cell fillers in plastic surgery [530], muscle tissue engineering [531], bone defect reconstruction [532] and cardiac tissue regeneration [533]. Bone marrow-derived mesenchymal stem cells are present in adipose tissue [534]. Arnalich-Montiel et al., (2008) [529] investigated the ability of human PLA cells to promote rabbit corneal stroma regeneration. Firstly, immunogenicity of human PLA cells was tested upon injection into a rabbit corneal stromal incision pocket created by excimer-induced stromal ablation. Still 10 weeks following surgery, the PLA cells had intermingled in

the stromal ECM, sustaining stromal structural integrity and corneal transparency. Human PLA cell regeneration capacity was then tested upon injection into a more acute epithelial layer flap opening with a 50µm deep stromal incision made with a microkeratatome. Afterwards, the flap was replaced. 12 weeks following surgery the human PLA cells again manifested integration into the corneal stroma in multilayers. Moreover, human PLA cells expressed markers of functional keratocyte cells, demonstrated by mRNA and protein expression of human (not rabbit) ALDH3A1 and KERA. In the host rabbit corneal stromas the PLA cells obtained a flattened and elongated keratocyte-like morphology (Fig.17).

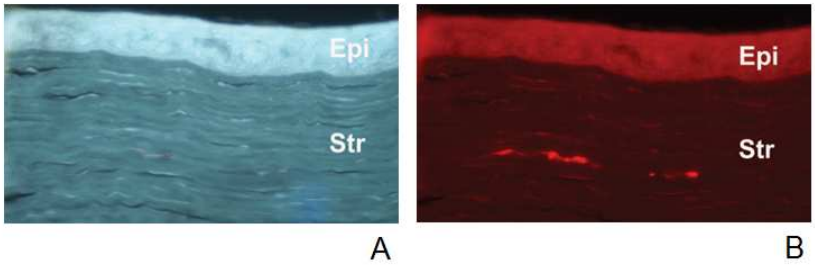


**Fig.17. PLA Cells Three Weeks after Corneal Stromal Injection.** A: Corneal stromal nuclei staining showing indistinguishable human and rabbit cell nuclei. B: Fluorescent CM-DiI (water-soluble fluorescent tag)-labeled human PLA cells interwoven into the corneal stroma showing a keratocyte-like morphology. X200 [529].

Newborn human umbilical cord-derived mesenchymal stem cells (UMSCs) show fibroblast-like cell morphology and express markers expressed by known mesenchymal stem cells. Newborn human umbilical hematopoietic stem cells (UHSC) also show expression of typical hematopoietic stem cell markers. Both cell populations are capable under correct conditions to differentiate into multiple cell types [535]. Liu et al., (2010) [535] transplanted both newborn human UMSCs and UHSCs into the corneal stromas of $Lum^{-/-}$ mice. Still three month following surgery UMSCs survived in mouse corneas and proliferated in the corneal stromas for up to 8 weeks following surgery, a feature of adult keratocytes in the corneal wound healing response. $Lum^{-/-}$ mice corneal transparency improved as corneal stroma thickness was increased. Collagen fibres were longer and more intact and UMSCs expressed markers of functional keratocyte cells. They assumed a flat, dendritic morphology and protein expressions of human (not mouse) LUM, KERA, CD34 and ALDH3A1 were elevated. On the other hand, UHSCs transplanted into mouse corneas began to apoptose as of 1 week

following surgery, as well as eliciting a significant immune response. Transparency was not restored in $Lum^{-/-}$ mice corneas. Overall this study further implies that bone marrow-derived mesenchymal stem cells even from different species can incorporate into the adult murine corneal stroma, without triggering graft rejection and improving corneal stroma transparency. UHSCs trigger an immune response and do not survive in the corneal stroma suggesting that previous expression of hematopietic stem cell markers may be from intermediate stages of progenitor cell differentiation pathways [513] and/or that hematopoietic progenitor cells differentiate early upon migration into the corneal stroma.

## 7 Implications of the Expression of Embryonic Stem Cell Markers by Corneal Stromal Progenitor Cells

As well as more restricted adult tissue stem cell markers, expression of a selection of embryonic stem cell markers (Pax6, Nestin, Six2, Six3, Notch1, Twist, Snail, Slug, Sox9) involved in neural crest and/or ocular tissue development were also found to be upregulated by normal adult corneal stromal progenitor cells [404, 457, 458]. Today, the reexpression of embryonic stem cell markers by “embryonic–like stem cells” in adult tissues is a captivating research area.

### 7.1 Embryonic-like Stem cells

Human pluripotent embryonic stem cells that derive from the inner cell mass of the blastocyst* can be propagated indefinitely in an undifferentiated state [536, 537]. Ethical and political issues concerning the use of human embryonic stem cells for research purposes led to the discovery that embryonic-like pluripotent stem cells can be generated directly from adult tissues. These cells have already been identified in several tissues, such as bone marrow [538, 539], amniotic fluid [540] inner ear [541], skeletal muscle [542, 543] and hair follicles [544]. The pluripotency of these cells can be easily demonstrated when they are grown in suspension, where they spontaneously differentiate and form cell aggregates named embryoid bodies in modes which recapitulate early events of embryonic development [545, 546]. Additionally, they can be differentiated into multiple cell lineages *in vitro* and *in vivo* that are not necessarily their cell lineage of origin, including mesenchymal, hematopoietic and neural tissues [547-552]. Transcription factors Sox2, Oct-3/4 and Nanog are required to maintain pluripotency of embryonic stem cells, independently and cooporatively [553-557].

### 7.2 Sox2, Oct-3/4 and Nanog Transcription Factors

Sox2 (HMG box gene*) is a member of a 20 member transcription factor family that are expressed in a variety of both embryonic and adult tissues [558, 559]. Sox2 is a member of Sox group B genes that participate in the earliest events of CNS differentiation in drosophila, xenopus, chick and mouse species [560]. During embryonic eye development, Sox2 expression is wide-spread and involved in optic vesicle, lens and neural retina formation [561, 562]. Co-operative expression of Pax6 and Sox2 is required for lens formation [561, 563, 564]. Concerning progenitor cells, Sox2 functions to maintain pluripotent neural stem cells. It is considered a marker of undifferentiated cells [553].

Oct-3/4 (also known as Pou5f1) is a transcription factor involved in self-renewal and proliferation of embryonic stem cells. Several studies have now shown that Oct-3⁄4 is expressed by a variety of adult tissue stem cells and in multipotent progenitor cells (i.e. stem cells from epithelium, bone marrow, liver) [565]. It has been suggested that it functions to sustain a self-renewal capacity in a manner analogous to its role in embryonic stem cells [566-568]. It is also used as a marker for undifferentiated cells [557].

Nanog is a recently identified transcription factor that is also expressed by embryonic stem cells, but not by differentiated mature somatic cells [555, 569]. It is thought to be a key factor in maintaining pluripotency [570], and when embryonic stem cells lose Nanog expression, they begin to differentiate [571].

A combination of Sox2, Oct-3/4 and Nanog transcription factors has been proved to be capable of inducing the expression of each other, and are essential for maintaining the self-renewing undifferentiated state of the inner cell mass of the blastocyst, as well as of embryonic stem cells [572].

### 7.3 Induced Pluripotent Stem Cells

Studies today based on embryonic-like stem cells and expression of Sox2, Oct-3/4 and Nanog is based on the recent ground breaking news showing that pluripotent stem cells can be induced directly from somatic adult cells upon addition of only Sox2, Oct-3/4 and Nanog factors (induced pluripotent stem cells). This was first discoved when isolated adult mouse fibroblast cells were transformed directly into embryonic stem cell-like cells once induced with Sox2, Oct-3/4 and Nanog [573]. Induced pluripotent stem cell generation is viewed as a multiple-step action mediated by these transcription factors that induce reverted expression of

embryonic stem cell markers, while at the same time suppressing the somatic cell genetic program. This highlights the potential importance of these factors for self-renewal and differentiation roles in maintaining pluripotency of adult stem cells.

## 7.4 Neural Crest-derived Embryonic Stem Cells

Embryonic neural crest mesenchymal cells, as well as participating in embryonic corneal stroma development, yield neuronal and glial* cells of the entire peripheral nervous system and in the head, they also give rise to cephalic tendons, cartilage, bone, dermis, vascular smooth muscle and adipocytes [574]. Original neural stem cells were considered to disappear upon differentiation as the neural tube* matures and neural crest cells mix with other cell types. However, it has been found that adult tissue locations such as the intestinal ganglia* [575], the spinal ganglia [576], the hair follicle [544, 577, 578], the tooth [579] and even bone marrow [580, 581] appear to be later niches for the maintenance of multipotnet neural crest-derived stem cells. This gave insights into the idea that the initial embryonic neural crest cell population could be constituted by a large proportion of lineage-restricted progenitor subpopulations with distinct cell fates* in adult tissues [582].

### 7.4.1 Embryonic Neural Precursor Characteristics of Late Embryonic Keratocyte Cells

Little is known about the relationship between adult corneal stromal keratocyte cells and their neural crest precursors. The Lwigale et al., (2005) [284] group used quail/chick chimeric grafts* to visually trace the invasion of and contribution of donor quail neural crest stromal cells in embryonic developing chick corneal stromas. Recipient chick embryos were first delivered quail dorsal neural tube grafts (Fig.18). Quail corneal stromal embryonic neural crest stromal cells (just before eyelid opening) were then injected under the chick embryo ectoderm at either side of the dorsal neural tube graft before the development of their secondary stroma (E8-9). Injected embryos were re-incubated from 0 hours to 15 days before being cryosectioning for immunohitochemical analyses.

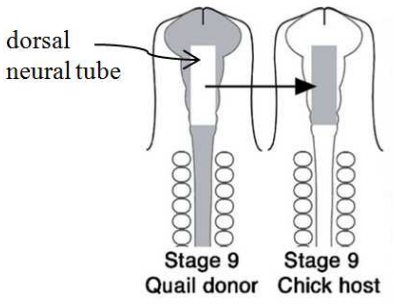


**Fig.18**. Schematic diagram illustrating the method for dorsal neural tube transplantation from quail to chick embryos (adapted from [284]).

Quail nucleus-specific antibody (QCPN) demonstrated contribution of quail donor neural crest cells to chick endothelial and stromal secondary layers during corneal development. Some donor keratocyte cells injected into the chick cornea migrated out of the injected cell mass, where they migrated alongside host migratory neural crest cells and proliferated in the surrounding head mesenchyme. Unlike the keratocyte cells that remained in the injected cell mass, the migratory cells ceased to synthesis keratin sulphate. However, the migrating quail cells did not mix with endogenous neural crest cells or express the neural crest cell marker (known as HNK-1). This suggests that the migratory quail donor keratcoyte cells did not fully lose their keratocyte phenotype, similar to keratocytes in the corneal wound healing process when they migrate into the wound zone, proliferate and differentiate into fibroblast-like cells and cease temporarily to produce and secrete keratocan sulphate [356].

Some injected donor quail keratocyte cells additionally contributed to the smooth muscle of cranial blood vessels. This was confirmed by expression of α-SMA by quail keratocyte cells. This suggests that the quail keratocyte cells responded to embryonic signaling events (such as TGF-β signaling) to acquire myofibroblast cell morphology, again similar to keratocyte responses following corneal wound healing.

The donor quail keratocyte cells failed to contribute to neurons in ganglia or branchial arch cartilage, illustrating that keratocyte cells are partially restricted progenitor cells rather than stem cells. This data demonstrates that at least some late-embryonic stromal keratocyte cells may not be terminally differentiated cells, but maintain a certain degree of plasticity and multipotency. These finding also suggest that some adult stromal keratocytes may retain more characteristics of their embryonic developmental potential than previously believed, and this

could be correlated with the different cell phenotypes identified in the corneal stromal wound healing cascade (repair fibroblasts, myofibroblast) [284].

Adding to these findings from the Lwigale et al., (2005) group [284], a new study demonstrated that late human embryonic neural crest cells were found to not only express partially committed progenitor cell markers, such as α-SMA protein, but they also synthesised Sox2, Oct-3/4 and Nanog proteins. These expressions were lost as neural crest cells developed into somatic cells [359]. Sox, Oct-3/4 and Nanog expression being emblematic of pluripotent embryonic stem cells implies that at least some adult neural crest cells could retain more of their embryonic precursor characteristics than previously thought [359].

Adult mesoderm progenitor cell lineages that differentiate into mesenchymal stromal progenitor cells from human bone marrow and umbilical cord have shown different progenitor lineage commitments, one being a Nestin expressing neural cell population. This was shown to be regulated by an Oct-3/4 molecular program [583]. This suggests that Sox2, Oct-3/4 and Nanog regulatory mechanisms for maintaining plasticity in embryonic stem cells could be similar in a range of adult stem cell lineages [584].

This same theory could be applied to the expression of embryonic-like developmental markers in the adult corneal stroma. For example, Pax6 is regarded as a multifunctional player regulating proliferation and differentiation of embryonic stem cells in a highly context-dependent manner [446, 585]. Recent work has now shown expression of Pax6 in regenerating adult neural crest-derived tissues, for example by neural and retinal progenitor cells [446, 447, 585]. Similarly, *in vitro* work on the adult mammary gland confirmed an important role for Notch signaling in cell fate* decisions, showing a role in stem cell self-renewal and expansion, as well as differentiation of specific progenitor cells [437]. Furthermore, Notch-dependent regulation of neural progenitors has already been discovered in the adult rat spinal cord [586], showing an important role for Notch signaling in mature neural crest-derived tissues. Expression of such markers in the adult corneal stroma could similarly correspond to neural crest-derived progenitor cell regulation of corneal stromal cell regeneration.

### 7.5 Sox2, Oct-3/4 and Nanog in Adult Tissue Regeneration

Most studies have investigated the role of Sox2 alone in adult tissue regeneration taking into account its well documented and wide CNS and ocular expression patterns

throughout embryonic development [560-564]. Sox2 mirrors the same roles for cell survival and cell differentiation in adult tissues as those identified in embryonic cells. Millimaki et al., (2010) [587] demonstrated that in adult zebrafish Sox2 is required for both adult hair cell survival, as well as for transdifferentiation of support cells* into hair cells during adult hair regeneration. Considering that aspects maintaining stem cell pluripotency in embryonic stem cells and adult stem cells have some parallels, the role of Sox2, Oct-3/4 and Nanog as a trio-transcription factor network in stem cells involved in adult tissue regeneration soon and lately became a curiosity. A small handful of reports have demonstrated expression of Sox2, Oct-3/4 and Nanog in adult stem cells, emerging new roles for these transcription factors in adult tissues homeostasis and repair [588].

## 8 Revision: Cornea Stromal Progenitor Cells

Several *in vitro* cell studies have tried to characterise an adult corneal stromal progenitor side population with a potential keratocyte replenishment function. These progenitor cells could derive from at least neural crest-derived and external bone marrow-derived mesenchymal lineages suggested by their expression profiles of a range of different stem cell markers. These progenitor cells also express embryonic stem cell-like markers usually expressed by neural and/or ocular tisssues. Evidence that some late embryonic neural crest-derived cells retain some cell plasticity, and express not only α-SMA, but also Sox2, Nanog and Oct-3/4, undifferentiated stem cell markers is interesting as we could also hypothesise a role of embryonic stem cell-like cells in adult corneal stromal wound repair.

## 8 Récapitulatif: Cellules progénitrices cornénnes stromales

Plusieurs études menées *in vitro,* ont essayé de caractériser une sous population de cellules progénitrices du stroma cornéen adulte avec un rôle potentiel dans la régénération de kératocytes adultes. Ces progéniteurs expriment des marqueurs de cellules souches issus de tissus adultes variés, indiquant que ces cellules progénitrices dérivent au moins d'une population cellulaire mésenchymeuse de la crête neurale qui résident dans le stroma cornéen, et d'une population cellulaire mésenchymeuse de la moelle osseuse. Ces cellules progénitrices expriment aussi des marqueurs de cellules souches embryonnaires qui sont également exprimés lors du développement des tissus issus de la crête neurale et/ou tissus oculaires. Une partie des cellules souches embryonnaires tardives de la crête neurale maintiennent une

plasticité cellulaire et expriment des marqueurs de cellules souches pluripotentes (α-SMA, Sox2, Nanog, Oct-3/4). Ce constat est intéressant car nous pouvons émettre l'hypothèse de l'existence d'une population de cellules souches adultes qui adoptent un phénotype embryonnaire dans le stroma cornéen adulte lors de la cicatrisation.

# II Aims

Since 2005 several *in vitro* cell studies have suggested the localisation of clonal, multipotent stromal progenitor cells in the adult cornea that not only express a variety of known adult tissue and embryonic stem cell markers, but are also capable of expressing functional keratocyte-like markers [403, 404, 457, 458, 513]. Stem cell marker expression profiles suggest localisation of more than one progenitor pool in the normal corneal stroma; at least resident progenitors and external corneal recruited progenitors [510-513]. When I began studying mouse corneal wound healing in 2009, it was shown that *in vivo* injected human corneal stromal progenitor cells hold the ability to restore corneal stromal organisation and transparency in mice with strucurally disordered stromas [527]. Together, these studies provide evidence for the potential existence of progenitor cells in the stroma with keratocyte regeneration potential. Consequently, the important issue to determine was whether a subpopulation of corneal stromal progenitor cells exists *in vivo.* **Thus, we aimed to use an *in vivo* adult mouse corneal wound healing model upon full thickness corneal incision to test for the localisation of cells expressing stem cell markers in stromal wound repair, and if so, what the tissue lineage origin of these cells could be.** We compared changes in expressions of stem cell markers in control versus wounded stromas at various times throughout stromal repair. We selected the following stem cell markers known to be expressed in adult stem cells and/or pluripotent embryonic stem cells:

1. **Adult tissue stem cell markers**: **Abcg2**, **CD133, Pax6** and Telomerase Reverse Transcriptase (**Tert**). Of interest to us is that in normal human corneal stromal ABCG2-positive cells were found to coexpress PAX6 [403], a marker also expressed throughout embryonic nervous system/ocular development [589]. Pax6 has now been found expressed by a range of adult ocular progenitor cells [446, 448, 585]. We also chose CD133 as it has been found to be expressed by a range of different tissue adult stem cells [515-518] and has been found to be increased in expression in human diseased corneal stromas [513]. Tert preserves telomere length during cell division-dependent DNA replication, and Tert activity is also considered a stem cell marker since it is upregulated in regenerative progenitor cells compared to somatic cells [590, 591].

2. **Neural stem cell marker**: This was in order to check if the *in vivo* wounded stroma could harbour *in situ* corneal stromal progentior cells, or if the majority of progenitor cells were more likely to be from different tissue stem cell populations. The **Nestin** marker is of special interest to us regarding it is expressed by neural crest cells during early embryogenesis (thus keratocyte cells) [460-462], but also it has also been found to be expressed in several adult stem cells, including murine corneal stromal progenitor cells [457, 465, 466]. Additionally we investigated the possibility of **external recruitment** of different tissue progenitor cells via an *in vivo* wounded corneal **lymphatic system**. For this purpose we used the **Lyve-1** lymphatic vessel endothelial cell-specific marker.

3. **Pluripotent embryonic stem cell-like markers**: We wanted to test for the localisation of corneal stromal cells that revert to reexpressing their former embryonic precursor cell markers throughout the *in vivo* stromal wound response. These markers were embryonic stem cells markers **Sox2**, **Oct-3/4**, **Nanog,** known to be expressed by embryonic cells throughout the development of neural crest tissues [359].

**Les objectifs**

Des études menées *in vitro* et des études de thérapie cellulaire suggèrent qu'une population de cellules progénitrices réparatrices située dans la cornée stromale adulte pourrait jouer un rôle dans la régénération des kératocytes. Par conséquent, il était important de déterminer si cette population de cellules progénitrices existe dans la cornée stromale adulte *in vivo*. Nous avons donc utilisé un modèle de cicatrisation cornéenne chez la souris adulte comprenant une blessure incisionnelle complète de la cornée, pour étudier la localisation des cellules exprimant les marqueurs de cellules souches lors de la réparation stromale. Nous avons aussi sélectionné des marqueurs pour essayer de déterminer les tissus d'origine de ces cellules. L'expression des marqueurs dans des stromas contrôles ont été comparés aux stromas blessés lors des différents stades de la cicatrisation stromale. Les marqueurs choisis sont des marqueurs de cellules souches connus et exprimés par des cellules souches adultes et/ou embryonnaires pluripotentes :

1. Des marqueurs de cellules souches à l'origine des **tissus adultes** : **Abcg2, CD133, Pax6** et la Télomerase Reverse Transcriptase (**Tert**). La colocalisation des cellules positives pour ABCG2 et PAX6 trouvées dans le stroma humain adulte peut être

intéressante [403]. Pax6 qui est un marqueur des précurseurs embryonnaires dans le système nerveux et tissus oculaires [589], mais aussi un marqueur des cellules progénitrices adultes dans des tissus oculaires [446, 448, 585]. CD133 est un marqueur exprimé par une variété de cellules souches adultes [515-518], et son expression est augmentée dans la cornée stromale humaine malade [513]. Tert préserve la longueur des télomères en ajoutant des répétitions télomériques aux chromosomes lors de la division cellulaire. Il est connu pour être un marqueur des cellules souches avec augmentation dans les progéniteurs par rapport aux cellules somatiques [590, 591].

2. Marqueurs de cellules souches exprimé par des tissus **nerveux** (issus de **la crête neurale)**: Il était nécessaire de vérifier si le stroma blessé contient des cellules progénitrices *in situ*, d'origine cornéenne stromale, ou si la majorité des progéniteurs sont issus de tissus externes. Le marqueur de cellules souches neurales **Nestin** est intéressant car il est exprimé par des cellules issues de la crête neurale (notamment des kératocytes) dans le développement embryonnaire [460-462], mais aussi par plusieurs cellules souches adultes neurales lors de la régénération tissulaire [465, 466]. Pour vérifier l'hypothèse du recrutement des progéniteurs extérieurs à la cornée, nous avons étudié la formation des vaisseaux lymphatiques dans la cornée blessée à l'aide du marqueur **Lyve- 1** (spécifique aux cellules endothéliales des vaisseaux lymphatiques).
3. Marqueurs de cellules souches **embryonnaires** : Nous avons testé la localisation de cellules stromales dans le stroma blessé qui ré-expriment des marqueurs de leurs précurseurs embryonnaires. Les marqueurs sélectionnés sont les marqueurs pluripotents **Sox2**, **Oct-3/4** et **Nanog,** connus comme étant exprimés lors du développement embryonnaire de la crête neurale [359].

# III Materials and Methods

## 1 *In vivo* Animal Corneal Wound Healing Models

The study of corneal wound healing and haze formation has been carried our using rabbit [358, 592-594], rat [595], hen [596] and monkey [597, 598] animal models. Different wound healing responses can be generated depending on the corneal wounding method used. Less acute stromal wound responses are generated using epithelial scrapes (not damaging the epithelial basement membrane/Bowman's layer), compared to more acute responses following alkali burns and deeper incison techniques (direct incision, suturing). Jester et al., (1987) [357] were the first to report full thickness corneal incision in a rabbit model. Full thickness incision damages all layers of the cornea, including the endothelium. Briefly, these results report that within 4 hours following injury a fibrin plug was formed to close the opening of the wound zone. By seven days following injury, a matrix of stromal fibroblast-like cells replaced the fibrin plug, and transition of these cells into myofibroblast cells was observed by α-SMA expression. These cells secreted an ECM consisting of proteoglycans that left an opaque scar.

### 1.1 *In vivo* Mouse Corneal Wound Healing Models

Mice have not been extensively used for the study of corneal wound healing as their corneas are small and relatively resistant to haze generation from less severe corneal wounding techniques, such as epithelial scraping and PRK*. Generation of corneal haze requires more acute corneal damage, such as full corneal thickness incision [337], or combinations of wounding techniques, such as epithelial scrape followed by PRK* [599]. Several groups have extrapolated the same wound response observed following rabbit full corneal thickness incision wounding to the *in vivo* wounded mouse corneal incision model (Fig.40. left panel) [600, 601]. Miyazaki et al., (2008) [601] found α-SMA expression as soon as 3 days following full corneal incision of C57BL/6 mice, leading to corneal scarring. Myofibroblast cells began to decline as of 21 days post-wounding (Fig.40. right panel). We opted for the development of a full corneal mouse incision wounding model as this method generates an acute stromal wound response, involving corneal haze formation and early stroma remodelling and wound contraction phases within 1 month. This gave convenient time

periods for the collection of corneal tissues throughout different stages of a complete stromal wound response.

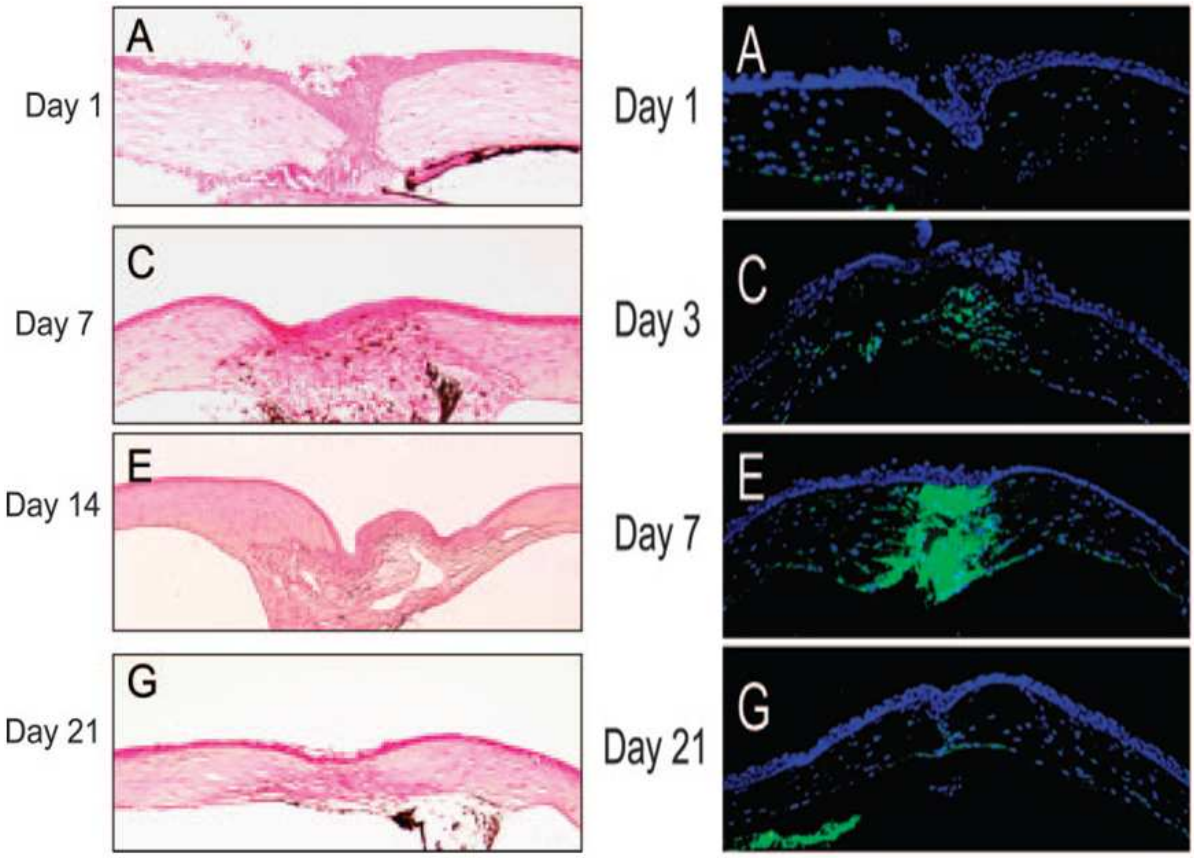


**Fig.19. Corneal Wound Healing Following Full Corneal Thickness Incision of C57BL/6 Mice**. Left panel: HE staining. Day 1: Wound zone occupied with epithelial cells in a fibrin plug. Day 7 and 14: Wound sealed with fibrotic scar tissue. Day 21: Scar tissue formed in the incision wound is more compact. Right panel: αSMA-positive stromal cells (green). Day 1: Almost no myofibroblasts are observed in the stroma. Day 3: Myofibroblasts are detected in the stroma. Day 7: Stromal wound zone is densely populated by myofibroblast cells. Day 21: Myofibroblast cell population has begun to decline. DAPI nuclei staining (blue) (adapted from [601]).

## 2 Our *in vivo* Mouse Corneal Wound Healing Model

### 2.1 The Surgery Protocol

Female C57BL/6 mice 12-16 weeks old were purchased from Charles River France (Arbresle, France) and maintained in Claude Bernard animal experimentation centre, Hôpital Purpan, CHU de Toulouse, France. All animals were treated in accordance with the Ethical Committee of the CPTP (Centre de Physiopathologie Toulouse Purpan, France) and

guidelines provided in the ARVO Statement for the use of Animals in Ophthalmic and Vision Research. Atropine (atropine sulphate 1% faure, Europhta Laboratoires, Monaco) was applied topically to the left (incised) eyes 10-20 minutes before surgery to dilate the iris. Use on humans has onset anaesthesia from 30 seconds, persisting for a minimum of 15 minutes, thus covering the duration of the mouse corneal incision surgery. This prevented the surgeon from damaging the corneal iris and preventing iridocorneal synergy (when the iris and corneal stroma fuse together). General injection anaesthesia regimen (Ketamine/Xylazine) was injected intraperitonealy and a local anaesthesia of 1.6 mg/0.4 ml oxybucaine chlorhydrate (Théa Laboratoires, Clermont-Ferrand, France) was applied. All surgery was performed by the same ophthalmologist surgeon with the same equipment. The full thickness of the centres of the corneas of the left eyes were perforated with a trephine 0.75 mm in diameter using a Zeiss® OPMI® CS operating microscope (Germany). This removed a button of corneal tissue from all corneal layers (Fig.21). 1 drop of 1% fucithalmic acid eye drop (LEO Laboratoires, St Quentin en Yvelines, France) was applied following the surgery. This is an antibiotic treatment developed against eye surface bacterial infection. The right eyes of incised mice did not undergo surgery. Mice with no surgery in either their left or right eyes served as controls (both eyes) for all experiments. 1 drop/day of fucithalmic acid and atropine were applied to incised eyes for 5 days after incision wounding, as for both eyes of control mice.

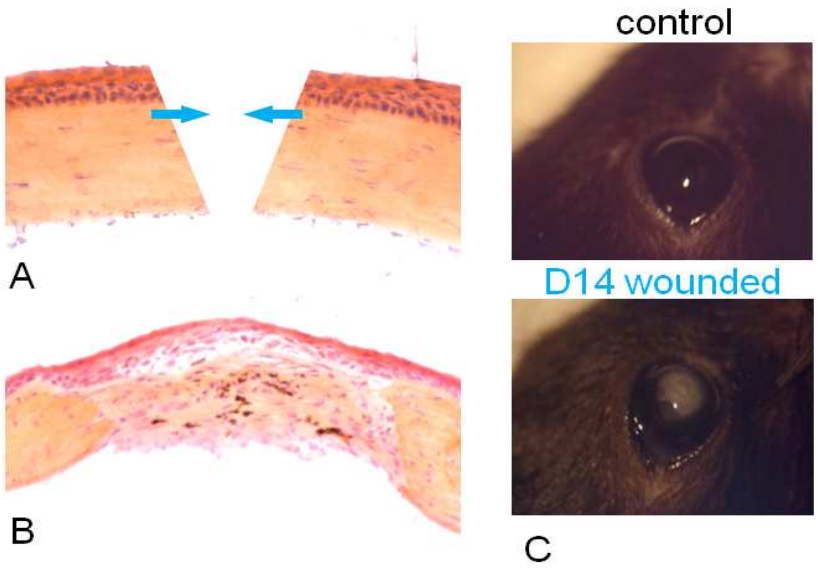


**Fig.20. Our *In vivo* Mouse Full Corneal Thickness Incision Model**. A: The incision penetrating all the corneal layers removing a button of corneal tissue (virtual incision). B: D14 stromal wound zone in the stroma remodelling process. (HE staining; X400). C: Corneal opacity developed by D14 post-wounding (digital photographs).

### 2.2 Clinical Observations

Corneal opacity levels were clinically measured with a slit-lamp* every week after wounding using a corneal transparency grade system [602]. Grade 0 describes a completely clear cornea, or with trace opacity obliquely illuminated with the slit-lamp. Grade 1 denotes less severe opacities that do not interfere with the visualisation of fine iris details. Grade 2 denotes moderate obscuration of the iris and lens, and grade 3 denotes complete opacification of the stroma in the incised area. Opacity grading was performed in a masked manner by two independent ophthalmologists. The presence of corneal blood vessel formation was rare. The majority of mouse corneas developed maximal corneal opacity by Day 14 (D14) post-wounding (Fig.21), showing an acute mouse corneal stromal wound healing response and upregulation of α-SMA confirmed myofibroblast generation [603]. Myofibroblast formation increased according with increasing opacity grade score (Fig. 22). In most mice both opacity formation and α-SMA expression gradually declined after D14 [603]. The morphological structures of wounded corneas from D7-D28 post-wounding corresponded to those in Fig. 23. D7 wounded corneas harbour a highly disorganised stromal cell and ECM organisation, and D14 wounded corneas show a dense population of stromal cells in the wound zone. By D21 and D28 the tissue in the wounded stroma is in the process of remodelling, and the relative position of cells to each other resembles that of a normal cornea. The epithelial, stromal and endothelial cell layers are well-distinguished, and the stromal cells are more elongated between the collagen fibres than in the D7 and D14 wounded stromal zones. Note that some differences were found in the sizes of wounded corneal tissues, the time taken for opacity to form and decline, and for corneal wound zones to remodel. This can be explained by biological variation between mice even from the same strain in corneal wound healing responses, but also due to slight unavoidable variability in the surgical procedure [592]. Mice that did not develop any corneal opacity by D28 post-wounding, or mice that still showed grade 3 corneal opacities at D28 post-wounding were not used for analysis in this project.

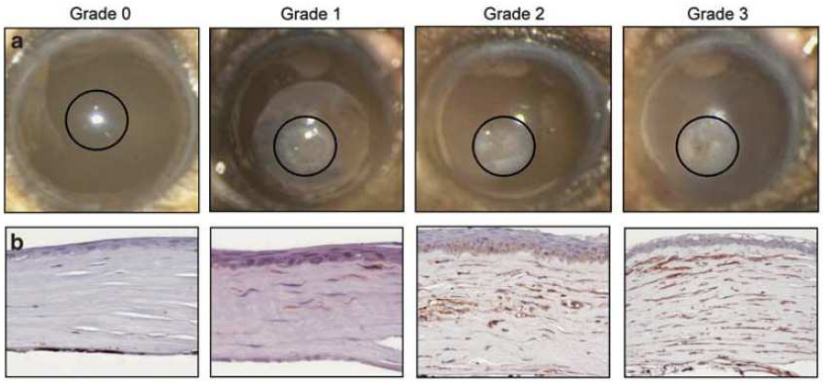


**Fig.21. Opacity Grading Scores with Corresponding Increase in Myofibroblast Formation**. Each grade is presented with corresponding histological observations of α-SMA expression (brown staining, X400). Increased expression of α-SMA with higher opacity grading (adapted from [603]).

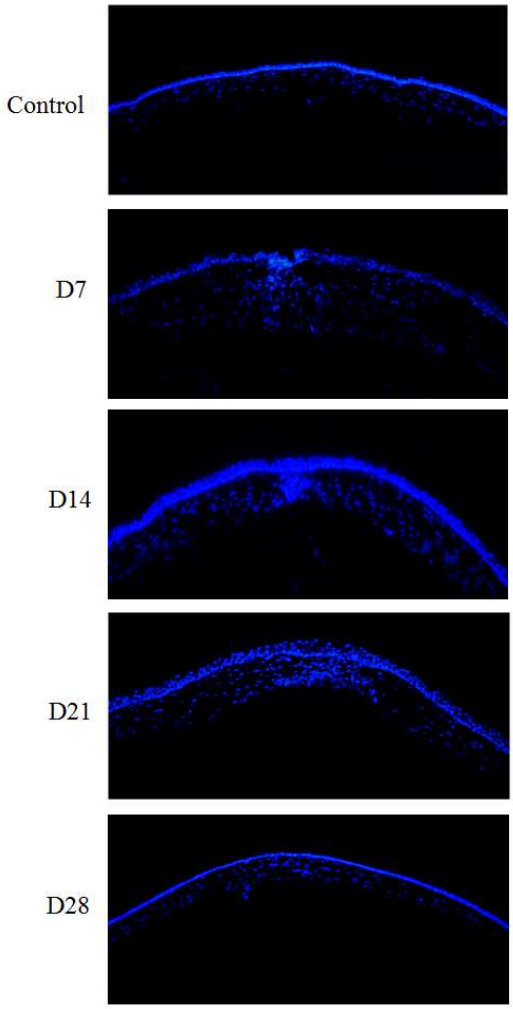


**Fig. 22. Morphological Structures of Wounded Corneas**. Control versus D7, D14, D21 and D28 wounded corneas following full thickness incision surgery (DAPI nuclei counterstaining). X100.

### 2.3 Tissue Collection

Incision wounded and control mice were euthanised using isoflurane and cervical dislocation after D7, D14, D21 and D28 post-wounding. The eyes were carefully enucleated and either cryo-embedded for immunohistochemical analyses, or the stroma was recuperated by removal of the epithelial and endothelial layers by gentle scraping with sterile surgical tweezers. These tissues were snap frozen in liquid nitrogen and used for mRNA and protein expression, and telomerase activity analyses. All tissues were stored at -80°C.

## 3 Quantitative RT-PCR

### 3.1 RNA Extraction and cDNA Synthesis

Total RNA was extracted from corneal stromal tissue using a 1ml micro tissue grinder (Wheaton, USA) at $^{+}$4°C and commerical protocol from the RNeasy® Mini Kit 50 (Cat. No. 74104, Qiagen, USA). RNA quantity and quality was controlled using the Agilent 2100 bioanalyzer with RNA 6000 nano chips (Agilent Technologies, USA). All RNA samples proceeded to cDNA synthesis, but RNAs with a RIN (RNA integrity number) ≥7/10 were preferentially used for qPCR analysis. Total cDNA was synthesised following the protocol from a commerically available SuperScript VILO Kit (Cat. No.v11754-250, Invitrogen, USA). Final 20µl cDNA volumes were stored at -20°C. Considering the small tissue size of the mouse corneal stroma, total cDNA concentrations were relatively low (approximately 3000 pg/µl per stroma).

### 3.2 Quantitative PCR

#### 3.2.1 Principle

QPCR is based on the possibility of tracing PCR amplification over time (“real time”) using fluorescence. Fluorescence data is collected throughout every PCR cycle and represents at the given time the quantity of primer amplified products. The higher the concentration of the amplicon under analysis in the cDNA sample, the lower the number of cycles required to obtain a fluorescent signal that is significantly higher than the background signal. This is defined as Ct, and relates to the beginning of the exponential (amplification) phase. qPCR does not study the concentration of final PCR products as do classical PCR methods, eliminating limiting factors during the plateau phase (notably primer and cDNA amount).

Thus, Ct readings are precise and reproducible for comparisons of concentrations of a gene of interest between cDNA samples.

### 3.2.2 Efficiency Calculations and Amplicon Specificity

For detection of small changes in expression it is required to calculate the efficiency (E) of the qPCR for a forward and reverse primer set. For this we carried out qPCR on a two-fold serial dilution of cDNA template. In theory, dilutions of cDNA template should each have amplification curves each one cycle behind each other, corresponding to a 100% E (referred to as 2). Ct values were presented graphically on a log scale graph, where the slope of the graph (linear regression, (-(1/log(1+E)) corresponded to the E. A -3.32 slope corresponds to a 100% E. The slope should always be <-3.32, otherwise E is >100%, meaning amplification of other non-specific amplicons. We calculated the mean E per primer set using 3 different wounded stromal cDNA templates. Only primers with a mean efficiency of 0.85-1.00 were used for further qPCR analysis.

The amplification specificity is controlled by a melting curve at the end of each PCR cycle; double-stranded DNA is denatured very slowly until the set primer annealing temperature is attained. This results in release of fluorescent label into the reaction mixture. The only fluorescent signal remaining corresponds to primer set amplicons, which is transformed into a peak. A single melting point curve peak corresponds to one single amplicon amplification. More than one peak corresponds to more than one amplicon product, in other words non-specific primers.

### 3.2.3 Experimentation

Primers for *Nestin*, as well as for two housekeeping control genes Beta-2 microglobulin *(B2m)* and Tyrosine 3-monooxygenase *(Th)* were designed using Primer Express 3.0 (Applied Bioystems) and purchased from Eurogentec S.A (Belgium). All primers were tested first on cDNA from embryonic mouse tissue, and optimal cDNA and primer concentrations were determined. For all assays complete 2X SYBR® Green ER® qPCR SuperMix Universal buffer (Cat. No. 11762-100, Invitrogen, USA) was mixed with 1µl cDNA, and 1µl forward and reverse primer mix. Total reaction volume was 10µl. *Nestin* mRNA expression was analysed in seventeen control, thirteen D7, thirteen D14, fourteen D21 and eleven D28 wounded stromal cDNA samples. Triplicate samples were used for all assays.

Reactions were performed in LightCycler 480 96-multiwell plates with sealing foils (Roche, UK) in the LightCycler 480 machine (Roche). PCR conditions were as follows: 50°C for 2 minutes, denaturation at 95°C for 10 minutes, and amplification for 40 cylces of 95°C for 15 seconds and 60°C for 1 minute.

### 3.2.4 Statistical Analysis

Housekeeping control gene expression should be the same in all control and wounded stromal cDNA samples analysed. This is important for taking into account fluctuations in data resulting from cDNA quality. We chose *Th* and *B2m* genes that showed a constant expression across numerous control and wounded stromal cDNA samples [603]. We initially tested these genes based on the published demonstration of the corresponding *Th* and *B2m* human genes as good housekeeping genes across many different human tissues [604]. Relative stromal cDNA sample expression data for each gene of interest was calculated by REST 2009 [605] software (Qiagen, Munich, Germany) that takes into account normalisation of primer set Ct standard deviation to:

- The *Nestin* primer set E calculation.
- The E calculations of both housekeeping control gene *Th* and *B2m* primer sets (known as the $2^{-\Delta\Delta CT}$ method [606]).
- The standard deviation of expression of both housekeeping control gene *Th* and *B2m* primer sets in control and wounded stromal cDNA samples.

Non-parametric Mann Whitney tests were used for group-to-group comparisons. A value of $p \leq 0.05$ was considered statistically significant, determining if gene expression changes were statistically significant between different stromal cDNA samples.

### 4 *Sox2* RT-PCR

A Quanti®Tect Primer Assay set for *Sox2* was purchased from Qiagen (Cat. No. QT01539055, Qiagen, France). *Sox2* mRNA expression was initially analysed by RT-qPCR, but a very high optimal concentration of cDNA template (600 pg/µl) was required for sufficient E calculations. Working with this cDNA sample concentration would have

exhausted the stock of stromal cDNA samples. We initially tried to overcome this problem by trying total RNA amplification using a combined RNA amplification and cDNA synthesis kit (Cat. No. L1016-01, SuperScript® RNA Amplification System). RNA amplification and/or cDNA synthesis was unsuccessful. Consequently, *Sox2* mRNA expression was analysed by agarose gel electrophoresis quantification of qPCR gene products in control and D14 wounded stromal cDNA samples. 5 µl of cDNA template (undiluted) was mixed with complete 2X LightCycler® 480 Green I master mix (Roche, UK) and 1.25 µl of forward and reverse primer mix at an optimised 10-fold dilution. Total reaction volume was 12.5 µl. PCR conditions were as follows: denaturation at 95°C for 15 minutes and amplification for 40 cycles of 94°C for 15 seconds, 72°C for 30 seconds and 72°C for 30 seconds. *Th* housekeeping gene was used as a control. Ct data was not calculated for Sox2 primer assays, but melting curves were checked for Sox2 primer specific amplification before gene product analysis by 2% agarose gel electrophoresis. 50 bp DNA ladder was used for molecular weight determination (Fermentas, France. Cat. No. SM1211).

Sox2 primer specificity was further confirmed by purifying *Sox2* qPCR products using the QIAquick Spin PCR Purification Kit (PCR products 100 bp to 10 kb, Quiagen). 5 µl of purified products were added to 25 µl urea–LB (0.5 mg/ml bromephenol blue (Sigma, France), 8 M urea (Sigma, France), 1% (v/v) NP-40 (Tergitol®, Sigma), 1mM Tris (pH 8)). The products were then denatured at 80°C for 5 minutes and ran on a 1M urea-2% agarose denaturing gel in TAE1X buffer (40 mM Tris base (Sigma, France), 20 mM acetate, 2 mM EDTA (pH 8)) at 75V for 1.5 hours at 4°C. The gel underwent numerous washes with TAE 1X buffer, followed by numerous washes with 100mM NaCl. The gel was incubated with SYBR® Gold Nucleic Acid Gel Stain (Molecular probes, Invitrogen, USA) for 30 minutes before visualisation under UV light of a band corresponding to the *Sox2* primer amplicon. The band was excised and purified according to manufacturer's instructions (QIAquick Gel Extraction Kit 50, Qiagen). Sequencing with a 3730xl sequencer (Applied Biosytems, MilleGen, Labège, France) using BigDye® Terminator v3.1 was carried out. The sequences obtained were compared to Mus musculus Sox2 sequence from Ensembl (Ensembl release 59-Aug 2010© WTSI/EBI).

## 5 Quantitative Telomerase Activity Analysis

### 5.1 Principle

Quantitative determination of telomerase activity was performed using the Quantitative Telomerase Detection Kit (MT3011 Biomax, US) that detects real-time PCR telomerase activity in lysed tissues and cells. Telomerase activity is quantified upon the sample extract ability to synthesise artificial telomeric repeats onto an artificial oligonucleotide substrate. The products are then amplified by PCR and direct detection of SYBR Green dye binding to the double-stranded DNA product monitors direct detection of the PCR product.

### 5.2 Experimentation

All reagents were supplied in the kit. All lysate preparation was carried out at $^{+}4$°C. Six D14 wounded and six control stromal tissues were pooled separately and lysed. Human KG1 myeloblastic cell line was used as a positive Tert activity and internal control (a gift from V. Mansat-De Mas, INSERM U563, Toulouse, France [607]). Cells were cultured at 37°C in IMDM medium (Invitrogen, Gibco, France) supplemented with 20% heat-inactivated fetal bovin serum (FBS), 100 U/ml penicillin and 100 µg/ml streptomycin in a humidified atmosphere containing 5% $CO_2$. Cells were maintained for 2 weeks at $3x10^5$ cells/ml by diluting with fresh medium every 2-3 days, and cell viability was assessed by trypan blue exclusion. A total of $1x10^5$ cells were lysed and centrifuged. A two-fold serial dilution of KG1 cells was made in lysate buffer. 12.5 µl of D14 wounded stromal or KG1 cell lysate was added to 12.5 µl of QTD premix in Thermo-Fast® 96 PCR detection plates (AB-1100, Abgene, Thermo Fisher Scientific, UK). PCR conditions were carried out in the ABI PRISM® 7000 Sequence Detection System (Applied BiosystemsTM, France) as follows:

- Telomerase “warm-up” reaction 25°C for 20 minutes.
- Initial activation: 95°C for 10 minutes.
- 40 cycles of: Denaturation at 95°C for 30 seconds, annealing at 60°C for 30 seconds and extension at 72°C for 30 seconds.

The Ct was used to detect the signal associated with an exponential growth of PCR products during the log-linear phase and compared between control and D14 wounded stromas. The same experiment was repeated 3 times using triplicate stromal and KG1 cell lysate samples, and a negative control (lysate buffer). Relative telomerase activity was

determined using REST 2009 software, and normalised to the negative control telomerase activity data. Non-parametric Mann Whitney tests were used for group-to-group comparisons. A value of $p \leq 0.05$ was considered statistically significant.

## 6 Immunohistochemistry

### 6.1 Sectioning and Fixation

Immunohistochemistry allows the visual localisation of protein in cell culture and tissues sample slices by the use of protein epitope antibody detection. Cryo-embedded enucleated mouse eyes were slowly frozen using isopentane before transport in liquid nitrogen for storage at -80°C. The eyes were then transported on dry ice for cryosectioning. Cryosections of a minimum of 7µm were required to maintain corneal structural integrity. For most primary antibodies used, sections were immediately fixed for 20 minutes in freshly prepared 4% paraformaldehyde at 4°C, then air dried before storage at -20°C. The anti-Nestin primary antibody required that sections were directly stored at -20°C after sectioning. These sections were then fixed just prior to immunostaining experimentation for 20 minutes in acetone at -20°C. For each eye sectioned, HE staining was carried out on a sample of slides to verify the state of the cornea before proceeding to primary antibody experimentation.

### 6.2 Immunodetection Experimentation

For immunostaining, a minimum of 3 different controls and 3 different D7, D14, and D28 wounded mouse eyes were tested with each antibody for consistency (except for Lyve-1/CD31 colocalisation experiments, for which we tested 5). Sections fixed in paraformaldehyde were incubated for 30 minutes in 0.1% $NaBH_4$ in PBS for antigen retrieval. All sections were permeabilised in 0.5% Triton X-100 in PBS. Non-specific binding was blocked by incubation in 10% FBS (Cat. No. 10106151, Invitrogen) for 30 minutes, followed by blocking for 30 minutes with Image-iT™ FX Signal Enhancer (Cat. No. I36933, Invitrogen, USA). Incubations of sections with primary antibodies against the proteins Abcg2, CD133, Tert, Sox2, Oct-3/4, Nanog, Pax6, Nestin, Lyve-1 and CD31, followed by a 1 hour incubation with 1/400 dilutions of secondary Alexa Fluor® antibodies (Molecular probes, Invitrogen, USA) were performed according to table 3 (*page 139*). All sections were washed for 5 x 5 minutes with 0.5% Triton X-100 in PBS after incubations with primary and secondary antibodies. 0.5% Triton X-100 in PBS was used for all serum, primary and

secondary antibody dilutions. Negative controls were carried out using 0.5% Triton X-100 in PBS, as well as rat isotype IgG antibody, rabbit and goat serums in replacement of the primary antibodies used on sections of control and wounded eyes (*see table 3 page 139*). Nuclei were counterstained and mounted using ProLong® Gold antifade reagent with DAPI (Cat. No. P36935, Invitrogen, USA). All experiments were carried out under the same conditions, and antibody controls and wounded cornea staining were performed concurrently.

### 6.2.1 Colocalisation Experiments

Colocalisation experiments are used to determine if ≥2 different proteins are localised to the same or different tissues, cells and even subcellular structures. Abcg2/Tert, Oct-3/4/Tert, Pax6/Sox2 and Lyve-1/CD31 colocalisation experiments were carried out. Note that for Lyve-1/CD31 colocalisation experiments, eye tissues were cryosectionned at 20µm in order to preserve vessel integrity for visualisation with confocal imaging. Different species primary and secondary antibodies were used to reduce non-specific background. The same protocol as in *section 6.2 page 136* was applied for colocalsiation experiments. Firstly, sections were incubated with one primary antibody, followed by incubation with its corresponding secondary antibody. This was then repeated for the second primary antibody with corresponding secondary antibody. Additional washes in 0.5% Triton X-100 in PBS were carried out before addition of the second primary and second antibodies, and before nuclei counterstaining with DAPI.

**Table 3** Primary and secondary antibodies used for protein detection with species, commercial, dilution and incubation information

| **Primary antibody** | **Supplier information** | **Dilution used** | **Incubation** | **Secondary antibody** |
|---|---|---|---|---|
| Rabbit polyclonal anti-CD133 | ab19898 Abcam, England | 1µg/µl | 2h/room temperature | Alexa 546, Cat. No. A11035 |
| Rat monoclonal anti-Abcg2 | ab24115 Abcam, England | 1µg/µl | 2h/room temperature | Alexa 555, Cat. No. A21434 |
| Goat polyclonal anti-Tert | sc-68721 Santa Cruz Biotechnolgy Inc, Germany | 4µg/µl | overnight/+4°C | Alexa 555, Cat. No. A21432 |
| Goat polyclonal anti-Sox2 | sc-17320 Santa Cruz Biotechnolgy Inc, Germany | 4µg/µl | overnight/+4°C | Alexa 555, Cat. No. A21434 |
| Rat monoclonal anti-Nestin | sc-101541 Santa Cruz Biotechnolgy Inc, Germany | 2µg/µl | overnight/+4°C | Alexa 555, Cat. No. A21434 |
| Rabbit polyclonal anti-Nanog | ab80892 Abcam, England | 2µg/µl | 2h/room temperature | Alexa 546, Cat. No. A11035 |
| Rabbit polyclonal anti-Oct4 | AB3209, Chemicon International Inc, USA | 2.5µg/µl | 2h/room temperature | Alexa 546, Cat. No. A11035 |
| Rabbit polyclonal anti-Pax6 | PRB-278P, Covance, California, USA | 3µg/µl | overnight/+4°C | Alexa 546, Cat. No. A11035 |
| Rat monoclonal anti-Lyve-1 (IgM) | sc-65647 Santa Cruz Biotechnolgy Inc, Germany | 0.4µg/µl | overnight/+4°C | Alexa 647, Cat. No. A21248 (IgM) |
| Rat monoclonal anti-CD31 | ab7388, Abcam, England | 0.2µg/µl | 2h/room temperature | Alexa 555, Cat No. A21434 |
| Rat IgG2 | MAB0061, R&D Systems Europe Ltd, England | 1µg/µl | overnight/+4°C | Alexa 555, Cat No. A21434 |
| Rabbit serum | R 9133, Sigma-Aldrich Inc, France | 1µg/µl | 2h/room temperature | Alexa 546, Cat No. A11035 |
| Goat serum | G 9023, Sigma-Aldrich Inc, France | 4µg/µl | overnight/+4°C | Alexa 555, Cat. No. A21432 |

### 6.3 Imagery

Firstly, slides were observed using 10X and 20X objectives (Leica DMR microscope) to select sections to proceed to confocal 20X objective and 63X oil objective microscopy (confocal Zeiss 710). For confocal microscopy a series of z-section images were acquired using Zen 2008 Software (Carl Zeiss GmbH SP1.1 Version 5.0). Fields were averaged 4 times to increase signal to noise ratio, and amplifier gain and offsets of each photomultiplier were adjusted for a given antibody, but were set constant for the sake of comparison between control and wounded corneas. Individual channels were devoid of fluorescence from other emission sources, thus eliminating bleed-through.

For Tert/Dapi colocalisation analysis, the Zen 2008 Software profile option was used to analyse the different colour fluorescence intensities per pixel of the image. This was presented graphically as a colocalisation profile. Fluorescence intensities were normalised to Zen software 2008 standard.

The free online ImageJ Plugin software (National Institutes of Health, USA) was used for quantification of colocalisaiton experiments using two different primary antobodies in different wounded corneal stromal regions (the direct stromal wound zones versus wounded stromal peripheries). ImageJ Plugin quantifies colour channel pixels by means of manual intensity threshold settings. The degree of colocalisation for the colour channels is positively related to the Mander's coefficient (M1), commonly known as the 'overlap coefficient' (OC) and is expressed as a percentage [608]. M1 was calculated in 25,000 pixel D14 stromal wound zone and D14 peripheral wounded stromal tissue areas. In this study, M1 corresponded to total percentage of red pixels that colocalised with green pixels. M1 was calculated 10 independent times for D14 stromal wound zone and for D14 wounded peripheral stromal tissue areas from 5 independent Oct-3/4 (red)/Tert (green) and 5 independent Pax6 (red)/Sox2 (green) colocalisation experiments. Two sample t-tests were carried out to test for a significant difference ($p \leq 0.05$) in M1 in D14 stromal wound zones compared to D14 wounded peripheral stromal tissues for both colocalisation experiments.

## 7 Immunoblotting

To begin with primary antibodies were tested on protein extracted from embryonic mouse heads (E11.5). This was to develop protein extraction methods and test antibody specificity. Accordingly, protein was extracted from control, D14 and D28 wounded stromal tissue samples using a 1ml micro tissue grinder (Wheaton, USA) in PBS with protease

inhibitor cocktail (Roche, France) at $^{+}$4°C. The supernatant was collected following a 10 minute 13,000 rpm centrifugation and protein concentration was determined using a Dc protein assay kit (BioRad, France). This is based on the Bradford Protein Assay method; a colour-based change in absorbance as Coomassie Blue binds to amino acids present in the protein lysate. 10 µg lysates were denatured in 5X sample loading buffer for 5 minutes at 95°C. Lysates were then run on 7.5-10% SDS-PAGE gels, transferred to Hybond-C extra nitrocellulose membranes (GE Healthcare, Canada) and blocked by incubation for 2 hours in 5% non-fat milk or BSA (Cat. No. 04-100-810-C, Euromedex, France). Proteins were then labeled using monoclonal rat anti-Abcg2 (Cat No. ab24115, Abcam, England), monoclonal rabbit anti-Pax6 (Cat. No. ARP32741_P050, Aviva Systems Biology, USA) or monoclonal rat anti-Nestin (Cat. No. MAB353, Chemicon, France) primary antibodies overnight at $^{+}$4°C. Monoclonal rabbit anti-Th (Cat No. ab75875, Abcam, England) primary antibody was used as a housekeeping control. Primary antibody dilutions were 1/500, 1/4000, 1/400 and 1/500 in their respective orders above. Labeling was followed by a 2 hour incubation at room temperature with 1/5000 dilutions of anti-rat and anti-rabbit IgG conjugated with horseradish peroxidase secondary antibodies (Cat. No. A5795 and A9169 respectively, Sigma, USA). Primary and secondary antibodies were diluted in 1% non-fat milk or BSA in PBS/Tween 1%. 3 x 10 minutes washes in PBS/Tween 1% were used between primary and secondary antibody incubations and before visualisation using an ECL-based detection system (Chemiluminescent Peroxidase Substrate-3 kit, Sigma, France). Prestained protein ladders were used for molecular weight determination (Cat. No. SM0671, SM1811, Fermentas, France).

## Figure 1

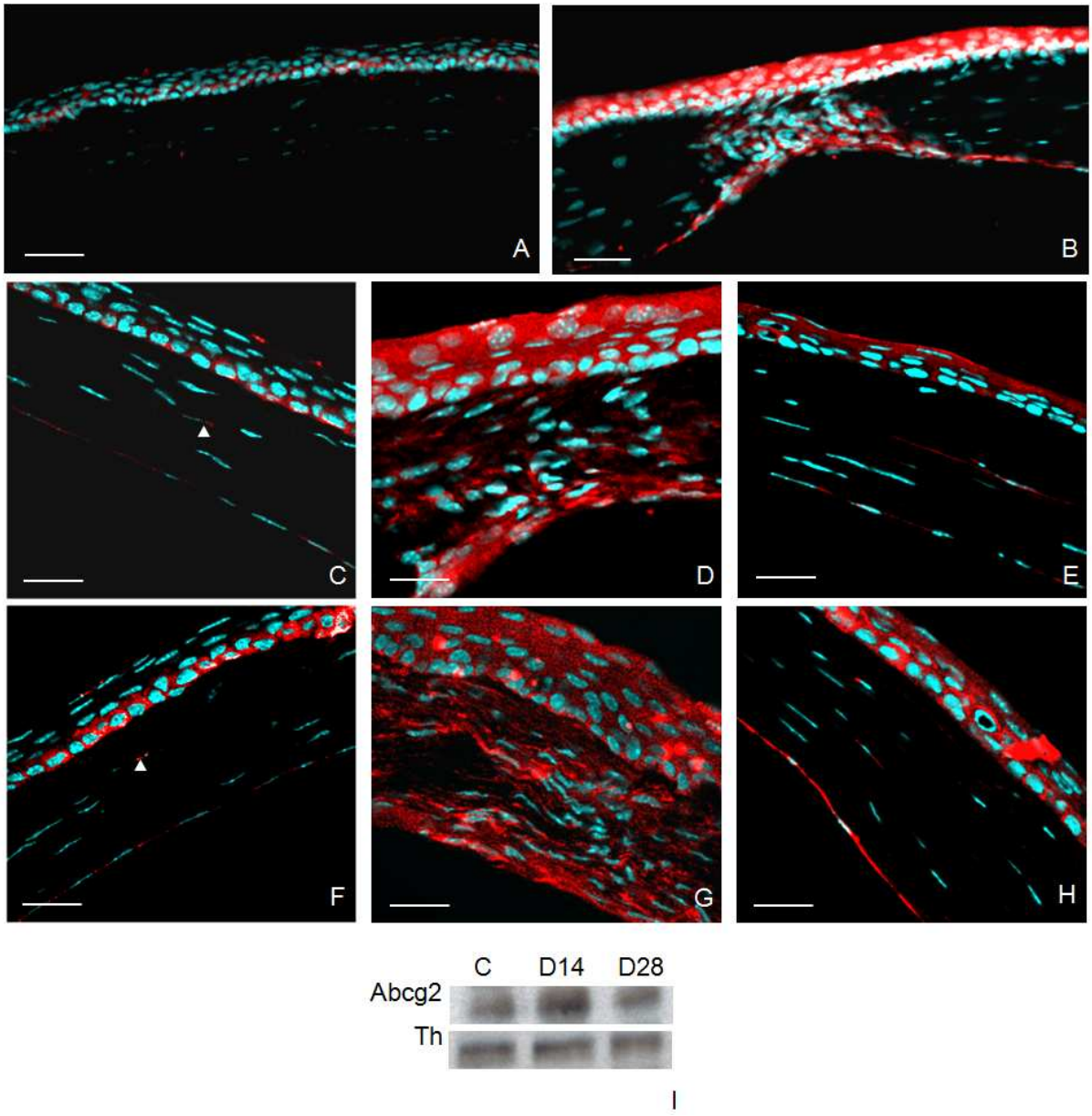


**Figure.1. Increased Expression of Keratocyte Progenitor Cell Markers during *in vivo* Corneal Wound Repair: ABCG2 and CD133.**

(A-E) Abcg2 immunostaining (red). (F-H) CD133 immunostaining. (A, C, F) Control cornea. Arrowheads highlight Abcg2-positive (C) or CD133-positive (F) cells. (B) D14 wounded cornea. (D, G) D14 wounded zone. (E, H) D28 wounded zone. Nuclei are counterstained with DAPI. (A-B) X200; scale bars represent 50 µm. (C-H) X630; scale bars represent 20 µm. (I) Western blot analysis of Abcg2 protein (72 Kda) expression in control (C), D14 and D28 wounded stromas. Th (59 Kda) was used as a housekeeping control in control (C), D14 and D28 wounded stromas.

# IV Results and Discussion

Previous studies have claimed the identification of a potential repair subpopulation of cells expressing stem cell markers in the corneal stroma of several different species [403-405, 457, 458, 511, 513]. These studies were based on either *in vitro* cell studies or unwounded corneas. **Here we report for the first time the identification of stromal stem cell markers in the *in vivo* murine wounded cornea**. Firstly, we demonstrate upregulation of known adult tissue stem cell markers in the wounded stroma. Secondly, the wounded stroma demonstrates upregulation of transcription factors important both for the maintenance of embryonic stem cell properties as well as ocular differentiation. Moreover, we show for the first time that the *in vivo* wounded corneal stroma can activate telomerase to extend cell division potential.

## 1 Increased Expression of Keratocyte Progenitor Cell Markers during *in vivo* Corneal Wound Repair

### 1.1 Abcg2 and CD133 Protein Expression is Increased in Stromal Wound Zones

Firstly, we wanted to know if the normal corneal stroma harboured Abcg2 and CD133 expression. We checked for this by simple immunostaining experiments. The control cornea expressed Abcg2 and CD133 in the limbal basal epithelial cell layer [521], and by a small number of stromal cells (Fig.1.A, C, F). This confirmed results by Du et al., (2005) [403] and Thill et al., (2007) [513] claiming that a minority of normal human stromal cells express Abcg2 and CD133 respectively. We then checked if Abcg2 and CD133 protein expression changed in wounded stromal tissues. D7 (data not shown) and D14 post-wounding, Abcg2 and CD133 expression appeared more intense in the epithelium, endothelium, and was particularly increased in the stromal wound zones (Fig.1.B, D, G). No Abcg2 (Fig.1.B) or CD133 (data not shown) protein expression was localised in the stroma beyond the wound zone. In D28 stromal wound zones, Abcg2 and CD133 expression still appeared higher than in the control cornea (Fig.1.E, H). Fig.1.I shows that immunoblot results for Abcg2 protein expression were consistent with the immunostaining data. Abcg2 protein expression was higher in D14 wounded stromas compared to control stromas.

In summary, upon corneal incision Abcg2 and CD133 protein expression increased in

## Figure 2

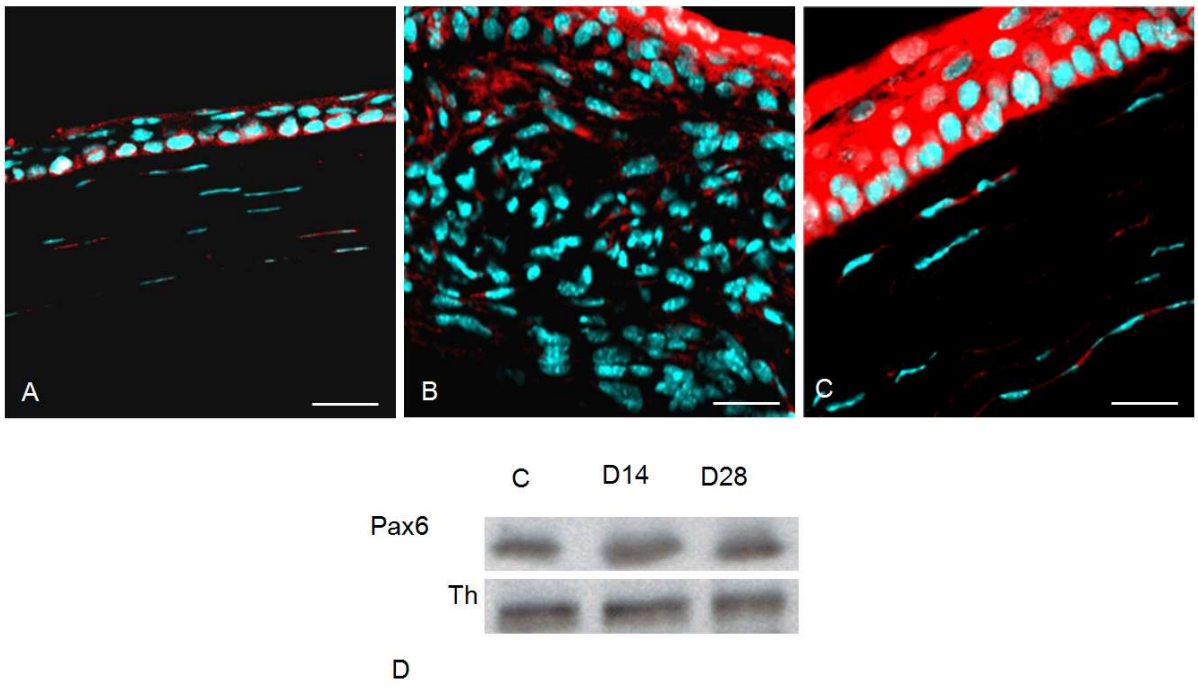


**Figure.2. Increased Expression of Keratocyte Progenitor Cell Markers during *in vivo* Corneal Wound Repair: Pax6.**

(A-C) Pax6 immunostaining (red). (A) Control cornea. (B) D14 wounded zone. (C) D28 wounded zone. Nuclei are counterstained with DAPI. X630; scale bars represent 20 µm. (D) Western blot analysis of Pax6 protein (48 Kda) expression in control (C), D14 and D28 wounded stromas. Th (59 Kda) was used as a housekeeping control in control (C) and D14 and D28 wounded stromas.

stromal wound zone cells, and this expression remained upregulated for 1 month. This implies that the normal corneal stroma could harbour a locally-derived Abcg2- and CD133-positive cell subpopulation that expands and is sustained in the stroma throughout the stroma remodelling process. This also correlates with an observation of elevated numbers of CD133-positive cells found in human diseased corneas by Thill et al., (2007) [513]. Both Abcg2 and CD133 protein expression was only localised within the stromal wound zone, and not within peripheral stromal tissue away from the wound, implying that these markers are **specific to a cell population recruited to the direct wound zone for a specific repair function**.

Given the wide adult tissue stem cell expression of the CD133 marker [515-518], the exact origin of the corneal stromal cells that express CD133 is unclear. At this stage both ideas of an *in situ* undifferentiated stromal progenitor cell marker [516-518], or an external bone marrow-derived progenitor cell marker [514, 515] are plausible.

### 1.2 Pax6 Expression is Increased in Stromal Wound Zones

We tested for an upregulation of Pax6 expression in wounded stromas. Again, we tested for differences in Pax6 protein expression between control and wounded corneas by immunostaining. Control corneal stroma showed low Pax6 protein expression by approximately half of stromal cells (Fig.2.A). In D7 (data not shown) and D14 stromal wound zones Pax6 protein expression was more intense, and still at least half of stromal wound zone cells were Pax6-positive (Fig.2.B). By D28 post-wounding, stromal Pax6 expression was still more intense than in the control stroma (Fig.2.C). Fig.2.D shows that immunoblotting results were consistent with immunostaining results for Pax6 protein expression. Pax6 protein expression was detected in control stroma, and expression was slightly increased in D14 and D28 wounded stromal tissue samples. Housekeeping control Th protein expression was constant across control, D14 and D28 wounded stromas.

Similar to Funderburgh et al., (2005) [404], Du et al., (2005) [403] and Du et al. (2007) [458], we found that Pax6 was expressed in the normal corneal stroma. However, these previous *in vitro* and *ex vivo* reports showed that only a small fraction (approximately 4%) of total bovine and human stromal cells were Pax6-positive. These results are concordant with total percentages of different progenitor cells in different muscle and skin dermal tissues. In these tissues progenitor cells account for 2- 9% of the total cell population of their cell niches [609-613]. On the contrary, we detected low levels of Pax6 protein in at least half of normal

**Figure 3.A**

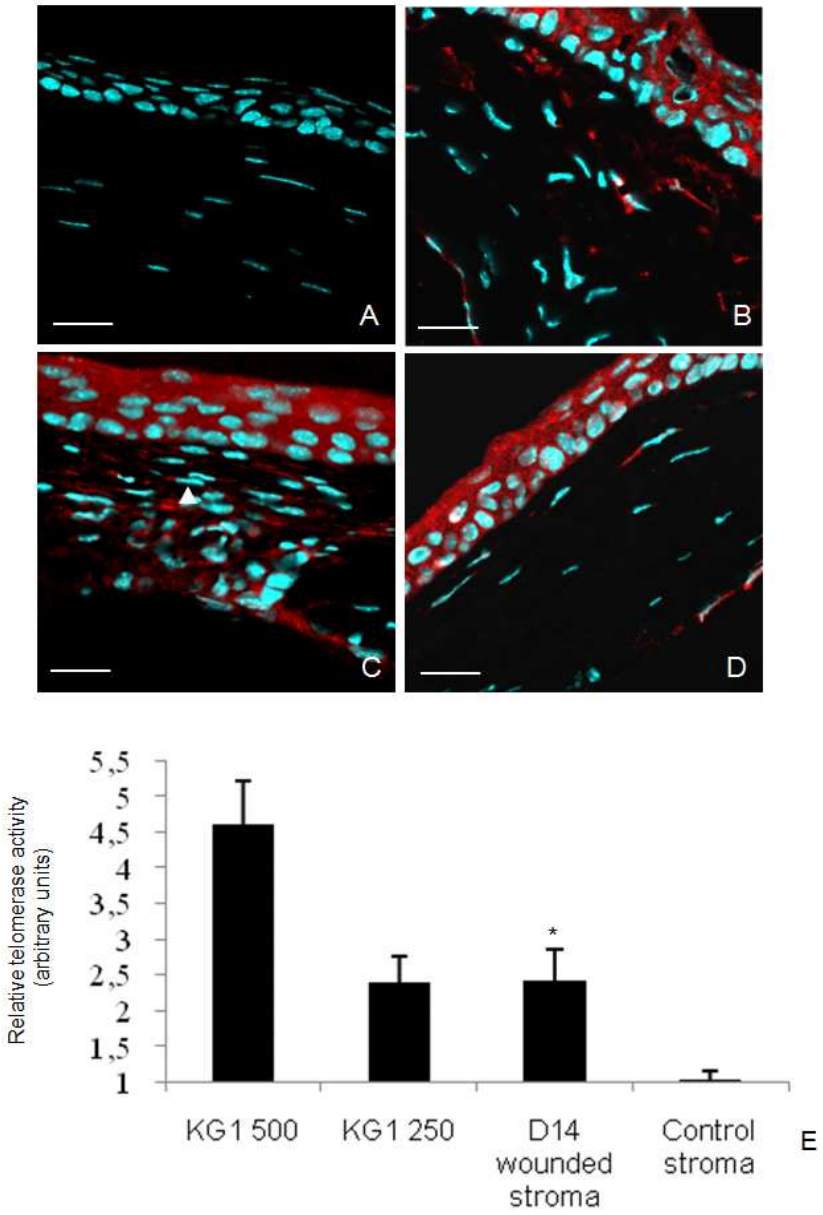


**Increased Expression of Keratocyte Progenitor Cell Markers during *in vivo* Corneal Wound Repair: Tert.**

Figure.3.A. Tert Protein Expression and Activity in Control and Wounded Stromas. (A-D) Tert immunostaining (red). (A) Control cornea. (B) D7 wounded zone. (C) D14 wounded zone. (D) D28 wounded zone. Nuclei are counterstained with DAPI. X630; scale bars represent 20 µm. (E) Telomerase activity assay. D14 wounded stromas were compared to control stromas. The stromas of six control corneas and the stromas of six D14 wounded corneas were pooled. Data (mean±SEM) are from three independent experiments. Activity is normalised to the negative control (lysate buffer). Human KG1 myeloblastic cells were used as a positive Tert activity control. KG1 500/250= 500/250 equivalent cells respectively. *p≤0.05. For arrowhead (C) see Fig.3.C.

corneal stromal cells. These different observations are likely to be down to inter-species differences. In our mouse model, Pax6 expression could correspond in majority to adult keratocyte cells, and in minority to a stromal progenitor cell subpopulation. This theory is supported by reports made on an axolotl tail regeneration model in which all embryonic, differentiated mature, and regenerating mature spinal cord (neural tube) tissues showed Pax6 expression [614]. In wounded corneal stromas, Pax6 protein expression increased in the stromal wound zone, and again at least half of the stromal cells expressed Pax6 protein. Overall, considering that Pax6 is expressed throughout ocular development [589], and there has been reports that Pax6 is expressed in regenerating adult ocular tissues [446, 448, 585], we can conclude that the majority of cells in the stromal wound zone are progenitor and/or keratocyte cells of ocular origin.

### 1.3 Identification of an Active Stromal Progenitor Cell Population: Increased Tert Protein Expression and Activity in Wounded Stromas

We wanted to know if stromal cells harboured functional progenitor cell function during corneal wound healing. Thus, we investigated Tert expression and activity as it is considered to be a stem cell marker upregulated in regenerative progenitor cells compared to somatic cells [590, 591]. Firstly, we compared Tert protein expression between control and wounded stromal tissues. Control cornea staining with Tert showed no reaction in the stroma, or the epithelial or endothelial cell layers (Fig.3.A.A). We observed an increase in Tert expression in wounded corneal epithelial and endothelial cells compared to the control cornea (Fig.3.A.B-D). Tert expression was increased in the D7 stromal wound zone, but not all stromal cells were Tert-positive (Fig.3.A.B). D14 wounded stromal zone showed high Tert expression and all stromal cells were Tert-positive. (Fig.3.A.C). At D28, the wounded stroma still showed higher Tert expression than in D7 and control stromas (Fig.3.A.D). We concluded that Tert stromal protein expression reached its highest level at approximately D14 of the stromal wound healing process, and then decreased by D28. Thus, D14 wounded stromas were used to compare Tert activity to control stromas. At D14 post-wounding telomerase activity was more than double (2.4-fold increase) in wounded stromas compared to unwounded stromas (Fig.3.A.E).

Figure.3.B.

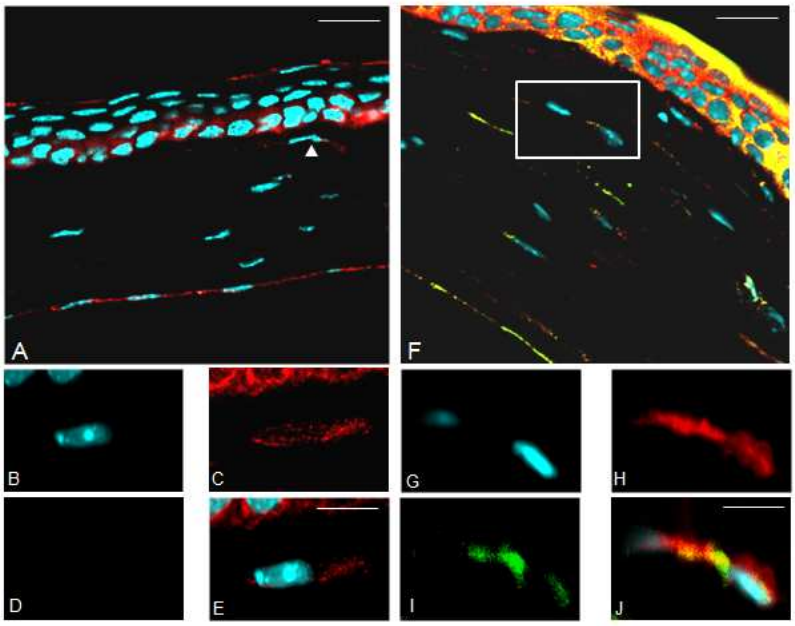


Figure.3.C.

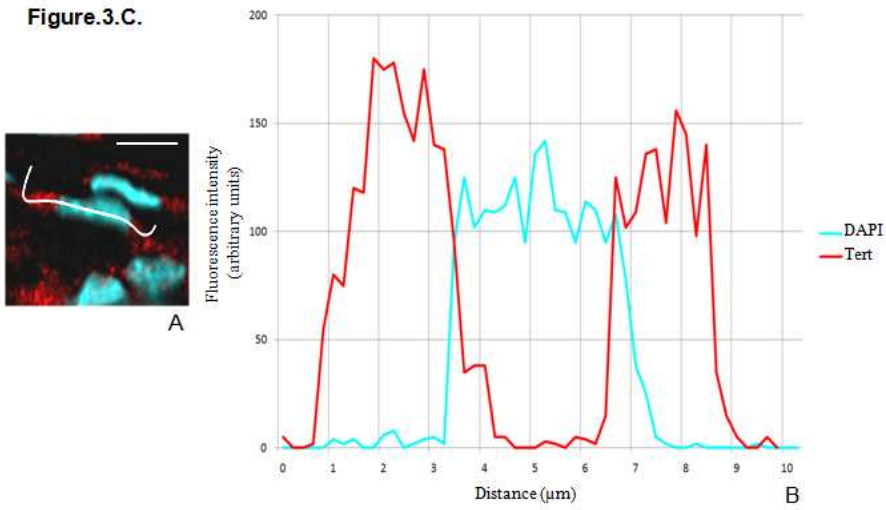


**Increased Expression of Keratocyte Progenitor Cell Markers during *in vivo* Corneal Wound Repair: Tert.**

Figure.3.B. Tert (green)/Abcg2 (red) colocalisation in Wounded Stromas. (A) Control cornea. X630; scale bar represents 20 µm. (B-E) X2500 magnification of arrowhead in Fig.A. Scale bar represents 5 µm. (F) D14 proximal wound zone stromal tissue. Proximal tissue corresponds to intact and more highly organised corneal tissue neighbouring the direct incision wound zone. X630; scale bar represents 20 µm. (G-J) X2500 magnification of inset in F. Scale bar represents 5 µm. Nuclei are counterstained with DAPI.

Figure.3.C. Cytoplasmic Tert Protein Localisation in D14 Wound Zone Stromal Cells. (A) X2500 magnification of cell arrowed in Fig.3.A.C. Scale bar represents 5µm. (B) Colocalisation profile of red (Tert) and blue (DAPI) fluorescence intensities per pixel along the line in A. Intensities are normalised to Zen software 2008 standard.

**This is first time in *vivo* evidence that the wounded corneal stroma has been observed to upregulate telomerase activity in response to corneal injury.** Moreover, Tert-positive cells in D7 (data not shown) and D14 (Fig.3.B) wounded stromas colocalised with Abcg2 protein. This suggests that Abcg2- and CD133-positive stromal cells are likely to correspond to **corneal stromal progenitor cells that are mitotically active in the wounded stroma.**

Tert preserves telomere length during cell division-dependent DNA replication and is considered a necessary enzyme to escape senescence, promote cell survival, and maintain the possibility of unlimited cell divisions [590, 591]. It would be expected that an increase in Tert activity would correlate with an increase in division of progenitor cells in the wounded stroma. Logically, for this Tert activity function, it was initially considered that Tert was only active once translocated into the nucleus and recruited to chromosome telomeres [615]. We would expect to observe this for cells undergoing mitosis. Note that Tert protein expression was found to be in majority cytoplasmic in D14 wounded stromal cells (Fig.3.C).

Interestingly, now, both cytoplasmic and nuclear Tert protein expression and activity has been demonstrated by mesenchymal stem cells from human amyotrophic lateral sclerosis subjects and glioblastomas [616], mesenchymal progenitor cells from human endometria [617] and embryonic neural cells [618]. Moreover, cytoplasmic Tert protein-interacting proteins and signaling events have been found to play a role in anti-apoptotic effects, suggesting a survival promoting function of cytoplasmic Tert [619]. Thus, Tert in corneal stromal progenitor cells could function to elicit not only protection throughout cell division, but additionally promote a survival signal during the stromal wound response. Contrarily, we cannot exclude that cytoplasmic Tert protein expression could correspond to mitochondrial trafficking of Tert for degradation [615], or translocation of inactive Tert protein back into the cytoplasm [620].

**Figure 4**

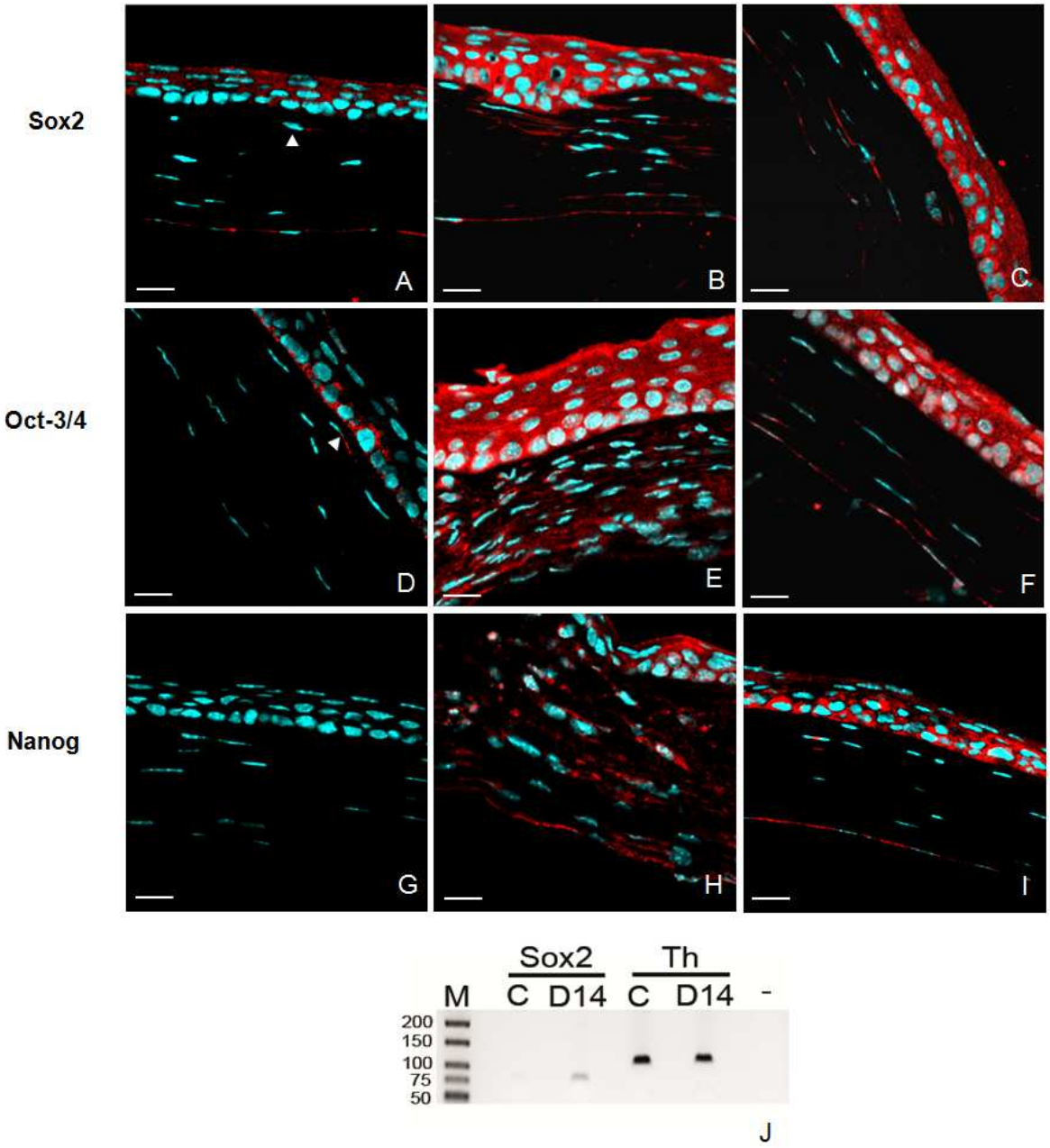


**Figure.4. Corneal Stromal Cells Reexpress Their Embryonic Stem Cell Markers.** (A-C) Sox2 immunostaining (red). (D-F) Oct-3/4 immunostaining (red). (G-I) Nanog immunostaining (red) (A, D, G) Control cornea. Arrowheads; Sox2-positive (A) and Oct-3/4 positive (D) cells. (B, E, H) D14 wounded zone. (C, F, I) D28 wounded zone. Nuclei are counterstained with DAPI. X630; scale bars represent 20 µm. (J) Agarose gel electrophoresis quantification of *Sox2* RT-qPCR products (75 bp amplicon) in control (C) and D14 wounded stromas. Controls: *Th* housekeeping gene control (110 bp amplicon) was used in control (C) and D14 wounded stromas. (-) Negative control. (M) DNA ladder, 50 bp.

## 2 Reexpression of Embryonic Cell Markers in the Wounded Stroma Corresponds to an Activated Adult Keratocyte Phenotype

### 2.1 Increased Sox2, Oct-3/4 and Nanog Expression in Wounded Stromas

Having demonstrated the existence of a potential stromal progenitor cell population, we investigated expression of embryonic stem cell markers expressed by neural crest-derived tissues to further investigate progenitor cell lineage. We tested for differences in Sox2, Oct-3/4 and Nanog protein expression between control and wounded stromal tissues by immunostaining. We found that Sox2 protein was expressed in the normal corneal epithelium and endothelium, and a small number of stroma cells were also Sox2-positive (arrowhead) (Fig.4.A). Oct-3/4 protein was expressed by limbal basal epithelial cells [621], and was also expressed by a minority of stroma cells (arrowhead) in the normal cornea (Fig.4.D). Nanog protein was not expressed in the normal cornea (Fig.4.G). In the D7 (data not shown) and D14 wounded stroma, Sox2 protein expression was more intense in the epithelium and in the stromal wound zone. The majority of the stromal cells showed Sox2 protein expression (Fig.4.B). In the D28 wounded stromal zone, Sox2 protein expression still appeared higher than in the control, and at least half of the stromal cells were Sox2-positive (Fig.4.C). The same increase in expression was observed for Oct-3/4 and Nanog proteins in D7 (data not shown), D14 (Fig.4.E, H) and D28 (Fig.4.F, I) wounded stromal zones. *Sox2* gene expression (mRNA) was assayed by RT-PCR and agarose gel electrophoresis in control and D14 wounded stromas (Fig.4.J). Control stroma showed low *Sox2* mRNA expression. *Sox2* mRNA expression was higher in the D14 wounded stroma compared to the control stroma, concordant with Sox2 immunostaining results. Housekeeping control gene *Th* mRNA expression was constant across control and D14 wounded stromas.

*Sox2* RT-qPCR product sequences corresponded to the published Mus musculus Sox2 sequence, confirming amplification of the Sox2 gene by our primers (data not shown).

In summary, we report an **upregulation of the expression of embryonic stem cell markers Sox2, Oct-3/4 and Nanog** throughout 1 month of the stromal wound repair process. Protein expression of the these stem cell markers in the stromal wound zone is likely to localise to the same stromal progenitor cells expressing adut tissue stem cell markers, as the majority of wound zone stromal cells were positive for adult and embryonic stem cell markers (Fig.1). As Sox2, Oct-3/4 and Nanog are expressed by late embryonic neural crest stem cells [359] implies that a high proportion of stromal wound zone cells could be progenitor cells of neural crest origin.

**Figure 5**

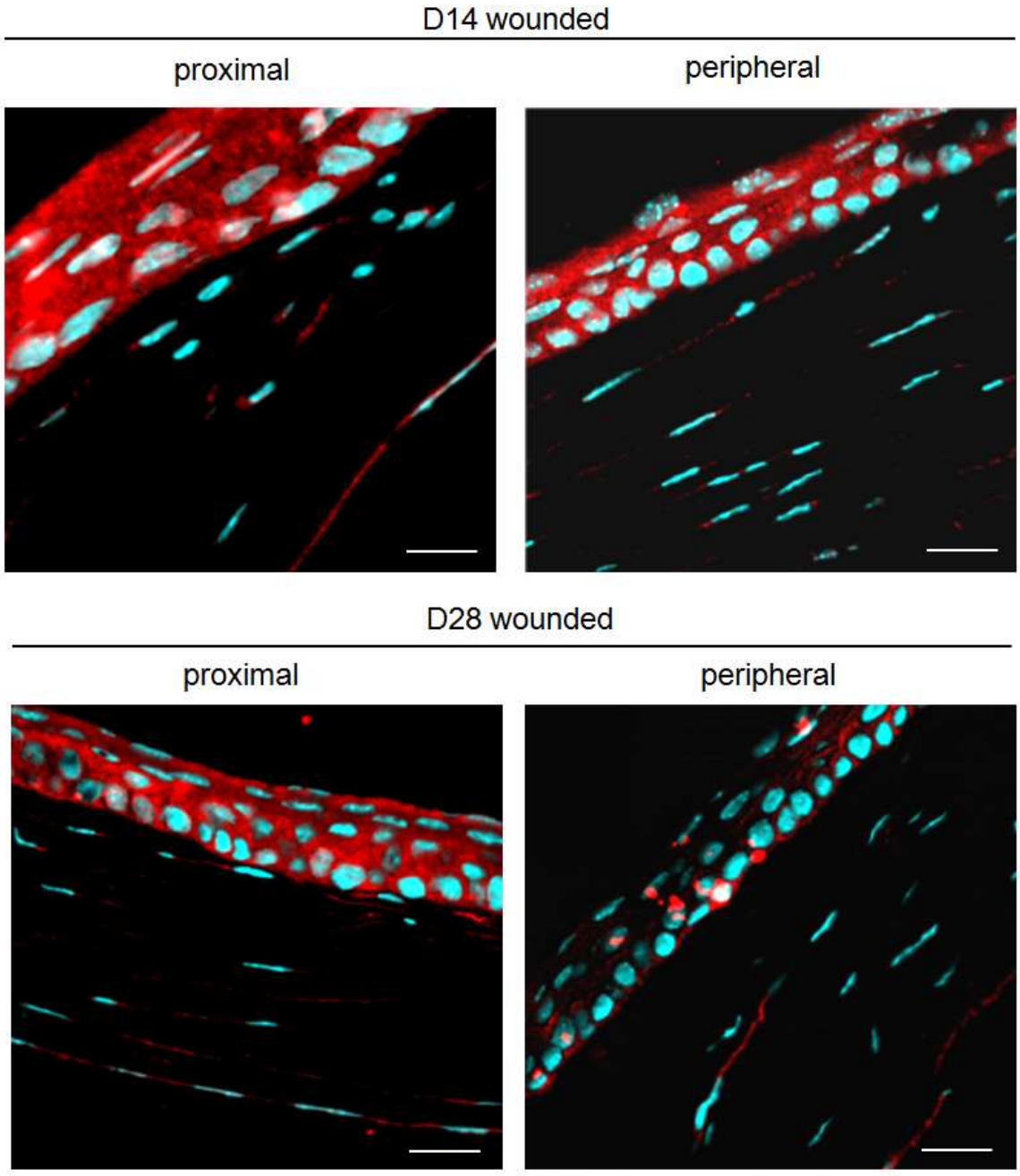
D14 wounded
proximal
peripheral
D28 wounded
proximal
peripheral

## 2.2 Upregulated Stem Cell Marker Exression throughout the Entire Wounded Stroma

Unlike Abcg2 and CD133 protein expression that was expressed exclusively in the stromal wound zone (Fig.1.B), we found Sox2 (Fig.5), Oct-3/4, Nanog, Pax6 and Tert (data not shown) protein was expressed throughout the entire wounded stroma at D7 (data not shown), D14 (Fig.5) and D28 (Fig.5) post-wounding. As well as protein expression localised in the stromal-incised wound zone as previously described, protein expression of these markers was also localised in proximal wound zone stromal tissue and in stromal tissue away from the wound zone (Fig.5). Proximal and peripheral wounded stromal tissue protein expression followed the same expression pattern as observed in the stromal wound zones; more stromal cells were positive for each protein marker in D14 wounded proximal and peripheral stromal tissues than in D28 wounded proximal and peripheral stromal tissues. By D28 post-wounding only a few cells in proximal and peripheral wounded stromal tissues showed protein expression, but expression still appeared higher than in equivalent control stromas.

Among reports demonstrating that Sox2, Oct-3/4 and Nanog expression in somatic multipotent progenitor cells functions in a manner that mirrors its roles in embryonic stem cells [566-568, 587], an *ex vivo* rat tracheal epithelial wound model showed that surviving $G_0$ blocked epithelial repair stem cells expressed Sox2, Oct-3/4 and Nanog proteins. However, these stem cells were a small population of cells among many other non-stem cell types (somatic cells), not expressing stem cell markers in the regenerating epithelial tissue [588]. **How can we explain this drastic upregulation of stem cell markers by adult stromal cells in the wounded cornea?**

## 2.3 A High Proportion of Sox2, Oct-3/4 and Nanog Expression in the Wounded Corneal Stroma does Not Correspond to Progenitor Cells

Based on the observation of global wounded corneal stromal tissue expression of stem cell markers, we thought that the expression of stem cell markers may not be specific to stromal progenitor cells as it seemed unrealistic to think that the wounded stroma could be populated by such a high quantity of progenitor cells. Taking into account that Tert is considered to be upregulated in progenitor cells compared to somatic adult cells [591], we carried out colocalisation experiments to determine if cells that expressed embryonic stem

Figure.6.A

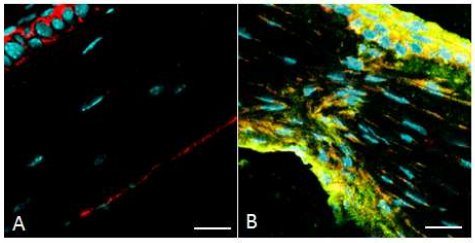


Figure.6.B

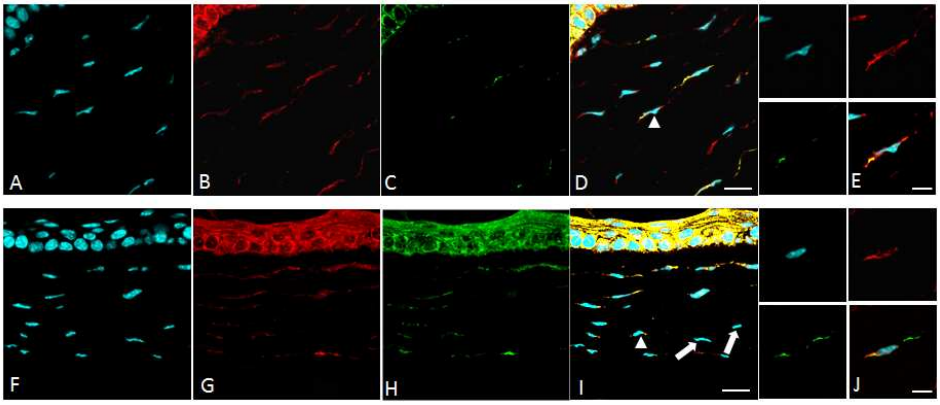


K

**i. Total % of Oct-3/4 stromal expression that colocalises with Tert expression**

| D14 wounded zone | | D14 wounded periphery | | |
|---|---|---|---|---|
| Mean | SEM | Mean | SEM | p-value |
| 95 | 0.01698 | 26 | 0.03057 | <0.0001* |

**ii. Total % of Pax6 stromal expression that colocalises with Sox2 expression**

| D14 wounded zone | | D14 wounded periphery | | |
|---|---|---|---|---|
| Mean | SEM | Mean | SEM | p-value |
| 96 | 0.01260 | 93 | 0.01079 | 0.0964** |

**Figure.6. Colocalisation of Stem Cell Markers in Wounded Stromas.**

**Figure.6.A. D14 Wounded Zone: Oct-3/4 (red) and Tert (green) coimmunostaining.** (A) Control cornea. (B) D14 wounded zone. X630; scale bar represents 20 µm.

**Figure.6.B. D14 Wounded Peripheral Tissue**: **(A-E) Oct-3/4 (red) and Tert (green) coimmunostaining** (E) Magnification (X2500) of cell (arrowhead) in (D). Scale bar represents 5 µm.

**(F-J) Pax6 (red) and Sox2 (green) coimmunostaining**. X630; scale bar represents 20 µm. (J) Magnification (X2500) of cell (arrowhead) in (I). Arrows indicate $Pax6^-/Sox^-$ cells. Scale bar represents 5 µm. Nuclei are counterstained with DAPI.

**(K) % Colocalisations in wounded stromas**. Calculations of M1 (total percentage of red pixels that colocalise with green pixels) in D14 wounded stromal zones and D14 wounded peripheral stromal tissues. (i) Stromal Oct-3/4 protein (red) expression colocalisation with Tert protein (green) expression. (ii) Stromal Pax6 protein expression (red) colocalisation with Sox2 protein (green) expression. The mean and SEM are calculated from 10 independent confocal images from 5 independent D14 wounded corneas. * represents a statistical significant difference in M1 in D14 wounded stromal zones compared to D14 wounded peripheral stromal tissues. ** represents no statistical significant difference in M1 in D14 wounded stromal zones compared to D14 wounded peripheral stromal tissues.

cells markers colocalised with Tert protein expression (likely to be progenitor cells) in wounded stromal tissues, or not.

Fig.6.A shows high colocalisation of Oct-3/4 and Tert expression in the D14 stromal wound zone (B) compared to in the control cornea (A). In the D14 wounded stromal periphery, only a small proportion of Oct-3/4-positive cells (red) were also Tert-positive (green) (Fig.6.B.(A-D)). Fig.6.B.(E) shows colocalisation of Oct-3/4 and Tert to the same stromal cell. Calculation of the Mander's coefficient (M1) demonstrated that total Oct-3/4 protein that colocalised with Tert protein in the D14 stromal wound zone (mean 95%) was significantly higher than within the D14 wounded stromal periphery (mean 26%) (Fig.6.B.(K.i)). Thus, we rejected the null hypothesis of equal means (t= 19.6498, df = 18, p-value = $1.306x10^{-13}$).

We also carried out Pax6 and Sox2 colocalisation experiments to test for the possible indication of non-ocular-derived progenitor cells in the wounded stromal peripheries that could express embryonic stem cell markers. Similar to Fig.6.A.(B), Pax6 and Sox2 protein colocalisation experiments showed high colocalisation of Pax6 and Sox2 protein expression within the D14 stromal wound zone (data not shown). The majority of Pax6-positive cells were also Sox2-positive in the D14 wounded stromal periphery (Fig.6.B.(F-I)). A small number of cells in the D14 wounded stromal periphery were negative for both Pax6 and Sox2 protein expression (Fig.6.B.I). Fig 6.B.(J) highlights colocalisation of Pax6 and Sox2 protein to the same stromal cells within the D14 wounded stromal periphery. We found no significant difference between the total percentage of Pax6 protein that colocalised with Sox2 protein in the D14 wound zone (mean 96%) compared to the D14 wounded stromal periphery (mean 93%) (Fig.6.B.(K.ii)). Thus, we accepted the null hypothesis of equal means (t = 1.7545, df = 18, p-value = 0.09635)

These results demonstrate that Oct-3/4 and Tert colocalisation was very high within cells in the stromal wound zones, whereas the majority of Oct-3/4-positive cells in the wounded stromal peripheries were Tert-negative, (even though a small number of Tert-positive cells were localised in the stromal peripheries). Together these findings indicate that:

1. The majority of wounded peripheral stromal cell expression of undifferentiated embryonic stem cell markers may not correspond to progenitor cells, but to **non-progenitor stromal cells**.

2. The minority of Tert-positive progenitor cells localised throughout the wounded peripheral stromal tissues (Abcg2/CD133-negative) could be a different progenitor population to those within the stromal wound zone, (Abcg2/CD133-positive).

These theories suggest that a high proportion of undifferentiated stem cell marker expression in the wounded stroma could actually correspond to non-progenitor adult keratocyte cells. We could deduce that adult **keratocyte cells generally revert to an activated wound response state in the wonded stroma**, even in stromal tissue away from the wound zone.

Secondly, given that the majority of peripheral wounded stromal cells were Pax6-positive, we can conclude that the wounded stromal peripheries are populated in majority by ocular-derived cells. Moreover, almost all Pax6-positive cells colocalsied with Sox2 protein, suggesting that the cells we observe in the peripheral wounded stromal tissues are highly likely to be activated adult keratocyte cells and progenitor cells. A minority of Pax6- and Sox2-negative cells were however localised in the D14 wounded peripheral stromal tissues. It is likely that these could cells correspond to either inflammatory cells or non-ocular cells that migrate into the stroma as previously decribed by Nakamura et al., (2005) [510], Sosnova et al., (2005) [511] and Barbosa et al., (2010) [369].

### 2.4 The "Half Way State"

Going back to the *ex vivo* rat tracheal epithelial cell wound model, once $G_0$ blocked epithelial repair stem cells differentiated into downstream ciliate, mucous or basal cells, expression of Sox2, Oct-3/4 and Nanog was lost [588]. Moreover, it has recently been shown that introducing transient Oct-3/4 expression to adult human keratinocyte cells was enough to change their differentiation pathway [622]. These studies show that transcription factors involved in early stem cell self-renewal can be contextually activated in more mature tissues to foster proliferation and susceptibility to environmental differentiation signals. These findings, along with our observations, allow us to hypothesise that the adult keratocyte cell could retain a relative plasticity, being able after an injury to reactivate embryonic pathways in order to heal the stromal wound. Together with the observations made that late embryonic keratocyte cells could retain a larger undifferentiated phenotype of their neural crest origins than initially considered [284, 359] implies that at least some wounded stromal cells identified

could in fact be **activated keratocyte cells that exhibit an "embryonic-like" phenotype**. Similarly, it has recently been demonstrated that other regenerative blastema-type tissues, notably the tip of the zebrafish fin, are regulated by a range of factors (notably Oct-3/4 and Sox2) do not fully depend on regulation by pluripotent factors, but may retain more embryonic features from their tissues of origin than previously considered [623, 624]. This has been termed the "**half way state**" [623]. In this project we cannot distinguish between marker profiles of the"activated keratocyte half way state" cell phenotype from the stromal progenitor cell phenotype as expression profiles overlap for the moment. Thus, our results additionally suggest that the minority of normal corneal stroma residing cells expressing embryonic stem cell markers could either correspond to a progenitor cell population and/or to a minority of adult keratocyte cells going through the turnover programme. Finally, a role for active half way state keratocyte cells in the stromal wound response remains undertermined, but we cannot exclude a migration of this cell type into the stromal wound zone for a repair function.

**Figure 7**

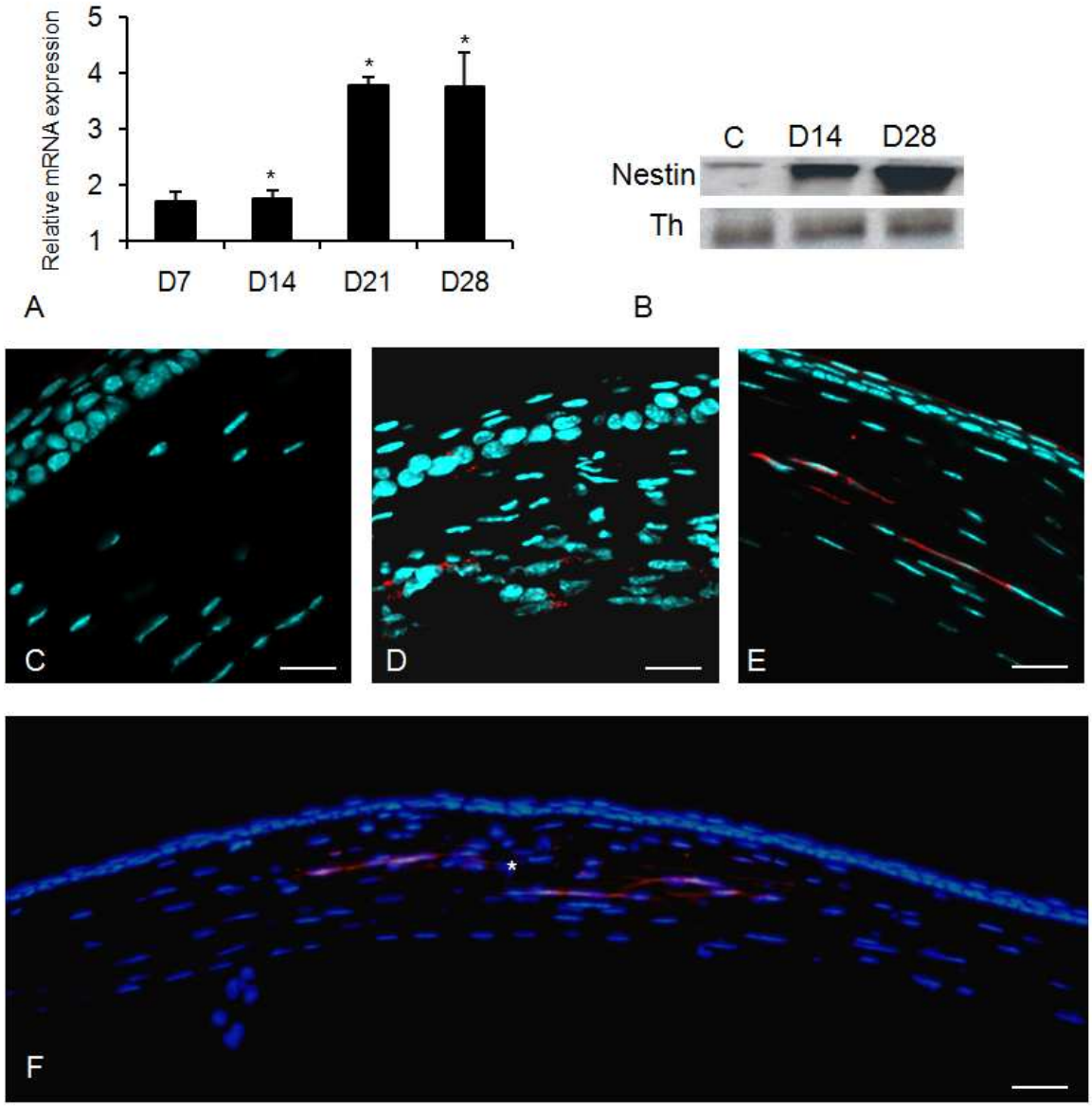


**Figure.7. A Neural Crest-Derived Repair Pathway Replenishes Lost Keratocyte Cells.** (A) *Nestin* mRNA was assayed in control and D7-D28 wounded stromas by RT-qPCR. Expression in wounded stromas is normalised to the expression in control stromas. *p≤0.05. Bars represent SEM for independent wounded stromal samples. (B) Western blot analysis of Nestin protein (220 Kda) expression in control (C), D14 and D28 wounded stromas. Th (59 Kda) was used as a housekeeping control in control (C), D14 and D28 wounded stromas. (C-F) Nestin immunostaining (red). (C) Control cornea. (D) D14 wounded zone. (E) D28 wounded zone. X630; scale bars represent 20 µm. (F) D28 wounded cornea. X200; scale bars represents 70µm. * corresponds to incision wound zone. Nuclei are counterstained with DAPI.

## 3 A Neural Crest-Derived Repair Pathway Replenishes Lost Keratocyte Cells

### 3.1 Increased Nestin Expression in Later Stroma Remodelling Stages

Nestin marker analysis demonstrated a different expression pattern to all other adult and embryonic stem cell markers analysed in this project. *Nestin* mRNA was found to be upregulated at D14 post-wounding (approximately 1.5-fold), but was upregulated to a greater extent at D21 and D28 post-wounding (approximately 3.7-fold) (Fig.7.A). Nestin protein expression analysed by both immunoblotting (Fig.7.B) and immunostaining (Fig.7.C-E) followed the same trend. Immunoblotting results showed low Nestin protein expression in control stromas. Nestin protein expression increased in D14 wounded stromas, but was most highly expressed in D28 wounded stromas. Housekeeping control Th protein expression was constant across control, D14 and D28 wounded stromas. Nestin immunostaining in control stroma showed no reaction (Fig.7.C). D7 (data not shown) and D14 wounded corneas show Nestin expression by a few stromal cells in the wound zone (Fig.7.D). Nestin protein expression was significantly increased in the stroma at D28 post-wounding (Fig.7.E). In the stromal wound zone Nestin-positive cells were arranged in a linear, grouped organisation and showed an elongated morphology, indicating also that Nestin protein expression of neighbouring cells overlapped. This implied a stromal cell-cell network, characteristic of normal stromal keratocyte cells embedded in the normal stromal ECM [269].

### 3.2 The “Half Way State” versus Dedifferentiation

Similar to Sox2, Oct-3/4 and Nanog, Nestin is known to be expressed by neural crest precursor cells during early embryogenesis [460-462], but also in several mitotically active adult stem cells [465, 466]. The Nestin promoter contains a POU-domain enhancer element [460], implying that the Oct-3/4 transcription factor may regulate Nestin expression. This theory has already been demonstrated where an Oct-3/4 molecular programme was thought to regulate the differentiation pathway of different adult mesoderm stem cell lineages into a Nestin-positive neural cell lineage [583]. An interesting point is that Nestin-positive cells were not found in peripheral corneal stromal tissues, but only in the direct stromal wound zone and proximal wounded stromal tissue. Expression was observed in the central stroma, not in epithelial- and endothelial-proximal stromal tissues (Fig.7.F). The Nestin-positive cells showed a highly similar cell morphology to adult keratocyte cells, but we know that Nestin is not expressed by adult keratocyte cells [467]. Nestin positive protein intermediate filaments

could be incompatible with specific cytoskeleton organisation required to maintain corneal stroma transparency. It could be that undifferentiated cell signals (notably Oct-3/4) regulate Nestin expression in some stromal wound zone cells, and that these cells then enter a keratocyte regeneration pathway to eventually replenish sites devoid of adult keratocytes. Thus, Nestin-positive cells could in fact be:

- **Neural crest-derived progenitor cells that could eventually differentiate into keratocyte cells** once Nestin expression is lost**.**
- **Activated keratocytes that have exceeded their "half way state" and need to dedifferentiate into keratocyte cells** once Nestin expression is lost via the reactivation of their embryological signaling pathways.

If this is the case, the Sox2/Oct-3/4/Nanog-positive and Nestin-negative cells localised throughout the remainder of the wounded stroma could correspond to activated keratocyte cells that do not go beyond their "half-way state", instead regaining their quiescent keratocyte state once they lose their expression of undifferentiated cell markers [572, 625].

## 4 Different Interpretations of the Upregulation of Progenitor Cell and Undifferentiated Keratocyte Cell Markers in the Wounded Stroma

Several alternative studies bringing forward interesting theories contest our ideas of the existence of an *in situ* corneal stromal progenitor subpopulation and of an undifferentiated adult keratocyte phenotype in the corneal stroma that are both activated following corneal injury.

### 4.1 What Happened to the Famous Myofibroblast Cells?

Literature clearly states that corneal stromal wounded areas must contain a lot of keratocyte cells that differentiate into myofibroblast cells [344], which are specifically identified by their expression of α-SMA [356, 357]. Our mouse corneal wound healing model also demonstrates increased expression of α-SMA in the wounded stromas [603]. Here in this project we demonstrate that the stromal wound zone harbours a high amount of cells that express both adult and embryonic stem cell markers. However, we know that late neural crest embryonic precursors also express α-SMA, in concert with Sox2, Oct-3/4 and Nanog expression [359]. It thus appears that it would be difficult to distinguish myofibroblast cells

from progenitor cells in the wounded stroma. Moreover, our results suggest that in fact myofibroblast cells may not be the major repair cell population in the stromal wound zone. Further work is however required to determine the stem cell expression profiles of myofibroblast cells before this theory can be developed further.

## 4.2 External Corneal Recruitment

### 4.2.1 Bone Marrow-derived Progenitor Cells

Bone marrow-derived cells have been found to migrate into the wounded murine corneal stroma, and then undergo differentiation into myofibroblast cells [512]. Moreover, injection of both bone-marrow derived mesenchymal stem cell lineages isolated from human adult adipose [529] and from human umbilical cord [535] have shown integration into murine (not human) stromal structures, and differentiation into keratocyte-like cells. These observations raise the possibility of external corneal recruitment of progenitor cells into the wounded corneal stroma. However, taking into account we demonstrated Pax6 expression by many cells in the wounded stroma implies that a high proportion of cells in the *in vivo* wounded stroma could be of ocular origin, meaning external ocular progenitor cells may not be the major progenitor cell population in the wounded stroma.

### 4.2.2 Lymphatic Vessel Formation

Considering that some external progenitor cells are highly likely to home to the wounded corneal stroma, and given the known immune cell trafficking role of lymph vessels in wound repair [400], we could hypothesise that lymphangiogenesis could enable the recruitment of these cells into the wounded cornea [393]. We thus analysed the formation of lymph vessels in our mouse corneal wound healing model by means of Lyve-1 immunostaining. Results demonstrated that the normal corneal stroma was not found to harbour either blood or lymph vessels as expected (data not shown). No D21 or D28 wounded corneal stromas showed formation of lymph vessels (data not shown). The majority of D7 (Fig.8.A, C) and D14 wounded (data not shown) stromas did not demonstrate either blood vessel or lymph vessel formation (3/5 mice per time period (60%)). Lymph vessel formation was observed in some central corneal D7 (Fig.8.B) and D14 (data not shown) wounded stromas (1/5 mice per time period (20%)). Lymph vessel formation in these mice was observed in ***proximal*** wound zone stromal tissues. Lymphatic vessel outgrowth from stromal

**Figure 8**

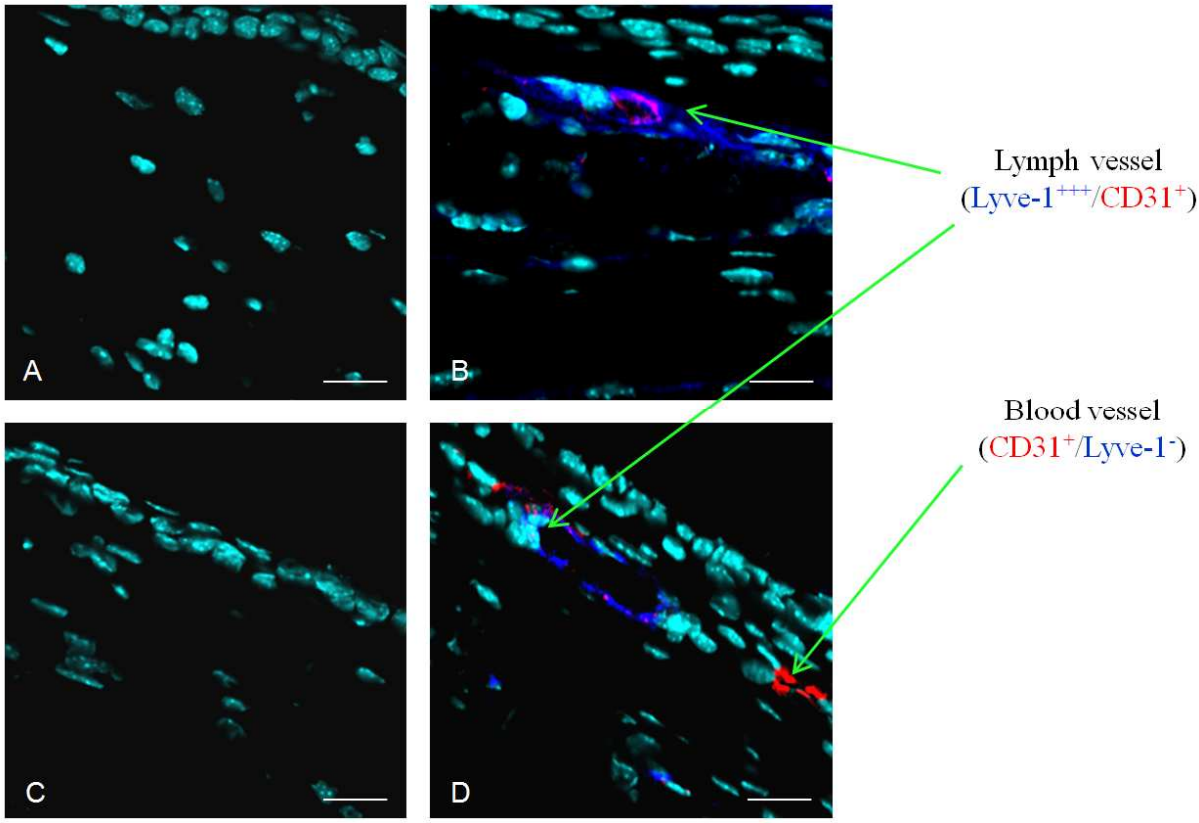


**Figure.8. Lymph Vessel Formation in Wounded Stromas.** Violet: Lyve-1. Red: CD31. Blue: Nuclear counterstaining with DAPI. (A-B) D7 proximal wound zone. (C-D) D7 peripheral wounded stromal tissue (adjacent to the limbal region). X630; scale bar represents 20 µm.

peripheries was also observed into some D7 (Fig.8.D) and D14 (data not shown) wounded stromas. In these mice, lymph vessel formation was observed only in ***peripheral*** wounded stromal tissues (1/5 mice per time period (20%)). Lymph vessel formation was identified in wounded stromas manifesting (Fig.8.D) or not manifesting (data not shown) corneal blood vessel outgrowth from the corneal limbal region, indicating that lymphangiogenesis in our corneal wound model can occur in the absence of blood vessel formation, as previously demonstrated by the same mouse species [395, 626].

Briefly, results showed a very high inter-mouse variance in the formation of lymph vessels in our mouse corneal wound healing model. However, all wounded mouse stromas showed an upregulation expression of progenitor cell markers, giving strong doubts that the formation of lymph vessels were responsible for the recruitment of progenitor cells into the wounded stroma of our wound model. Nevertheless, it is known that the mouse corneoscleral limbus vasculature harbors lymph vessels [627]. It could be that some repair cells are initially released in the limbal region, and then migrate into the wounded stroma. In this case, lymph vessel formation in proximity to the stromal wound zone may function to directly release supplementary repair cell into the stromal wound zone vicinity. The extent of lymph vessel formation could depend on inter-mouse variation in corneal wound responses, with more acute responses eliciting lymph vessel formation in proximity to the stromal wound zone. On the other hand, could lymph vessel formation function to supply repair cells from outside the cornea in proximity to the stromal wound zone? Further experimentation is required before such conclusions can be made.

### 4.3 Existence of a Limbal Stromal Cell Niche

First reports of the isolation of limbal stromal cells in a limbal niche were made in 2005 by Dravida et al., 2005 [628]. This group separated the limbal stromal zone from the epithelial limbal zone of corneas from human patients undergoing cataract surgery. Limbal fibroblast-like cells were then isolated via cell surface Stage-Specific Embryonic Antigen-4 (SSEA-4) expression. SSEA-4 is widely expressed by pluripotent human embryonic stem cells and adult bone marrow-derived mesenchymal stem cells [629]. Similar to wounded corneal stromal cells identified in this project, expression of embryonic stem cell markers was found by these isolated limbal stromal cells, notably expression of Sox2, Oct-4 and Nanog. Moreover, similar to stromal progenitor cells isolated from the adult cornea, these corneal limbal cells were also capable of growing clonally and had a multipotent differentiation

potential. They were capable of maturing into cells including neurons, chondrocytes, adipocytes, hepatocytes and corneal epithelial-like cells. Keratocyte cell generation was *not* reported or discussed.

Polisetty et al., (2008) [630] found that limbal mesenchymal cell cultures could be established from epithelialised and depithelialised human corneal limbal tissue from limbal epithelial transplantation donors. Resulting limbal mesenchymal cells demonstrated elongated spindle morphology, similar to bone marrow-derived mesenchymal stromal stem cells. Contrary to an embryonic-like stem cell expression profile of limbal fibroblast-like cells isolated by Dravida et al., (2005) [628], this group discovered a mesenchymal stem cell-like surface marker phenotype ($CD90^{+}$, $CD166^{+}$), with negative expression of hematopoietic stem cell markers ($CD14^{-}$, $CD31^{-}$,$CD45^{-}$).

Finally, it was recently shown that the murine corneal limbus is a source of cells which have fibroblastic morphology, are of neural crest origin, and certainly *in vivo* are multipotent. These cells have been termed "neural crest-derived stem cell-like cells" (NCDSCs) [631]. These cells were isolated by culturing limbal tissue from mice between postnatal days 1 and 8 (early eyelid opening stages). Interestingly, limbal tissue from mice older than this or from central corneal stromal tissue could not give rise to NCDSCs. NCDSCs were found to be Sca-1 positive, an important marker for mesenchymal stem cells. They additionally expressed adult tissue restricted stem cell markers, such as Abcg2, as well as embryonic neural crest development markers Twist, Slug, Snail, and Sox9. To determine the origin of these cells, it was shown that they were positive for corneal stromal keratocyte markers CD34, Lumican and Aldh1, weakly positive for endothelial cell markers, and negative for epithelial cells markers. This data indicates that NCDSCs are likely to be of stromal origin. Interestingly, these cells showed limited *in vitro* proliferative potential, losing it during the first 10 passages of culture, in a similar way to mesenchymal stem cells. This study indicates that NCDSCs are of neural crest origin and behave like multipotent stem cells. Note that these cells did not express Pax6, implying that this cell population is likely not to correspond to the half way state keratocyte phenotype identified by us in this project, but could however correspond to some progenitor cells. On the other hand, care in the interpretation of these results is required as the primary cultures mentioned here could have been contaminated with some epithelial cells that could have undergone EMT, also potentially accounting for this stem cell marker expression profile and morphological phenotype.

We cannot exclude that the limbal region may harbour progenitor cell populations that contribute to the stromal wound response upon migration into the wounded stroma from their limbal niche. These cells may also constantly migrate into the normal corneal stroma to function as guardians, accelerating migratory pathways and/or proliferation in order to expand the progenitor pool following corneal stromal injury.

### 4.4 Epithelial/Endothelial-to-mesenchymal Transitions

Limbal basal epithelial stem cells are well documented to express a wide variety of known progenitor cell fate* and undifferentiated cell markers [297, 621]. We documented an upregulated expression of all the markers analysed in this project (except neural crest-derived Nestin) in the wounded mouse corneal epithelium. In 1995 first evidence demonstrated the possibility of corneal intra-stroma invasion by surface epithelia using rabbit epithelial cells in corneal explants [632]. More recently, in some corneal opacity forming diseases, such as ocular pterygium* and limbal stem cell deficiency, the underlying mechanism of intra-stromal invasion by limbal basal epithelial stem cells, followed by migration, proliferation and EMT into fibroblast-like cells was put forward [633, 634]. Likewise, an *in vitro* rabbit corneal wound model based on culturing limbal extracts at the air-fluid interface (tissue air-lifting) was used to show that limbal basal epithelial cells can invade the underlying limbal stroma. It was also found that the epithelial stem cells underwent EMT in the limbal stroma [634]. The same group claims to have identified p63-positive corneal stromal cells from the pannus* of 3 human patients suffering from total limbal stem cell deficieny [635]. P63 being a putative limbal basal epithelial stem cell marker [295], puts forward a role of epithelial stem cell EMT in fibrotic eye diseases.

**Can we predict an epithelial cell role in adult stroma regeneration?**

We cannot at this stage determine to what extent epithelial stem cells could participate in the stromal wound response in our mouse corneal wound model. It would be hard to believe that epithelial stem cells could account for the global wounded stromal cell stem expression profiles. This would require invasion of the entire stroma. It would be more likely that epithelial stem cells invade the stromal wound zone early-on following injury, and then undergo EMT in order to elicit a stroma remodelling function to fill in just part of a proximal stromal gap.

Normal human corneal endothelial cells have shown expression of CD133 [636], and expression of Telomerase, Oct-3/4, Wnt-1, Pax6 and Sox2 has been shown by exposed

damaged endothelial cells in adult human corneal graft bed tissue [378]. Similarly, we document an upregulation of CD133, Abcg2, Tert, Sox2, Oct-3/4, Nanog, Pax6 protein expression in wounded endothelial tissues in our mouse wound model. Likewise, we cannot exclude migration, proliferation and endothelial-mesenchmyal transition (EnMT) of corneal endothelial progenitor cells into the stromal wound zone [637], and to what extent in keratocyte replenishment this could bear. However, again it would be hard to imagine that the single cell endothelial cell layer could account for this entire stromal cell wound response. In summary, **we concluded that the observations made in this report were in majority due to stromal cell responses.**

## 5 Summary of Results

In conclusion, we report identification of more restricted adult tissue stem cell, neural crest-derived stem cell and embryonic stem cell markers throughout the *in vivo* mouse corneal stromal wound response (*summarised in table 4 page 166*). Our results show for the first time the localisation of a stromal cell subpopulation that expands to provide a progenitor pool during *in vivo* stromal wound repair. Whether these cells are present *in situ* or migrate from the limbus or elsewhere is not clear. For the first time we also demonstrate that the *in vivo* adult keratocyte could actually be an embryonic-like precursor in the wounded stroma, with a more plastic phenotype than previously considered. Expression of an adult and embryonic neural stem cell marker in later stromal wound healing stages in stromal wound zones could correspond equally to both hypothesises of a keratocyte replenishment function via the activation of keratocyte dedifferentiation and stromal progenitor cell differentiation.

## 5 Résumé des résultats

En conclusion, nous montrons l’expression de marqueurs de cellules souches qui sont exprimés par des tissus adultes, des cellule souches issues de la crête neural et des cellules souches pluripotentes lors de la réponse *in vivo* de cicatrisation cornéenne stromale adulte (*résumé dans le tableau 4 page 166*). Nos résultats *in vivo* démontrent pour la première fois la localisation d’une sous population de cellules progénitrices dans le stroma qui se multiplient lors du remodelage du stroma. Il reste à déterminer si ces cellules sont *in situ*, ou migrent du limbe, ou encore sont recrutées d’autres tissus. Notre étude suggère pour la première fois que le kératocyte adulte peut acquérir le phénotype de son précurseur embryonnaire dans le stroma blessé, concluant que son phénotype semble être plus plastique qu’on le considère.

L’expression d’un marqueur de cellule souche embryonnaire et adulte exprimé par des tissus neuraux a été localisée dans des cellules stromales exclusivement dans la zone blessée lors des stades tardifs de la cicatrisation. Cette expression pourrait correspondre à une voie de dédifférenciation des kératocytes, ainsi qu’à une différenciation des progéniteurs du stroma afin de régénérer les kératocytes perdus dans les zones du stroma blessé.

**Table 4** Changes in protein expression, mRNA expression (when indicated) and activity (when indicated) of stem cell markers in wounded compared to control stromas. Note that for Pax6, mRNA and protein expression patterns do not concord.

| Stem cell marker | Stromal expression | | | | | | |
|---|---|---|---|---|---|---|---|
| | **Tissue Sample** | **Control** | **D7** | **D14** | **D28** | **Wound zone** | **Periphery** |
| **Abcg2** | Protein | Low | ++ | ++ | + | + | - |
| **CD133** | Protein | Low | ++ | ++ | + | + | - |
| **Tert** | Protein | Low | + | ++ | + | + | + |
| | Activity | - | NI | + | NI | NA | NA |
| **Sox2** | mRNA | Low | NI | ++ | NI | NA | NA |
| | Protein | Low | ++ | ++ | + | + | + |
| **Oct-3/4** | Protein | Low | ++ | ++ | + | + | + |
| **Nanog** | Protein | - | ++ | ++ | + | + | + |
| **Pax6** | mRNA | detected | constant | constant | constant | NA | NA |
| | Protein | ≥50% stromal cells | + | + | + | + | + |
| **Nestin** | mRNA | detected | + | + | ++ | NA | NA |
| | Protein | - | + | + | ++ | + | - |

- : No expression/activity
+ : Increased expression
constant: No change in expression
NA: Not applicable
NI: Not investigated

**Figure 9**

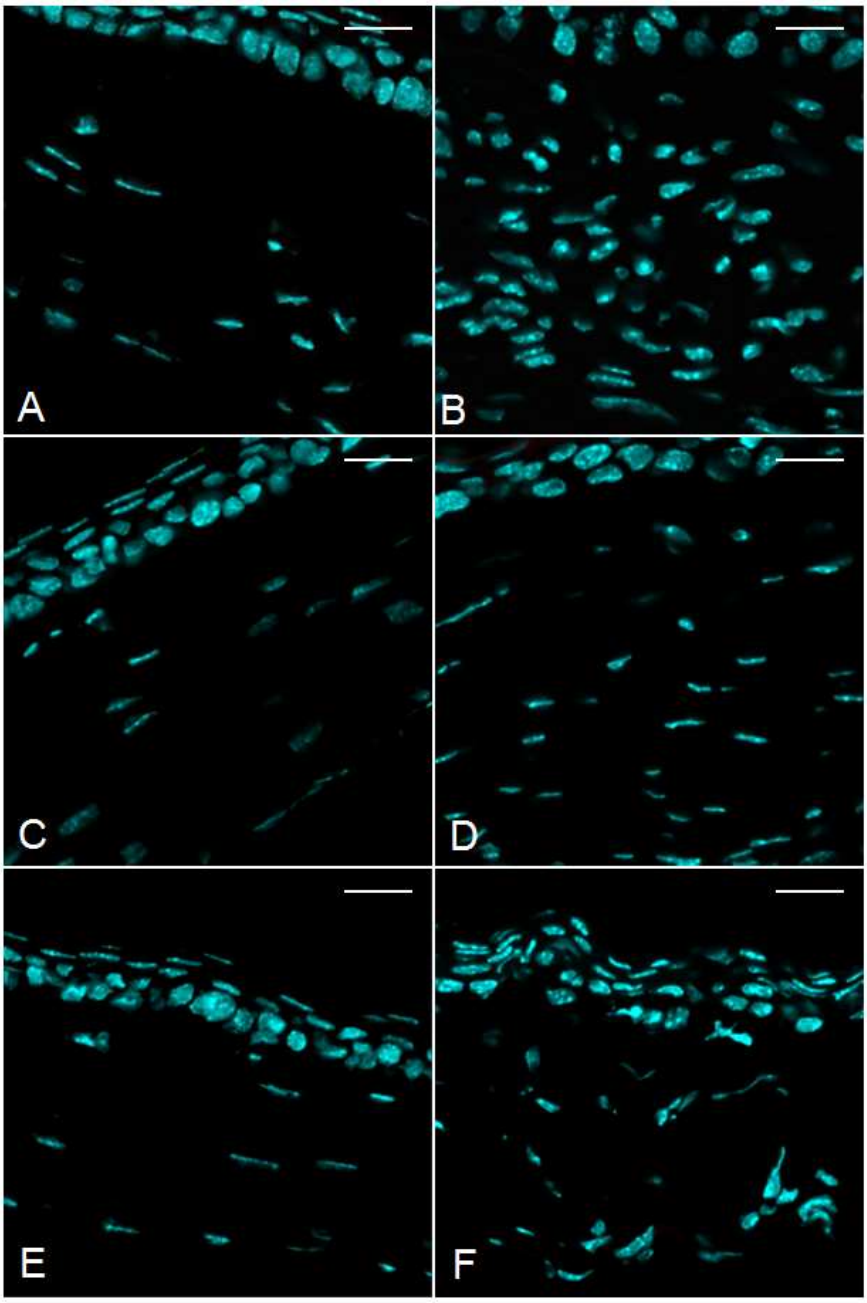


**Supplementary Figure.9.** Negative Control Immunostaining (red staining) using rat isotype IgG antibody (A-B), rabbit (C-D) and goat (E-F) serums in replacement of the primary antibodies on control (A, C, E) and D7 or D14 wounded (B, D, F) corneas. X630; scale bars represent 20 µm. Nuclei counterstained with DAPI.

# 6 Article Manuscript

**Manuscript title:** *In vivo* reexpression of stem cell markers in adult stromal cells during murine corneal wound repair

**Jacqueline Butterworth**, Dawiyat Massoudi, Angélique Erraud, Pierre Fournié, Christine Peres, Emilie Ancele, Matthias Macé, François Malecaze, Michèle Allouche, Patrick Calvas and Stéphane Galiacy

Submitted to ***Cell Research***

*In vivo* reexpression of stem cell markers in adult stromal cells during murine corneal wound repair.

Jacqueline Butterworth [a,b,*], Dawiyat Massoudi [a,b,*], Angélique Erraud [a,b], Pierre Fournié [a,b,c], Christine Peres [a,b], Emilie Ancele [b,c], Matthias Macé [a], François Malecaze [a,b,c], Michèle Allouche [a,b], Patrick Calvas [a,b,d] and Stéphane D. Galiacy [a,b,#]

[a] Inserm, U563, Centre de Physiopathologie de Toulouse Purpan, Toulouse, France

[b] Université Toulouse III Paul-Sabatier, UMRs563, Toulouse, France

[c] CHU de Toulouse, Hôpital Purpan, Service d'Ophtalmologie, Toulouse, France

[d] CHU de Toulouse, Hôpital Purpan, Service de Génétique Médicale, Toulouse, France

[*] JB and DM contributed equally to this work

[#] Corresponding author. Tel: 00 33 5 62 74 45 09; fax: 00 33 5 62 74 45 58

E-mail address: stephane.galiacy@inserm.fr

**Running title:**

Stem cell markers' reexpression in wounded corneal stroma

**Abstract**

Corneal scarring following trauma, inflammation or surgery, impairs vision for many affected individuals and can lead eventually to corneal blindness. The normal corneal repair process involves successive phases of inflammation, apoptosis, cell proliferation and extracellular matrix synthesis and remodelling. Understanding the role played by adult corneal stroma cells in tissue regeneration is important to improve prevention or treatment of corneal opacities. Corneal stroma keratocytes develop from mesenchymal cells originating in the cranial neural crest. Several *in vitro* studies have tried to identify an adult corneal stroma progenitor cell able to differentiate into keratocyte-like cells. However the localisation and tissue lineage of this putative stroma progenitor is still elusive. In this study, we used an *in vivo* mouse model of full thickness corneal incision wounding to study the phenotype of cells involved in stroma wound repair. We characterised the localisation and dynamic changes in expression of a range of stem cell markers between control and wounded corneal stromas at various time periods after corneal incision by means of immunohistochemical, immunoblotting and RT-qPCR analyses. We report increased expression of restricted adult tissue stem cell (Abcg2), ocular development / nervous system (Pax6, Nestin) markers and increased telomerase activity in the wounded stroma. Moreover we observe that the majority of adult keratocytes can reexpress stem cell (Sox2, Pou5f1 (Oct3/4), Nanog) markers throughout stroma remodelling. Our *in vivo* results strongly suggest the existence of a normal adult stroma progenitor cell pool able to expand during corneal wound healing.

**Keywords:** cornea, keratocyte, wound healing, progenitor cells, stem cells, neural crest

## Introduction

Corneal scarring following trauma, inflammation or surgery, impairs vision for many affected individuals and can lead eventually to corneal blindness. The normal corneal repair process involves successive phases of inflammation, apoptosis, cell proliferation and extracellular matrix synthesis (ECM) and remodelling. Understanding the role played by adult cornea stroma cells in tissue regeneration is important to improve prevention or treatment of corneal opacities. The corneal stroma accounts for approximately 90% of total corneal thickness. It consists of neural crest-derived mesenchymal cells embedded between collagenous lamellae. These cells, named keratocytes, are responsible for the secretion of a unique ECM of glycoproteins and proteoglycans that is required for maintaining stroma integrity and transparency necessary for clear vision [1]. Mammalian adult keratocytes are largely quiescent. However, in response to acute injury, keratocytes neighbouring the wound become mitotically active, proliferate, adopt a fibroblast phenotype and migrate into the injured area [2]. Depending on the extent of the injury, so-called myofibroblast cells characterised by alpha-smooth muscle actin (alpha-SMA) expression can also be observed in the stroma.

Since 2005, *in vitro* cell studies in a range of species (bovine, mouse, rabbit and human) isolated a subpopulation of corneal stroma cells capable of growing clonally and expressing a variety of known stem cell markers [3-7]. These cells are multipotent and capable of switching phenotype to express keratocyte-specific markers [5, 6, 8]. This subpopulation could represent putative adult corneal stroma cell progenitors. Among the different stem cell markers identified in the aforementioned studies are the restricted adult tissue stem cell marker Abg2 (also known as BCRP) and the embryonic ocular precursor marker Pax6 [3-6, 8]. Abcg2 is an ATP-binding cassette transporter G family member. This transporter protein has been used as a marker for many types of stem cells, including hematopoietic [9-11], mesenchymal [11], muscular [11], neural [12, 13], cardiac [14], pancreatic islet [15], keratinocyte [16, 17] and corneal limbal epithelial stem cells [18]. Together with Pax6, ABCG2 has been found to be

expressed in around 4% of adult stroma cells in human and bovine cornea [3]. Pax6 is the product of a developmental homeobox gene expressed by ocular precursor cells in early development [19]. Pax6 expression continues in the adult corneal epithelium, but was initially considered to be absent from adult keratocytes [20]. Only recently has Pax6 expression been identified in regenerating adult tissues, for example, in neural and retinal progenitor cells [21-23]. Pax6-mediated regulation of adult progenitor cell fate mirrors that in embryonic tissues [21]. Moreover, these *in vitro* cell studies have reported that cornea stroma progenitor cells express undifferentiated embryonic stem cell markers involved in embryonic neural crest development and/or ocular development, such as Six2, Six3, Notch1, Twist, Snail, Slug, and Sox9 [4, 6, 8].

An important issue is to determine whether a subpopulation of corneal stromal cell progenitors can be demonstrated *in vivo,* and if so, to localize and find out the tissue lineage origin of this putative progenitor. In this study we used an *in vivo* mouse corneal wound healing model developed upon full thickness incision of the central cornea [24]. We aimed to characterise the dynamic changes in expression of stem cell markers throughout the corneal stroma wound healing response. We selected stem cell markers known to be expressed in multi/pluripotent embryonic and/or adult stem cells. Of particular interest to us is that late embryonic neural crest-derived stem cells , which participate in corneal stroma formation, express Sox2 (also known as SRY-related HMG-box gene 2), Nanog, Pou5f1 (also known as Oct-3/4) and Nestin [25]. Nestin is a type VI intermediate filament protein mainly express in rapidly dividing cells during the early stages of development in the nervous system and myogenic tissue. Thus it is widely used as a neural stem cell markers [26]. It's worth to note that its expression is down regulated upon cell differentiation, however it is induced transiently in response to injury in several tissues where it was found in the development process [27, 28]. Moreover, the Nestin promoter contains several enhancer elements and essentially a POU-domain. It is worthy to note that Sox2, Pou5f1 and Nanog transcription factors can maintain the pluripotency of embryonic stem cells individually and cooperatively

in humans and mice [29-35]. However, loss of expression of one of these factors ultimately leads to the extinction of the others [36].

Looking at various times after corneal incision, our *in vivo* study demonstrates an increased expression of restricted adult tissue stem cell (Abcg2), ocular development/nervous system (Pax6, Nestin) markers and increased telomerase activity in the wounded stroma. Moreover, we observe that the majority of adult keratocytes can reexpress stem cell markers (Sox2, Pou5f1 (Oct3/4), Nanog) throughout stroma remodelling, suggesting a relative plastic phenotype of these cells. These *in vivo* results strongly suggest the existence of a normal adult stroma progenitor cell pool able to expand during corneal wound healing.

## Results

### Increased expression of keratocyte progenitor cell markers *in vivo* during corneal wound repair

Immunostaining showed that Abcg2 is expressed in control corneas in the limbal basal epithelial cell layer [37] and by a small number of stroma cells. We found that intermittent endothelial cells also expressed Abcg2 (Fig.1.A, C). At D7 (7-days) (data not shown) and D14 post-wounding, Abcg2 expression was more intense in the epithelium, endothelium and was particularly increased in the wounded stroma zone. No expression was detected in the stroma beyond the wound zone (Fig.1.B, D). In the D28 wounded stroma, Abcg2 expression was still higher than in the control cornea, and approximately half of stromal cells were Abcg2-positive (Fig.1.E). By D28 the tissue in the stroma wound zone was in the process of remodelling, and the relative positions of cells to one another resembled those of the normal control cornea. The epithelial, stromal and endothelial cell layers were well-distinguished, and the stromal cells were more elongated between the collagen fibres than in the D7 and D14 wound zones (Fig.1). Immunoblot results for Abcg2 expression were consistent with the immunostaining data (Fig.1.E). Abcg2 protein expression was highest in D14 wounded stroma tissue, and remained slightly increased in D28 wounded stroma tissue compared to control stroma tissue. Protein expression of the Housekeeping control gene Th was constant between control, D14 and D28 wounded stroma tissues.

Immunostaining results showed that Pax6 protein expression increased in wounded corneal epithelia and endothelia (Fig.2.A-C). Control corneal stroma showed low Pax6 expression by at least half of the stromal cells (Fig.2.A). In D7 (data not shown) and D14 wounded stromas Pax6 protein expression was more intense, but still only approximately half of the stromal cells were Pax6-positive (Fig.2.B). Stromal Pax6 expression at D28 post-wounding was still more intense than the control stroma (Fig.2.C). Fig.4.D shows that immunoblotting results were consistent with immunostaining data for Pax6 protein expression. Pax6 protein

expression was detected in control stroma, and its expression was slightly increased in D14 and D28 wounded stroma tissues. Housekeeping control gene Th protein expressions were constant between control, D14 and D28 wounded stroma tissues. *Pax6* gene expression assayed by RT-qPCR showed no significant difference in expression between control stromas and D7, D14, D21 and D28 wounded stromas ($p \leq 0.05$) (data not shown). *Pax6* gene amplifications in control and D7, D14, D21 and D28 wounded stroma samples gave an average Ct (cycle threshold) value of 24.64 (SEM 0.38), indicating *Pax6* mRNA expression in both control and wounded stromas.

**Increased Tert protein expression and Telomerase activity in wounded stromas**

Control cornea immunostaining with Tert showed no reaction in the stroma, nor the epithelial or endothelial cell layers, as expected (Fig.3.A). We observed an increase in Tert expression in wounded corneal epithelium and endothelium cell layers (Fig.3.B-D). Tert expression increased in the D7 stroma wound zone, but not all cells were Tert-positive (Fig.3.B). D14 wounded stroma showed high Tert expression and all stromal cells were Tert-positive. (Fig.3.C.). At D28, the wounded stroma still showed higher Tert expression than the control stroma (Fig.3.D), and epithelial and endothelial cells were Tert-positive. We concluded that Tert stroma protein expression reached its highest level at approximately D14 of the stromal wound healing process, and then decreased by D28. Thus, D14 wounded stromas were used to compare Tert activity to control stromas. At D14 post-wounding telomerase activity was increased by 2.4-fold in wounded stromas compared to unwounded stromas (Fig.3.E). Control stromas showed no Tert activity. KG1 myeloblastic cells were used as a control [38].

**Corneal Stroma cells re express stem cells markers**

Immunostaining showed Sox2 protein expression in the normal corneal epithelium and

endothelium (Fig.4.A). A small number of stroma cells were also Sox2-positive (arrowhead). In the D7 (data not shown) and D14 wounded stroma, Sox2 protein staining was more intense in the epithelium and the stroma wound zone, and the majority of the stromal cells were Sox2-posiitve (Fig.4.B). Sox2 protein expression in proximal and peripheral stroma wound zone tissues followed the same Sox2 expression pattern as in the stroma wound zone. Briefly, Sox2 protein in D14 wounded proximal and peripheral stromal tissue increased compared to equivalent control stroma tissues (Fig.4.C-D). In the D28 wounded zone, Sox2 protein expression remained higher than in the control and most of the cells were Sox2-positive (Fig.4.F). Only a few cells in the proximal and peripheral wounded stromal tissues were Sox2-positive, but expression was still higher than in the control stroma (Fig.5.G-H). The same expression pattern for Sox2 protein expression was observed for Pou5f1 (D14 post-wound is shown in Fig.5) and Nanog proteins in D7, D14 and D28 wounded stromal tissue (data not shown).

*Sox2* gene expression (mRNA) was assayed by RT-PCR and agarose gel electrophoresis in control and D14 wounded stromas (Fig.4.E). Control stroma tissue showed low *Sox2* mRNA expression. *Sox2* mRNA expression was upregulated in D14 wounded stroma tissue compared to control stroma tissue, concordant with immunostaining results. mRNA expression of the Housekeeping control gene *Th* was constant between control and D14 wounded stroma tissue.

**Increased colocalisation of Pou5f1-positive stromal cells with Tert protein in wounded stroma zones**

Pou5f1 and Tert coimmunostaining results in control corneas showed no Tert expression, whereas Pou5f1 was expressed by the limbal basal epithelial layer [39] and by a small number of stromal cells (Fig.5.A). D14 wounded stroma showed both increased expression of both Pou5f1 and Tert expression by stromal cells within and in proximity to the wound zone. In the

D14 wounded stroma periphery, only a small proportion of Pou5f1-positive cells were also Tert-positive (Fig.5.G). Fig.5.D-G illustrates the colocalisation of Pou5f1 and Tert protein in the same stromal cells within D14 wounded peripheral stroma tissue. We computed the degree of colocalisation of Tert and Pou5f1. Calculations of M1 (Mander's coefficient) for the total Pou5f1 protein that colocalised with Tert protein in the D14 stroma wound zone (mean 95%) was significantly higher than in the D14 wounded stroma periphery (mean 26%). We rejected the null hypothesis of equal means ($t= 19.6498$, $df = 18$, p-value = $1.306 \times 10^{-13}$).

**Increased Nestin mRNA and protein expression in wounded stromas**

RT-qPCR results showed that *Nestin* mRNA was upregulated at D14 post-wounding (approximately 1.5-fold), and was upregulated to a greater extent at D21 and D28 post-wounding (approximately 3.7-fold) (Fig.6.A). Nestin immunoblotting results (Fig.6.B) showed very low Nestin protein expression in control stroma tissue. Nestin protein expression increased in D14 wounded stroma tissue, but was most highly expressed in D28 wounded stroma tissue. Housekeeping control gene Th protein expression was constant between control, D14 and D28 wounded stroma tissues. Nestin immunostaining results were concordant with immunoblotting results. The control stroma showed no reaction with Nestin protein staining (Fig.6.C). D7 (data not shown) and D14 wounded corneas showed Nestin expression by stromal cells in the wound zone (Fig.6.D). Nestin protein expression was significantly increased in the stroma at D28 post-wounding (Fig.6.E). In the stroma wound zone Nestin-positive cells were arranged in a linear, grouped organisation and showed an elongated morphology, indicating also that Nestin protein expression of neighbouring cells overlapped. Nestin protein expression was not found in peripheral wounded corneal stroma tissue (Fig.6.F).

## Discussion

Understanding the mechanisms of corneal repair could open new therapeutic strategy to treat permanent corneal opacities and thus prevent corneal transplantation. Little is known about stromal cells renewal after corneal injury. In this study, we aimed to decipher whether a subpopulation of corneal stroma cell progenitors could be localised *in vivo* in response to a corneal injury. Here we report for the first time the expression of stem cell markers in the stroma of *in vivo* murine wounded cornea.

### Identification of an active stromal progenitor cell population

We found that Abcg2 and Pax6 were expressed by a small number of stromal cells in unwounded mouse stromal tissue, consistent with reports made by Du *et al.* [3] claiming that a minority of normal stroma cells express Abcg2 and Pax6. Upon corneal incision, Abcg2 and Pax6 protein expression was increased in cells in the stroma wound zone, and this expression remained upregulated throughout 1 month. This result implies that the normal corneal stroma harbours an Abcg2- and Pax6-positive cell subpopulation that expands and is sustained in the stroma throughout the stroma remodelling process. Abcg2 protein expression was only localised within the stroma wound zone and not within wounded peripheral stroma tissue, implying that this markers is specific to a cell population recruited to the direct wound zone for a repair function. Concerning Pax6, while we found an increased expression in the wounded area, but we also found this marker was expressed widely by a majority of normal keratocyte cells, which is different from findings for human and bovine stroma. As previous murine studies focused only on the mouse epithelium, we can hypothesise that this difference is mostly due to species and strain specificity. Still, as it has recently been showed that Pax6 expression have been identified in regenerating adult ocular tissues [21-23], we can conclude that most of the cells present in the wound area are of ocular origin. Finally, we wanted to know if stromal cells harboured functional progenitor function during corneal wound healing. Thus we investigated Tert expression and activity as it is

considered to be a stem cell marker upregulated in regenerative progenitor cells compared to somatic cells. Tert preserves telomere length during cell division-dependent DNA replication and is considered a necessary enzyme to maintain the possibility of unlimited cell divisions [40, 41]. We showed that Tert protein expression peaked between D7 and D14 of the stromal wound healing response and remained upregulated throughout 1 month post wounding. Tert activity was more than doubled in D14 wounded stromas compared to control stromas. This is the first time *in vivo* that stromal cells have been observed to upregulate telomerase in response to corneal injury, confirming the presence of progenitor cells that can be activated in the wounded stroma.

**Upregulation of stem cell markers in the wounded stroma**

Having demonstrated the expression of a putative stromal progenitor cell population, we investigated expression of stem cells markers to investigate their lineage. We report that Sox2, Pou5f1 and Nanog expression are thus also upregulated throughout the *in vivo* stromal wound healing response. This change in expression was more drastic than expected. Increased expression was observed throughout the whole cornea, in the stroma wound zone, but also outside the wound area in the uninjured corneal stromal tissue. Among reports demonstrating that Sox2, Pou5f1 and Nanog function in somatic cells and multipotent somatic progenitor cells in a manner that mirrors their roles in embryonic stem cells [42-45]; an *ex vivo* rat trachea epithelial wound model showed that surviving $G_0$-blocked epithelial stem cells undergoing proliferation also express Sox2, Pou5f1 and Nanog proteins. Once these cells differentiated into downstream ciliate, mucous or basal cells, expression of the three transcription factors was lost [46]. Moreover, it was recently shown that introducing transient Pou5f1 expression to adult keratinocyte cells is sufficient to alter their differentiation pathways [47]. These studies indicate that transcription factors involved in early stem cell self-renewal can be contextually activated in more mature tissues to foster proliferation and

susceptibility to environmental differentiation signals. Moreover, Lwigale et al. recently show in an elegant model of quail/chick graft that late embryonic keratocyte cells are actually multipotent cells and as such have highly plastic phenotype[48]. Taken together with our data, we thus confirm that the adult keratocyte retains a relative plasticity and is able after an injury to express stem cells markers. It's worthy to note that this markers are also express by neural crest cells during embryongenesis [25]. However, analysis of lineage specific markers such as Sox9 or Twist should allow us to determine putative neural crest origin of these cells. Nevertheless, somatic cells able to retain embryonic features from their tissue of origin has been termed "the half way state" [49, 50]. Precise role of the adult keratocyte in the wound area remain to be determined but we cannot exclude a migration and an active participation of this cell in the repair area. Finally, we demonstrated that Pou5f1 and Tert colocalisation was visibly higher within cells in the stromal wound zone, whereas the majority of Pou5f1-positive cells in the wounded stromal periphery were Tert-negative. This further implies that cells in the wound zone must be actively dividing and protecting their telomeres; most probably keratocyte progenitors. This last point could be in contradiction with the literature stating that the wounded area in such severe injury must contain a lot of myofibroblast cells [24, 51] which are specifically stained for alpha-SMA. However, embryonic neural crest cells and keratocyte precursors *in vitro* also express alpha-SMA [25, 52]. Thus, in the acute phase of injury distinction between both cell types might be difficult and it would be interesting to investigate permanent opacities in our model several months after wounding by performing co-staining of alpha-SMA and Nestin which are also co-express in neural crest cells and keratocyte precursors [25, 52]. Nestin is of special interest not only regarding keratocytes as it is expressed by neural crest cells during early embryogenesis, but also as it is expressed in several adult stem cells, such as progenitor cells of the skin [53]. By homology with skin and central nervous system [54], we would have expect that adult keratocyte progenitors would express Nestin. However, as previously described by Espana et al. adult stromal cells do not express Nestin [55]. Our hypothesis is that Nestin expression is related to mitotically active cells, however keratocytes are relatively quiescent cells with low turn-over. Moreover, Nestin expression might be

incompatible with specific cytoskeleton organisation required to maintain corneal transparency. We observed a strong *Nestin* mRNA expression increase from 14 days post-wounding. Stromal Nestin protein expression mirrored this increase and was still high 28 days post-wounding. The most striking feature is that Nestin-positive cells were localised exclusively in the wound zone. At 28 days post-wounding, we can observe Nestin-positive stromal cells presenting a linear network orientation, where inter-cell intermediate filaments appeared to overlap, implying a stromal cell-cell network. This structural organisation is characteristic of normal stromal keratocytes embedded in stromal ECM [56]. The cells also exhibited an elongated and compact morphology, characteristic of the normal keratocyte cell phenotype [1]. This last result confirms the presence of stromal cells, which re-activate stem cells signaling pathways in order to rebuild the lost corneal stroma. Nestin expression most probably mean than these cells originate for the neural embryonic area but more investigation will be needed to confirm this hypothesis. Moreover, while we showed that most of the cells present in the wound area should be from ocular origin, we still cannot exclude that other cell types than adult keratocytes and their progenitors might be involved in stromal wound repair as Pax6 staining did not cover all the cell population. Thus, bone-marrow derived mesenchymal progenitor cell lineages directly isolated from adult adipose [57] and from newborn human umbilical cord [58] have shown integration into the stromal structure and differentiation into functional keratocyte-like cells when injected into the corneal stroma. This raises the possibility of the recruitment of some external progenitor cells into the corneal stroma. For example, lymphogenesis in the cornea during wound healing could enable the recruitment of progenitor cells [59], which then could migrate and proliferate. Stromal-like cells expressing stem cell markers have been isolated from the corneal limbus [60-62]. We cannot exclude migration of limbal cells directly into the stroma following corneal wounding. However, neural crest-like stem cell-like limbal stromal cells showed upregulation of a range of stem cell markers, and were notably Nestin-positive but Pax6-negative [60]. This indicates that these cells could account for a neural crest-derived stroma progenitor cell population, but not for the Pax6-positive undifferentiated keratocyte cell phenotype. In addition, epithelial

stem cells are well documented to express a wide variety of known stem cell and progenitor cell fate markers. In some cornea-opacity forming diseases, such as limbal basal stem cell deficiency and ocular pterygium, the underlying mechanism of intra-stromal invasion by epithelial stem cells, followed by migration, proliferation and epithelial-mesenchymal transition into fibroblast-like cells has been proposed [63, 64]. It has also been described in a Pax6 heterozygous mouse corneal wound model that epithelial cells undergo a mesenchymal transition and thus express myofibroblast markers such as alpha-SMA [65]. We cannot at this stage exclude invasion into the stroma by epithelial stem cells, or determine to what extent epithelial stem cells could fill in the stromal gap and replenish keratocyte cells. Expression of Tert, Pou5f1, Pax6 and Sox2 has been shown in adult human corneal graft bed tissue exposing damaged corneal endothelial cells [66]. Likewise, we cannot exclude migration, proliferation and endothelial-mesenchymal transition of corneal endothelial progenitor cells into the stroma wound zone [67], and to what extent in keratocyte replenishment this could bear.

Comprehension of stromal repair process is fundamental to understand how permanent corneal opacities develop. We demonstrated than in response to an injury, the corneal stroma cells reexpress stem cells markers. Moreover, our results strongly suggest the existence of a normal adult stromal progenitor cell pool able to expand during corneal wound healing. Further investigations are required to determine the precise role of these cells in the stroma regeneration, and their potential clinical implications.

## Materials and methods

### Animals and surgery

Female C57/BL6 mice 12-16 weeks old were purchased from Charles River France (Arbresle, France) to generate a corneal wound healing model. All animals were treated in accordance with the Ethical Committee of the CPTP (Centre de Physiopathologie Toulouse Purpan, France) and guidelines provided in the ARVO Statement for the use of Animals in Ophthalmic and Vision research. Atropine (atropine sulphate 1% Faure; Laboratoires ERUOPHTA, Monaco) was applied topically to the left (incised) eyes of mice 10-20 minutes before surgery to dilate the iris. A general injection anaesthesia regimen (Ketamine/Xylazine) was injected intraperitonealy and a local anaesthesia of oxybuprocaine chlorhydrate (Laboratoires Théa 1.6 mg/0.4 ml Clermont-Ferrand, France) was applied. The full thickness of the centres of the corneas of the left eyes were perforated with a trephine 0.75 mm in diameter using a Zeiss® OPMI® CS operating microscope (Germany). All surgeries were performed by the same surgeon. The right eyes of incised mice did not undergo surgery. Mice with no surgery in either left or right eyes served as controls for all experiments. One drop of 1% fucithalmic acid (LEO Laboratoires, St Quentin en Yvelines, France) was also applied for the surgery. One drop/day of fucithalmic acid and atropine were applied to incised eyes for 5 days after incision. Both eyes of control mice underwent identical treatment. After 7 (D7), 14 (D14), 21 (D21) and 28 (D28) days following incision mice were euthanised using isoflurane and cervical dislocation. Right and left eyes were either enucleated for cryo-embedding (Tissue-Tek® Sakura Finetek 4583 OCT Compound, USA), or the stroma was collected by removal of the epithelial and endothelial layers by gentle scraping with sterile surgical tweezers, then snap frozen in liquid nitrogen. All tissues were stored at -80°C.

### Quantitative RT-PCR

Total RNA was extracted from the cornea stromas using the commercial protocol from the

RNeasy® Mini Kit 50 (Cat. No. 74104, Qiagen, USA) and quantified using Agilent 2100 bioanalyser with RNA 6000 nano chips (Agilent Technologies, USA). Total cDNA was synthesised following the protocol from a commercially available SuperScript VILO Kit (Cat. No. 11754-250, Invitrogen, USA) and stored at -20°C. Primers for *Nestin*, as well as for two housekeeping control genes Beta-2 microglobulin (*B2m*) and Tyrosine 3-monooxygenase (*Th*), were designed using Primer Express 3 (Applied Biosystems, California, USA) and purchased from Eurogentec S.A (Belgium). Primers for *Nestin* were 5'-CTCTCGCTTGCAGACACCTG-3' (forward) and 5'-GATGGGAGTGCTGGCCAA-3' (reverse). Primers for *B2m* were 5'-TTCTGGTGCTTGTCTCACTGA-3' (forward) and 5'-CAGTATGTTCGGCTTCCCATTC-3' (reverse). Primers for *Th* were 5'-TGGATAAGAGTGAGCTGGTACA-3' (forward) and 5'-CGTGTCCCTGCTCTGTTACG-3' (reverse). A Quanti®Tect Primer Assay for *Sox2* was purchased from Qiagen (Qiagen, France, Cat. No. QT01052786 and QT01539055 respectively). All primers were first tested on cDNA from embryonic mouse tissue, and efficiency calculations were then made using three wounded stroma cDNA samples. Only primers with a mean efficiency of 0.85-1.00 were used. For *Nestin* assays complete 2X SYBR® Green ER® qPCR SuperMix Universal buffer (Cat. No. 11762-100, Invitrogen, USA) was mixed with 1µl cDNA (optimal concentration 50 pg/µl) and 1µl forward and reverse primer mix (optimal concentration 10µM). The total reaction volume was 10µl. *Nestin* mRNA expression was analysed in seventeen control stroma, thirteen D7 wounded stroma, thirteen D14 wounded stroma, fourteen D21 wounded stroma and eleven D28 wounded stroma cDNA samples. For *Pax6* assays, complete 2X LightCycler® 480 Green I master mix (Roche, UK) was mixed with 2µl cDNA (optimal concentration 75 pg/µl) and 2 µl forward and reverse primer mix (optimal 10-fold dilution). The total reaction volume was 10 µl. *Pax6* mRNA was analysed in thirty-six control, seven D7 wounded, seven D14 wounded, seven D21 wounded and seven D28 wounded stroma cDNA samples. *Sox2* mRNA expression was assayed in four control and four D14 wounded cDNA samples. 5 µl of cDNA template (high optimal concentration of 600 pg/µl) was mixed with complete 2X LightCycler® 480 Green I master mix (Roche, UK) and

1.25 µl of forward and reverse primer mix (optimal 10-fold dilution). The total reaction volume was 12.5 µl. Triplicate samples were used for all assays. All reactions were performed in LightCycler 480 96-multiwell plates with sealing foils (Roche, UK) in the LightCycler 480 machine (Roche). PCR conditions for *Nestin* assays were as follows: 50°C for 2 minutes, denaturation at 95°C for 10 minutes, and amplification for 40 cylces of 95°C for 15 seconds and 60°C for 1 minute. PCR conditions for *Pax6* and *Sox2* assays were as follows: denaturation at 95°C for 15 minutes and amplification for 40 cycles of 94°C for 15 seconds, 72°C for 30 seconds and 72°C for 30 seconds. The Ct was used to detect the increase in the signal associated with an exponential growth of PCR product during the log-linear phase. The relative expression was calculated using REST 2009 software (Qiagen, Munich, Germany) using the $2^{-\Delta\Delta CT}$ method [68] to normalise data according to expression of the housekeeping genes. Data was then normalised to expression in the control stroma samples. Non-parametric Mann-Whitney tests were used for group-to-group comparisons. A value of $p \leq 0.05$ was considered statistically significant. *Pax6* amplicons from control, D7 wounded, D14 wounded, D21 wounded and D28 wounded stroma samples were analysed by 2% agarose gel electrophoresis. Ct data were not calculated for *Sox2* primer assays, but melting curves were checked for *Sox2* primer specific amplification. *Sox2* gene products were then analysed by 2% agarose gel electrophoresis. The *Th* housekeeping gene was used as a control. 50 bp DNA ladder was used for molecular weight determination (Fermentas, France. Cat. No. SM1211).

**Telomerase activity analysis**

Quantitative determination of telomerase activity was performed using the Quantitative Telomerase Detection Kit (MT3011 Biomax, US). All lysate preparation was carried out at $^{+}4$°C. Six D14 wounded stromas and six control stromas were pooled separately and lysed. The human KG1 myeloblastic cell line was used as a positive Tert activity and internal

control (a gift from V. Mansat-De Mas, INSERM U563, Toulouse, France [38]). A total of 1 x$10^5$ cells were lysed and centrifuged. A two-fold serial dilution of KG1 cells was made in lysate buffer. Either 12.5 µl of D14 wounded stromal or KG1 cell lysate was added to 12.5 µl of QTD premix in Thermo-Fast® 96 PCR detection plates (AB-1100, Abgene, Thermo Fisher Scientific, UK). Telomerase activity was determined by the ability of telomeric repeat synthesis onto an oligonucleotide substrate and subsequent PCR amplification and direct detection of SYBR Green dye binding to the double-strand DNA product using the ABI PRISM® 7000 Sequence Detection System (Applied BiosystemsTM, France). PCR conditions were according to the manufacturer's instructions. Ct data was used to detect the signal associated with an exponential growth of PCR product during the log-linear phase and compared between control and D14 wounded stromas. The same experiment was repeated three times using triplicate stroma and KG1 cell lysate samples and a negative control (lysate buffer). Relative telomerase activity was determined using REST 2009 software (Qiagen, Munich, Germany) and normalised to the negative control telomerase activity. A non-parametric Mann-Whitney test was used for group-to-group comparisons. A value of $p \leq 0.05$ was considered statistically significant.

**Immunohistochemistry**

Cornea cryosections of 7 µm thickness were immediately fixed for 20 minutes in freshly prepared 4% paraformaldehyde at 4°C and then air dried before storage at -20°C. The anti-Nestin antibody required that sections were directly stored at -20°C after sectioning. These sections were then fixed prior to immunostaining for 20 minutes in acetone at -20°C. For each eye, a hematoxylin and eosin staining was carried out on a sample of slides to verify the state of the cornea. A minimum of three different controls and three different D7, D14, and D28 wounded mouse eyes were tested with each antibody for consistency. For immunostaining, sections fixed in paraformaldehyde were incubated for 30 minutes in 0.1%

NaBH4 in PBS for antigen retrieval and all sections were permeabilised in 0.5% Triton X-100 in PBS. Non-specific binding was blocked by incubation in 10% foetal bovine serum (Cat. No. 10106151, Invitrogen) for 30 minutes, followed by blocking for 30 minutes with Image-iT™ FX Signal Enhancer (Cat. No. I36933, Invitrogen, USA). Incubation of sections with primary antibodies against Abcg2, CD133, Tert, Sox2, Pou5f1, Nanog, Pax6 or Nestin followed by a 1 hour incubation with 1/400 dilutions of secondary Alexa Fluor® antibodies (Molecular probes, Invitrogen, USA) were performed according to table 1. Pou5f1/Tert and Pax6/Sox2 colocalisation experiments were carried out using different species primary and secondary antibodies to reduce non-specific background. Negative controls were performed using 0.5% Triton X-100 in PBS and rat isotype IgG antibody, rabbit or goat serums instead of the primary antibodies used on sections of wounded eyes (table 1). Nuclei were counterstained and mounted using ProLong® Gold antifade reagent with DAPI (Cat. No. P36935, Invitrogen, USA). For washes between each step and for dilutions of all serums and antibodies, 0.5% Triton X-100 in PBS was used. All experiments were carried out under the same conditions, and antibody controls and wounded cornea staining were performed concurrently. Slides were observed using a 20X objective (Leica DMR microscope), and a 20X objective and 63X oil objective (confocal Zeiss 710 microscope). For confocal microscopy a series of z-section images were acquired using Zen 2008 Software (Carl Zeiss GmbH SP1.1 Version 5.0). Fields were averaged four times to increase signal to noise ratio, and amplifier gain and offsets of each photomultiplier were adjusted for a given antibody, but were kept constant for the sake of comparison between control and wounded corneas. Individual channels were devoid of fluorescence from other emission sources, thus eliminating bleed-through. For colocalisation experiments, free online ImageJ Plugin software (National Institutes of Health, USA) was used to quantify overlapping red and green colour pixels by means of manual intensity threshold settings in 25,000 pixel D14 stroma wound zone and D14 wounded peripheral stroma tissue areas (encompassing approximately seven stromal cells). The degree of colocalisation for the proteins was positively related to the Mander's coefficient (M1), known commonly as the 'overlap coefficient' (OC), and is expressed as a percentage

[69]. In this study, M1 corresponded to the total percentage of red pixels that colocalised with green pixels. M1 was calculated 10 independent times for D14 stroma wound zones and for D14 wounded peripheral stroma tissue areas from 5 independent Pou5f1/Tert and 5 independent Pax6/Sox2 colocalisation experiments. Two sample *t*-tests were carried out to test for a significant difference ($p \leq 0.05$) in M1 in D14 stroma wound zones compared to D14 wounded peripheral stroma tissue for both colocalisation experiments.

**Immunoblotting**

Protein was extracted from control, D14 and D28 wounded stroma tissue samples using a 1ml micro tissue grinder (Wheaton, USA) in PBS with a protease inhibitor cocktail (Roche, France). The supernatant was collected following a 10 minute 13,000 rpm centrifugation and protein concentration was determined using a Dc protein assay kit (BioRad, France). 10 µg lysates were run on 7.5-10% SDS-PAGE gels, transferred to Hybond-C extra nitrocellulose membranes (GE Healthcare, Canada) and blocked in 5% non-fat milk or BSA (Euromedex, France. Cat. No. 04-100-810-C) for 2 hours. Proteins were then labelled using monoclonal rat anti-Abcg2 (Abcam, England, Cat No. ab24115), monoclonal rabbit anti-Pax6 (Aviva Systems Biology, USA, Cat. No. ARP32741_P050) or monoclonal rat anti-Nestin (Chemicon, France, Cat. No. MAB353) primary antibodies overnight at $^{+}4°C$. Monoclonal rabbit anti-Th (Abcam, England, Cat No. ab75875) primary antibody was used as a housekeeping control. Primart antibody dilutions were 1/500, 1/4000, 1/400 and 1/500 in their respective order. Labeling was followed by a 2 hour incubation at room temperature with 1/5000 dilutions of anti-rat and anti-rabbit IgG conjugated with horseradish peroxidase (Sigma, USA. Cat. No. A5795 and A9169 respectively). Washes in PBS/Tween 1% were used between primary and secondary antibodies and before visualisation using an ECL-based detection system (Chemiluminescent Peroxidase Substrate-3 kit, Sigma, France). Prestained protein ladders were used for molecular weight determination (Fermentas, France. Cat. No. SM0671,

SM1811).

**Table 1** Primary and secondary antibodies used for protein detection with species, commercial, dilution and incubation information.

| Primary antibody | Supplier information | Dilution used | Incubation | Secondary Alexa Fluor® antibody |
|---|---|---|---|---|
| Rat monoclonal anti-Abcg2 | ab24115 Abcam, England | 1 µg/µl | 2 h/room temperature | Alexa 555, Cat. No. A21434 |
| Goat polyclonal anti-Tert | sc-68721 Santa Cruz Biotechnology Inc, Germany | 4 µg/µl | overnight/+4°C | Alexa 555, Cat. No. A21432 |
| Goat polyclonal anti-Sox2 | sc-17320 Santa Cruz Biotechnology Inc, Germany | 4 µg/µl | overnight/+4°C | Alexa 555, Cat. No. A21434 |
| Rat monoclonal anti-Nestin | sc-101541 Santa Cruz Biotechnology Inc, Germany | 2 µg/µl | overnight/+4°C | Alexa 555, Cat. No. A21434 |
| Rabbit polyclonal anti-Nanog | ab80892 Abcam, England | 2 µg/µl | 2 h/room temperature | Alexa 546, Cat. No. A11035 |
| Rabbit polyclonal anti-Oct4 | AB3209, Chemicon International Inc, USA | 2.5 µg/µl | 2 h/room temperature | Alexa 546, Cat. No. A11035 |
| Rabbit polyclonal anti-Pax6 | PRB-278P, Covance, California, USA | 3 µg/µl | overnight/+4°C | Alexa 546, Cat. No. A11035 |
| Rat IgG | MAB0061, R&D Systems Europe Ltd, England | 1 µg/µl | overnight/+4°C | Alexa 555, Cat. No. A21434 |
| Rabbit serum | R 9133, Sigma-Aldrich Inc, France | 1 µg/µl | 2 h/room temperature | Alexa 546, Cat. No. A11035 |
| Goat serum | G 9023, Sigma-Aldrich Inc, France | 4 µg/µl | overnight/+4°C | Alexa 555, Cat. No. A21432 |

**Acknowledgements**

The authors would like to thank staff from INSERM U563 histology and confocal imaging services and the Claude Bernard animal experimentation centre, Hôpital Purpan, CHU de Toulouse, France. The authors thank Dr. Sophie Allart for her confocal expertise (INSERM U563), Dr. Hélène Coppin for her RT-qPCR expertise and Dr. Heather Etchevers for help with the manuscript. The authors also thank Stéphane Roga, Dr. Nathalie Ortega and Dr. Christine Moussion for help with the figures. This work received funding from the European Commission's Sixth Framework Programme through the Marie Curie Research Training Network 'MY EUROPIA' (MRTN-CT-2006-034021).

## References


1 Hay ED. Development of the vertebrate cornea. *Int Rev Cytol* 1979; **63**:263-322.
2 Fini ME. Keratocyte and fibroblast phenotypes in the repairing cornea. *Prog Retin Eye Res* 1999; **18**:529-551.
3 Du Y, Funderburgh ML, Mann MM, SundarRaj N, Funderburgh JL. Multipotent stem cells in human corneal stroma. *Stem Cells* 2005; **23**:1266-1275.
4 Funderburgh ML, Du Y, Mann MM, SundarRaj N, Funderburgh JL. PAX6 expression identifies progenitor cells for corneal keratocytes. *Faseb J* 2005; **19**:1371-1373.
5 Thill M, Schlagner K, Altenahr S *et al*. A novel population of repair cells identified in the stroma of the human cornea. *Stem Cells Dev* 2007; **16**:733-745.
6 Yoshida S, Shimmura S, Nagoshi N *et al*. Isolation of multipotent neural crest-derived stem cells from the adult mouse cornea. *Stem Cells* 2006; **24**:2714-2722.
7 Yoshida S, Shimmura S, Shimazaki J, Shinozaki N, Tsubota K. Serum-free spheroid culture of mouse corneal keratocytes. *Invest Ophthalmol Vis Sci* 2005; **46**:1653-1658.
8 Du Y, Sundarraj N, Funderburgh ML, Harvey SA, Birk DE, Funderburgh JL. Secretion and organization of a cornea-like tissue in vitro by stem cells from human corneal stroma. *Invest Ophthalmol Vis Sci* 2007; **48**:5038-5045.
9 Abbott BL. ABCG2 (BCRP) expression in normal and malignant hematopoietic cells. *Hematol Oncol* 2003; **21**:115-130.
10 Scharenberg CW, Harkey MA, Torok-Storb B. The ABCG2 transporter is an efficient Hoechst 33342 efflux pump and is preferentially expressed by immature human hematopoietic progenitors. *Blood* 2002; **99**:507-512.
11 Zhou S, Schuetz JD, Bunting KD *et al*. The ABC transporter Bcrp1/ABCG2 is expressed in a wide variety of stem cells and is a molecular determinant of the side-population phenotype. *Nat Med* 2001; **7**:1028-1034.
12 Cai J, Cheng A, Luo Y *et al*. Membrane properties of rat embryonic multipotent neural stem cells. *J Neurochem* 2004; **88**:212-226.
13 Jang YK, Park JJ, Lee MC *et al*. Retinoic acid-mediated induction of neurons and glial cells from human umbilical cord-derived hematopoietic stem cells. *J Neurosci Res* 2004; **75**:573-584.
14 Martin CM, Meeson AP, Robertson SM *et al*. Persistent expression of the ATP-binding cassette transporter, Abcg2, identifies cardiac SP cells in the developing and adult heart. *Dev Biol* 2004; **265**:262-275.
15 Lechner A, Leech CA, Abraham EJ, Nolan AL, Habener JF. Nestin-positive progenitor cells derived from adult human pancreatic islets of Langerhans contain side population (SP) cells defined by expression of the ABCG2 (BCRP1) ATP-binding cassette transporter. *Biochem Biophys Res Commun* 2002; **293**:670-674.
16 Terunuma A, Jackson KL, Kapoor V, Telford WG, Vogel JC. Side population keratinocytes resembling bone marrow side population stem cells are distinct from label-retaining keratinocyte stem cells. *J Invest Dermatol* 2003; **121**:1095-1103.
17 Triel C, Vestergaard ME, Bolund L, Jensen TG, Jensen UB. Side population cells in human and mouse epidermis lack stem cell characteristics. *Exp Cell Res* 2004; **295**:79-90.
18 Dua HS, Shanmuganathan VA, Powell-Richards AO, Tighe PJ, Joseph A. Limbal epithelial crypts: a novel anatomical structure and a putative limbal stem cell niche. *Br J Ophthalmol* 2005; **89**:529-532.
19 Cvekl A, Tamm ER. Anterior eye development and ocular mesenchyme: new insights from mouse models and human diseases. *Bioessays* 2004; **26**:374-386.
20 Sivak JM, Mohan R, Rinehart WB, Xu PX, Maas RL, Fini ME. Pax-6 expression and activity are induced in the reepithelializing cornea and control activity of the transcriptional promoter for matrix metalloproteinase gelatinase B. *Dev Biol* 2000; **222**:41-54.
21 Osumi N, Shinohara H, Numayama-Tsuruta K, Maekawa M. Concise review: Pax6

transcription factor contributes to both embryonic and adult neurogenesis as a multifunctional regulator. *Stem Cells* 2008; **26**:1663-1672.
22 Thummel R, Enright JM, Kassen SC, Montgomery JE, Bailey TJ, Hyde DR. Pax6a and Pax6b are required at different points in neuronal progenitor cell proliferation during zebrafish photoreceptor regeneration. *Exp Eye Res* 2010; **90**:572-582.
23 Thummel R, Kassen SC, Enright JM, Nelson CM, Montgomery JE, Hyde DR. Characterization of Muller glia and neuronal progenitors during adult zebrafish retinal regeneration. *Exp Eye Res* 2008; **87**:433-444.
24 Galiacy SD, Fournie P, Massoudi D *et al.* Matrix metalloproteinase 14 overexpression reduces corneal scarring. *Gene Ther* 2010.
25 Thomas S, Thomas M, Wincker P *et al.* Human neural crest cells display molecular and phenotypic hallmarks of stem cells. *Hum Mol Genet* 2008; **17**:3411-3425.
26 Michalczyk K, Ziman M. Nestin structure and predicted function in cellular cytoskeletal organisation. *Histol Histopathol* 2005; **20**:665-671.
27 Namiki J, Tator CH. Cell proliferation and nestin expression in the ependyma of the adult rat spinal cord after injury. *J Neuropathol Exp Neurol* 1999; **58**:489-498.
28 Vaittinen S, Lukka R, Sahlgren C *et al.* The expression of intermediate filament protein nestin as related to vimentin and desmin in regenerating skeletal muscle. *J Neuropathol Exp Neurol* 2001; **60**:588-597.
29 Avilion AA, Nicolis SK, Pevny LH, Perez L, Vivian N, Lovell-Badge R. Multipotent cell lineages in early mouse development depend on SOX2 function. *Genes Dev* 2003; **17**:126-140.
30 Boyer LA, Lee TI, Cole MF *et al.* Core transcriptional regulatory circuitry in human embryonic stem cells. *Cell* 2005; **122**:947-956.
31 Chambers I, Colby D, Robertson M *et al.* Functional expression cloning of Nanog, a pluripotency sustaining factor in embryonic stem cells. *Cell* 2003; **113**:643-655.
32 Loh YH, Wu Q, Chew JL *et al.* The Oct4 and Nanog transcription network regulates pluripotency in mouse embryonic stem cells. *Nat Genet* 2006; **38**:431-440.
33 Mitsui K, Tokuzawa Y, Itoh H *et al.* The homeoprotein Nanog is required for maintenance of pluripotency in mouse epiblast and ES cells. *Cell* 2003; **113**:631-642.
34 Muller T, Fleischmann G, Eildermann K *et al.* A novel embryonic stem cell line derived from the common marmoset monkey (Callithrix jacchus) exhibiting germ cell-like characteristics. *Hum Reprod* 2009; **24**:1359-1372.
35 Niwa H, Miyazaki J, Smith AG. Quantitative expression of Oct-3/4 defines differentiation, dedifferentiation or self-renewal of ES cells. *Nat Genet* 2000; **24**:372-376.
36 Babaie Y, Herwig R, Greber B *et al.* Analysis of Oct4-dependent transcriptional networks regulating self-renewal and pluripotency in human embryonic stem cells. *Stem Cells* 2007; **25**:500-510.
37 Dua HS, Joseph A, Shanmuganathan VA, Jones RE. Stem cell differentiation and the effects of deficiency. *Eye (Lond)* 2003; **17**:877-885.
38 Beyne-Rauzy O, Recher C, Dastugue N *et al.* Tumor necrosis factor alpha induces senescence and chromosomal instability in human leukemic cells. *Oncogene* 2004; **23**:7507-7516.
39 Zhou SY, Zhang C, Baradaran E, Chuck RS. Human corneal basal epithelial cells express an embryonic stem cell marker OCT4. *Curr Eye Res* 2010; **35**:978-985.
40 Amit M, Carpenter MK, Inokuma MS *et al.* Clonally derived human embryonic stem cell lines maintain pluripotency and proliferative potential for prolonged periods of culture. *Dev Biol* 2000; **227**:271-278.
41 Hiyama E, Hiyama K. Telomere and telomerase in stem cells. *Br J Cancer* 2007; **96**:1020-1024.
42 Millimaki BB, Sweet EM, Riley BB. Sox2 is required for maintenance and regeneration, but not initial development, of hair cells in the zebrafish inner ear. *Dev Biol* 2010; **338**:262-269.
43 Nayernia K, Lee JH, Drusenheimer N *et al.* Derivation of male germ cells from bone marrow stem cells. *Lab Invest* 2006; **86**:654-663.

44 Pallante BA, Duignan I, Okin D *et al.* Bone marrow Oct3/4+ cells differentiate into cardiac myocytes via age-dependent paracrine mechanisms. *Circ Res* 2007; **100**:e1-11.
45 Zhang S, Jia Z, Ge J *et al.* Purified human bone marrow multipotent mesenchymal stem cells regenerate infarcted myocardium in experimental rats. *Cell Transplant* 2005; **14**:787-798.
46 Song N, Jia XS, Jia LL *et al.* Expression and role of Oct3/4, Nanog and Sox2 in regeneration of rat tracheal epithelium. *Cell Prolif* 2010; **43**:49-55.
47 Racila D, Winter M, Said M *et al.* Transient expression of OCT4 is sufficient to allow human keratinocytes to change their differentiation pathway. *Gene Ther* 2010.
48 Lwigale PY, Cressy PA, Bronner-Fraser M. Corneal keratocytes retain neural crest progenitor cell properties. *Dev Biol* 2005; **288**:284-293.
49 Christen B, Robles V, Raya M, Paramonov I, Belmonte JC. Regeneration and reprogramming compared. *BMC Biol* 2010; **8**:5.
50 Kragl M, Knapp D, Nacu E *et al.* Cells keep a memory of their tissue origin during axolotl limb regeneration. *Nature* 2009; **460**:60-65.
51 Stramer BM, Zieske JD, Jung JC, Austin JS, Fini ME. Molecular mechanisms controlling the fibrotic repair phenotype in cornea: implications for surgical outcomes. *Invest Ophthalmol Vis Sci* 2003; **44**:4237-4246.
52 Mimura T, Amano S, Yokoo S, Uchida S, Usui T, Yamagami S. Isolation and distribution of rabbit keratocyte precursors. *Mol Vis* 2008; **14**:197-203.
53 Li L, Mignone J, Yang M *et al.* Nestin expression in hair follicle sheath progenitor cells. *Proc Natl Acad Sci U S A* 2003; **100**:9958-9961.
54 Johansson CB, Lothian C, Molin M, Okano H, Lendahl U. Nestin enhancer requirements for expression in normal and injured adult CNS. *J Neurosci Res* 2002; **69**:784-794.
55 Espana EM, Kawakita T, Di Pascuale MA *et al.* The heterogeneous murine corneal stromal cell populations in vitro. *Invest Ophthalmol Vis Sci* 2005; **46**:4528-4535.
56 Muller LJ, Pels L, Vrensen GF. Novel aspects of the ultrastructural organization of human corneal keratocytes. *Invest Ophthalmol Vis Sci* 1995; **36**:2557-2567.
57 Arnalich-Montiel F, Pastor S, Blazquez-Martinez A *et al.* Adipose-derived stem cells are a source for cell therapy of the corneal stroma. *Stem Cells* 2008; **26**:570-579.
58 Liu H, Zhang J, Liu CY *et al.* Cell therapy of congenital corneal diseases with umbilical mesenchymal stem cells: lumican null mice. *PLoS One* 2010; **5**:e10707.
59 Cursiefen C, Maruyama K, Jackson DG, Streilein JW, Kruse FE. Time course of angiogenesis and lymphangiogenesis after brief corneal inflammation. *Cornea* 2006; **25**:443-447.
60 Brandl C, Florian C, Driemel O, Weber BH, Morsczeck C. Identification of neural crest-derived stem cell-like cells from the corneal limbus of juvenile mice. *Exp Eye Res* 2009; **89**:209-217.
61 Dravida S, Pal R, Khanna A, Tipnis SP, Ravindran G, Khan F. The transdifferentiation potential of limbal fibroblast-like cells. *Brain Res Dev Brain Res* 2005; **160**:239-251.
62 Polisetty N, Fatima A, Madhira SL, Sangwan VS, Vemuganti GK. Mesenchymal cells from limbal stroma of human eye. *Mol Vis* 2008; **14**:431-442.
63 Kato N, Shimmura S, Kawakita T *et al.* Beta-catenin activation and epithelial-mesenchymal transition in the pathogenesis of pterygium. *Invest Ophthalmol Vis Sci* 2007; **48**:1511-1517.
64 Kawakita T, Espana EM, He H, Li W, Liu CY, Tseng SC. Intrastromal invasion by limbal epithelial cells is mediated by epithelial-mesenchymal transition activated by air exposure. *Am J Pathol* 2005; **167**:381-393.
65 Ou J, Walczysko P, Kucerova R *et al.* Chronic wound state exacerbated by oxidative stress in Pax6+/- aniridia-related keratopathy. *J Pathol* 2008; **215**:421-430.
66 McGowan SL, Edelhauser HF, Pfister RR, Whikehart DR. Stem cell markers in the human posterior limbus and corneal endothelium of unwounded and wounded corneas. *Mol Vis* 2007; **13**:1984-2000.
67 Reneker LW, Bloch A, Xie L, Overbeek PA, Ash JD. Induction of corneal myofibroblasts by lens-derived transforming growth factor beta1 (TGFbeta1): a transgenic mouse model.

*Brain Res Bull* 2010; **81**:287-296.
68 Livak KJ, Schmittgen TD. Analysis of relative gene expression data using real-time quantitative PCR and the 2(-Delta Delta C(T)) Method. *Methods* 2001; **25**:402-408.
69 Manders EM, Stap J, Brakenhoff GJ, van Driel R, Aten JA. Dynamics of three-dimensional replication patterns during the S-phase, analysed by double labelling of DNA and confocal microscopy. *J Cell Sci* 1992; **103 ( Pt 3)**:857-862.

**Titles and legends to figures**

**Figure 1. Increased expression of keratocyte progenitor cell markers *in vivo* during corneal wound repair: ABCG2**

(A-E) Abcg2 immunostaining (red). (A, C) Control cornea. Arrowheads (C) indicate Abcg2-positive stromal cells. (B) D14 wounded cornea. (D) D14 wound zone. (E) D28 wound zone. Nuclei were counterstained with DAPI. (A-B) X200; scale bars represent 50 µm. (C-E) X630; scale bars represent 20 µm. (F) Western blot analysis of Abcg2 protein (72 KDa) expression in control (C), D14 and D28 wounded stromas. Th (59 KDa) was used as a housekeeping control in control (C), D14 and D28 wounded stromas.

**Figure 2. Increased expression of keratocyte progenitor cell markers *in vivo* during corneal wound repair: Pax6**

(A-C) Pax6 immunostaining (red). (A) Control cornea. (B) D14 wound zone. (C) D28 wound zone. Nuclei were counterstained with DAPI. X630; scale bars represent 20 µm. The magnification of Fig. 2B has not been altered according to the other confocal images (X630). We observed some inter-mouse differences in the sizes of wounded corneal tissues. (D) Western blot analysis of Pax6 protein (48 KDa) expression in lanes control (C), D14 and D28 wounded stromas. Th (59 KDa) was used as a housekeeping control in control (C), D14 and D28 wounded stromas.

**Figure 3. Tert protein expression and activity in control and wounded stromas.**

(A-D) Tert immunostaining (red). (A) Control cornea. (B) D7 wound zone. (C) D14 wound zone. (D) D28 wound zone. Nuclei were counterstained with DAPI. X630; scale bars represent 20 µm. (E) Telomerase activity revealed by a PCR assay. D14 wounded stromas were compared to control stromas. The stromas of six control corneas and the stromas of six D14 wounded corneas were pooled. Data (mean±SEM) are from three independent

experiments. Activity is normalised to the negative control (lysate buffer). Human KG1 myeloblastic cells were used as a housekeeping positive control. KG1 500/250 = 500/250 equivalent cells respectively. * p≤0.05.

**Figure 4. Corneal Stroma cells re express stem cells markers**

Sox2 immunostaining (red). Proximal wounded tissue corresponds to intact and more highly organised corneal tissue neighbouring the direct wound zone. Peripheral wounded tissue corresponds to corneal tissue towards the limbus. (A) Control cornea. Arrowhead; Sox2-positive stromal cell. (B) D14 wound zone. (C) D14 proximal wound zone cornea. (D) D14 peripheral cornea. (F) D28 wound zone. (G) D28 proximal wound zone cornea. (H) D28 peripheral cornea. Nuclei were counterstained with DAPI. X630; scale bars represent 20 µm.

Sox2 mRNA (E) Agarose gel electrophoresis quantification of *Sox2* RT-qPCR products (75 bp amplicon) in control C and D14 wounded stromas. Controls: *Th* housekeeping control gene (110 bp amplicon) in control C and D14 wounded stromas. (-) Negative control. (M) DNA ladder, 50 bp.

**Figure 5. Increased colocalisation of Pou5f1-positive stromal cells with Tert protein in wounded stroma zones.**

(A-G) Pou5f1 (red) and Tert (green) coimmunostaining. (A) Control cornea. Arrowhead indicates a Pou5f1-positive cell. (B) D14 wound zone. (C) D14 peripheral wounded cornea. X630; scale bar represents 20 µm. (D-G) Magnification (X2500) of stromal cell arrowed in (C). Scale bar represents 5 µm.

**Figure 6. Nestin mRNA and protein expression.**

(A) *Nestin* mRNA was assayed in control and D7-D28 wounded stromas by RT-qPCR. Expression in wounded stromas is normalised to the expression in control stromas. p≤0.05.

Bars represent SEM for independent wounded stroma samples. (B) Western blot analysis of Nestin protein (200-220 KDa) expression in control (C), D14 and D28 wounded stromas. Th (59 KDa) was used as a housekeeping control in control (C), D14 and D28 wounded stromas. Nestin immunostaining (red). (C) Control cornea. (D) D14 wound zone. (E) D28 wound zone. X630; scale bars represent 20 µm. (F) D28 wounded cornea. X200; scale bars represents 70µm. Arrowhead corresponds to wound zone. Nuclei were counterstained with DAPI.

**Figure.1**

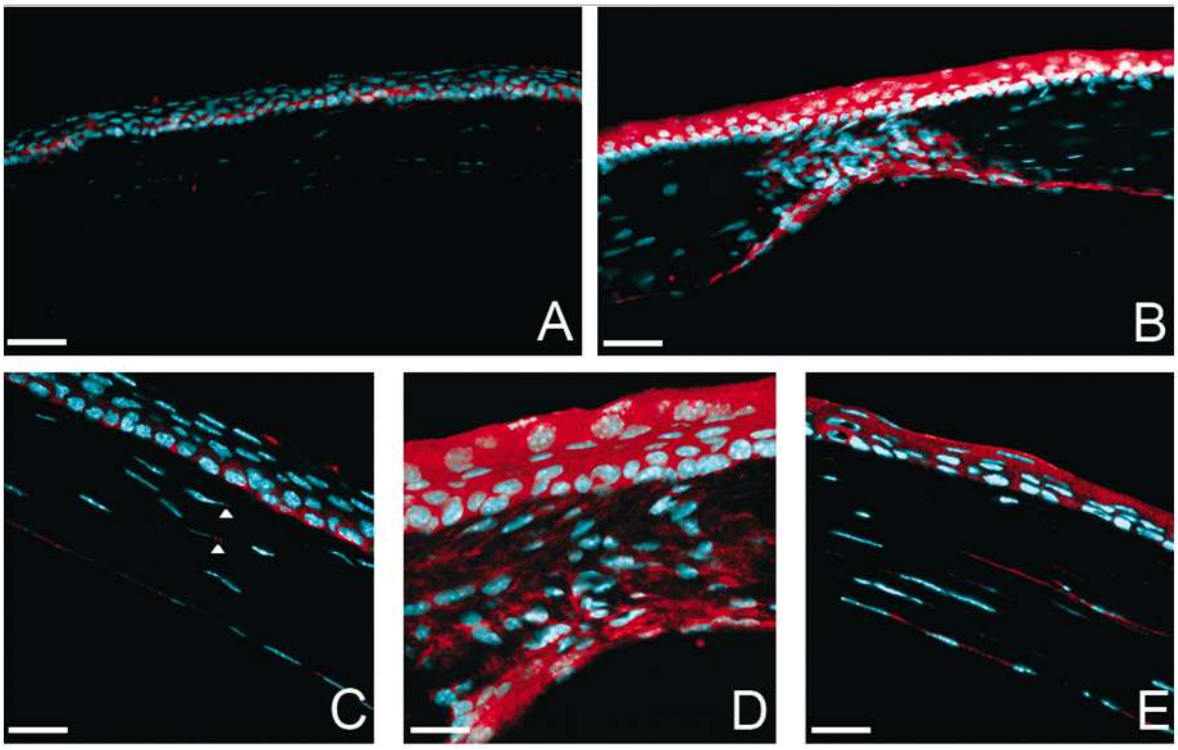


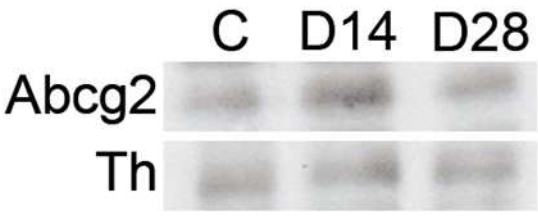


F

**Figure.2**

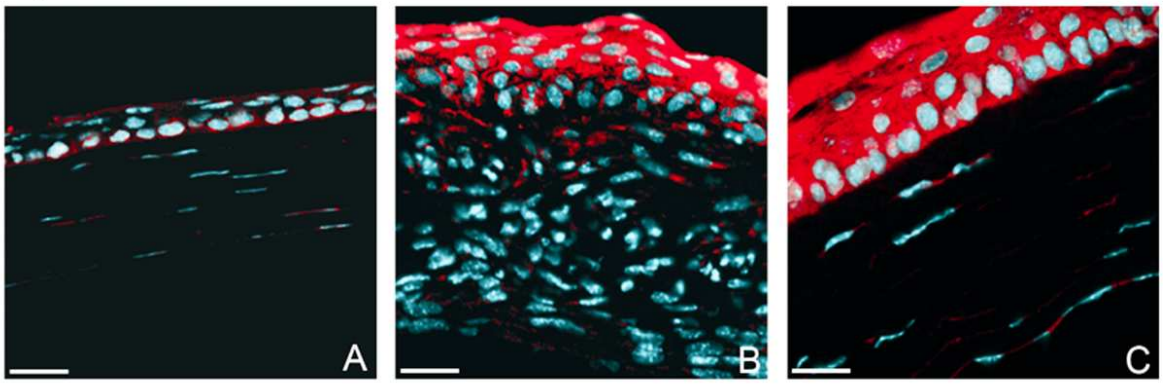


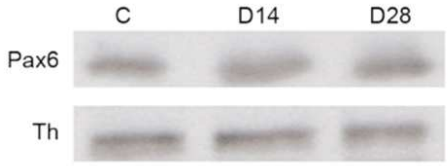


D

Figure.3

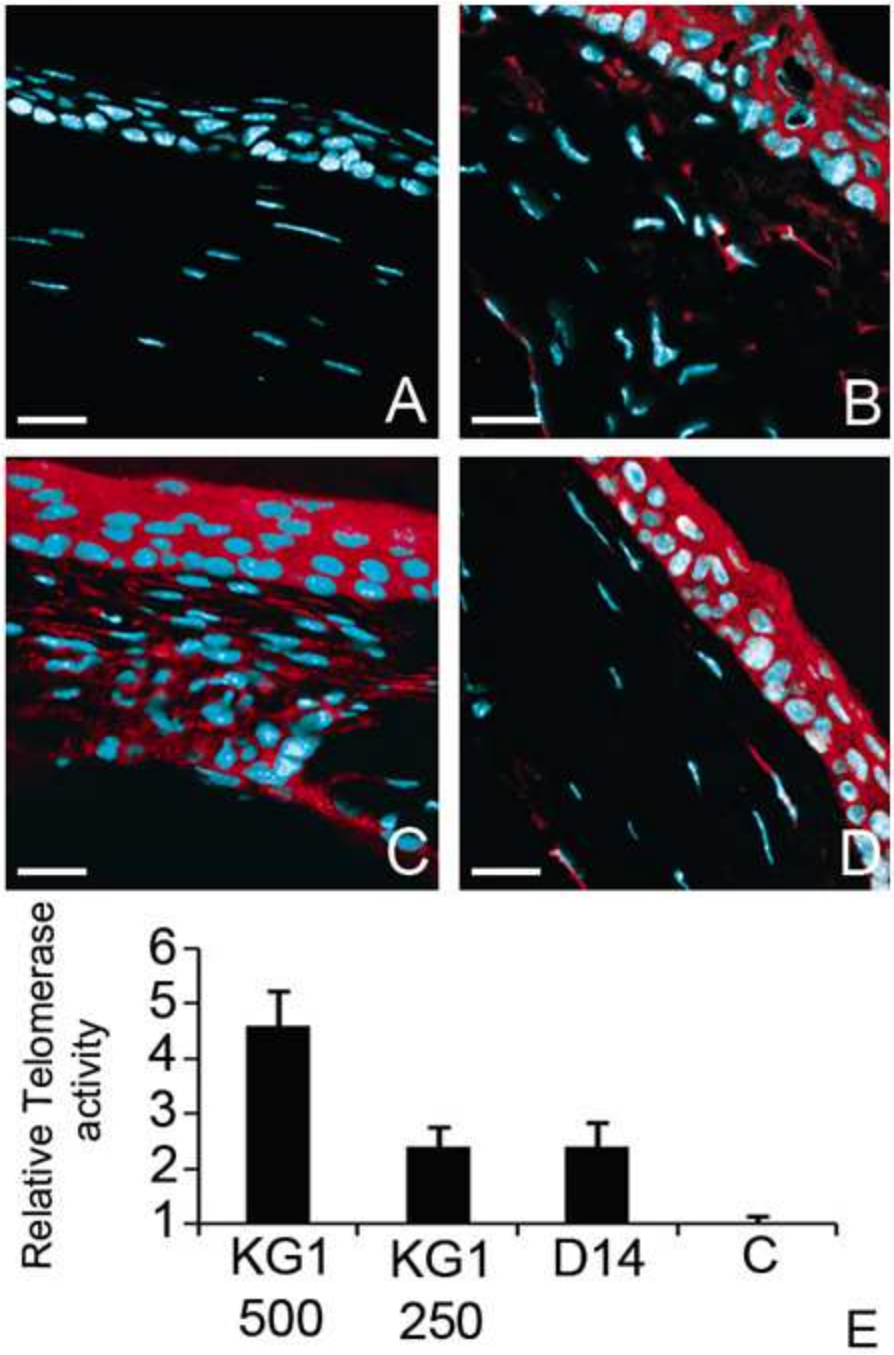
A
B
C
D
Relative Telomerase activity
6
5
4
3
2
1
KG1 500
KG1 250
D14
C
E

Figure.4

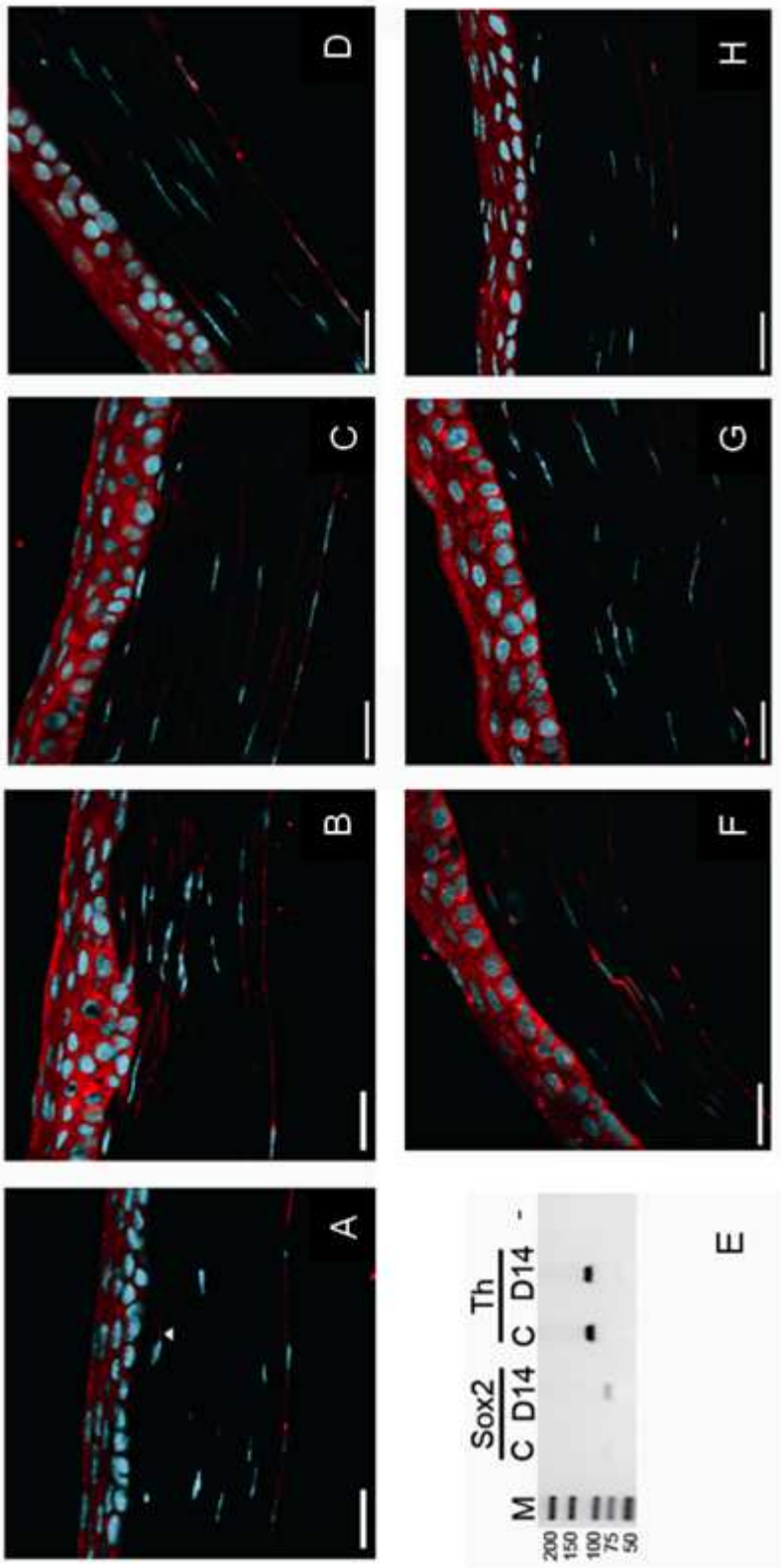

**Figure.5**

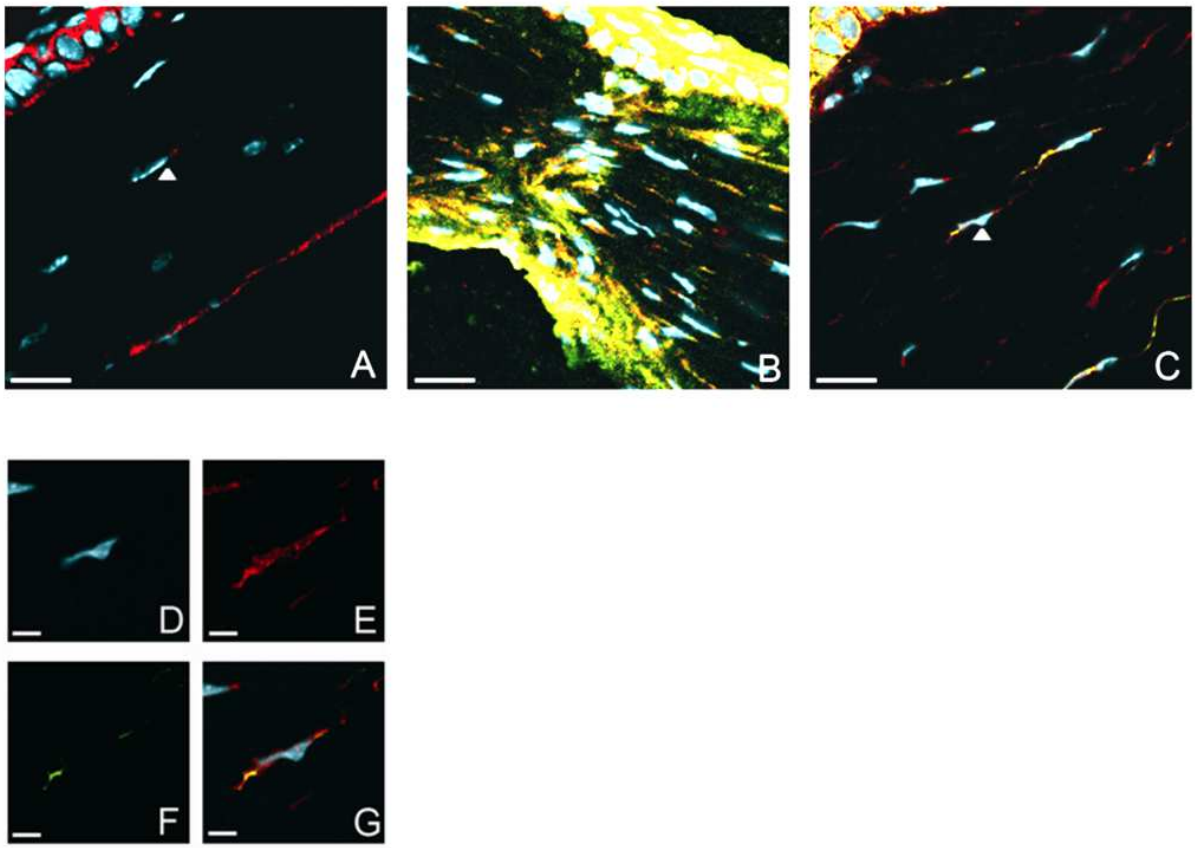

**Figure.6**

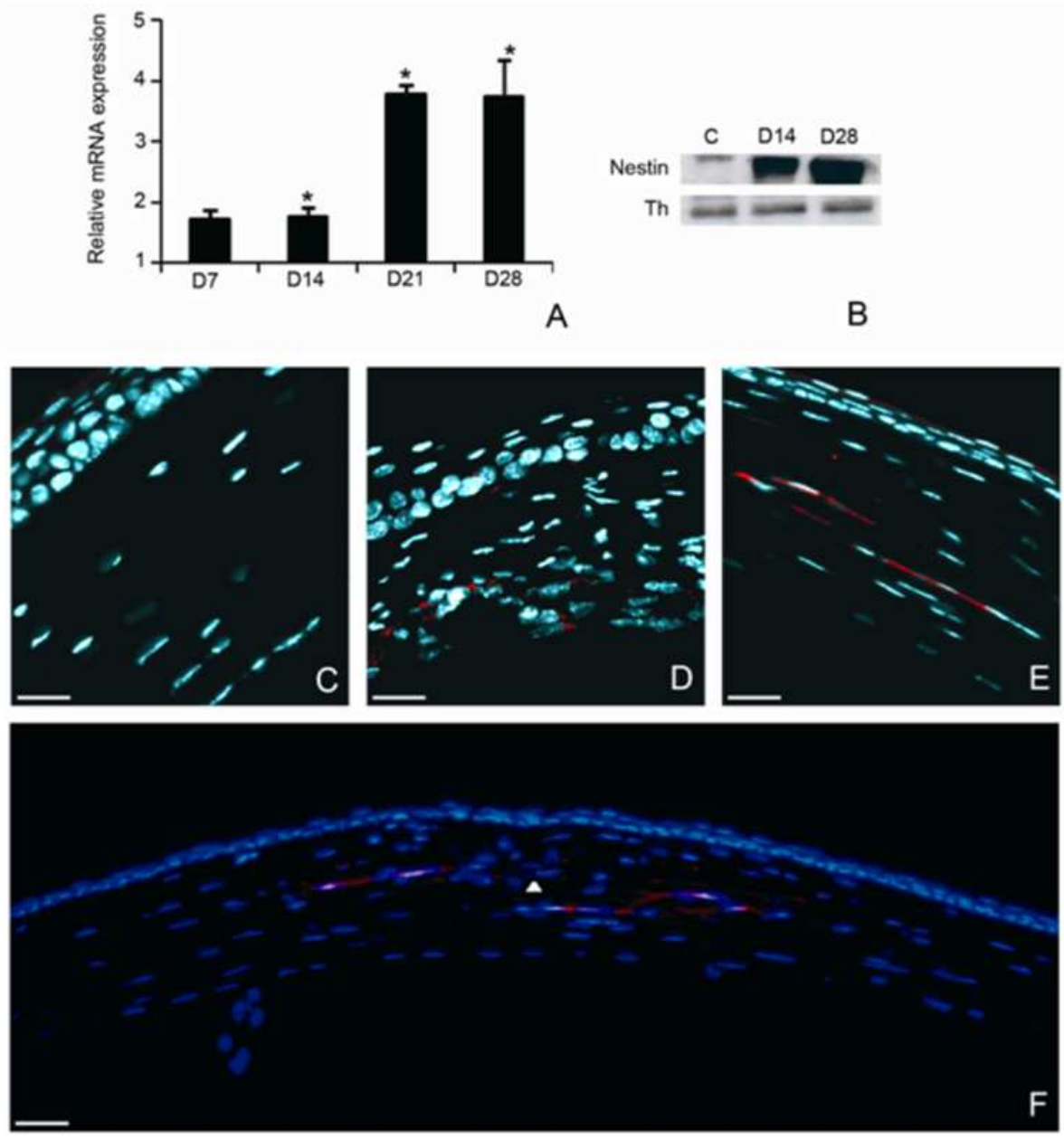
Relative mRNA expression
5
4
3
2
1
D7
D14
D21
D28
A
C
D14
D28
Nestin
Th
B
C
D
E
F

# V General Discussion

To date only *in vitro* cell studies and therapeutic cell injection studies have put forward the suggestion of the existence of a corneal stromal progenitor subpopulation with a keratocyte cell replenishment function. This project has not only shown the potential presence of a stromal progenitor cell population that expands throughout the *in vivo* corneal wound response, but has also demonstrated that the adult keratocyte may revert to an embryonic-like cell phenotype in the *in vivo* wounded stroma. The identification of these two new *in vivo* cell populations indicates the presence of unknown repair events that still need to be determined in the *in vivo* wounded stroma, involving at least these two cell populations. Two major questions need to be answered, **what are the functions of these cells in the stromal wound response, and where do they originate from?**

## 1. Different Adult Tissue Regeneration Models

In an attempt to answer these questions we can consider the underlying mechanisms of wound healing responses in other adult tissues following injury.

### 1.1 The Skin

The skin has been abundantly studied for its regenerative capacity considering its exposed and therefore easy access location for experimentation. Similar to the cornea, the skin is an epithelial-lined organ, where the epidermis corresponds to the outer complex stratified squamous epithelial cell layer. The dermis is the thick underlying structural component that is constituted in majority by collagen and ECM, as well as hair follicles, sebaceous glands, apocrine glands, adipocytes, lymphatic and blood vessels. Thus, the dermis is a more complex tissue than the corneal stroma, harbouring at least three different stem cell lineages [638]. It does however contain the adult fibroblast cell, being the morphological and functional equivalent of the corneal stromal keratocyte cell. Similar to the cornea, much more attention has been placed on the definition and behavior of outer epidermal layer stem cells that are responsible for the maintenance of the skin barrier. Knowledge is still incomplete on how the dermis is coordinated at the cellular level during skin wound repair, but results have strongly shown the presence of a multipotent resident bone marrow-derived fibroblast-like stem cell subpopulation [638]. It has been suggested that this stem cell population has more of an “enhancer” role throughout wound healing, having a significant *effect on* the signalling

events involved in wound healing [638]. These cells secrete a variety of growth factors, cytokines* and chemokines* known to enhance cell growth [639-641], as well as factors that down-modulate inflammatory cytokines [642, 643], and this release has been found to be up to seven-fold higher than the release by activated adult fibroblast cells [639]. This implies a paracrine* signalling function of these stem cells to enhance, or guide the wound response of other cells in the tissue [638, 644]. On the other hand, some reports indicate that resident dermal stem cells also provide committed daughter progenitor cells that differentiate and directly contribute to the structural repair of wounds [644]. This suggests that bone marrow-derived resident stem cells could elicit at least two different roles in dermis wound repair; **guide other cells along their repair pathway, and themselves regenerate new cells for wound repair**.

### 1.2 Skeletal Muscles

Another interesting point is that in more complex tissues, not one, but *multiple* different progenitor cell populations have been identified. In skeletal muscle there has been at least four different stem/progenitor cell populations characterised. These cells are side-population cells, muscle-derived stem cells, CD133-positive progenitor cells and the Satellite progenitor cells [645]. Extensive cell isolation studies have found that these cells exist as independent populations based on their differences in surface antigens and origins; some are externally recruited via blood vessels [645]. Satellite progenitors are dormant cells localised in a specific niche found at the periphery of skeletal fibres and are largely considered to date the myogenic muscle repair cell population. In response to muscle stress or trauma, Satellite cells are activated, migrate and proliferate and differentiate into myogenic cells for regeneration [646]. To date the roles of the other stem/progenitor cell populations remains elusive [645].

### 1.3 Neural Tissues

Adult neurogenesis is generally considered an active process encompassing the proliferation and cell fate* specification of endogenous adult neural progenitors, and their subsequent differentiation, maturation and functional integration into the existing neuronal circuitry [647]. In the adult CNS, active neurogenesis occurs in two discrete ‘neurogenic’ regions in the brain; essentially a specialised compartement in the forebrain for supporting high rates of cell proliferation, and a subcompartment in the hippocampus involved in

memory consolidation [648, 649]. Experimental animal models of adult CNS inflammatory disorders, such as multiple sclerosis and autoimmune encephalomyelitis (both multipfocal demyelinating disorders), demonstrate that progenitor cells can suvbvert to migration to the areas of demyelination [650, 651]. Here these cells release an array of molecules containing immunomodulatory substances, neutrophic growth factors and stem cell regulators that coordinate progenitor cell proliferation, followed by their differentiation into glial cells [652]. Again the same conclusion can be made concerning the intrinsic function of progenitor cells in adult neurogenesis; they not only guide other cells along their repair pathway, they themselves contribute directly to the wound response by replacing lost somatic cells. Again, adult neural tissues undergoing repair have been found to harbour a heterogenous cell population, containing not only neural crest-derived stem cells, but bone marrow-derived mesencymal and haematopoietic stem cells [653].

The regenerative theories raised here can be somewhat extrapolated to try and decipher the mechanisms underlying the corneal stromal wound response (leaving merge for tissue and species differences).

## 2. Functions and Origins of the Corneal Stromal Progenitor Cell Subpopulation(s)

The stromal wound zone progenitor cells identified in our study could be the equivalent of the muscle Satellite cell; resident in the normal stroma as a “dormant” subpopulation, but activates and proliferates following corneal injury, following differentiation into adult keratocyte cells in later stromal repair phases. Additionally, we could also expect progenitor cells to elicit a paracrine* signalling role to enhance endogenous adult keratocyte cell activation and inflammatory cell responses. Finally, work by Du et al., (2007) [458] demonstrated that *in vitro* corneal stromal progenitor cells were more efficient in novel stromal ECM production and secretion compared to corneal stroma-derived repair fibroblast cells. Thus, could we even attribute a direct contribution of wound zone progenitor cells to new ECM deposition?

In our mouse corneal wound healing model, the progenitor cell population in the stromal wound zone ($\underline{Tert}^{+}$/Abcg2$^{+}$/CD133$^{+}$) did not harbour expression of the same adult stem cell markers to the minor progenitor cell population within peripheral wounded stromal tissue ($\underline{Tert}^{+}$/Abcg2$^{-}$/CD133$^{-}$). Are these cells from a different tissue cell lineage? Do these cells elicit different functions? Progenitor cells localised within wounded peripheral stromal

tissue could elicit paracrine* signaling roles that guide other cells, in particular activated keratocyte cells, along their repair pathway. Tert expression could be involved in cell survival signals, as previously reported in mesenchymal stem and progenitor cells from several different human cell lineages [616-618]. This signal may involve inhibition of keratocyte cell apoptosis [619], while at the same time activating their half way state in the case of a requirement to adopt a repair fibroblast or myofibroblast phenotype for repair fucntion.

To my knowledge the localisation of just one progenitor cell lineage in an adult tissue has not been reported. Likewise, given the heterogeneity of the stem cell marker profiles identified in the *in vitro* studies that have tried to characterise corneal stromal progenitor cells [404, 457, 458, 513], we can expect some external corneal tissue progenitor cells to home to the wounded stroma. These are most likely to be progenitor cells of bone marrow-derived cell lineages [510-512]. On the other hand, skin, muscle and CNS neural tissues are more complex tissues than the cornea, involving many more cell types, so we could expect there to be less different progenitor subpopulations in the stroma than those that come into play in these tissues. Further *in vivo* cell isolation studies need to be carried out to determine progenitor surface antigens to identify the different progenitor lineages present in the normal and wounded stroma.

### 3. Roles of the New Half Way State Keratocyte Phenotype

Animal models based on determining the extent of dermal wound healing from adult mesenchymal stem cell function has been carried out upon application of mesenchymal stem cells to a wound bed within an isolated wound chamber (all surrounding skin tissue is removed). It was discovered that wounds only healed when a mixture of both mesenchymal stem cells ***with embryonic skin cells*** were applied to the wound chamber [654]. These results suggest that the resident dermal mesenchymal stem cells required the coexistence of other dermal cells for tissue regeneration. This finding, along with the theory made that similar signal upregulation is found in the developing CNS as in regenerative adult CNS, implies similarities between somatic cell responses in both embryonic development and adult tissue regeneration [614, 653]. In other words, it appears that pre-existing cells are required not only for a mechanical structure for tissue regeneration [638], but also for dedifferentiation to replenish lost cells [655] and for the release of signaling molecules to guide endogenous cell responses [638]. Accordingly, we could apply these same functions to the embryonic-like activated keratocyte cell in the wounded stroma. Their upregulation of undifferentiated

markers Sox2, Oct-3/4 and Nanog throughout the wounded stroma could play a role in self-renewal and differentiation signaling events, as previously demonstrated in other adult tissues [553, 555, 566-569, 587, 588]. Initial upregulation followed by an expected loss of these signals would be important for keratocyte signals to respectively:

1. Activate other keratocyte cells within the wound zone to proliferate. There could be additionally a role for these signals to activate stromal wound zone cells to adopt the repair fibroblast phenotype, or differentiate into myofibroblast cells, for wound repair.
2. Activate the later stromal remodelling phase keratocyte regeneration pathway in order for myofibroblast cells in the wound zone to eventually differentiate into keratocyte cells to replace the cells lost from apoptosis.

However, self-renewal and differentiation signals could equally be activated keratocyte-progenitor signals. We could expect a role of activated keratocyte cells in the regulation of progenitor cell expansion throughout the early stages of the *in vivo* corneal stromal wound response. Likewise differentiation signals could activate progenitor cell differentiation once stroma remodelling is complete.

### 4. The Wounded Stromal Response; A Complex Network of Cell Repair Signals

We can observe the stromal wound response as a controlled network of signaling events. Taking into account the different possible combinations of repair signals at play, we can start to assemble a complex network of stromal cell repair responses, with different signal pathways activated in different wound healing stages. Taking into account published observations and the results from this project; **I put forward the following schematic representation of the cell responses in the *in vivo* corneal wound response**:

## 4.1 The Normal Stroma

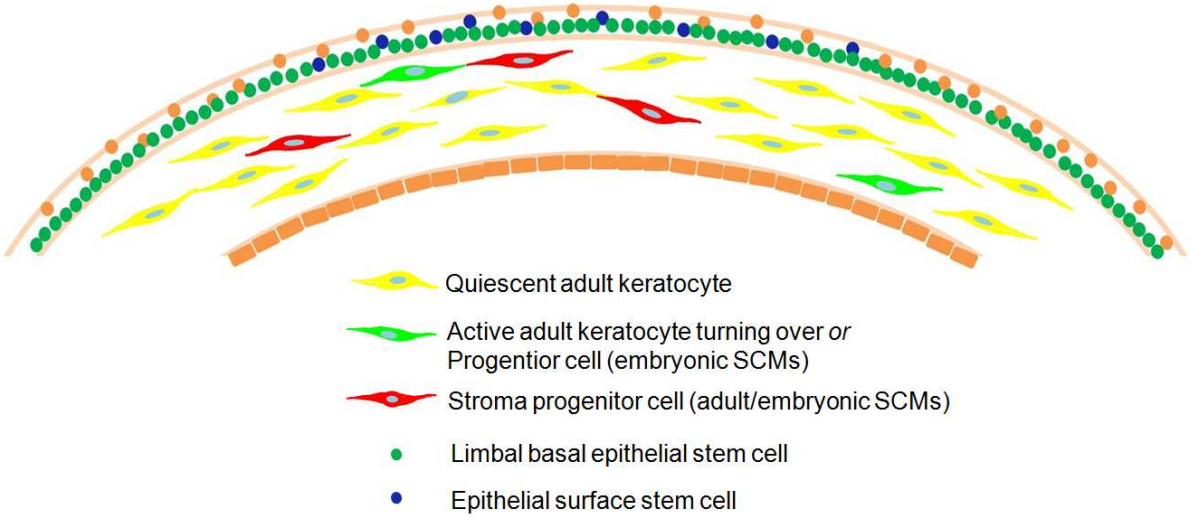


The most abundant corneal stroma cell type is the quiescent adult keratocyte that does not express adult stem cell markers (SCMs), but is likely to express Pax6. The normal stroma is thought to harbour a progenitor cell subpopulation. Morphologically these cells are not distinguishable from adult keratocyte cells in order to retain the transparent corneal quality, but surface marker expression of adult stem cell markers allows us to distinguish them. There is also thought to be a minor subpopulation of cells that express embryonic stem cell markers, but we cannot yet determine if these cells are keratocyte cells turning over and/or progenitor cells. We do not know at present if the progenitor cell subpopulation is an *in situ* stromal cell population, or if progenitor cells migrate and reside in the stroma from a limbal niche of from external corneal tissues via the limbal region. Progentior cells in the normal stroma could act as guardians, ready to proliferate and elicit their stromal repair functions in the respone to corneal injury.

## 4.2 The Wounded Stroma

### 4.2.1 D7-D14: The Stromal Wound Stabilisation Phase

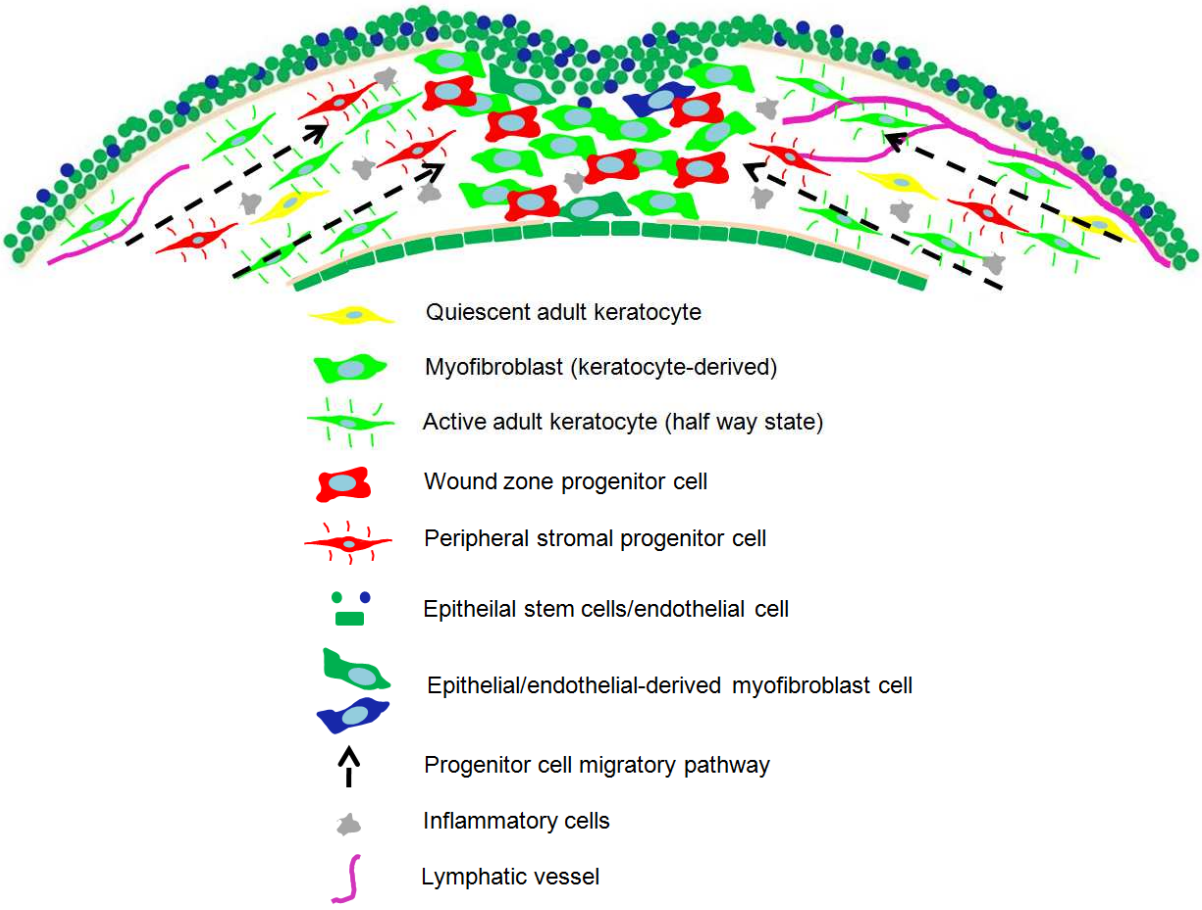


The earlier wound response stages could be considered as a coordinated network of signals and responses to promote repair cell synthesis and deposition of a new ECM to fill in lost stromal tissue [644]. We could expect the following cellular events (with many occurring simultaneously):

- A decrease in adult keratocytes cells in the stromal wound vicinity due to apoptosis.
- Keratocyte apoptosis and epithelium-stroma cell interactions activate the progenitor cell subpopulation, resulting in progenitor cell expansion in the wound zone. Progenitor cells within the wound zone could contribute to new ECM production. These cells express adult and embryonic stem cell markers. We could expect these cells to have a repair myofibroblast cell phenotype, and they could also express α-SMA.

- Progenitor cell signals (and perhaps half way state keratocyte cell signals) and epithelium-stroma cell interactions stimulate the differentiation of wound zone keratocyte cells into myofibroblast cells to synthesise and deposit new ECM. I would expect these cells to show an upregulation of α-SMA expression, and perhaps express both adult and embryonic stem cell markers. These cells could be considered as keratocytes that go beyond their half way state.
- Progenitor cells away from the wound zone could be involved in paracrine* signaling events that enhance the activation of keratocyte cells throughout the entire wounded stroma, while proximal activated wound zone keratocyte cells could initiate the activation of other keratocyte cells via their ECM network. The keratocyte half way state phenotype would be adopted by adult keratocytes throughout the stroma.
- We expect EMT/EnMT of some epithelial and endothelial cells respectively. Thse cells would migrate into *proximal* wounded stromal tissue to contribute to ECM synthesis.
- We expect some influx migration of external stromal progenitor cells into the wounded stroma from the the limbal region and/or the blood circulation.
- The formation of lymph vessels could also be observed, either directly in proximal wound zone stromal tissue or from limbal outgrowths into peripheral stromal tissue. These vessels could participate in influx of inflammatory and external stromal progenitor cells.

### 4.2.2 D21-D28: The Stromal Repair Phase

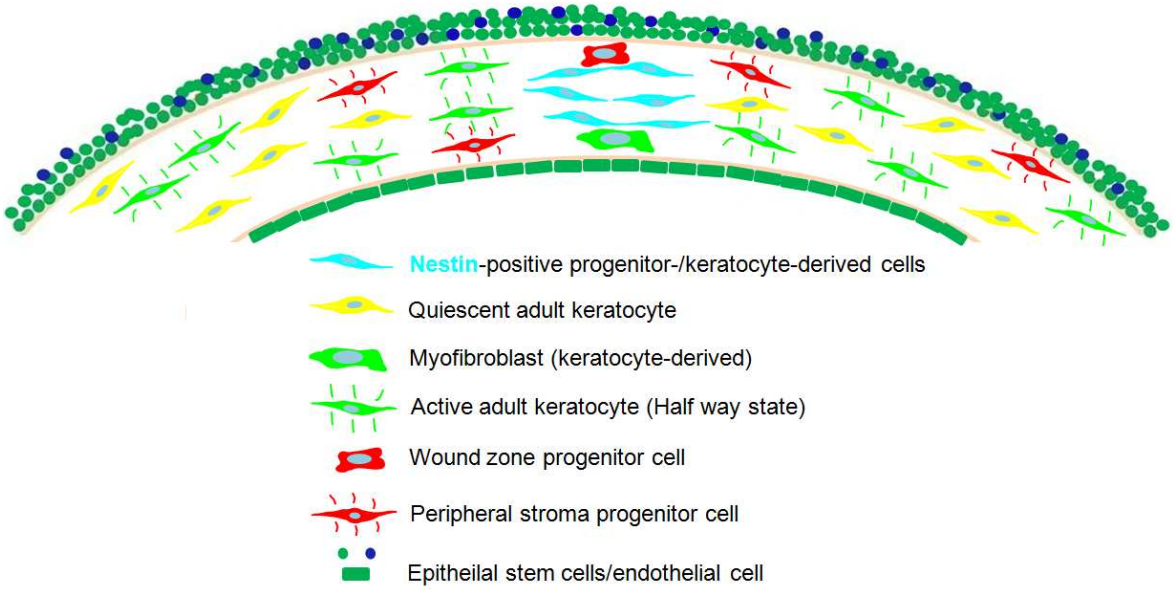


The later wound healing phase corresponds to the eventual replacement of lost keratocyte cells by cells with similar functional characteristics in the new ECM [644]. We could expect the following signals and cellular events to activate this response:

- Progenitor and half way state keratocyte undifferentiated cell signals (essentially Oct-3/4) could induce Nestin expression in wound zone repair cells. Nestin expression could be regarded as a marker for cells going through, or at the beginning of a keratocyte regeneration pathway. We could expect Nestin-positive cells to be both neural crest-derived progenitor cells and/or keratocyte-derived myofibroblast cells that need to differentiate and dedifferenitate respectively to regenerate normal keratocyte cells required for restoring normal stromal transparency.
- Half way state keratocyte cells away from the wound zone would begin to revert back to their quiescent adult keratocyte state.
- We cannot exclude that epithelial- and endothelial-derived myofibroblast cells in stromal wound zones could regenerate keratocyte cells via the same Nestin-positive pathway.
- We would expect migration of external progenitor cells to have stopped at this stage, unless of course some or all of the Nestin-positive cells in the stromal wound zone

correspond to a specific progenitor population recruited into the stromal wound zone at later stromal repair stages to regenerate adult kratocyte cells.

### 4.2.3 > D28; Back to the Norm, or Not

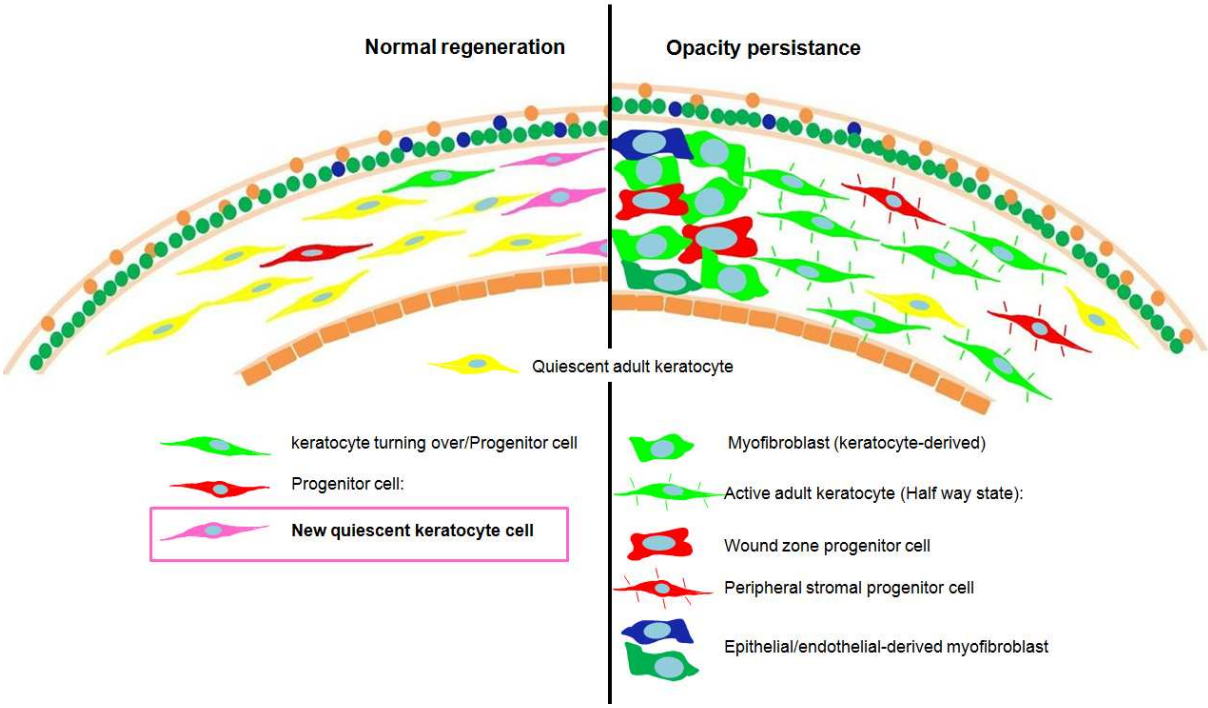


#### A Normal Corneal Stromal Repair

The majority of mouse corneas from our wound healing model lost their stromal opacity formation gradually after D14 post-wounding. We expect their new stromal ECM and cell types to eventually compare to that of a normal stroma. There would be a:

- Decrease in undifferentiated cell signals (due to a decrease in progenitor and half way state keratocyte cells throughout the whole stroma)
- Decrease in Nestin-positive cells
- Increase in quiescent adult keratocyte-like cells.

There still remains many unanswered questions regarding which cell types in the wounded stroma regenerate kertaocyte cells. It is unknown if there are specific cell types, or subsets of cells types that apoptose once stroma remodelling is complete, and if some cells

can revert back to a quiescent keratocyte-like cell phenotype in order to restore corneal transparency. For example, do some progenitor cells apoptose, or retain a more quiescent keratocyte-like phenotype to restore a progenitor pool, or do all progenitor cells differentiate into fucntional keratocyte cells? In the wound zone we could expect a subset of myofibroblast cells to apoptose, and a different subset to dedifferentiate [311, 333, 355, 358, 368, 369, 656]. However, more work is required to determine which cell subsets do what i.e. Could it be that neural crest-derived progenitor wound zone myofibroblast cells apoptose once the keratocyte-derived myofibroblast cells dedifferentiate into keratocyte cells, or vice versa.

### B Persistant Corneal Stromal Opacities

Some of our mice retained a corneal stromal opacity for many month post-wounding. Corneal stromal opacity is due to the persistence of myofibroblast cells in the stroma [272]. Based on our findings in this project, we can now hypothesise many new factors that could contribute to the maintenance of myofibroblast cell phenotypes in the wounded stroma. Here are some examples:

- A defect in activated half way state keratocyte cells i.e. they remain blocked in their activated state, meaning a constant upregulation of undifferentiated cell signals could inhibit the differentiation pathway of some myofibroblast/progenitor cells in the stromal wound zone.
- A defect in/loss of progenitor paracrine* signaling events could lead to a lack of differentiation signals to myofibroblast cells, or lack of signals to deactivate the keratocyte half way state. It could also be that a subset of myofibroblast cells that undergo apoptosis rely on correct functioning of progenitor signals (i.e. loss of Tert survival signals).
- The loss of a complete progenitor cell population required for the regeneration of keratocyte cells in the stromal wound zone. This could be due to a defect in *in situ* stromal progenitor cells, or a defect in the migration of progenitor cells from different tissues into the wounded stroma.
- A defect in/incapability of epithelial/endotheial cell-derived myofibroblast cells to differenitatiate into keratocyte-like cells.

On the whole, we suggest that the *in vivo* stromal wound response could be **more complex** than previously considered. There are now more cell types to consider in the wounded stroma; half way keratocyte cells and *local* progenitor cells, not to mention the probable recruitment of *external* progenitor cells from different tissues that could also be capable of differentiating into myofibroblast-like cells to contribute to ECM restoration and keratocyte cell regeneration. There are likely to be interconnected repair cell signals and functions between progenitor and undifferentiated keratocyte cells. A loss or defect in the wound repsonse of one of these cell populations could perhaps lead to inhibition of myofibroblast cell differentiation events, and in turn lead to corneal opacity formation. A summary of the possible network of signals at play among repair cells is *summarised in the diagram below*.

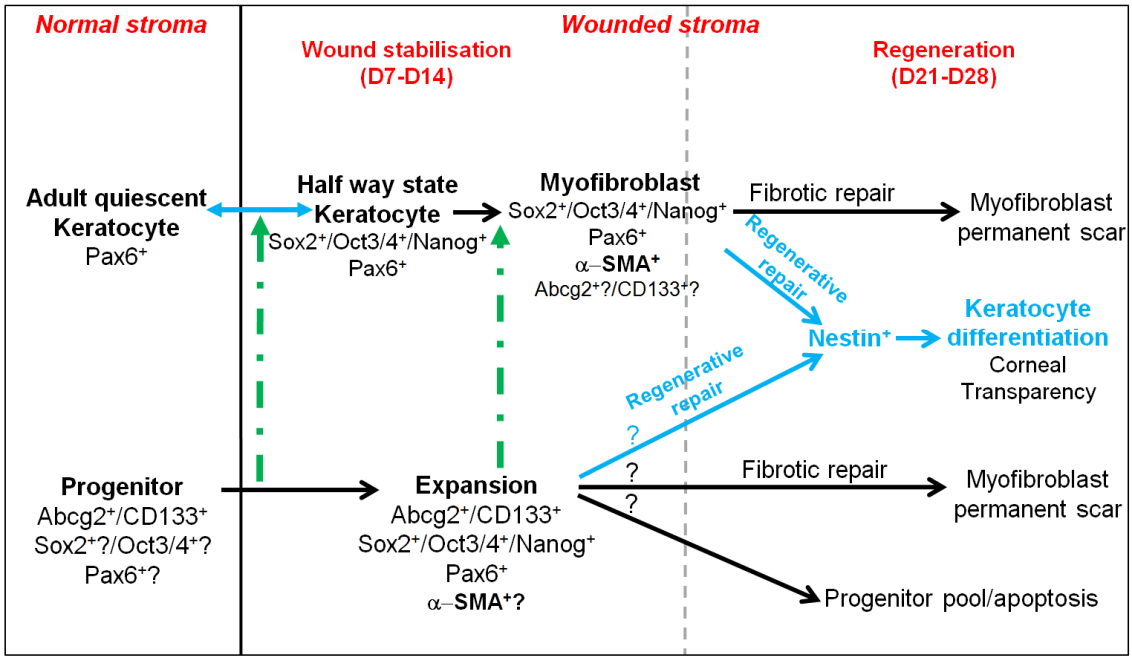


Schematic representation of the model for progenitor and keratocyte cell fates* and signalling events in corneal stromal wound healing. Dotted green arrows indicate progenitor guiding paracrine signals. The blue arrow indicates the role of undifferentiated cell signals that activate the dedifferentiation of keratocyte cells having exceeded their half-way state and/or progenitor cells to regenerate keratocyte cells for normal corneal transparency. ? Represents possible cell fates* of stromal progenitor cells. Note the bidirectional cell state between the quiescent and half way state keratocyte cell. We expect the repair fibroblast phenotype to appear between the half way state and myofibroblast cell phenotypes.

# VI Perspectives

## 1 Short Term Experimentation Currently Underway

### 1.1 Regeneration of Keratocyte-like Cells

*In vitro* cell studies and therapeutic cell injection studies suggest that stromal progenitor cells differentiate into functional keratocyte-like cells [403-405, 457, 458, 513, 527]. The next step in this study is to determine if once stromal wound zone cells lose their Nestin expression; do they express keratocyte markers? We are collecting wounded stromas at 2 and 3 months post-wounding to investigate changes in Nestin and keratocyte-specific marker expressions (Keratocan, Keratocan sulphate, ALDH3A1) compared to D28 wounded stromas. A donwregulation of Nestin expression followed by an upregulation of keratocyte-specific marker expressions would suggest keratocyte regeneration by wound zone stromal cells via a Nestin-positive regeneration pathway.

### 1.2 Investigation of Permament Corneal Opacities

We have also prolonged the sacrification times of some mice in which we observed grade 3 corneal opacities still at D28 post-wounding. We will test out the theory that stromas with opacity could harbour global expression of activated half way state keratocyte cells. This could confirm the requirement, or not, of inactivation of these cells for myofibroblast cells and/or progenitor cells to differentiate into keratocyte cells. We are also investigating co-staining of α-SMA and Nestin in these stromal tissues to give an indication if persistant Nestin-positive myofibroblast cells are present in the stroma. If so, it could be a defect in the keratocyte regeneration pathway that underlies myofibroblast persistence and opacity formation.

### 1.3 Contribution of Epithelial EMT to Stromal Wound Repair

Considering that I hypothesise a small contribution of epithelial EMT in the stromal wound zone to myofibroblast formation, we are in the process of investigating for the expression of p63 by fibroblast-like cells in D7 and D14 wounded stromal tissues by immunostaining. P63 has already been used as a putative marker to trace epithelial stem cells that invade underlying fibrotic stromal tissue and undergo EMT [635]. The results will hopefully give us an insight into the extent of the contribution from epithelial cells in the our observed stromal wound response.

### 1.4 Additional Stem Cell Markers

There is an extensive list of other adult and embryonic stem cell markers that could be additionally investigated to continue the identification of progenitor cell lineages and undifferentiated cell functions at play in the wounded stroma. We are in the process of carrying out CD45 (bone marrow-derived hematopietic stem cell marker) RT-qPCR and immunohistochemical anlyses in order to test for the migration of external bone marrow-derived progenitor cells [484] into the *in vivo* wounded stroma.

It would also be interesting to study the expression of other known embryonic stem cell markers known to regulate stem cell proliferation and differentiation. Among neural crest-derived embryonic stem cell markers identified by the handful of *in vitro* corneal stromal cell studies [404, 457, 458], Notch was identified as a stromal progenitor stem cell marker. This is an attractive target considering Sox2 has been shown to be downstream of Notch signaling in the mouse [657]. Similar to Sox2 signaling, Notch signaling has shown both regulatory roles over progenitor cell proliferation and differentiation in mammalian embryogenesis and adult stem cells [658-662]. In all cases, Notch signaling upregulation is known to lead to progenitor cell maintenance, and loss of Notch signals results in progenitor cell differentiation [2, 663]. Notch signaling cascades involved in self-renewal and differentiation in the developing and adult nervous sytsem bring into play a complex network of extracellular signals involving Wnt, β-catenin and Hedgehog proteins [658]. The Wnt/β-Catenin pathway regulates cell fate* decisions during development of vertebrates and invertebrates. There is currently an active neuroscience research area based on the Wnt/β-catenin signal network shown to promote neural stem cell proliferation and migration, but inhibition of differentiation into new neurons throughout adult neurogenesis [664]. Similarly, the Sonic hedgehog (Shh) signalling molecule assumes various roles in the CNS during vertebrate development via regulation of neural progenitor cell proliferation and differentiation [665]. Also, new research areas are beginning to question the function of the expression of Shh identified in both mature and regenerating neural stem cells [614, 666, 667]. In addition, very recently it was shown that Twist activation is upstream of Notch signaling in adult muscle progenitor cells, suggesting that these two factors co-regulate maintenance and differentiation of embryonic and adult progenitor cells [668]. The fact that Twist2 activity loss in the normal adult mouse corneal stroma leads to corneal thinning due to keratocyte cell loss [495], implies that Twist may also be involved in this network of

undifferentiated cells signals we observed in the *in vivo* wounded stroma. We could perhaps predict a mirrored upregulation of these markers mentioned above with Sox2, Oct-3/4 and Nanog expression by activated keratocyte cells. Results will give speculations on the entity of the network of embryonic stem cell signals at play and their functions in the wounded stroma.

## 2 Long Term Experimentation to Develop

### 2.1 Identification and Isolation of Wounded Stromal Cell Populations

The identification of the surface antigens of the repair cell populations involved in the *in vivo* wounded stroma is necessary to determine the number of different repair cell populations present, and their origins. This will be carried carried out using fluorescent-activated cell sorting (FACS). This technique allows sorting of heterogenous mixtures of cells based on multiple fluorescence signals from specific secondary antibodies via cell surface antigens of interest, giving quantitative cell numbers as well as physical isolation of cells of interest. This technique is considered to be of high sensitivity, selecting cell surface markers with higher specificity than simple immunostaining and microscopy observations that can take into account background noise from cells that do not actually bind the primary antibody [669]. Briefly experimental procedure would entail; removal of the epithelial and endothelia cell layers from corneal stromas (control, D7, D14 and D28). The stromas would then be diced into small cubes and cultured. After a maximum of 4 passages the cells would be saturated with primary and secondary antibodies before fluorescence analysis by FACS. A selection of primary antibodies based on markers from this project, with additional kertocyte-specific, adult bone marrow-derived stem cell and neural crest-derived stem cell, ocular development and neural crest-derived embryonic stem cell markers could be tested. This technique will allow us to determine the heterogeneity of progenitor cell lineages involved in the *in vivo* stromal wound response, giving not only insights to where cells originate from, but also indications into the proportions of each cell population in the wounded stroma. Determination of more specific marker profiles of the stromal cells will allow us to isolate these cells for *in vitro* analysis of their functions in the wounded stroma.

### 2.2 Functional Analysis of Adult Keratocyte to Embryonic-like Cell Phenotype Switching

We aim to functionally determine if keratocytes do veritably switch to an embryonic phenotype in the *in vivo* wounded stroma. We aim to construct an adenoassociated viral

vector carrying GFP-mouse Oct-3/4 cDNA to transfect normal cornea stromal cells, as experimentally carried out by Galiacy et al. (2010) [603]. Transfected corneas will then undergo full thickness incision wounding, resulting in an upregulation of GFP expression by activated Oct-3/4-transfected cells. GFP-positive cells will be isolated from the cornea for FACS determination of their cell surface antigen profiles, which will give us insights into the quantity of total wounded stromal Oct-3/4-positive cells that are generated from adult keratocytes and from progenitor cells. Also, a simple coimmunostaining of the GFP-positive cells with adult stem cell markers would also give us a rough estimate of the proportion of Oct-3/4 positive cells that correspond to progenitor, and thus activated keratocyte cells.

## 3 Therapeutic Implications for Corneal Opacity Treatments: Autologous Grafts

Unfortunately human allogenic corneal transplants are not widely used to replace corneal stromas with opacity formation. This is due to not only a lack of donors, but also due to immune rejection and an increasing popularity of laser eye surgery, often making corneas unsuitable for transplantation [670]. In the case for patients suffering from unilateral corneal opacity, it can be too much of a risk to transfer a sample of corneal stromal cells from the healthy eye to the defect eye. Such a stromal incision could activate the same opacity-forming response in the healthy contralateral eye, leaving the patient completely blind.

The solution? Wounded rat corneal epithelium with limbal stem cell deficiency has shown complete restoration once transplanted with autologous mesenchymal stem cells [671]. Autologous isolation and injection of neural crest-/bone marrow-derived mesenchymal stem cells directly into the corneal stroma could be tested using $Lum^{-/-}$ animal models. This technique would supply the opacity bearing corneal stroma with an active progenitor pool, of which we could analyse injected stem cell capacities to differentiate into functional keratocyte-like cells, potentially reducing corneal stromal opacities.

On the other hand, patients could benefit from recent developments in the new huge research area based on the generation of pluripotent embryonic-like stem cells from human adult tissues, notably neural stem cells, skin fibroblast and keratinocyte cells [573, 622, 672]. Recently, a mouse sickle cell anemia model has shown successful replacement of defected cells with adult hematopietic stem cells generated from autologous induced pluripotent stem cells [673]. This shows that adult cells from a different, but autologous tissue can be reprogrammed into cells with a pluripotent embryonic-like cell phenotype to replace defective

cells and restore a normal non-diseased phenotype. **Could induced pluripotent stem cells be injected into corneal stromas harbouring opacities?** Following injection, induced pluripotent stem cells may differeniate into functional keratocyte-like cells in the stroma (Fig.10). Could we go as far as thinking that injected pluripotent cells could even stimulate pre-existing stromal myofibroblast cells (being the defective cell phenotype) to differentiate into keratocyte cells or apoptose? Not only would this technique overcome the problem of corneal graft limitations and failures, but would restore normal corneal stromal transparency, restoring vision for corneal opacity sufferers.

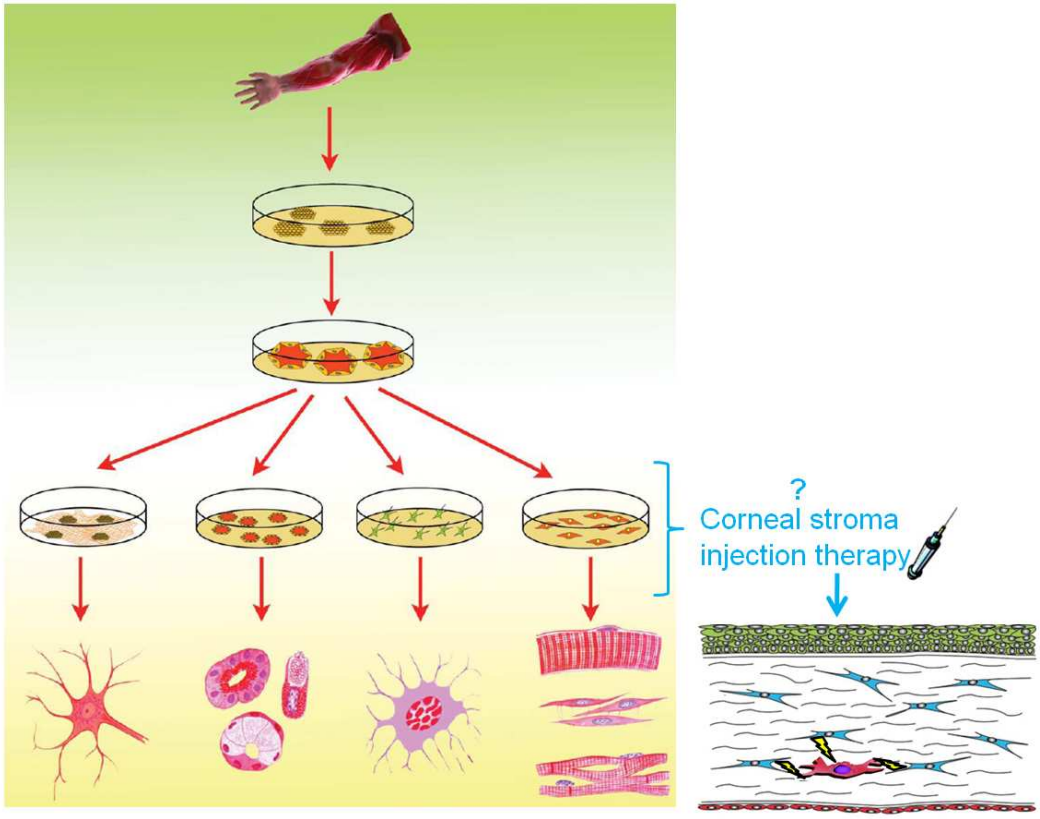


**Schematic representation of adult cell types generated from induced pluripotent stem cells** involving reprogramming of human skin fibroblasts with genetic factors, and their subsequent differentiation into ectodermal, mesodermal and endodermal cell types [674]. Right: Added adaptation representing the idea of using **induced pluripotent stem cells to restore corneal stromal transparency.** Do these cells have the ability to repopulate corneal stromas with keratocyte cells, and stimulte differentiation and/or apoptosis of pre-existing myofibroblast cells?

## 4 Conclusion: Project 2

*In vitro* cell studies have suggested that the normal adult corneal stroma harbours a cell subpopulation that expresses stem cell markers. These cells express a range of adult and embryonic stem cell markers, are multipotent and capable of switching phenotype to that of functional keratocyte-like cells. The idea of these cells being stromal progenitor cells with a keratocyte replenishment function has been discussed, but never investigated in adult corneal stroma repair.

We have localised for the first *in vivo* two different repair cell populations expressing a range of stem cell markers in the adult mouse wounded corneal stroma. The first population is a stromal progenitor cell subpopulation expressing both adult tissue and embryonic stem cell markers. This cell population expands essentially in the stromal wound zone following corneal injury, suggesting a potential repair role of these cells. Wether this population is *in situ* or migrates from the limbus or elsewhere is unclear. Secondly, we unexpectedly found that the majority of *in vivo* adult keratocyte cells could be more plastic cells than were previously considered to date, being capable of reexpressing their embryonic developmental markers (Sox2, Oct-3/4 and Nanog) to play a role in the stromal wound response. Finally, the expression of an adult and embryonic neural stem cell marker exclusively by wound zone stromal cells in later stroma remodelling stages could correspond equally to both hypothesises of activation of keratocyte dedifferentiation and neural crest-derived stromal progenitor cell differentiation to eventually regenerate adult keratocyte cells.

The precise stem cell marker expression profiles of these repair cell populations are required to allow us to distinguish between both cell types, and determine their roles in the stromal wound response. Further work is required to deduce the contributions of external stromal progenitors and their tissues of origin in order for us to construct a complete flow of stromal wound repair cellular events that lead to the regeneration of adult keratocyte cells and corneal transparency following injury.

## 4 Conclusion: Projet 2

Des études cellulaires *in vitro* ont suggéré que le stroma cornéen adulte comporte une sous population cellulaire qui exprime des marqueurs de cellules souches adultes et embryonnaires. Ces cellules sont multipotentes et capable de se différencier en keratocytes phénotypiques et fonctionnels ; l'hypothèse émise est que ces cellules sont des progéniteurs

du stroma avec un rôle dans la régénération des kératocytes. Cette hypothèse n'a jamais été mise en évidence lors de la réparation stromale *in vivo*.

Pour la première fois, nous avons localisé *in vivo* deux populations de cellules différentes exprimant des marqueurs de cellules souches lors de la cicatrisation cornéenne stromale adulte. La première population est une population de progéniteurs du stroma exprimant des marqueurs de cellules souches adultes et embryonnaires. Suite à une blessure cornéenne, cette population progénitrice se multiplie principalement dans la zone du stroma blessé, suggérant un rôle réparateur potentiel de ces cellules. Ces progéniteurs sont peut être *in situ,* migrent d'une niche limbique ou d'un autre tissu. Nous suggérons également qu'*in vivo* la majorité des kératocytes adultes du stroma cornéen blessé acquièrent le phénotype de leurs précurseurs embryonnaires (expression du Sox2, Oct-3/4 et Nanog) pour jouer un rôle dans la réparation du stroma. Ces cellules sont vraisemblablement plus plastiques qu'on le considère. Finalement, nous montrons l'expression du marqueur Nestin par des cellules présentes exclusivement dans la zone stromale blessée lors des stades tardifs de la cicatrisation. Nestin n'est pas exprimé par des kératocytes adultes, mais exprimé par des cellules souches adultes et embryonnaires neurales, nous laissant penser que la régénération des kératocytes pourrait se faire via la différenciation de cellules progénitrices issues de la crête neurale et la dédifférenciation des kératocytes.

Les profils d'expression des marqueurs de cellules souches de chacune de ces populations cellulaires sont importants afin de pouvoir les distinguer entre elles et déterminer leurs rôles dans la réponse de la cicatrisation stromale. Plus de travaux sont nécessaires pour déterminer la contribution au remodelage du stroma par des cellules progénitrices à l'exterieur du stroma et leurs tissus d'origine.

## Summary

High myopia, known as severe shortsightedness, affects 4% of the western population and can in extreme cases lead to blindness. In the French Caucasian population high myopia is a heterogeneous complex disease, and previous attempts to localise the multiple underlying genes have failed. A new GWAS study has been designed based on limiting complex trait confounders by changing the previously used phenotype inclusion criterion from refractive error to axial length. A new cohort was recruited but not sufficiently completed, thus to overcome small cohort effects power calculations indicated the requirement to use a severe axial length cohort in a first genome scan, followed by a mutli-step replication analysis that is still underway today. The identification of genes involved in myopia development is the first step in the understanding of the physiopathology of the disease, but also in the development of alternative treatments that today depend on spectacles and contact lens wearing.

Myopia can be treated by refractive error surgery. This requires damaging the cornea which can in an average of 1.75% of patients lead to the development of corneal stromal opacities. The mechanisms underlying both normal corneal stromal wound responses and stromal opacity formations are not fully elucidated. A handful of *in vitro* cell studies have tried to localise corneal stromal progenitor cells that differentiate into keratocyte-like cells. Thus, we investigated the phenotype of cells involved in *in vivo* stromal wound repair using a mouse model of full thickness corneal incision wounding. For the first time *in vivo* we suggest the localisaiton of a normal adult stromal progenitor cell pool that expands in response to corneal wounding. We also demonstrate that the majority of adult keratocyte cells in the *in vivo* wounded stroma could revert to a late neural crest embryonic-like cell phenotype (expression of Sox2, Oct-3/4, Nanog), indicating that adult keratocyte cells could be relatively plastic cells. Expression of a neural adult and embryonic stem cell marker exclusively by wound zone stromal cells in later stroma remodelling stages suggests keratocyte cells could regenerate via neural crest-derived progenitor cell differentiation and keratocyte dedifferentiation. Together our results give new insights into novel stromal progenitor and keratocyte cell stromal wound repair functions which could help develop new targets for the prevention and treatment of corneal opacity formations.

# Resumé

La myopie forte est un trouble sévère de la vision de loin, qui touche 4% de la population occidentale, et dans des cas extrêmes peut conduire à la cécité. Dans la population française caucasienne la myopie forte est une maladie complexe et les tentatives précédentes de localiser les multiples gènes de susceptibilité se sont soldées par des échecs. Une nouvelle étude d'association pangénomique a été développée afin de limiter l'hétérogénéité de la myopie forte en remplaçant le phénotype d'inclusion d'erreur de réfraction par la longueur axiale. Une nouvelle cohorte a été recrutée mais pas suffisamment étoffée. Pour contourner les effets d'une petite cohorte, les calculs de puissance ont mis en évidence le besoin d'effectuer un premier scan pangénomique d'une cohorte incluant des phénotypes de longueur axiale extrême, suivi par une analyse de réplication multi-étapes qui est toujours en cours. L'identification des gènes impliqués dans le développement de la myopie forte est le premier pas pour la compréhension de la physiopathologie de la maladie, mais également pour le développement de traitements alternatifs qui se limitent actuellement à une correction de la réfraction par le port des lunettes et de lentilles.

La myopie peut être traitée par la chirurgie réfractive. Cette chirurgie consiste à blesser la cornée, ce qui peut conduire à des opacités stromales chez une moyenne de 1,75% des patients opérés. Les mécanismes sous-jacents de la réponse réparatrice du stroma et la formation des opacités stromales sont élusifs. Des études menées *in vitro* ont essayé de caractériser une population de cellules progénitrices cornéennes stromales qui peuvent se différencier en cellules avec un phénotype et une fonction kératocytaire. Nous avons donc analysé les phénotypes des cellules impliquées dans la réparation du stroma *in vivo* à l'aide d'un modèle de cicatrisation cornéenne comprenant une blessure incisionnelle de la cornée complète chez la souris adulte. Pour la première fois *in vivo* nous avons identifié une population de cellules stromales progénitrices qui se multiplie à la suite d'une blessure cornéenne. Nos montrons également que *in vivo*, la majorité des kératocytes adultes du stroma cornéen après blessure semble acquérir un phénotype de leurs précurseurs embryonnaires (expression de Sox2, Oct-3/4, Nanog). Ceci suggère que ces cellules sont potentiellement plus plastiques qu'on le considère. L'expression d'un marqueur des cellules souches embryonnaires et adultes neuronales par des cellules exclusives de la zone stromale blessée lors des stades tardifs de la cicatrisation, laisserait penser que la régénération des kératocytes pourrait se faire via la différenciation de cellules progénitrices issues de la crête neurale et aussi la dédifférenciation des kératocytes. Nos résultats donnent de nouvelles perspectives sur les fonctions des cellules progénitrices stromales et cellules kératocytes adultes dans le stroma blessé, fournissant de nouvelles cibles potentielles pour la prévention et le traitement des opacités cornéennes.

## Annex 1

## Project 1: Published Review 1 entitled "Axial length: An underestimated endophenotype of myopia

Medical Hypotheses 74 (2010) 252–253

Contents lists available at ScienceDirect

Medical Hypotheses

journal homepage: www.elsevier.com/locate/mehy

# Axial length: An underestimated endophenotype of myopia

Weihua Meng, Jacqueline Butterworth, Francois Malecaze, Patrick Calvas*

*Centre of Physiopathology, INSERM U563, Purpan Hospital, Toulouse 31024, France*

ARTICLE INFO

*Article history:*
Received 8 September 2009
Accepted 13 September 2009

ABSTRACT

Myopia is a major threat for vision health across the world. Around 1 in 4 in the West and over 3 in 4 in the East are suffering from this common eye disorder. It is a complex trait affected by both genetic and environmental determinants. Axial length is an essential man-made parameter generated from ocular biometric components. It represents a combination of anterior chamber depth, lens thickness and vitreous chamber depth. Meanwhile, it is an endophenotype of the phenotype of myopia. In the mainstream genetic studies on vision science, it is always treated only as a parameter rather than an endophenotype. However, in this article, the potential advantages are discussed for axial length analysed as an endophenotype independently. It may provide solutions for the exploration of myopia genetics.



### Introduction

Myopia or shortsightedness is one of the most common eye disorders worldwide. It affects around 25% of people in the Western and over 80% in some Asian populations [1,2]. Based on a recent report from the World Health Organization (WHO), the number of people who have visual impairment caused by myopia and other ocular disorders succeeds over 161 million in 2002 [3]. Furthermore, myopia accounts for almost 75% of the refractive error-related complications [4]. Thus, despite being a non-life threatening disease, it has a huge social and economic burden for public health systems [5]. The phenotype of myopia is described by spherical equivalent (SE) using dioptre (D) measurements. Most studies classify mild myopia ranging from −0.5D to −6D and high myopia less than −6D. Some suggested that the underlying mechanisms maybe different for these 2 types of myopia [6]. But no further evidence has been generated so far. Axial length (AL) is the largest determinant of refractive error [7]. It represents a combination of anterior chamber depth, lens thickness and vitreous chamber depth. It is well confirmed that there is a negative relationship between AL and myopia (the longer the AL, the more severe the myopia) [8,9]. AL can be treated as a parameter or as an endophenotype of myopia. Under most genetic studies on vision science, AL was treated, however, only as a parameter.

### Hypotheses

AL can provide extra advantages if treated as an endophenotype in the exploration of myopia genetics.

* Corresponding author. Tel.: +33 (0)561779079.
*E-mail address:* calvas.p@chu-toulouse.fr (P. Calvas).

0306-9877/$ - see front matter © 2009 Elsevier Ltd. All rights reserved.
doi:10.1016/j.mehy.2009.09.025

### Evaluation and discussion of the hypotheses

Myopia is a complex trait affected by both genetic and environmental factors [10]. It is suggested that environmental factors such as near work is responsible for 12% of phenotypic variance and the rest is due to genetic components [11]. In general, researchers agree that genetic factors may account for over 50% of population variance [12]. So far, more than 18 chromosomal regions have been put forward for mild myopia and high myopia by linkage studies but no genes have been pinpointed [12]. Evidence showed that AL may have some special characteristics which are different from myopia [13,14]. The comparison between the heritability of myopia and AL was summarised in Table 1. It is clear that the heritability of myopia varied significantly among twin studies, sibling studies and nuclear family studies [13]. The more distant the samples are, the less heritability they possess. In terms of AL, the heritability remained consistent among studies which indicated the first benefit of using AL as an endophenotype in genetic studies [14]. Using AL as an endophenotype can avoid or minimise the bias caused by the more complex myopic trait. Second, since the heritability of AL was more stable, it is possible that the endophenotype of AL may be encoded by less genes than the phenotype of myopia. Although AL is still under polygenetic control, traits with fewer genes are relatively easier to be decoded [15]. Furthermore, environmental factors had less effect on AL than myopic spherical equivalence [13,14]. Trait variance of AL caused by environment was only around 6% contrasting that of SE from 14% to 33%. It is also suggested that AL may share common genes with the phenotype of myopia [16]. Finally, myopia is commonly accompanied with other eye disorders such as cataract, glaucoma and chorioretinal abnormalities [17]. These eye disorders would be annoying confounders and would decrease the power of genetic studies.

**Table 1**
Comparison of the heritability of myopia and axial length.

| Trait | Heritability | | |
|---|---|---|---|
| | Twins | Sibs | Nuclear families |
| Myopia | 0.82 | 0.50 | 0.21 |
| AL | 0.88 | 0.73 | 0.75 |

AL: axial length.

On the contrary, AL is a very clean endophenotype and it follows normal distribution in populations. The measurement of AL can be preceded at the same time with the evaluation of SE during the clinical patient recruitment examinations [18]. Therefore, there are no extra expenses.

AL is the sum of the anterior chamber depth, lens thickness and the length of vitreous chamber. Theoretically, any genes which contribute to these 3 components will have an effect on AL. Evidence revealed the heritability of AL is partly mediated by anterior chamber depth [18]. Meanwhile, more attention was focused on the length of the vitreous chamber. Based on animal models, the sclera, the tough tissue containing the eyeball was found to be a dynamic tissue [19]. The decreased collagen content of the sclera during myopia development would increase its elasticity [20]. As a consequence, it could facilitate the increase of the vitreous chamber and thus lengthen AL. A signalling cascade was involved in this remodelling process [19]. The first attempt to locate AL genes discovered a region in chromosome 5q [21]. But it has not been replicated yet. Recently, one study of animal models on axial myopia also suggested the involvement of genes controlling body size [22].

## Conclusion

Like other refractive-error disorders, myopia is a consequence of uncoordinated contributions of ocular components to the overall eye structure. Axial length as an endophenotype of myopia has its own genetic components, some of which shared with myopia. The value of analysing AL lies in the fact that the heritability of AL varies little among multiple family structures. If AL is used as an endophenotype, it is possible to avoid or minimise the bias potentially caused by the more complex myopic trait. AL is a clean endophenotype with no obvious confounders which exist in the studies of myopia. Therefore, it may bring some opportunities to unravel its own genetic basis and its genetic connection with myopia if further investigations could be performed.

## Conflict of interest statement

None declared.

## Acknowledgement

We thank Paul Baird for providing information in Table 1.

## References

[1] Kempen JH, Mitchell P, Lee KE, et al. The prevalence of refractive errors among adults in the United States, Western Europe, and Australia. Arch Ophthalmol 2004;122:495–505.
[2] Lam CS, Goldschmidt E, Edwards MH. Prevalence of myopia in local and international schools in Hong Kong. Optom Vis Sci 2004;81:317–22.
[3] Resnikoff S, Pascolini D, Etya'ale D, et al. Global data on visual impairment in the year 2002. Bull World Health Organ 2004;82:844–51.
[4] Casson RJ, Newland HS, Muecke J, et al. Prevalence and causes of visual impairment in rural Myanmar: the Meiktila eye study. Ophthalmology 2007;114:2302–8.
[5] Rein DB, Zhang P, Wirth KE, et al. The economic burden of major adult visual disorders in the United States. Arch Ophthalmol 2006;124:1754–60.
[6] Tron EJ. The optical elements of the refractive power of the eye. In: Ridley F, Sorsby A, editors. Modern trends in ophthalmology. New York: Paul B Hoeber; 1940.
[7] Young TL, Metlapally R, Shay AE. Complex trait genetics of refractive error. Arch Ophthalmol 2007;125:38–48.
[8] Mallen EA, Gammoh Y, Al-Bdour M, Sayegh FN. Refractive error and ocular biometry in Jordanian adults. Ophthal Physiol Opt 2005;25:302–9.
[9] Chen MJ, Liu YT, Tsai CC, Chen YC, Chou CK, Lee SM. Relationship between central corneal thickness, refractive error, corneal curvature, anterior chamber depth and axial length. J Chin Med Assoc 2009;72:133–7.
[10] Tang WC, Yap MK, Yip SP. A review of current approaches to identifying human genes involved in myopia. Clin Exp Optom 2008;91:4–22.
[11] Saw SM, Tan SB, Fung D, et al. IQ and the association with myopia in children. Invest Ophth Vis Sci 2004;45:2943–8.
[12] Schache M, Chen CY, Pertile KK, et al. Fine mapping linkage analysis identifies a novel susceptibility locus for myopia on chromosome 2q37 adjacent to but not overlapping MYP12. Mol Vis 2009;15:722–30.
[13] Chen CY, Scurrah KJ, Stankovich J, et al. Heritability and shared environment estimates for myopia and associated ocular biometric traits: the genes in myopia (GEM) family study. Hum Genet 2007;121:511–20.
[14] Dirani M, Chamberlain M, Shekar SN, et al. Heritability of refractive error and ocular biometrics: the genes in myopia (GEM) twin study. Invest Ophth Vis Sci 2006;47:4756–61.
[15] Paget S, Vitezica ZG, Malecaze F, Calvas P. Heritability of refractive value and ocular biometrics. Exp Eye Res 2008;86:290–5.
[16] Dirani M, Shekar SN, Baird PN. Evidence of shared genes in refraction and axial length: the genes in myopia (GEM) twin study. Invest Ophth Vis Sci 2008;49:4336–9.
[17] Saw SM, Gazzard G, Shih-Yen EC, Chua WH. Myopia and associated pathological complications. Ophthal Physiol Opt 2005;25:381–91.
[18] Klein AP, Suktitipat B, Duggal P, et al. Heritability analysis of spherical equivalent, axial length, corneal curvature, and anterior chamber depth in the Beaver Dam eye study. Arch Ophthalmol 2009;127:649–55.
[19] Rada JA, Shelton S, Norton TT. The sclera and myopia. Exp Eye Res 2006;82:185–200.
[20] McBrien NA, Jobling AI, Gentle A. Biomechanics of the sclera in myopia: extracellular and cellular factors. Optom Vis Sci 2009;86:E23–30.
[21] Zhu G, Hewitt AW, Ruddle JB, et al. Genetic dissection of myopia: evidence for linkage of ocular axial length to chromosome 5q. Ophthalmology 2008;115:1053–7.
[22] Prashar A, Hocking PM, Erichsen JT, Fan Q, Saw SM, Guggenheim JA. Common determinants of body size and eye size in chickens from an advanced intercross line. Exp Eye Res 2009;89:42–8.

**Annex 2**

**Project 1: Published Review 2 entitled "Axial length of Myopia: A Review of Current Research**

EURETINA – Review

Ophthalmologica

Ophthalmologica 2011;225:127–134
DOI: 10.1159/000317072

Received: March 3, 2010
Accepted after revision: June 3, 2010
Published online: October 16, 2010

# Axial Length of Myopia: A Review of Current Research

Weihua Meng[a] Jacqueline Butterworth[a] François Malecaze[a, b, d]
Patrick Calvas[a, c, d]

[a]Physiopathology Centre, INSERM U563, and Departments of [b]Ophthalmology and [c]Medical Genetics, Purpan Hospital, Toulouse, and [d]University Paul Sabatier, Toulouse, France

**Key Words**
Axial length · Myopia · Genetics · Refractive error · Endophenotype

**Abstract**
Myopia, or nearsightedness, is a worldwide common type of refractive error. It is a non-life-threatening disorder with huge social and economic consequences due to its increasing prevalence. Axial length (AL) is the primary determinant of non-syndromic myopia. It is a parameter representing the combination of anterior chamber depth, lens thickness and vitreous chamber depth of the eye. AL can also be treated as an endophenotype of myopia and may provide extra advantages in the investigation of its genetic basis. The study of AL will not only identify the determinants of eye elongation, but also provide aetiological evidence for myopia. The purpose of this review is to outline the current state of AL research. Epidemiological evidence, genetic determinants, the relationship with other eye components and relative animal models of AL are summarised.



## Introduction

Myopia is a major threat for vision health across the world. It is responsible for around 75% of the refractive-error-related complications, with serious social and economical consequences [1, 2]. Patients with severe forms of myopia or high myopia are more susceptible to other ocular abnormalities such as lacquer cracks, retinal detachment, chorioretinal atrophy and glaucoma [3]. In Western Europe, the estimated prevalence of myopia is over 25% [3]. Similar results have been reported in some regions such as the Middle East and South America. Table 1 summarises myopia prevalences of middle-aged groups in different areas [3–12]. Those studies revealed a relatively higher morbidity of myopia in some East Asian countries. The difference was found to be greater if preschool and school age children were evaluated (table 2) [13–24]. Studies on schoolchildren in Hong Kong and medical students in Singapore even revealed extremely high prevalences of 82% and 90% [25, 26]. According to a recent report from the World Health Organisation, the number of people who have visual impairment caused by myopia and other ocular disorders reached over 161 million in 2002 whereas some researchers worried that this figure was greatly underestimated [27, 28].

Myopia can be classified using different criteria [29]. For example, physiological myopia and pathological myopia are differentiated by the presence of degenerative changes and the value of the refractive error (normally in diopters). Based on the age of onset, myopia can also be divided into 3 groups: youth-onset myopia (less than 20 years old), early adult-onset myopia (aged between 20 and 40) and late adult-onset myopia (over 40 years old). Other classifications include: axial myopia and non-axial my-

KARGER
Fax +41 61 306 12 34
E-Mail karger@karger.ch
www.karger.com


0030–3755/11/2253–0127$38.00/0

Accessible online at:
www.karger.com/oph

Prof. Patrick Calvas
Physiopathology Centre, Purpan Hospital, INSERM U563
FR–31024 Toulouse (France)
Tel. +33 561 779 079, Fax +33 561 779 073, E-Mail calvas.p@chu-toulouse.fr

**Table 1.** Prevalence of myopia and high myopia in middle-aged populations

| Country or region | Sample number | Age distribution, years | Definition of | | Prevalence of | |
|---|---|---|---|---|---|---|
| | | | myopia, dpt | high myopia, dpt | myopia, % | high myopia, % |
| Japan [4] | 3,021 | 58.4 ± 11.8 | <–0.5 | <–5 | 41.8 | 8.2 |
| Iran [5] | 1,367 | 63.7 ± 7.1 | <–0.5 | | 27.2 | |
| Bangladesh [6] | 11,624 | 44 ± 12.6 | <–0.5 | <–5 | 22.1 | 1.8 |
| China, north [7] | 6,491 | >30 | <–0.5 | <–5 | 26.7 | 1.8 |
| China, south [8] | 1,269 | >50 | <–0.5 | <–5 | 32.3 | 5 |
| India [9] | 3,642 | >40 | <–0.5 | <–5 | 34.6 | 4.5 |
| Singapore [10] | 1,113 | >40 | <–0.5 | <–5 | 38.7 | 9.1 |
| Europe, west [3] | 6,543 | >40 | <–1 | <–5 | 26.6 | 4.6 |
| USA [3] | 14,414 | >40 | <–1 | <–5 | 25.4 | 4.5 |
| Australia [3] | 8,324 | >40 | <–1 | <–5 | 16.4 | 2.8 |
| Norway [11] | 1,889 | 40–45 | <–0.5 | | 30.3 | |
| Spain [12] | 417 | 40–79 | <–0.5 | | 25.4 | |

Age distribution is preferred to be presented as means ± standard deviation. If the references did not provide such information, then other forms of age range are shown.

opia; low myopia (0 to –3 dpt), moderate myopia (–3 to –6 dpt) and high myopia (<–6 dpt); syndromic myopia and non-syndromic myopia. To some extent, a graded classification is artificial. In the genetic domain, non-syndromic myopia can be separated into 2 categories: myopia following complex traits, which is determined by both genetic and environmental factors; myopia showing a mendelian pattern of inheritance (autosomal dominant, autosomal recessive and so on), which is normally found by family studies and mainly caused by genetic mutations.

### Axial Length

There are 4 ocular structures contributing to the refractive status of a given human eye, including the cornea, aqueous humour, lens and the vitreous humour. Myopia and other refractive-error disorders are consequences of uncoordinated contributions of ocular components to overall eye structures. In other words, the cornea and lens fail to compensate for axial length (AL) elongation (myopia) or shortening (hyperopia). Thus, parameters closely linked to measurements of these parts such as corneal curvature, anterior chamber depth (ACD), lens thickness, vitreous chamber depth and AL are widely evaluated in the study of eye diseases [30]. Among these components, AL received most attention since it is a main parameter for both myopia and hypermyopia [30].

As early as the mid last century, researchers found that AL showed a bimodal distribution in an adult myopic population [31]. When grouping samples in 2 categories, a first peak appears around the AL of 24 mm for low myopia (–6 dpt < refractive error < 0 dpt) while the second peak appears roughly at the AL of 30 mm for high myopia (refractive error <–6 dpt). This indicates that the physiopathological mechanisms of different severities of myopia may differ and partly explains why it is necessary to separate myopia cases according to the severity to explore its genetic basis. Meanwhile, the distribution of AL is reported to be positively skewed in the general population, and it is under a normal distribution in some selected cohorts [32, 33]. Table 3 shows a summary of AL and its corresponding refractive error in multiple populations from different countries [33–39]. Nowadays, ophthalmologists use ultrasound velocity reading machinery and optical partial coherence interferometry to determine the AL of their patients to clarify the severity of myopia. Most agree that AL is the largest determinant of refractive error [40]. A great number of reports have shown a negative relationship between AL and myopia. In other words, the longer the AL, the severer the myopia [41, 42]. Olsen et al. [35] found that when considering the contribution of AL, lens power and corneal power together, using multiple linear regression analyses, it can explain up to 96% of the variation of refraction in populations. Age-related AL differences were discovered in some investigations. Older people were likely to have shorter AL than younger par-

**Table 2.** Prevalence of myopia in preschool and school age children

| Country or region | Sample number | Age distribution | Definition of myopia dpt | Prevalence of myopia % |
|---|---|---|---|---|
| Singapore [13] | 3,009 | 6–72 months | <–0.5 | 11.0 |
| USA | | | | |
| Urban and white [14] | 1,030 | 6–71 months | <–1 | 0.7 |
| African [15] | 2,994 | 6–72 months | <–1 | 6.6 |
| Hispanic [15] | 3,030 | | | 3.7 |
| Australia [16] | | | | |
| Urban | 322 | 11–14 years | <–0.5 | 17.8 |
| Rural | 270 | | | 6.9 |
| China [17] | 1,892 | 14.7 ± 0.8 years | <–0.5 | *62.3* |
| Iran [18] | 815 | 6 years | <–0.5 | 1.7 |
| UK [19] | 7,600 | 7 years | <–1 | 1.1 |
| Singapore [20] | 631 | 7 years | <–0.5 | 29.0 |
| | 470 | 8 years | | 34.7 |
| | 352 | 9 years | | *53.1* |
| Poland [21] | | | | |
| Urban | 1,200 | 11.9 ± 1.4 years | <–0.5 | 13.7 |
| Rural | 1,006 | | | 7.5 |
| Indian [22] | | | | |
| Urban | 1,789 | 7–15 years | <–0.5 | *51.4* |
| Rural | 1,525 | | | 16.7 |
| Sweden [23] | 143 | 4–15 years | <–0.5 | 6.0 |
| Malaysia [24] | 705 | 6–12 years | <–0.5 | 5.4 |

Age distribution is preferred to be presented as means ± standard deviation. If the references did not provide such information, then other forms of age range are shown. The highest 3 are italicised.

ticipants [38]. Warrier et al. [34] suggested that these differences were related to cohort effects. For example, near work was more intensive in the younger age group, which is a factor increasing AL probably due to a defocus-induced disturbance of emmetropisation [43]. However, the Los Angeles Latino Eye Study did not reveal an age-related AL difference based on a population of 5,588 participants over a period of 40 years [44]. Meanwhile, it is well agreed that women tend to have a shorter AL [34, 35], partly explained by stature [45]. AL has some predicted values for the onset of myopia but only within the 2–4 years preceding onset [46]. It reaches its fastest rate of change during the year before the onset of myopia and then axial elongation follows relatively slowly, with more stable rates of change after onset [46].

### AL and Ocular Biometric Components

The visual system is not well developed until 3 years of age. In general, AL increases rapidly in the early stage of life, then slowly increases until adulthood, then decreases in old age. Data from Biino et al. [33] showed a quadratic relationship between AL and age. A cohort study reported that the average axial length for full-term infants increases from 16.8 to 23.6 mm when they become adults [47]. This increase in AL would cause a serious shift to myopia, which was however offset by corresponding changes in other parts of the eye structure. For example, the lens will reduce its refractive power when AL increases [48]. A 1-mm elongation of AL without other compensation is equivalent to a myopia shift of –2 or –2.5 dpt. Evidence shows that each component of the visual system has close interaction with the other components during the maturation process. Lambert [49] deduced from animal experiments that if the lens were removed from human eyes at an early stage (within the first 2 months), a retardation of eye growth would occur. Human data also support the contention that the AL of eyes after cataract surgery is shorter than in age-matched controls [50, 51], although some authors have observed opposite effects [52]. A decrease in lens power is correlated with the elongation of AL but knowledge on whether this is an active or a passive emmetropisation process is rather limited to make a decisive conclusion [53]. AL was also reported to be significantly negatively correlated with corneal power and documented to have a positive correlation with ACD and a negative correlation with lens thickness [35, 54–56]. Osuobeni [55] suggested that the ratio between AL and corneal radius may be a better indicator of myopia. AL undergoes diurnal fluctuation of around 15–40 μm, with a mean period of approximately 21 h [57]. The maximum AL appears at midday. It is reasonable to hypothesise that this phenomenon is caused by the daily change of intraocular pressure (IOP) since IOP follows diurnal fluctuation as well [58]. However, this assumption is under debate [58, 59]. Read et al. [59] found the association between the change in AL and the change in IOP while no evidence was found by Wilson et al. [58] that IOP fluctuation appears to cause diurnal AL fluctuation.

### AL and Genetic Determinants

Myopia can be treated as a mendelian trait, caused by a single gene, or a complex trait, affected by multiple genetic factors and environmental factors depending on the

**Table 3.** AL information and its corresponding refractive error in middle-aged populations

| Country or region | Supplemental information | Age distribution years | Study type | Sample number | AL mm | Corresponding refractive error dpt |
|---|---|---|---|---|---|---|
| Sardinia, Italy [33] | right eye<br>left eye | 41 ± 19 | family | 741 | 23.57 ± 1.15<br>23.51 ± 1.06 | −0.27 ± 2.11<br>−0.24 ± 1.78 |
| Myanmar [34] | male<br>female | 56.2 ± 11.5 | population | 605<br>893 | 23.12 ± 0.98<br>22.54 ± 1.04 | −1.33 ± 3.40<br>−1.16 ± 3.12 |
| Denmark [35] | male<br>female | 67.9<br>68.1 | population | 325<br>398 | 23.74 ± 1.01<br>23.20 ± 0.98 | 1.05 ± 2.19<br>1.28 ± 2.12 |
| Mongolia [36] | male<br>female | 40–49 | population | 241<br>368 | 23.40 ± 1.30<br>23.00 ± 1.30 | 0.10 ± 1.80<br>−0.30 ± 1.60 |
| Jordan [37] | male<br>female | 29.3 ± 7.45<br>27.4 ± 6.45 | population | 450<br>643 | 23.33 ± 1.02<br>22.99 ± 0.97 | −0.74 ± 1.84<br>−0.95 ± 1.58 |
| Singapore [38] | male<br>female | >40 | population | 457<br>547 | 23.54 ± 1.10<br>22.98 ± 1.16 | −0.40 ± 2.41<br>−0.56 ± 2.89 |
| Australia [39] | | 46.5 ± 19.6 | family | 723 | 25.53 ± 1.50 | −2.10 ± 3.12 |

Age distribution is preferred to be presented as means ± standard deviation. If the references did not provide such information, then other forms of age range are shown.

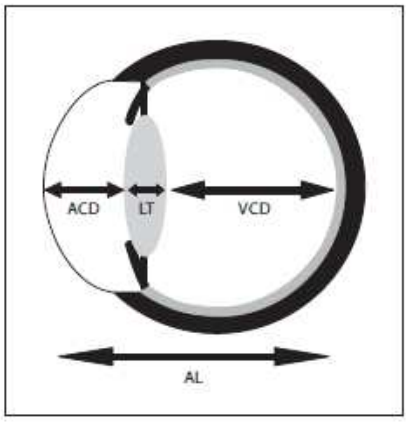


**Fig. 1.** Illustration of AL. ACD = Anterior chamber depth; LT = Lens thickness; VCD = vitreous chamber depth.

underlying mechanism. So far, more than 20 chromosomal areas have been proposed to contain potential myopia genes, but further attempts need to narrow down these regions and pinpoint the corresponding genes [60]. Evidence supports strong genetic components in the determination of AL. Children with myopic parents have a higher chance of being affected and have longer AL than those without myopic parents [61]. Twin studies also demonstrated that AL is highly heritable and genetic effects can explain up to 88% of this parameter [62, 63]. Segregation analyses suggested that AL is under polygenic control [64]. Moreover, a large proportion of correlation between AL and myopia can be explained by these genetic effects, which indicates that AL and myopia may share common genes [65]. AL reflects the sum of the thickness of the lens, ACD and the length of the vitreous chamber (fig. 1) [66]. Research has shown that part of the heritability of AL is mediated by ACD [67]. In 2004, Biino et al. [33] performed a linkage analysis on extended pedigrees and discovered a locus on 2p24 possibly containing a gene for AL. Afterwards, using twin samples, Zhu et al. [68] reported the evidence for linkage of AL to the long arm of chromosome 5. To our knowledge, these were the only 2 regions reported so far for AL and have not been fine mapped yet.

AL is an endophenotype of myopia. Both AL and myopia (in refractive error) can be analysed as a quantitative trait using linkage studies. However, AL is much more suitable. The phenotype of myopia, especially high myopia, is commonly accompanied with other eye disorders

**Table 4.** Heritability comparisons between AL and myopia

| Trait | Heritability | | |
|---|---|---|---|
| | twins | sibs | nuclear families |
| AL [65] | 0.88 | 0.73 | 0.75 |
| Myopia [39] | 0.82 | 0.50 | 0.21 |

**Table 5.** Comparison between heritability of AL and heritability of refractive error (RE)

| Country or region | Study type | Heritability of AL, % | Heritability of RE, % |
|---|---|---|---|
| Sardinia, Italy [33] | | | |
| Male | family | 60 | 18–27 |
| Female | family | 31 | |
| Taiwan [70] | twin | 67 | 33 |
| | twin | 94 | 89–91 |
| USA [67] | population | 67 | 58 |
| France [64] | family | 20 | 20 |

Only references containing both AL and RE heritability information are selected.

such as cataract, glaucoma and chorioretinal abnormalities [69], thus would inevitably involve some confounders and may lead to biased conclusions. However, AL, as a clean trait, could be studied in general optical healthy populations and subjects with low myopia to avoid those confounders. Some reported that the heritability of myopia varies significantly among studies with different family structures, while the heritability of AL remains quite consistent (table 4) [39, 65]. Trait variance of AL caused by environmental factors was only around 6% contrasting that of myopia from 14 to 33% [39, 65]. Thus, using AL as an endophenotype could avoid or minimise the substantial bias caused by a more complex myopic trait due to instability of heritability. Table 5 summarises the studies that calculated both heritability of AL and heritability of refractive error [33, 64, 67, 70]. Most studies showed a higher heritability of AL than refractive error. AL as a clean and simple endophenotype may bring some advantages to the research field of myopia. This conclusion was partly supported by the first genome-wide association study (GWAS) on myopia performed by a Japanese group [71]. In addition to using general populations as controls, they defined high myopia as AL >28 mm regardless of refractive error information. A susceptible locus on 11q24.1 was then discovered by this case-control GWAS approach.

### AL and Myopia Animal Models

It is well confirmed that ocular growth is affected by the quality of visual experience during early life. Failure to induce myopia in dark-reared animals suggests that visual experience is a trigger of eye growth [72]. Animal models of myopia have been successfully established in several species including the monkey, tree shrew, marmoset, chick and the pig [30]. Various methods can be applied to achieve myopia, such as form deprivation, minus lens-induced optical defocus and restricted visual environment conditions [30]. Eyes with induced myopia were observed to have longer AL. For example, negative lenses produce hyperopic defocus and increase the rate of eye growth in monkeys [73]. Conversely, positive lenses lead to myopic defocus and decrease eye growth [74]. It is worth mentioning that such eyes with induced myopia showed evidence of recovery when the inducing factors were removed, and this recovery was inversely related to age [75, 76]. The monkey eyes showed evidence of strong recovery ability. Even 1 h/day of unrestricted viewing can reduce around 50% of the myopia induced by a 17-week period of deprivation [77]. This suggests the existence of an active emmetropisation mechanism, which controls the location of the retina by remodelling of the sclera so that images can be focused on the focal plane [78]. A molecular signalling cascade seems to be involved in this process. This is probably through the neuro-epithelium and the choroid, and involves a remodelling of the scleral extracellular matrix. In turn, this would cause AL to increase due to lengthening of the vitreous chamber [79, 80]. Scientists are working on strengthening the sclera in order to prevent the elongation of AL. One method is called collagen cross-linking, which will generate a more stable internal structure of the sclera by inducing intra- and interfibrillar collagen cross-links [81]. Physical cross-linking by combined riboflavin-ultraviolet or riboflavin-blue light and chemical cross-linking by glyceraldehydes, glutaraldehyde and aliphatic β-nitro alcohols were proven to increase biomechanical strength in both human and animal sclera [81–85]. Compared with other treatments of myopia, cross-linking would correct a cause instead of an effect. However, severe side effects can happen to other ocular structures such as the retina and cornea when cross-linking [81, 82]. Recently, successful cross-

linking approaches without severe side effects were reported by Wollensak and Iomdina [86, 87]. Chick models on axial myopia also suggested the involvement of genes controlling body size [88].

### Questions Requiring Answers in the Future

Myopia, as a complex trait, is influenced by both genetic and environmental factors. However, none of the myopia genes have been confirmed so far despite multiple candidate loci being proposed. Currently, 18 regions from MYP1 to MYP18 have been approved by the HUGO Gene Nomenclature Committee. These regions were well described by Tang et al. [60] except the latest one – the MYP18 region. This spans from 14q21.1 to 14q24.2 and was recently found in a consanguineous Chinese family [89]. This is the first report of an autosomal recessive inheritance model of high myopia.

Candidate genes such as *PAX6*, *MFRP*, *MYOC*, *MMP*, *UMODL1* and collagen genes have been studied on single or multiple single-nucleotide polymorphism bases [90]. These candidates have good biological evidence to participate in the process of myopia genesis or progression. For example, polymorphisms in the *MMP* genes may affect the activities of enzymes degrading matrix proteins and modulate sclera extensibility. However, lessons from GWAS studies on other complex traits such as coronary heart disease showed that most of the traditional candidate genes with solid biological connection with the trait could not be replicated in the GWAS [91]. And those discovered loci were not previously suspected as candidates [91]. GWAS is a good approach to detect major genes for myopia and sheds light on the molecular basis of this disorder as well as identifies possible pathways. However, special care needs to be taken when designing GWAS to avoid possible confounders.

It still remains unclear as to what roles the environmental factors play in relation to human myopia. Are they only triggers or decisive factors? It has been suggested that environmental factors such as extensive near work act as triggers of myopia [29]. The expression of *AL* genes activated by environmental factors leads to the elongation of AL. In environments of extensive near work, such as some high schools in East Asia, where students perform more reading and writing due to higher education pressure, a case-control GWAS study design would be helpful to discover trigger genes for axial myopia or in other words, genes for AL. Sorsby and Leary [92] suggested that ocular growth ceases around the age of 14–15 years based on a cross-section study involving 1,500 individuals aged from 3 to 22 years. On the other hand, myopia progress will not stop until the mid twenties for those hard-working students. In these 10 years, adolescents will experience significant changes due to pubertal development. Then the question is whether anything related to puberty, for example endocrine changes, will also affect the progress of myopia or the elongation of AL. If the extensive near work occurs after the age of 30 years, will it have the same consequence as when it occurs in teenagers? Why does AL generally decrease in the old? Is this process a simple reversal of axial elongation or completely caused by a different mechanism?

Animal models have provided useful and interesting theories concerning myopia and AL but species-specific differences in ocular structures make current extrapolations to human eye development somewhat tenuous. Creative new studies of myopia and its primary determinant, AL, will be able to provide valuable predictive information and effective treatment of this widespread disorder.

### References


1 Casson RJ, Newland HS, Muecke J, McGovern S, Durkin S, Sullivan T, Aung T: Prevalence and causes of visual impairment in rural Myanmar: the Meiktila Eye Study. Ophthalmology 2007;114:2302–2308.

2 Rein DB, Zhang P, Wirth KE, Lee PP, Hoerger TJ, McCall N, Klein R, Tielsch JM, Vijan S, Saaddine J: The economic burden of major adult visual disorders in the United States. Arch Ophthalmol 2006;124:1754–1760.

3 Kempen JH, Mitchell P, Lee KE, Tielsch JM, Broman AT, Taylor HR, Ikram MK, Congdon NG, O'Colmain BJ, Eye Diseases Prevalence Research Group: The prevalence of refractive errors among adults in the United States, Western Europe, and Australia. Arch Ophthalmol 2004;122:495–505.

4 Sawada A, Tomidokoro A, Araie M, Iwase A, Yamamoto T, Tajimi Study Group: Refractive errors in an elderly Japanese population: the Tajimi study. Ophthalmology 2008;115:363–370.

5 Yekta AA, Fotouhi A, Khabazkhoob M, Hashemi H, Ostadimoghaddam H, Heravian J, Mehravaran S: The prevalence of refractive errors and its determinants in the elderly population of Mashhad, Iran. Ophthalmic Epidemiol 2009;16:198–203.

6 Bourne RR, Dineen BP, Ali SM, Noorul Huq DM, Johnson GJ: Prevalence of refractive error in Bangladeshi adults: results of the National Blindness and Low Vision Survey of Bangladesh. Ophthalmology 2004;111:1150–1160.

7 Liang YB, Wong TY, Sun LP, Tao QS, Wang JJ, Yang XH, Xiong Y, Wang NL, Friedman DS: Refractive errors in a rural Chinese adult population: the Handan eye study. Ophthalmology 2009;116:2119–2127.
8 He M, Huang W, Li Y, Zheng Y, Yin Q, Foster PJ: Refractive error and biometry in older Chinese adults: the Liwan eye study. Invest Ophthalmol Vis Sci 2009;50:5130–5136.
9 Krishnaiah S, Srinivas M, Khanna RC, Rao GN: Prevalence and risk factors for refractive errors in the South Indian adult population: the Andhra Pradesh Eye disease study. Clin Ophthalmol 2009;3:17–27.
10 Wong TY, Foster PJ, Hee J, Ng TP, Tielsch JM, Chew SJ, Johnson GJ, Seah SK: Prevalence and risk factors for refractive errors in adult Chinese in Singapore. Invest Ophthalmol Vis Sci 2000;41:2486–2494.
11 Midelfart A, Kinge B, Midelfart S, Lydersen S: Prevalence of refractive errors in young and middle-aged adults in Norway. Acta Ophthalmol Scand 2002;80:501–505.
12 Anton A, Andrada MT, Mayo A, Portela J, Merayo J: Epidemiology of refractive errors in an adult European population: the Segovia study. Ophthalmic Epidemiol 2009;16:231–237.
13 Dirani M, Chan YH, Gazzard G, Hornbeak DM, Leo SW, Selvaraj P, Zhou B, Young TL, Mitchell P, Varma R, Wong TY, Saw SM: Prevalence of refractive error in Singaporean Chinese children: the Strabismus, Amblyopia, and Refractive Error in Young Singaporean Children (STARS) Study. Invest Ophthalmol Vis Sci 2010;51:1348–1355.
14 Giordano L, Friedman DS, Repka MX, Katz J, Ibironke J, Hawes P, Tielsch JM: Prevalence of refractive error among preschool children in an urban population: the Baltimore Pediatric Eye Disease Study. Ophthalmology 2009;116:739–746.
15 Multi-Ethnic Pediatric Eye Disease Study Group: Prevalence of myopia and hyperopia in 6- to 72-month-old African American and Hispanic children: the Multi-Ethnic Pediatric Eye Disease Study. Ophthalmology 2010;117:140–147.
16 Ip JM, Rose KA, Morgan IG, Burlutsky G, Mitchell P: Myopia and the urban environment: findings in a sample of 12-year-old Australian school children. Invest Ophthalmol Vis Sci 2008;49:3858–3863.
17 Congdon N, Wang Y, Song Y, Choi K, Zhang M, Zhou Z, Xie Z, Li L, Liu X, Sharma A, Wu B, Lam DS: Visual disability, visual function, and myopia among rural Chinese secondary school children: the Xichang Pediatric Refractive Error Study (X-PRES) – report 1. Invest Ophthalmol Vis Sci 2008;49:2888–2894.
18 Jamali P, Fotouhi A, Hashemi H, Younesian M, Jafari A: Refractive errors and amblyopia in children entering school: Shahrood, Iran. Optom Vis Sci 2009;86:364–369.
19 Barnes M, Williams C, Lumb R, Harrad RA, Sparrow JM, Harvey I, ALSPAC study team: The prevalence of refractive errors in a UK birth cohort of children aged 7 years. Invest Ophthalmol Vis Sci 2001;42:S389.
20 Saw SM, Carkeet A, Chia KS, Stone RA, Tan DT: Component dependent risk factors for ocular parameters in Singapore Chinese children. Ophthalmology 2002;109:2065–2071.
21 Czepita D, Mojsa A, Zejmo M: Prevalence of myopia and hyperopia among urban and rural schoolchildren in Poland. Ann Acad Med Stetin 2008;54:17–21.
22 Uzma N, Kumar BS, Khaja Mohinuddin Salar BM, Zafar MA, Reddy VD: A comparative clinical survey of the prevalence of refractive errors and eye diseases in urban and rural school children. Can J Ophthalmol 2009;44:328–333.
23 Gronlund MA, Andersson S, Aring E, Hard AL, Hellstrom A: Ophthalmological findings in a sample of Swedish children aged 4–15 years. Acta Ophthalmol Scand 2006;84:169–176.
24 Hashim SE, Tan HK, Wan-Hazabbah WH, Ibrahim M: Prevalence of refractive error in malay primary school children in a suburban area of Kota Bharu, Kelantan, Malaysia. Ann Acad Med Singapore 2008;37:940–946.
25 Lam CS, Goldschmidt E, Edwards MH: Prevalence of myopia in local and international schools in Hong Kong. Optom Vis Sci 2004;8:317–322.
26 Woo WW, Lim KA, Yang H, Lim XY, Liew F, Lee YS, Saw SM: Refractive errors in medical students in Singapore. Singapore Med J 2004;45:470–474.
27 Resnikoff S, Pascolini D, Etya'ale D, Kocur I, Pararajasegaram R, Pokharel GP, Mariotti SP: Global data on visual impairment in the year 2002. Bull World Health Organ 2004;82:844–851.
28 Dandona L, Dandona R: What is the global burden of visual impairment? BMC Med 2006;4:6.
29 Zejmo M, Forminska-Kapuscik M, Pieczara E, Filipek E, Mrukwa-Kominek E, Samochowiec-Donocik E, Leszczynski R, Smuzyńska M: Etiopathogenesis and management of high-degree myopia. Part I. Med Sci Monit 2009;15:199–202.
30 Young TL, Metlapally R, Shay AE: Complex trait genetics of refractive error. Arch Ophthalmol 2007;125:38–48.
31 Tron EJ: The optical elements of the refractive power of the eye; in Ridley F, Sorsby A (eds): Modern Trends in Ophthalmology. New York, Hoeber Press, 1940, p 245.
32 Fotedar R, Wang JJ, Burlutsky G, Morgan IG, Rose K, Wong TY, Mitchell P: Distribution of axial length and ocular biometry measured using partial coherence laser interferometry (IOL Master) in an older white population. Ophthalmology 2010;117:417–423.
33 Biino G, Palmas MA, Corona C, Prodi D, Fanciulli M, Sulis R, Serra A, Fossarello M, Pirastu M: Ocular refraction: heritability and genome-wide search for eye morphometry traits in an isolated Sardinian population. Hum Genet 2005;116:152–159.
34 Warrier S, Wu HM, Newland HS, Muecke J, Selva D, Aung T, Casson RJ: Ocular biometry and determinants of refractive error in rural Myanmar: the Meiktila Eye Study. Br J Ophthalmol 2008;92:1591–1594.
35 Olsen T, Arnarsson A, Sasaki H, Sasaki K, Jonasson F: On the ocular refractive components: the Reykjavik Eye Study. Acta Ophthalmol Scand 2007;85:361–366.
36 Wickremasinghe S, Foster PJ, Uranchimeg D, Lee PS, Devereux JG, Alsbirk PH, Machin D, Johnson GJ, Baasanhu J: Ocular biometry and refraction in Mongolian adults. Invest Ophthalmol Vis Sci 2004;45:776–783.
37 Mallen EA, Gammoh Y, Al-Bdour M, Sayegh FN: Refractive error and ocular biometry in Jordanian adults. Ophthalmic Physiol Opt 2005;25:302–309.
38 Wong TY, Foster PJ, Ng TP, Tielsch JM, Johnson GJ, Seah SK: Variations in ocular biometry in an adult Chinese population in Singapore: the Tanjong Pagar Survey. Invest Ophthalmol Vis Sci 2001;42:73–80.
39 Chen CY, Scurrah KJ, Stankovich J, Garoufalis P, Dirani M, Pertile KK, Richardson AJ, Mitchell P, Baird PN: Heritability and shared environment estimates for myopia and associated ocular biometric traits: the Genes in Myopia (GEM) family study. Hum Genet 2007;121:511–520.
40 Young TL, Metlapally R, Shay AE: Complex trait genetics of refractive error. Arch Ophthalmol 2007;125:38–48.
41 Mallen EA, Gammoh Y, Al-Bdour M, Sayegh FN: Refractive error and ocular biometry in Jordanian adults. Ophthalmic Physiol Opt 2005;25:302–309.
42 Chen MJ, Liu YT, Tsai CC, Chen YC, Chou CK, Lee SM: Relationship between central corneal thickness, refractive error, corneal curvature, anterior chamber depth and axial length. J Chin Med Assoc 2009;72:133–137.
43 Hung GK, Ciuffreda KJ: Model of human refractive error development. Curr Eye Res 1999;19:41–52.
44 Shufelt C, Fraser-Bell S, Ying-Lai M, Torres M, Varma R, Los Angeles Latino Eye Study Group – refractive error, ocular biometry, and lens opalescence in an adult population: the Los Angeles Latino Eye Study. Invest Ophthalmol Vis Sci 2005;46:4450–4460.
45 Lee KE, Klein BE, Klein R, Quandt Z, Wong TY: Association of age, stature, and education with ocular dimensions in an older white population. Arch Ophthalmol 2009;127:88–93.
46 Mutti DO, Hayes JR, Mitchell GL, Jones LA, Moeschberger ML, Cotter SA, Kleinstein RN, Manny RE, Twelker JD, Zadnik K, CLEERE Study Group: Refractive error, axial length, and relative peripheral refractive error before and after the onset of myopia. Invest Ophthalmol Vis Sci 2007;48:2510–2519.
47 Gordon RA, Donzis PB: Refractive development of the human eye. Arch Ophthalmol 1985;103:785–789.
48 Brown NP, Koretz JF, Bron AJ: The development and maintenance of emmetropia. Eye 1999;13:83–92.

49 Lambert SR: The effect of age on the retardation of axial elongation following a lensectomy in infant monkeys. Arch Ophthalmol 1998;116:781–784.
50 Kugelberg U, Zetterstrom C, Syren-Nordqvist S: Ocular axial length in children with unilateral congenital cataract. Acta Ophthalmol Scand 1996;74:220–223.
51 Flitcroft DI, Knight-Nanan D, Bowell R, Lanigan B, O'Keefe M: Intraocular lenses in children: changes in axial length, corneal curvature, and refraction. Br J Ophthalmol 1999;83:265–269.
52 Leiba H, Springer A, Pollack A: Ocular axial length changes in pseudophakic children after traumatic and congenital cataract surgery. J AAPOS 2006;10:460–463.
53 Mutti DO, Mitchell GL, Jones LA, Friedman NE, Frane SL, Lin WK, Moeschberger ML, Zadnik K: Axial growth and changes in lenticular and corneal power during emmetropization in infants. Invest Ophthalmol Vis Sci 2005;46:3074–3080.
54 Jivrajka R, Shammas MC, Boenzi T, Swearingen M, Shammas HJ: Variability of axial length, anterior chamber depth, and lens thickness in the cataractous eye. J Cataract Refract Surg 2008;34:289–294.
55 Osuobeni EP: Ocular components values and their intercorrelations in Saudi Arabians. Ophthalmic Physiol Opt 1999;19:489–497.
56 Su DH, Wong TY, Foster PJ, Tay WT, Saw SM, Aung T: Central corneal thickness and its associations with ocular and systemic factors: the Singapore Malay Eye Study. Am J Ophthalmol 2009;147:709–716.
57 Stone RA, Quinn GE, Francis EL, Ying GS, Flitcroft DI, Parekh P, Brown J, Orlow J, Schmid G: Diurnal axial length fluctuations in human eyes. Invest Ophthalmol Vis Sci 2004;45:63–70.
58 Wilson LB, Quinn GE, Ying GS, Francis EL, Schmid G, Lam A, Orlow J, Stone RA: The relation of axial length and intraocular pressure fluctuations in human eyes. Invest Ophthalmol Vis Sci 2006;47:1778–1784.
59 Read SA, Collins MJ, Iskander DR: Diurnal variation of axial length, intraocular pressure, and anterior eye biometrics. Invest Ophthalmol Vis Sci 2008;49:2911–2918.
60 Tang WC, Yap MK, Yip SP: A review of current approaches to identifying human genes involved in myopia. Clin Exp Optom 2008;91:4–22.
61 Kurtz D, Hyman L, Gwiazda JE, Manny R, Dong LM, Wang Y, Scheiman M, COMET Group: Role of parental myopia in the progression of myopia and its interaction with treatment in COMET children. Invest Ophthalmol Vis Sci 2007;48:562–570.
62 He M, Hur YM, Zhang J, Ding X, Huang W, Wang D: Shared genetic determinant of axial length, anterior chamber depth, and angle opening distance: the Guangzhou Twin Eye Study. Invest Ophthalmol Vis Sci 2008;49:4790–4794.
63 Lopes MC, Andrew T, Carbonaro F, Spector TD, Hammond CJ: Estimating heritability and shared environmental effects for refractive error in twin and family studies. Invest Ophthalmol Vis Sci 2009;50:126–131.
64 Paget S, Vitezica ZG, Malecaze F, Calvas P: Heritability of refractive value and ocular biometrics. Exp Eye Res 2008;86:290–295.
65 Dirani M, Shekar SN, Baird PN: Evidence of shared genes in refraction and axial length: the Genes in Myopia (GEM) twin study. Invest Ophthalmol Vis Sci 2008;49:4336–4339.
66 Phillips JR: Monovision slows juvenile myopia progression unilaterally. Br J Ophthalmol 2005;89:1196–1200.
67 Klein AP, Suktitipat B, Duggal P, Lee KE, Klein R, Bailey-Wilson JE, Klein BE: Heritability analysis of spherical equivalent, axial length, corneal curvature, and anterior chamber depth in the Beaver Dam Eye Study. Arch Ophthalmol 2009;127:649–655.
68 Zhu G, Hewitt AW, Ruddle JB, Kearns LS, Brown SA, Mackinnon JR, Chen CY, Hammond CJ, Craig JE, Montgomery GW, Martin NG, Mackey DA: Genetic dissection of myopia: evidence for linkage of ocular axial length to chromosome 5q. Ophthalmology 2008;115:1053–1057.
69 Saw SM, Gazzard G, Shih-Yen EC, Chua WH: Myopia and associated pathological complications. Ophthalmic Physiol Opt 2005;25:381–391.
70 Tsai MY, Lin LL, Lee V, Chen CJ, Shih YF: Estimation of heritability in myopic twin studies. Jpn J Ophthalmol 2009;53:615–622.
71 Nakanishi H, Yamada R, Gotoh N, Hayashi H, Yamashiro K, Shimada N, Ohno-Matsui K, Mochizuki M, Saito M, Iida T, Matsuo K, Tajima K, Yoshimura N, Matsuda F. A genome-wide association analysis identified a novel susceptible locus for pathological myopia at 11q24.1. PLoS Genet 2009;5:e1000660.
72 Raviola E, Wiesel TN: An animal model of myopia. N Engl J Med 1998;312:1609–1615.
73 Hung LF, Crawford ML, Smith EL: Spectacle lenses alter eye growth and the refractive status of young monkeys. Nat Med 1995;1:761–765.
74 Norton TT, Siegwart JT Jr: Animal models of emmetropization: matching axial length to the focal plane. J Am Optom Assoc 1995;66:405–414.
75 Zhou X, Lu F, Xie R, Jiang L, Wen J, Li Y, Shi J, He T, Qu J: Recovery from axial myopia induced by a monocularly deprived facemask in adolescent (7-week-old) guinea pigs. Vision Res 2007;47:1103–1111.
76 Siegwart JT Jr, Norton TT: The susceptible period for deprivation-induced myopia in tree shrew. Vision Res 1998;38:3505–3515.
77 Smith EL 3rd, Hung LF, Kee CS, Qiao Y: Effects of brief periods of unrestricted vision on the development of form-deprivation myopia in monkeys. Invest Ophthalmol Vis Sci 2002;43:291–299.
78 Rada JA, Shelton S, Norton TT: The sclera and myopia. Exp Eye Res 2006;82:185–200.
79 Siegwart JT Jr, Norton TT: Regulation of the mechanical properties of tree shrew sclera by the visual environment. Vision Res 1999;39:387–407.
80 McBrien NA, Jobling AI, Gentle A: Biomechanics of the sclera in myopia: extracellular and cellular factors. Optom Vis Sci 2009;86:23–30.
81 Wollensak G, Iomdina E, Dittert DD, Salamatina O, Stoltenburg G: Cross-linking of scleral collagen in the rabbit using riboflavin and UVA. Acta Ophthalmol Scand 2005;83:477–482.
82 Wollensak G, Spoerl E: Collagen crosslinking of human and porcine sclera. J Cataract Refract Surg 2004;30:689–695.
83 Paik DC, Wen Q, Braunstein RE, Airiani S, Trokel SL: Initial studies using aliphatic beta-nitro alcohols for therapeutic corneal cross-linking. Invest Ophthalmol Vis Sci 2009;50:1098–1105.
84 Danilov NA, Ignatieva NY, Iomdina EN, Semenova SA, Rudenskaya GN, Grokhovskaya TE, Lunin VV: Stabilization of scleral collagen by glycerol aldehyde cross-linking. Biochim Biophys Acta 2008;1780:764–772.
85 Iseli HP, Spoerl E, Wiedemann P, Krueger RR, Seiler T: Efficacy and safety of blue-light scleral cross-linking. J Refract Surg 2008;24:S752–S755.
86 Wollensak G, Iomdina E: Long-term biomechanical properties of rabbit sclera after collagen crosslinking using riboflavin and ultraviolet A (UVA). Acta Ophthalmol 2009;87:193–198.
87 Wollensak G, Iomdina E: Long-term biomechanical properties after collagen crosslinking of sclera using glyceraldehyde. Acta Ophthalmol 2008;86:887–893.
88 Prashar A, Hocking PM, Erichsen JT, Fan Q, Saw SM, Guggenheim JA: Common determinants of body size and eye size in chickens from an advanced intercross line. Exp Eye Res 2009;89:42–48.
89 Yang Z, Xiao X, Li S, Zhang Q: Clinical and linkage study on a consanguineous Chinese family with autosomal recessive high myopia. Mol Vis 2009;15:312–318.
90 Hornbeak DM, Young TL: Myopia genetics: a review of current research and emerging trends. Curr Opin Ophthalmol 2009;20:356–362.
91 Wang Q: Molecular genetics of coronary artery disease. Curr Opin Cardiol 2005;20:182–188.
92 Sorsby A, Leary GA: A longitudinal study of refraction and its components during growth. Spec Rep Ser Med Res Counc (GB) 1969;309:1–41.

# Annex 3

## Project 1 Recruitment protocol

**Protocole – Etude Génétique de la Myopie**

**Contacts:** **Jackie Butterworth (Doctorante)**

**INSERM U563**

**Dépt Génétique**

**Equipe Malecaze/Calvas**

**Bureau B513 (Couloir bleu)**

**Tél Bureau : 05 62 74 45 09**

**Mon portable : 06 37 64 98 19**

jacqueline.butterworth@toulouse.inserm.fr

**Bérengère Goderiaux (Orthoptiste)**

**Portable : 06 59 86 29 22**

goderiauxberengere@yahoo.fr

**Description vulgarisée de l'étude (pour les patients):**

**Une ancienne étude sur une population de familles françaises a localisé une région sur le chromosome 7 qui semble contenir un gène impliqué dans le déterminisme de la myopie forte. Pour la suite, il est nécessaire de recruter plus de volontaires pour poursuivre l'étude génétique (analyse d'association en utilisant le génotypage de 600 marqueurs d'ADN) dans cette région. Ceci devrait permettre d'identifier le gène causal (sur les 67 présents dans la région).**

Le patient s'intéresse parfois aux résultats, il faut donc expliquer que la durée de ce projet est estimée à 3 ans. Les patients peuvent nous contacter (numéro du bureau) pour en savoir plus.

**Patients que vous pouvez recruter** :

1. **Des myopes forts bilatéraux ≥ -6D (à l'œil le moins atteint)**

2. **Des témoins sains**

**SIGNATURE DU CONSENTEMENT INDISPENSABLE**

**Il faut indiquer si le patient myope fort est un cas familial ou un cas sporadique:**

- **Cas familial – quand il existe ≥1 myope fort bilatéral (≥ 6D) chez les frères/sœurs/parents/oncles et tantes/grands-parents/les enfants du patient.**

- **Cas sporadique – quand le patient n'a pas d'autres myopes fortes dans sa famille (frères/sœurs/parents/oncles et tantes/grands-parents/leurs enfants). Myopes faibles bilatéraux (-1D > -6D) acceptés.**

**Arbre généalogique obligé pour chaque patient myope fort et témoin qui montre les frères/sœurs, parents (avec oncles/tantes), grands-parents et leurs enfants sains et myopes faibles/myopes fortes.**

- Indiquez bien les membres de la familles qui sont myopes faibles ou myopes fortes.

- Noms/prénoms dans la mesure du possible.

- Notez les valeurs de réfraction connues des autres membres, sinon récupérez des numéros de téléphone des membres douteux si possible.

- Si le patient **ne sait pas** s'il existe d'autres myopes dans la famille (membres de la famille décédés ou injoignables): il est toujours possible de le recruter mais bien préciser qu'on n'a pas pu le classer comme un cas familial ou sporadique.

**Utiliser ce système de symboles :**

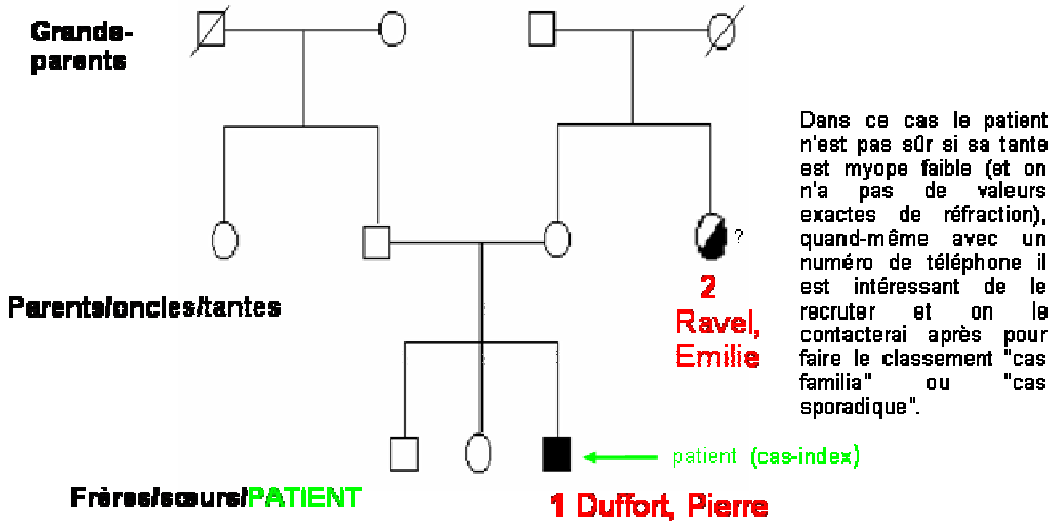


carré = garçon

cercle = fille

= sain (emmétrope) et on a des valeurs de réfraction (OD et OG)

= sain probable (emmétrope) mais on ne sait pas des valeurs de réfraction (par exemple on sait qu'il/elle ne porte pas des lunettes mais c'est tout pour le moment)

= myope fort (≥ 5D) et on a des valeurs de réfraction (OD et OG)

= myope fort (≥ 5D) probable mais on n'a pas des valeurs de réfraction

= myope faible (-1D > -5D) et on a des valeurs de réfraction (OD et OG)

= myope faible (-1D > -5D) probable mais on n'a pas de valeurs de réfraction

= décédé/injoignable

- **Témoins – des patients emmétropes sans des myopes fortes dans la famille (frères/sœurs/parents/oncles et tantes/grands-parents/leurs enfants).**

**- Il faut toujours remplir les mêmes feuilles (avec l'examen ophtalmo complet)**

- Le plus simple est de prendre les conjoints, amis etc qui accompagnent le patient à la consultation.

- On peut prendre des emmétropes qui n'appartiennent pas à la **même famille du patient, mais pas les conjoints des mères/pères des patients myopes fortes !!!**

**<u>Les détails civils du patient et origines ethno-géographiques de sa famille</u>**

- ***Numéro de téléphone (domicile) le plus important!!!***
- Il faut préciser **l'origine ethno-géographique (lieu de naissance) du patient, parents et grands-parents**.

-On peut être plus vague pour les grands-parents, comme le numéro du département, le pays ou dans le pire de cas le groupe ethnique (par exemple, Asiatique, Maghrébin) si le pays n'est pas connu.

-Si le patient n'est pas sûr il faut le préciser (avec ?), il ne faut pas deviner !

**L'examen ophtalmo complet** (sur la feuille et dans la base de données)

## Obligatoire pour les patients myopes forts et les témoins

- Besoin de savoir si le patient est né(e) prématuré(e) ou pas et une valeur à peu près pour le poids de naissance (si le patient ne sait pas entrer ? dans la BDD).
- **L'âge du début de la myopie** – important mais une estimation me suffit (par exemple une tranche d'âge 10-12 ans).
- Topographie pour les témoins.

Je ne peux accepter aucun patient :

- **Atteint d'autres maladies oculaires** (la rétinite pigmentaire, la rétinopathie du prématuré, dystrophie cornéenne, keratocône, Maladie de Wagner)
- **Patients opérés** de cataracte ou laser (**sauf si on peut récupérer l'examen ophtalmo qui précède la chirurgie**).
- **Myopie avec un fort astigmatisme (≤-2)**
- **Myopie syndromique** (Syndrome de Marfan/Syndrome de Stickler type 1 et 2/Syndrome d'Ehlers-Danlos/Juvenile glaucoma/Maladie de Bornholm).

**Prélèvements –** par les infirmières, on a fourni des tubes 10 ml (EDTA) et les aiguilles dans un placard d'une salle de consultation (voir avec Martine Castillon).

# Annex 4

## Project 1 Patient recruitment file



HOPITAL : PURPAN RANGUEIL

DATE.....

MYOPE FORT ☐ TEMOIN ☐
-FAMILIAL ☐
-SPORADIQUE ☐
-INCERTAIN ☐

**INFORMATIONS CIVILES DU PATIENT**

NOM : ..... NOM DE JEUNE FILLE : .....

PRENOM : ..... SEXE : M F

DATE DE NAISSANCE : .....

ADRESSE : .....

Complément adresse : .....

CODE POSTAL : ..... VILLE : ..... PAYS : .....

TEL DOMICILE : ..... TEL PORTABLE : ..... TEL TRAVAIL : .....

NOM DU CONJOINT : ..... EMAIL : .....

NOM DES ENFANTS :

1. .....
2. .....
3. .....
4. .....
5. .....
6. .....
7. .....
8. .....

**INFORMATIONS CIVILES DES PARENTS**

| MERE | PERE |
|---|---|
| NOM : ..... | NOM : ..... |
| PRENOM : ..... | PRENOM : ..... |
| ADRESSE : ..... | ADRESSE : ..... |
| ..... | ..... |
| Complément adresse : ..... | Complément adresse : ..... |
| CODE POSTAL : ..... | CODE POSTAL : ..... |
| VILLE : ..... | VILLE : ..... |
| TEL DOMICILE : ..... | TEL DOMICILE : ..... |

NOM : ..... PRENOM : .....

## ORIGINE ETHNO-GEOGRAPHIQUE DE LA FAMILLE

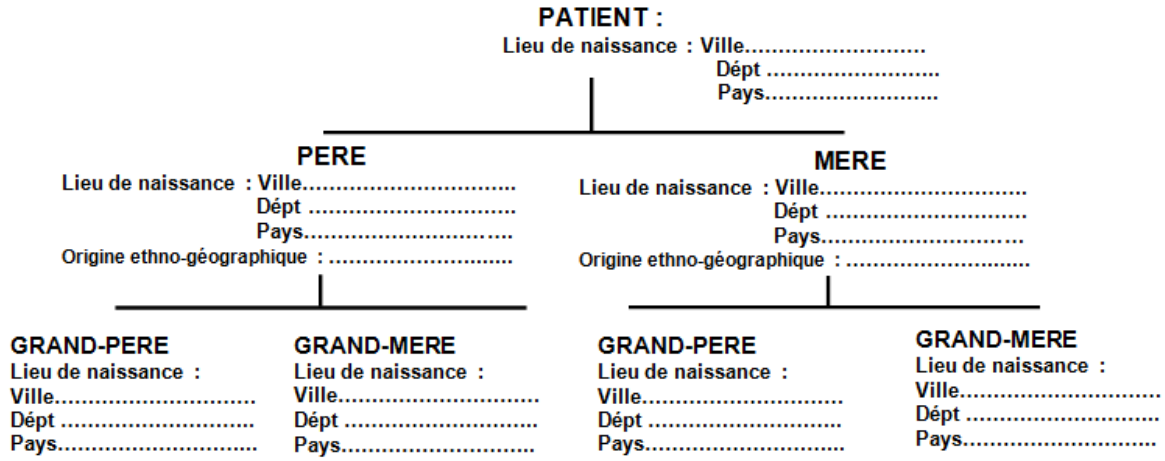


## ARBRE GENEALOGIQUE :

**L'EXAMEN OPHTALMO** 3/3

NOM : ..... PRENOM : .....

**NO DOSSIER OPHTALMO : ..... NOM OPHTALMO : .....**

**VISITE: CONSULTATION HOSPITALISE** : Si hospitalisé, pour quelle raison: .....

**VILLE D'OPHTALMO HABITUEL : .....**

---

N° DE GROSSESSES : ..... PREMATURE : OUI NON POIDS NAISS : ..... grammes

AGE DEBUT MYOPIE : .....

ANTEDECENTS OPHTALMO : .....

.....

CHIRURGIE OPHTALMOLOGIQUE : NON OUI : PRECISER .....

ANTEDECENTS DIVERS : .....

MEDICAMENTS : .....

---

EN CAS DE CHIRURGIE OPHTALMOLOGIQUE, VALEURS MESUREES AVANT OPERATION : NON OUI : si oui DATE : .....

AV LOIN OD : /10 ou < 1 / 20 AV LOIN OG : /10 ou < 1 / 20

AV PRES OD P : 1.5 2 3 4 5 6 8 10 14 <14

AV PRES OG P : 1.5 2 3 4 5 6 8 10 14 <14

SPHERICITE OD : ..... CYL OD : ..... AXE OD : ..... ES OD: .....

SPHERICITE OG : ..... CYL OG : ..... AXE OG : ..... ES OG : .....

ADD VP OD : ..... KERATOMETRIE MOYENNE OD : .....

ADD VP OG : ..... KERATOMETRIE MOYENNE OG : .....

VISION DE LOIN : CORRECTION : LENTILLES ..... D *ou* LUNETTES ..... D

| OD | OG |
|---|---|
| CORNEE : NORMALE EXCIMER KR AUTRE | CORNEE : NORMALE EXCIMER KR AUTRE |
| CA : NORMAL IOL neg | CA : NORMAL IOL neg |
| CRIST : CLAIR OPAQUE APHAQUE PSEUDOPHAQUE | CRIST : CLAIR OPAQUE APHAQUE PSEUDOPHAQUE |
| DR : OUI NON | DR : OUI NON |
| LESION MACULAIRE : OUI NON | LESION MACULAIRE : OUI NON |
| STAPHYLOME : OUI NON | STAPHYLOME : OUI NON |
| TONUS : ..... BIOMETRIE : ..... | TONUS : ..... BIOMETRIE : ..... |
| PHOTO FOND ŒIL : OUI NON | PHOTO FOND ŒIL : OUI NON |
| TOPOGRAPHIE (POUR LES TEMOINS) : OUI NON | TOPOGRAPHIE (POUR LES TEMOINS) : OUI NON |

---

CONSENTEMENT SIGNE : OUI NON

PRELEVEMENT : OUI NON

# Annex 5

## Project 1 Volonteer recruitment press articles



Cobayes miros pour y voir clair

**« Progresser dans la connaissance des mécanisme de la myopie »**. C'est l'objectif d'une étude menée par deux professeurs du CHU de Purpan. Ils recherchent des volontaires « myopes forts » mais aussi, pour comparer les marqueurs génétiques, des « cobayes » sans aucun trouble de la vue. Les candidats devront remplir un questionnaire et consentir à une prise de sang « de quelques millilitres ». *Rens. au 05 62 74 45 09.*

Magazine, 20 minutes, Toulouse

Myopie : appel aux volontaires

Santé. Les chercheurs ont besoin de 400 sujets dotés d'une vue parfaite.



La myopie concerne 25 % de la population. Photo DDM, archives

Depuis la fin de l'année 2008, les équipes des professeurs François Malecaze du CHU Purpan et Pierre Calvas de l'Inserm se penchent sur la composante génétique de la myopie, maladie qui touche actuellement un quart de la population.

« On sait que des facteurs liés aux conditions de vie, comme le travail sur ordinateur, les jeux vidéos, favorisent la myopie mais on ne sait pas pourquoi la elle survient. Ce qui nous intéresse c'est de déterminer la part génétique de la maladie », précise Pierre Calvas.

Pour ce travail de recherche, les équipes toulousaines ont réussi à recueillir les analyses de 400 sujets atteints de myopie sévère (plus de six dioptries). Un succès puisque seulement 10 % des myopes sont atteints de myopie sévère. « Nous avons, en plus, réussi à réunir des sujets issus de la même zone géographique - la région toulousaine - ce qui va permettre d'être plus pointus sur notre étude », explique François Malecaze.

L'équipe de chercheurs a désormais besoin de réunir 400 sujets non myopes pour comparer leur patrimoine génétique avec celui des myopes sévères. « Nous allons faire des statistiques et voir si un gène influe dans la survenue de la myopie», ajoute Pierre Calvas.

Une simple prise de sang est demandée aux volontaires. Ils peuvent s'adresser par téléphone à Mme Godenaux au service d'ophtalmologie du CHU Purpan au 05 61 77 99 99 (le matin) ou Mme Butterworth au 05 62 74 45 09 ou 06 37 64 98 19. Par courriel : malecaze.sec@chu-toulouse.fr ; jacqueline.butterworth@inserm.fr

On-line, La dépêche, Toulouse



La parole à **Patrick Calvas et François Malecaze**

Les professeurs Patrick Calvas et François Malecaze, professeur de génétique et ophtalmologiste et au CHU de Purpan.

"25% des Français souffrent de myopie"

Les Toulousains François Malecaze et Patrick Calvas recrutent actuellement des volontaires afin de poursuivre leurs travaux sur la myopie. Explications.

**Pourquoi recruter des volontaires à Toulouse concernant la myopie ?**

En France, près de 2 millions de personnes sont atteintes de myopie forte, maladie très invalidante. Les personnes qui en sont atteintes ne peuvent ni conduire ni travailler sur ordinateur. Au sein de notre laboratoire, basé à Toulouse et appartenant au réseau My Eurogtia, notre effort de recherche porte sur la génétique. L'objectif est de comprendre quels sont les gènes qui aboutissent à cette forme de myopie. Nous recherchons 2 000 volontaires (1 000 myopes forts et 1 000 "sains"), afin de leur faire un prélèvement sanguin et de comparer leurs gènes.

**2 000**

C'est le nombre de volontaires recherchés pour cette étude. Rens. : Mme Godenaux, service d'ophtalmologie, CHU Purpan, 05 61 77 99 99 (le matin) ou malecaze.sec@chu-toulouse.fr.

**Quel est l'état de la recherche sur la myopie ?**

Près d'un quart de la population française en souffre. Sur ces 25%, seuls 2 à 3% sont concernés par la myopie forte. Cela fait plusieurs années que nous travaillons avec une centaine de familles sur la transmission génétique de cette forme de myopie. Une étape supplémentaire dans la recherche passe par l'appel aux volontaires.

**Quelles avancées espérez-vous obtenir avec cette recherche ?**

On espère comprendre les mécanismes de l'infection afin de réfléchir sur un traitement d'ici à quelques années. En nous concentrant sur la myopie forte, nous espérons trouver un traitement pour toutes les formes de myopie, y compris celles qui se soignent avec des lunettes, des lentilles ou une opération. PROPOS RECUEILLIS PAR PHILIPPE FONT

Magazine à lire aussi article metrofrance.com/toulouse

Magazine, Le métro, Toulouse

# Bibliography


1. Oyster C, *The Human Eye Structure and Function*. Formation of the human eye. 1999, Sunderland, Massachusetts: Sinauer Associates, Inc. 57-70.
2. Harris WA. Pax-6: where to be conserved is not conservative. Proc Natl Acad Sci U S A 1997; **94**: (6): 2098-2100
3. Gilbert S, *Developmental biology*. 6th edition ed. Development of the Vertebrate Eye. 2000, Sunderland, Massachusetts: Sinauer Associates, Inc.
4. Gilmartin B. Myopia: precedents for research in the twenty-first century. Clin Experiment Ophthalmol 2004; **32**: (3): 305-324
5. Mutti DO, Mitchell GL, Jones LA et al. Axial growth and changes in lenticular and corneal power during emmetropization in infants. Invest Ophthalmol Vis Sci 2005; **46**: (9): 3074-3080
6. Young TL, Metlapally R, Shay AE. Complex trait genetics of refractive error. Arch Ophthalmol 2007; **125**: (1): 38-48
7. Chavaud D. Traitement chirurgical des complications rétiniennes de la myopei forte. Rev Prat 2001; **51**: (15): 1629-1630
8. Flament J, *Opthalmologie, pathologie du système visuel*. 2002, Paris: Masson.
9. Meng W, Butterworth J, Malecaze F et al. Axial Length of Myopia: A Review of Current Research. Ophthalmologica 2010; **225**: (3): 127-134
10. Xu L, Li Y, Wang S et al. Characteristics of highly myopic eyes: the Beijing Eye Study. Ophthalmology 2007; **114**: (1): 121-126
11. Jacobi FK, Zrenner E, Broghammer M et al. A genetic perspective on myopia. Cell Mol Life Sci 2005; **62**: (7-8): 800-808
12. Han W, Yap MK, Wang J et al. Family-based association analysis of hepatocyte growth factor (HGF) gene polymorphisms in high myopia. Invest Ophthalmol Vis Sci 2006; **47**: (6): 2291-2299
13. Leung YF, Tam PO, Baum L et al. TIGR/MYOC proximal promoter GT-repeat polymorphism is not associated with myopia. Hum Mutat 2000; **16**: (6): 533
14. Grosvenor T. A review and a suggested classification system for myopia on the basis of age-related prevalence and age of onset. Am J Optom Physiol Opt 1987; **64**: (7): 545-554
15. McBrien NA, Gentle A. Role of the sclera in the development and pathological complications of myopia. Prog Retin Eye Res 2003; **22**: (3): 307-338
16. Brown NP, Koretz JF, Bron AJ. The development and maintenance of emmetropia. Eye (Lond) 1999; **13 ( Pt 1)**: 83-92
17. Chen MJ, Liu YT, Tsai CC et al. Relationship between central corneal thickness, refractive error, corneal curvature, anterior chamber depth and axial length. J Chin Med Assoc 2009; **72**: (3): 133-137
18. Mallen EA, Gammoh Y, Al-Bdour M et al. Refractive error and ocular biometry in Jordanian adults. Ophthalmic Physiol Opt 2005; **25**: (4): 302-309
19. Bamashmus MA, Matlhaga B, Dutton GN. Causes of blindness and visual impairment in the West of Scotland. Eye (Lond) 2004; **18**: (3): 257-261
20. Buch H, Vinding T, La Cour M et al. Prevalence and causes of visual impairment and blindness among 9980 Scandinavian adults: the Copenhagen City Eye Study. Ophthalmology 2004; **111**: (1): 53-61
21. Iwase A, Araie M, Tomidokoro A et al. Prevalence and causes of low vision and blindness in a Japanese adult population: the Tajimi Study. Ophthalmology 2006; **113**: (8): 1354-1362
22. Kelliher C, Kenny D, O'Brien C. Trends in blind registration in the adult population of the Republic of Ireland 1996-2003. Br J Ophthalmol 2006; **90**: (3): 367-371

23. Klaver CC, Wolfs RC, Vingerling JR et al. Age-specific prevalence and causes of blindness and visual impairment in an older population: the Rotterdam Study. Arch Ophthalmol 1998; **116**: (5): 653-658
24. Krumpaszky HG, Ludtke R, Mickler A et al. Blindness incidence in Germany. A population-based study from Wurttemberg-Hohenzollern. Ophthalmologica 1999; **213**: (3): 176-182
25. Munier A, Gunning T, Kenny D et al. Causes of blindness in the adult population of the Republic of Ireland. Br J Ophthalmol 1998; **82**: (6): 630-633
26. Saw SM, Gazzard G, Shih-Yen EC et al. Myopia and associated pathological complications. Ophthalmic Physiol Opt 2005; **25**: (5): 381-391
27. Sorsby A, Benjamin B, Bennett AG. Steiger on refraction: a reappraisal. Br J Ophthalmol 1981; **65**: (12): 805-811
28. Touzeau O, Allouch C, Borderie V et al. [Correlation between refraction and ocular biometry]. J Fr Ophtalmol 2003; **26**: (4): 355-363
29. Lyhne N, Sjolie AK, Kyvik KO et al. The importance of genes and environment for ocular refraction and its determiners: a population based study among 20-45 year old twins. Br J Ophthalmol 2001; **85**: (12): 1470-1476
30. Kempen JH, Mitchell P, Lee KE et al. The prevalence of refractive errors among adults in the United States, Western Europe, and Australia. Arch Ophthalmol 2004; **122**: (4): 495-505
31. Goh WS, Lam CS. Changes in refractive trends and optical components of Hong Kong Chinese aged 19-39 years. Ophthalmic Physiol Opt 1994; **14**: (4): 378-382
32. Lam CS, Goldschmidt E, Edwards MH. Prevalence of myopia in local and international schools in Hong Kong. Optom Vis Sci 2004; **81**: (5): 317-322
33. Lin LL, Shih YF, Lee YC et al. Changes in ocular refraction and its components among medical students--a 5-year longitudinal study. Optom Vis Sci 1996; **73**: (7): 495-498
34. Woo WW, Lim KA, Yang H et al. Refractive errors in medical students in Singapore. Singapore Med J 2004; **45**: (10): 470-474
35. Fuchs A. Frequency of myopia gravis. Am J Ophthalmol 1960; **49**: 1418-1419
36. Wong TY, Foster PJ, Hee J et al. Prevalence and risk factors for refractive errors in adult Chinese in Singapore. Invest Ophthalmol Vis Sci 2000; **41**: (9): 2486-2494
37. Bar Dayan Y, Levin A, Morad Y et al. The changing prevalence of myopia in young adults: a 13-year series of population-based prevalence surveys. Invest Ophthalmol Vis Sci 2005; **46**: (8): 2760-2765
38. Bloom RI, Friedman IB, Chuck RS. Increasing rates of myopia: the long view. Curr Opin Ophthalmol 2010; **21**: (4): 247-248
39. Schaeffel F, Howland HC. Mathematical model of emmetropization in the chicken. J Opt Soc Am A 1988; **5**: (12): 2080-2086
40. Siegwart JT, Jr., Norton TT. The susceptible period for deprivation-induced myopia in tree shrew. Vision Res 1998; **38**: (22): 3505-3515
41. Smith EL, 3rd, Bradley DV, Fernandes A et al. Form deprivation myopia in adolescent monkeys. Optom Vis Sci 1999; **76**: (6): 428-432
42. Wallman J, Adams JI. Developmental aspects of experimental myopia in chicks: susceptibility, recovery and relation to emmetropization. Vision Res 1987; **27**: (7): 1139-1163
43. Phillips JR, Khalaj M, McBrien NA. Induced myopia associated with increased scleral creep in chick and tree shrew eyes. Invest Ophthalmol Vis Sci 2000; **41**: (8): 2028-2034
44. Schaeffel F, Burkhardt E, Howland HC et al. Measurement of refractive state and deprivation myopia in two strains of mice. Optom Vis Sci 2004; **81**: (2): 99-110
45. Shen W, Vijayan M, Sivak JG. Inducing form-deprivation myopia in fish. Invest Ophthalmol Vis Sci 2005; **46**: (5): 1797-1803
46. Sherman SM, Norton TT, Casagrande VA. Myopia in the lid-sutured tree shrew (Tupaia glis). Brain Res 1977; **124**: (1): 154-157

47. Troilo D, Judge SJ. Ocular development and visual deprivation myopia in the common marmoset (Callithrix jacchus). Vision Res 1993; **33**: (10): 1311-1324
48. Wallman J, Turkel J, Trachtman J. Extreme myopia produced by modest change in early visual experience. Science 1978; **201**: (4362): 1249-1251
49. Wiesel TN, Raviola E. Myopia and eye enlargement after neonatal lid fusion in monkeys. Nature 1977; **266**: (5597): 66-68
50. Norton TT, Amedo AO, Siegwart JT, Jr. Darkness causes myopia in visually experienced tree shrews. Invest Ophthalmol Vis Sci 2006; **47**: (11): 4700-4707
51. Wallman J, Winawer J. Homeostasis of eye growth and the question of myopia. Neuron 2004; **43**: (4): 447-468
52. Lu F, Zhou X, Zhao H et al. Axial myopia induced by a monocularly-deprived facemask in guinea pigs: A non-invasive and effective model. Exp Eye Res 2006; **82**: (4): 628-636
53. Curtin BJ, Iwamoto T, Renaldo DP. Normal and staphylomatous sclera of high myopia. An electron microscopic study. Arch Ophthalmol 1979; **97**: (5): 912-915
54. McBrien NA, Cornell LM, Gentle A. Structural and ultrastructural changes to the sclera in a mammalian model of high myopia. Invest Ophthalmol Vis Sci 2001; **42**: (10): 2179-2187
55. McBrien NA, Gentle A. The role of visual information in the control of scleral matrix biology in myopia. Curr Eye Res 2001; **23**: (5): 313-319
56. Gentle A, McBrien NA. Modulation of scleral DNA synthesis in development of and recovery from induced axial myopia in the tree shrew. Exp Eye Res 1999; **68**: (2): 155-163
57. Moring AG, Baker JR, Norton TT. Modulation of glycosaminoglycan levels in tree shrew sclera during lens-induced myopia development and recovery. Invest Ophthalmol Vis Sci 2007; **48**: (7): 2947-2956
58. Norton TT, Rada JA. Reduced extracellular matrix in mammalian sclera with induced myopia. Vision Res 1995; **35**: (9): 1271-1281
59. Rada JA, Shelton S, Norton TT. The sclera and myopia. Exp Eye Res 2006; **82**: (2): 185-200
60. Di Girolamo N, Lloyd A, McCluskey P et al. Increased expression of matrix metalloproteinases in vivo in scleritis tissue and in vitro in cultured human scleral fibroblasts. Am J Pathol 1997; **150**: (2): 653-666
61. Gaton DD, Sagara T, Lindsey JD et al. Matrix metalloproteinase-1 localization in the normal human uveoscleral outflow pathway. Invest Ophthalmol Vis Sci 1999; **40**: (2): 363-369
62. Guggenheim JA, McBrien NA. Form-deprivation myopia induces activation of scleral matrix metalloproteinase-2 in tree shrew. Invest Ophthalmol Vis Sci 1996; **37**: (7): 1380-1395
63. Kim JW, Lindsey JD, Wang N et al. Increased human scleral permeability with prostaglandin exposure. Invest Ophthalmol Vis Sci 2001; **42**: (7): 1514-1521
64. Shelton L, Rada JS. Effects of cyclic mechanical stretch on extracellular matrix synthesis by human scleral fibroblasts. Exp Eye Res 2007; **84**: (2): 314-322
65. Siegwart JT, Jr., Norton TT. Selective regulation of MMP and TIMP mRNA levels in tree shrew sclera during minus lens compensation and recovery. Invest Ophthalmol Vis Sci 2005; **46**: (10): 3484-3492
66. Siegwart JT, Jr., Norton TT. The time course of changes in mRNA levels in tree shrew sclera during induced myopia and recovery. Invest Ophthalmol Vis Sci 2002; **43**: (7): 2067-2075
67. Wallman J, Gottlieb MD, Rajaram V et al. Local retinal regions control local eye growth and myopia. Science 1987; **237**: (4810): 73-77
68. Troilo D, Gottlieb MD, Wallman J. Visual deprivation causes myopia in chicks with optic nerve section. Curr Eye Res 1987; **6**: (8): 993-999
69. Winawer J, Wallman J. Temporal constraints on lens compensation in chicks. Vision Res 2002; **42**: (24): 2651-2668
70. Bormann J. The 'ABC' of GABA receptors. Trends Pharmacol Sci 2000; **21**: (1): 16-19

71. Chebib M, Johnston GA. GABA-Activated ligand gated ion channels: medicinal chemistry and molecular biology. J Med Chem 2000; **43**: (8): 1427-1447
72. Stone RA, Liu J, Sugimoto R et al. GABA, experimental myopia, and ocular growth in chick. Invest Ophthalmol Vis Sci 2003; **44**: (9): 3933-3946
73. Chebib M, Hinton T, Schmid KL et al. Novel, potent, and selective GABAC antagonists inhibit myopia development and facilitate learning and memory. J Pharmacol Exp Ther 2009; **328**: (2): 448-457
74. Hasegawa S, Terazono K, Nata K et al. Nucleotide sequence determination of chicken glucagon precursor cDNA. Chicken preproglucagon does not contain glucagon-like peptide II. FEBS Lett 1990; **264**: (1): 117-120
75. Drucker DJ, Asa S. Glucagon gene expression in vertebrate brain. J Biol Chem 1988; **263**: (27): 13475-13478
76. Larsen PJ, Holst JJ. Glucagon-related peptide 1 (GLP-1): hormone and neurotransmitter. Regul Pept 2005; **128**: (2): 97-107
77. Buck C, Schaeffel F, Simon P et al. Effects of positive and negative lens treatment on retinal and choroidal glucagon and glucagon receptor mRNA levels in the chicken. Invest Ophthalmol Vis Sci 2004; **45**: (2): 402-409
78. Vessey KA, Lencses KA, Rushforth DA et al. Glucagon receptor agonists and antagonists affect the growth of the chick eye: a role for glucagonergic regulation of emmetropization? Invest Ophthalmol Vis Sci 2005; **46**: (11): 3922-3931
79. Ashby R, Kozulin P, Megaw PL et al. Alterations in ZENK and glucagon RNA transcript expression during increased ocular growth in chickens. Mol Vis 2010; **16**: 639-649
80. Massague J, Wotton D. Transcriptional control by the TGF-beta/Smad signaling system. Embo J 2000; **19**: (8): 1745-1754
81. Jobling AI, Nguyen M, Gentle A et al. Isoform-specific changes in scleral transforming growth factor-beta expression and the regulation of collagen synthesis during myopia progression. J Biol Chem 2004; **279**: (18): 18121-18126
82. Jobling AI, Gentle A, Metlapally R et al. Regulation of scleral cell contraction by transforming growth factor-beta and stress: competing roles in myopic eye growth. J Biol Chem 2009; **284**: (4): 2072-2079
83. Cornell RA, Kimelman D. Activin-mediated mesoderm induction requires FGF. Development 1994; **120**: (2): 453-462
84. Pickering JG, Ford CM, Tang B et al. Coordinated effects of fibroblast growth factor-2 on expression of fibrillar collagens, matrix metalloproteinases, and tissue inhibitors of matrix metalloproteinases by human vascular smooth muscle cells. Evidence for repressed collagen production and activated degradative capacity. Arterioscler Thromb Vasc Biol 1997; **17**: (3): 475-482
85. Schonherr E, Hausser HJ. Extracellular matrix and cytokines: a functional unit. Dev Immunol 2000; **7**: (2-4): 89-101
86. Rohrer B, Stell WK. Basic fibroblast growth factor (bFGF) and transforming growth factor beta (TGF-beta) act as stop and go signals to modulate postnatal ocular growth in the chick. Exp Eye Res 1994; **58**: (5): 553-561
87. Mao J, Liu S, Wen D et al. Basic fibroblast growth factor suppresses retinal neuronal apoptosis in form-deprivation myopia in chicks. Curr Eye Res 2006; **31**: (11): 983-987
88. Rohrer B, Tao J, Stell WK. Basic fibroblast growth factor, its high- and low-affinity receptors, and their relationship to form-deprivation myopia in the chick. Neuroscience 1997; **79**: (3): 775-787
89. Goss DA. Clinical accommodation and heterophoria findings preceding juvenile onset of myopia. Optom Vis Sci 1991; **68**: (2): 110-116

90. Gwiazda J, Thorn F, Held R. Accommodation, accommodative convergence, and response AC/A ratios before and at the onset of myopia in children. Optom Vis Sci 2005; **82**: (4): 273-278
91. Mutti DO, Mitchell GL, Hayes JR et al. Accommodative lag before and after the onset of myopia. Invest Ophthalmol Vis Sci 2006; **47**: (3): 837-846
92. Grigorenko EL. The inherent complexities of gene-environment interactions. J Gerontol B Psychol Sci Soc Sci 2005; **60 Spec No 1**: 53-64
93. Saw SM. A synopsis of the prevalence rates and environmental risk factors for myopia. Clin Exp Optom 2003; **86**: (5): 289-294
94. Mavracanas TA, Mandalos A, Peios D et al. Prevalence of myopia in a sample of Greek students. Acta Ophthalmol Scand 2000; **78**: (6): 656-659
95. Sperduto RD, Seigel D, Roberts J et al. Prevalence of myopia in the United States. Arch Ophthalmol 1983; **101**: (3): 405-407
96. Rosenfield M, Ciuffreda KJ. Cognitive demand and transient nearwork-induced myopia. Optom Vis Sci 1994; **71**: (6): 381-385
97. Beedle SL, Young FA. Values, personality, physical characteristics, and refractive error. Am J Optom Physiol Opt 1976; **53**: (11): 735-739
98. Mutti DO, Mitchell GL, Moeschberger ML et al. Parental myopia, near work, school achievement, and children's refractive error. Invest Ophthalmol Vis Sci 2002; **43**: (12): 3633-3640
99. Young FA, Leary GA, Baldwin WR et al. The transmission of refractive errors within eskimo families. Am J Optom Arch Am Acad Optom 1969; **46**: (9): 676-685
100. Garner LF, Owens H, Kinnear RF et al. Prevalence of myopia in Sherpa and Tibetan children in Nepal. Optom Vis Sci 1999; **76**: (5): 282-285
101. Morgan RW, Munro M. Refractive problems in Northern natives. Can J Ophthalmol 1973; **8**: (2): 226-228
102. Morgan RW, Speakman JS, Grimshaw SE. Inuit myopia: an environmentally induced "epidemic"? Can Med Assoc J 1975; **112**: (5): 575-577
103. Wensor M, McCarty CA, Taylor HR. Prevalence and risk factors of myopia in Victoria, Australia. Arch Ophthalmol 1999; **117**: (5): 658-663
104. Au Eong KG, Tay TH, Lim MK. Education and myopia in 110,236 young Singaporean males. Singapore Med J 1993; **34**: (6): 489-492
105. Paritsis N, Sarafidou E, Koliopoulos J et al. Epidemiologic research on the role of studying and urban environment in the development of myopia during school-age years. Ann Ophthalmol 1983; **15**: (11): 1061-1065
106. Rosner M, Belkin M. Intelligence, education, and myopia in males. Arch Ophthalmol 1987; **105**: (11): 1508-1511
107. Angle J, Wissmann DA. The epidemiology of myopia. Am J Epidemiol 1980; **111**: (2): 220-228
108. Richler A, Bear JC. Refraction, nearwork and education. A population study in Newfoundland. Acta Ophthalmol (Copenh) 1980; **58**: (3): 468-478
109. Zadnik K, Satariano WA, Mutti DO et al. The effect of parental history of myopia on children's eye size. Jama 1994; **271**: (17): 1323-1327
110. Zylbermann R, Landau D, Berson D. The influence of study habits on myopia in Jewish teenagers. J Pediatr Ophthalmol Strabismus 1993; **30**: (5): 319-322
111. Irving EL, Sivak JG, Callender MG. Refractive plasticity of the developing chick eye. Ophthalmic Physiol Opt 1992; **12**: (4): 448-456
112. Siegwart JT, Jr., Norton TT. Regulation of the mechanical properties of tree shrew sclera by the visual environment. Vision Res 1999; **39**: (2): 387-407
113. Smith EL, 3rd, Hung LF. The role of optical defocus in regulating refractive development in infant monkeys. Vision Res 1999; **39**: (8): 1415-1435

114. Wildsoet C, Wallman J. Choroidal and scleral mechanisms of compensation for spectacle lenses in chicks. Vision Res 1995; **35**: (9): 1175-1194
115. Zhan MZ, Saw SM, Hong RZ et al. Refractive errors in Singapore and Xiamen, China--a comparative study in school children aged 6 to 7 years. Optom Vis Sci 2000; **77**: (6): 302-308
116. Jones LA, Sinnott LT, Mutti DO et al. Parental history of myopia, sports and outdoor activities, and future myopia. Invest Ophthalmol Vis Sci 2007; **48**: (8): 3524-3532
117. Cordain L, Eaton SB, Brand Miller J et al. An evolutionary analysis of the aetiology and pathogenesis of juvenile-onset myopia. Acta Ophthalmol Scand 2002; **80**: (2): 125-135
118. Tang WC, Yap MK, Yip SP. A review of current approaches to identifying human genes involved in myopia. Clin Exp Optom 2008; **91**: (1): 4-22
119. Lander ES, Schork NJ. Genetic dissection of complex traits. Science 1994; **265**: (5181): 2037-2048
120. Dirani M, Chamberlain M, Shekar SN et al. Heritability of refractive error and ocular biometrics: the Genes in Myopia (GEM) twin study. Invest Ophthalmol Vis Sci 2006; **47**: (11): 4756-4761
121. Hammond CJ, Snieder H, Gilbert CE et al. Genes and environment in refractive error: the twin eye study. Invest Ophthalmol Vis Sci 2001; **42**: (6): 1232-1236
122. Hu DN. Twin study on myopia. Chin Med J (Engl) 1981; **94**: (1): 51-55
123. Lin LL, Chen CJ. A twin study on myopia in Chinese school children. Acta Ophthalmol Suppl 1988; **185**: 51-53
124. Teikari JM. Myopia and stature. Acta Ophthalmol (Copenh) 1987; **65**: (6): 673-676
125. Feingold J. [Multifactorial diseases: a nightmare for the geneticist]. Med Sci (Paris) 2005; **21**: (11): 927-933
126. Alsbirk PH. Anterior chamber of the eye. A genetic and anthropological study in Greenland Eskimos. Hum Hered 1975; **25**: (5): 418-427
127. Alsbirk PH. Variation and heritability of ocular dimensions. A population study among adult Greenland Eskimos. Acta Ophthalmol (Copenh) 1977; **55**: (3): 443-456
128. Alsbirk PH. Refraction in adult West Greenland Eskimos. A population study of spherical refractive errors, including oculometric and familial correlations. Acta Ophthalmol (Copenh) 1979; **57**: (1): 84-95
129. Biino G, Palmas MA, Corona C et al. Ocular refraction: heritability and genome-wide search for eye morphometry traits in an isolated Sardinian population. Hum Genet 2005; **116**: (3): 152-159
130. Chen CY, Scurrah KJ, Stankovich J et al. Heritability and shared environment estimates for myopia and associated ocular biometric traits: the Genes in Myopia (GEM) family study. Hum Genet 2007; **121**: (3-4): 511-520
131. Pacella R, McLellan J, Grice K et al. Role of genetic factors in the etiology of juvenile-onset myopia based on a longitudinal study of refractive error. Optom Vis Sci 1999; **76**: (6): 381-386
132. Goldschmidt E. [On the etiology of myopia. An epidemiological study]. Acta Ophthalmol (Copenh) 1968; Suppl 98:91+
133. Goss DA, Hampton MJ, Wickham MG. Selected review on genetic factors in myopia. J Am Optom Assoc 1988; **59**: (11): 875-884
134. Naiglin L, Clayton J, Gazagne C et al. Familial high myopia: evidence of an autosomal dominant mode of inheritance and genetic heterogeneity. Ann Genet 1999; **42**: (3): 140-146
135. Yang Z, Xiao X, Li S et al. Clinical and linkage study on a consanguineous Chinese family with autosomal recessive high myopia. Mol Vis 2009; **15**: 312-318
136. Farbrother JE, Kirov G, Owen MJ et al. Linkage analysis of the genetic loci for high myopia on 18p, 12q, and 17q in 51 U.K. families. Invest Ophthalmol Vis Sci 2004; **45**: (9): 2879-2885

137. Hammond CJ, Andrew T, Mak YT et al. A susceptibility locus for myopia in the normal population is linked to the PAX6 gene region on chromosome 11: a genomewide scan of dizygotic twins. Am J Hum Genet 2004; **75**: (2): 294-304
138. Klein AP, Duggal P, Lee KE et al. Confirmation of linkage to ocular refraction on chromosome 22q and identification of a novel linkage region on 1q. Arch Ophthalmol 2007; **125**: (1): 80-85
139. Naiglin L, Gazagne C, Dallongeville F et al. A genome wide scan for familial high myopia suggests a novel locus on chromosome 7q36. J Med Genet 2002; **39**: (2): 118-124
140. Nallasamy S, Paluru PC, Devoto M et al. Genetic linkage study of high-grade myopia in a Hutterite population from South Dakota. Mol Vis 2007; **13**: 229-236
141. Paluru P, Ronan SM, Heon E et al. New locus for autosomal dominant high myopia maps to the long arm of chromosome 17. Invest Ophthalmol Vis Sci 2003; **44**: (5): 1830-1836
142. Paluru PC, Nallasamy S, Devoto M et al. Identification of a novel locus on 2q for autosomal dominant high-grade myopia. Invest Ophthalmol Vis Sci 2005; **46**: (7): 2300-2307
143. Schwartz M, Haim M, Skarsholm D. X-linked myopia: Bornholm eye disease. Linkage to DNA markers on the distal part of Xq. Clin Genet 1990; **38**: (4): 281-286
144. Stambolian D, Ciner EB, Reider LC et al. Genome-wide scan for myopia in the Old Order Amish. Am J Ophthalmol 2005; **140**: (3): 469-476
145. Stambolian D, Ibay G, Reider L et al. Genomewide linkage scan for myopia susceptibility loci among Ashkenazi Jewish families shows evidence of linkage on chromosome 22q12. Am J Hum Genet 2004; **75**: (3): 448-459
146. Stambolian D, Ibay G, Reider L et al. Genome-wide scan of additional Jewish families confirms linkage of a myopia susceptibility locus to chromosome 22q12. Mol Vis 2006; **12**: 1499-1505
147. Wojciechowski R, Moy C, Ciner E et al. Genomewide scan in Ashkenazi Jewish families demonstrates evidence of linkage of ocular refraction to a QTL on chromosome 1p36. Hum Genet 2006; **119**: (4): 389-399
148. Young TL, Ronan SM, Alvear AB et al. A second locus for familial high myopia maps to chromosome 12q. Am J Hum Genet 1998; **63**: (5): 1419-1424
149. Zhang Q, Guo X, Xiao X et al. A new locus for autosomal dominant high myopia maps to 4q22-q27 between D4S1578 and D4S1612. Mol Vis 2005; **11**: 554-560
150. Zhang Q, Guo X, Xiao X et al. Novel locus for X linked recessive high myopia maps to Xq23-q25 but outside MYP1. J Med Genet 2006; **43**: (5): e20
151. Zhang Q, Li S, Xiao X et al. Confirmation of a genetic locus for X-linked recessive high myopia outside MYP1. J Hum Genet 2007; **52**: (5): 469-472
152. Lam DS, Tam PO, Fan DS et al. Familial high myopia linkage to chromosome 18p. Ophthalmologica 2003; **217**: (2): 115-118
153. LaFramboise T. Single nucleotide polymorphism arrays: a decade of biological, computational and technological advances. Nucleic Acids Res 2009; **37**: (13): 4181-4193
154. A haplotype map of the human genome. Nature 2005; **437**: (7063): 1299-1320
155. Carlson CS, Eberle MA, Kruglyak L et al. Mapping complex disease loci in whole-genome association studies. Nature 2004; **429**: (6990): 446-452
156. Feuk L, Carson AR, Scherer SW. Structural variation in the human genome. Nat Rev Genet 2006; **7**: (2): 85-97
157. Abu Bakar S, Hollox EJ, Armour JA. Allelic recombination between distinct genomic locations generates copy number diversity in human beta-defensins. Proc Natl Acad Sci U S A 2009; **106**: (3): 853-858
158. Redon R, Ishikawa S, Fitch KR et al. Global variation in copy number in the human genome. Nature 2006; **444**: (7118): 444-454
159. Lupski JR, Stankiewicz P. Genomic disorders: molecular mechanisms for rearrangements and conveyed phenotypes. PLoS Genet 2005; **1**: (6): e49

160. Iafrate AJ, Feuk L, Rivera MN et al. Detection of large-scale variation in the human genome. Nat Genet 2004; **36**: (9): 949-951
161. Sebat J, Lakshmi B, Troge J et al. Large-scale copy number polymorphism in the human genome. Science 2004; **305**: (5683): 525-528
162. Paget S, Julia S, Vitezica ZG et al. Linkage analysis of high myopia susceptibility locus in 26 families. Mol Vis 2008; **14**: 2566-2574
163. Young TL, Ronan SM, Drahozal LA et al. Evidence that a locus for familial high myopia maps to chromosome 18p. Am J Hum Genet 1998; **63**: (1): 109-119
164. Risch N, Merikangas K. The future of genetic studies of complex human diseases. Science 1996; **273**: (5281): 1516-1517
165. Spielman RS, Ewens WJ. The TDT and other family-based tests for linkage disequilibrium and association. Am J Hum Genet 1996; **59**: (5): 983-989
166. Hattersley AT, McCarthy MI. What makes a good genetic association study? Lancet 2005; **366**: (9493): 1315-1323
167. Lin HJ, Wan L, Tsai Y et al. The TGFbeta1 gene codon 10 polymorphism contributes to the genetic predisposition to high myopia. Mol Vis 2006; **12**: 698-703
168. Wang IJ, Chiang TH, Shih YF et al. The association of single nucleotide polymorphisms in the 5'-regulatory region of the lumican gene with susceptibility to high myopia in Taiwan. Mol Vis 2006; **12**: 852-857
169. Hasumi Y, Inoko H, Mano S et al. Analysis of single nucleotide polymorphisms at 13 loci within the transforming growth factor-induced factor gene shows no association with high myopia in Japanese subjects. Immunogenetics 2006; **58**: (12): 947-953
170. Heath S, Robledo R, Beggs W et al. A novel approach to search for identity by descent in small samples of patients and controls from the same mendelian breeding unit: a pilot study on myopia. Hum Hered 2001; **52**: (4): 183-190
171. Lam DS, Lee WS, Leung YF et al. TGFbeta-induced factor: a candidate gene for high myopia. Invest Ophthalmol Vis Sci 2003; **44**: (3): 1012-1015
172. Liang CL, Hung KS, Tsai YY et al. Systematic assessment of the tagging polymorphisms of the COL1A1 gene for high myopia. J Hum Genet 2007; **52**: (4): 374-377
173. Young TL, Atwood LD, Ronan SM et al. Further refinement of the MYP2 locus for autosomal dominant high myopia by linkage disequilibrium analysis. Ophthalmic Genet 2001; **22**: (2): 69-75
174. Schache M, Chen CY, Pertile KK et al. Fine mapping linkage analysis identifies a novel susceptibility locus for myopia on chromosome 2q37 adjacent to but not overlapping MYP12. Mol Vis 2009; **15**: 722-730
175. Wang P, Li S, Xiao X et al. High myopia is not associated with the SNPs in the TGIF, lumican, TGFB1, and HGF genes. Invest Ophthalmol Vis Sci 2009; **50**: (4): 1546-1551
176. Ma JH, Shen SH, Zhang GW et al. Identification of a locus for autosomal dominant high myopia on chromosome 5p13.3-p15.1 in a Chinese family. Mol Vis 2010; **16**: 2043-2054
177. Hysi PG, Young TL, Mackey DA et al. A genome-wide association study for myopia and refractive error identifies a susceptibility locus at 15q25. Nat Genet 2010; **42**: (10): 902-905
178. Solouki AM, Verhoeven VJ, van Duijn CM et al. A genome-wide association study identifies a susceptibility locus for refractive errors and myopia at 15q14. Nat Genet 2010; **42**: (10): 897-901
179. Li YJ, Goh L, Khor CC et al. Genome-Wide Association Studies Reveal Genetic Variants in CTNND2 for High Myopia in Singapore Chinese. Ophthalmology 2011; **118**: (2): 368-375
180. Genome-wide association study of 14,000 cases of seven common diseases and 3,000 shared controls. Nature 2007; **447**: (7145): 661-678
181. Weedon MN, Lango H, Lindgren CM et al. Genome-wide association analysis identifies 20 loci that influence adult height. Nat Genet 2008; **40**: (5): 575-583

182. Zippel R, Gnesutta N, Matus-Leibovitch N et al. Ras-GRF, the activator of Ras, is expressed preferentially in mature neurons of the central nervous system. Brain Res Mol Brain Res 1997; **48**: (1): 140-144
183. Nakanishi H, Yamada R, Gotoh N et al. A genome-wide association analysis identified a novel susceptible locus for pathological myopia at 11q24.1. PLoS Genet 2009; **5**: (9): e1000660
184. Jacobi FK, Pusch CM. A decade in search of myopia genes. Front Biosci 2010; **15**: 359-372
185. Lam CY, Tam PO, Fan DS et al. A genome-wide scan maps a novel high myopia locus to 5p15. Invest Ophthalmol Vis Sci 2008; **49**: (9): 3768-3778
186. Guo X, Xiao X, Li S et al. Nonsyndromic high myopia in a Chinese family mapped to MYP1: linkage confirmation and phenotypic characterization. Arch Ophthalmol 2010; **128**: (11): 1473-1479
187. Chen CY, Stankovich J, Scurrah KJ et al. Linkage Replication of the MYP12 Locus in Common Myopia. Invest Ophthalmol Vis Sci 2007; **48**: (10): 4433-4439
188. Tang WC, Yip SP, Lo KK et al. Linkage and association of myocilin (MYOC) polymorphisms with high myopia in a Chinese population. Mol Vis 2007; **13**: 534-544
189. Fingert JH, Ying L, Swiderski RE et al. Characterization and comparison of the human and mouse GLC1A glaucoma genes. Genome Res 1998; **8**: (4): 377-384
190. Michels-Rautenstrauss KG, Mardin CY, Budde WM et al. Juvenile open angle glaucoma: fine mapping of the TIGR gene to 1q24.3-q25.2 and mutation analysis. Hum Genet 1998; **102**: (1): 103-106
191. Nguyen TD, Chen P, Huang WD et al. Gene structure and properties of TIGR, an olfactomedin-related glycoprotein cloned from glucocorticoid-induced trabecular meshwork cells. J Biol Chem 1998; **273**: (11): 6341-6350
192. Jhamandas JH, Simonin F, Bourguignon JJ et al. Neuropeptide FF and neuropeptide VF inhibit GABAergic neurotransmission in parvocellular neurons of the rat hypothalamic paraventricular nucleus. Am J Physiol Regul Integr Comp Physiol 2007; **292**: (5): R1872-1880
193. Schulz HL, Stoehr H, White K et al. Genomic structure and assessment of the retinally expressed RFamide-related peptide gene in dominant cystoid macular dystrophy. Mol Vis 2002; **8**: 67-71
194. Paget S, Vitezica ZG, Malecaze F et al. Heritability of refractive value and ocular biometrics. Exp Eye Res 2008; **86**: (2): 290-295
195. Metlapally R, Li YJ, Tran-Viet KN et al. COL1A1 and COL2A1 genes and myopia susceptibility: evidence of association and suggestive linkage to the COL2A1 locus. Invest Ophthalmol Vis Sci 2009; **50**: (9): 4080-4086
196. Ciner E, Ibay G, Wojciechowski R et al. Genome-wide scan of African-American and white families for linkage to myopia. Am J Ophthalmol 2009; **147**: (3): 512-517 e512
197. Klein AP, Suktitipat B, Duggal P et al. Heritability analysis of spherical equivalent, axial length, corneal curvature, and anterior chamber depth in the Beaver Dam Eye Study. Arch Ophthalmol 2009; **127**: (5): 649-655
198. Tsai MY, Lin LL, Lee V et al. Estimation of heritability in myopic twin studies. Jpn J Ophthalmol 2009; **53**: (6): 615-622
199. He M, Hur YM, Zhang J et al. Shared genetic determinant of axial length, anterior chamber depth, and angle opening distance: the Guangzhou Twin Eye Study. Invest Ophthalmol Vis Sci 2008; **49**: (11): 4790-4794
200. Lopes MC, Andrew T, Carbonaro F et al. Estimating heritability and shared environmental effects for refractive error in twin and family studies. Invest Ophthalmol Vis Sci 2009; **50**: (1): 126-131
201. Dirani M, Shekar SN, Baird PN. Evidence of shared genes in refraction and axial length: the Genes in Myopia (GEM) twin study. Invest Ophthalmol Vis Sci 2008; **49**: (10): 4336-4339

202. Dirani M, Chan YH, Gazzard G et al. Prevalence of refractive error in Singaporean Chinese children: the strabismus, amblyopia, and refractive error in young Singaporean Children (STARS) study. Invest Ophthalmol Vis Sci 2010; **51**: (3): 1348-1355
203. Yap M, Wu M, Liu ZM et al. Role of heredity in the genesis of myopia. Ophthalmic Physiol Opt 1993; **13**: (3): 316-319
204. Zadnik K, Mutti DO. Myopia--a challenge to optometric research. J Am Optom Assoc 1995; **66**: (3): 145-146
205. Meng W, Butterworth J, Malecaze F et al. Axial length: an underestimated endophenotype of myopia. Med Hypotheses 2010; **74**: (2): 252-253
206. McCarthy MI, Abecasis GR, Cardon LR et al. Genome-wide association studies for complex traits: consensus, uncertainty and challenges. Nat Rev Genet 2008; **9**: (5): 356-369
207. Price AL, Patterson NJ, Plenge RM et al. Principal components analysis corrects for stratification in genome-wide association studies. Nat Genet 2006; **38**: (8): 904-909
208. Voight BF, Pritchard JK. Confounding from cryptic relatedness in case-control association studies. PLoS Genet 2005; **1**: (3): e32
209. Jakobsson M, Scholz SW, Scheet P et al. Genotype, haplotype and copy-number variation in worldwide human populations. Nature 2008; **451**: (7181): 998-1003
210. Lao O, Lu TT, Nothnagel M et al. Correlation between genetic and geographic structure in Europe. Curr Biol 2008; **18**: (16): 1241-1248
211. Li JZ, Absher DM, Tang H et al. Worldwide human relationships inferred from genome-wide patterns of variation. Science 2008; **319**: (5866): 1100-1104
212. Moskvina V, Smith M, Ivanov D et al. Genetic Differences between Five European Populations. Hum Hered 2010; **70**: (2): 141-149
213. Novembre J, Johnson T, Bryc K et al. Genes mirror geography within Europe. Nature 2008; **456**: (7218): 98-101
214. Rosenberg NA, Mahajan S, Ramachandran S et al. Clines, clusters, and the effect of study design on the inference of human population structure. PLoS Genet 2005; **1**: (6): e70
215. Seldin MF, Shigeta R, Villoslada P et al. European population substructure: clustering of northern and southern populations. PLoS Genet 2006; **2**: (9): e143
216. Rosenberg NA, Pritchard JK, Weber JL et al. Genetic structure of human populations. Science 2002; **298**: (5602): 2381-2385
217. Roberson ED, Pevsner J. Visualization of shared genomic regions and meiotic recombination in high-density SNP data. PLoS One 2009; **4**: (8): e6711
218. Li Q, Yu K. Improved correction for population stratification in genome-wide association studies by identifying hidden population structures. Genet Epidemiol 2008; **32**: (3): 215-226
219. Purcell S, Cherny SS, Sham PC. Genetic Power Calculator: design of linkage and association genetic mapping studies of complex traits. Bioinformatics 2003; **19**: (1): 149-150
220. Ding K, Kullo IJ. Genome-wide association studies for atherosclerotic vascular disease and its risk factors. Circ Cardiovasc Genet 2009; **2**: (1): 63-72
221. Amin N, van Duijn CM, Janssens AC. Genetic scoring analysis: a way forward in genome wide association studies? Eur J Epidemiol 2009; **24**: (10): 585-587
222. Colhoun HM, McKeigue PM, Davey Smith G. Problems of reporting genetic associations with complex outcomes. Lancet 2003; **361**: (9360): 865-872
223. Gateva V, Sandling JK, Hom G et al. A large-scale replication study identifies TNIP1, PRDM1, JAZF1, UHRF1BP1 and IL10 as risk loci for systemic lupus erythematosus. Nat Genet 2009; **41**: (11): 1228-1233
224. Todd JA. Statistical false positive or true disease pathway? Nat Genet 2006; **38**: (7): 731-733
225. Lenth RV. Statistical power calculations. J Anim Sci 2007; **85**: (13 Suppl): E24-29
226. Skol AD, Scott LJ, Abecasis GR et al. Joint analysis is more efficient than replication-based analysis for two-stage genome-wide association studies. Nat Genet 2006; **38**: (2): 209-213

227. Satagopan JM, Venkatraman ES, Begg CB. Two-stage designs for gene-disease association studies with sample size constraints. Biometrics 2004; **60**: (3): 589-597
228. Satagopan JM, Verbel DA, Venkatraman ES et al. Two-stage designs for gene-disease association studies. Biometrics 2002; **58**: (1): 163-170
229. Thomas D, Xie R, Gebregziabher M. Two-Stage sampling designs for gene association studies. Genet Epidemiol 2004; **27**: (4): 401-414
230. Thomas DC, Casey G, Conti DV et al. Methodological Issues in Multistage Genome-wide Association Studies. Stat Sci 2009; **24**: (4): 414-429
231. Hirschhorn JN, Daly MJ. Genome-wide association studies for common diseases and complex traits. Nat Rev Genet 2005; **6**: (2): 95-108
232. Altshuler D, Hirschhorn JN, Klannemark M et al. The common PPARgamma Pro12Ala polymorphism is associated with decreased risk of type 2 diabetes. Nat Genet 2000; **26**: (1): 76-80
233. Lowe CE, Cooper JD, Chapman JM et al. Cost-effective analysis of candidate genes using htSNPs: a staged approach. Genes Immun 2004; **5**: (4): 301-305
234. van den Oord EJ, Sullivan PF. False discoveries and models for gene discovery. Trends Genet 2003; **19**: (10): 537-542
235. Craig DW, Pearson JV, Szelinger S et al. Identification of genetic variants using bar-coded multiplexed sequencing. Nat Methods 2008; **5**: (10): 887-893
236. Zayats T, Young TL, Mackey DA et al. Quality of DNA extracted from mouthwashes. PLoS One 2009; **4**: (7): e6165
237. Weirich-Schwaiger H, Weirich HG, Gruber B et al. Correlation between senescence and DNA repair in cells from young and old individuals and in premature aging syndromes. Mutat Res 1994; **316**: (1): 37-48
238. Hardy GH. Mendelian Proportions in a Mixed Population. Science 1908; **28**: (706): 49-50
239. Hosking L, Lumsden S, Lewis K et al. Detection of genotyping errors by Hardy-Weinberg equilibrium testing. Eur J Hum Genet 2004; **12**: (5): 395-399
240. Ashburner M, Ball CA, Blake JA et al. Gene ontology: tool for the unification of biology. The Gene Ontology Consortium. Nat Genet 2000; **25**: (1): 25-29
241. Rual JF, Venkatesan K, Hao T et al. Towards a proteome-scale map of the human protein-protein interaction network. Nature 2005; **437**: (7062): 1173-1178
242. Solomon KD, Fernandez de Castro LE, Sandoval HP et al. LASIK world literature review: quality of life and patient satisfaction. Ophthalmology 2009; **116**: (4): 691-701
243. Dupps WJ, Jr., Wilson SE. Biomechanics and wound healing in the cornea. Exp Eye Res 2006; **83**: (4): 709-720
244. Kapadia MS, Wilson SE. One-year results of PRK in low and moderate myopia: fewer than 0.5% of eyes lose two or more lines of vision. Cornea 2000; **19**: (2): 180-184
245. Stojanovic A, Ringvold A, Nitter T. Ascorbate prophylaxis for corneal haze after photorefractive keratectomy. J Refract Surg 2003; **19**: (3): 338-343
246. Wilson SE. Analysis of the keratocyte apoptosis, keratocyte proliferation, and myofibroblast transformation responses after photorefractive keratectomy and laser in situ keratomileusis. Trans Am Ophthalmol Soc 2002; **100**: 411-433
247. Ehlers N, Hjortdal J. Corneal thickness: measurement and implications. Exp Eye Res 2004; **78**: (3): 543-548
248. Nishida T. [The cornea: stasis and dynamics]. Nippon Ganka Gakkai Zasshi 2008; **112**: (3): 179-212; discussion 213
249. Land MF. Visual optics: The sandlance eye breaks all the rules. Curr Biol 1999; **9**: (8): R286-288
250. Muller LJ, Marfurt CF, Kruse F et al. Corneal nerves: structure, contents and function. Exp Eye Res 2003; **76**: (5): 521-542

251. Hamrah P, Dana MR. Corneal antigen-presenting cells. Chem Immunol Allergy 2007; **92**: 58-70
252. Streilein JW. Ocular immune privilege: therapeutic opportunities from an experiment of nature. Nat Rev Immunol 2003; **3**: (11): 879-889
253. Maurice DM. The structure and transparency of the cornea. J Physiol 1957; **136**: (2): 263-286
254. Fabiani C, Barabino S, Rashid S et al. Corneal epithelial proliferation and thickness in a mouse model of dry eye. Exp Eye Res 2009; **89**: (2): 166-171
255. Ehlers N, Heegaard S, Hjortdal J et al. Morphological evaluation of normal human corneal epithelium. Acta Ophthalmol 2009;
256. Goldman JN, Benedek GB. The relationship between morphology and transparency in the nonswelling corneal stroma of the shark. Invest Ophthalmol 1967; **6**: (6): 574-600
257. Birk DE, Fitch JM, Linsenmayer TF. Organization of collagen types I and V in the embryonic chicken cornea. Invest Ophthalmol Vis Sci 1986; **27**: (10): 1470-1477
258. Fini ME, Stramer BM. How the cornea heals: cornea-specific repair mechanisms affecting surgical outcomes. Cornea 2005; **24**: (8 Suppl): S2-S11
259. Funderburgh JL, *Corneal proteoglycans*. Proteoglycans: Structure, Biology, and Molecular Interactions, ed. I. R. 2000, New York: Marcel Dekker, Inc. 237–273.
260. Funderburgh JL, Mann MM, Funderburgh ML. Keratocyte phenotype mediates proteoglycan structure: a role for fibroblasts in corneal fibrosis. J Biol Chem 2003; **278**: (46): 45629-45637
261. He J, Bazan NG, Bazan HE. Mapping the entire human corneal nerve architecture. Exp Eye Res **91**: (4): 513-523
262. Hay ED. Development of the vertebrate cornea. Int Rev Cytol 1979; **63**: 263-322
263. Scott JE, Bosworth TR. A comparative biochemical and ultrastructural study of proteoglycan-collagen interactions in corneal stroma. Functional and metabolic implications. Biochem J 1990; **270**: (2): 491-497
264. Paulsson M. Basement membrane proteins: structure, assembly, and cellular interactions. Crit Rev Biochem Mol Biol 1992; **27**: (1-2): 93-127
265. Wilson SE, Hong JW. Bowman's layer structure and function: critical or dispensable to corneal function? A hypothesis. Cornea 2000; **19**: (4): 417-420
266. Hayashi S, Osawa T, Tohyama K. Comparative observations on corneas, with special reference to Bowman's layer and Descemet's membrane in mammals and amphibians. J Morphol 2002; **254**: (3): 247-258
267. Kafarnik C, Murphy CJ, Dubielzig RR. Canine duplication of Descemet's membrane. Vet Pathol 2009; **46**: (3): 464-473
268. Nakayasu K, Tanaka M, Konomi H et al. Distribution of types I, II, III, IV and V collagen in normal and keratoconus corneas. Ophthalmic Res 1986; **18**: (1): 1-10
269. Muller LJ, Pels L, Vrensen GF. Novel aspects of the ultrastructural organization of human corneal keratocytes. Invest Ophthalmol Vis Sci 1995; **36**: (13): 2557-2567
270. Moller-Pedersen T, Ledet T, Ehlers N. The keratocyte density of human donor corneas. Curr Eye Res 1994; **13**: (2): 163-169
271. Beales MP, Funderburgh JL, Jester JV et al. Proteoglycan synthesis by bovine keratocytes and corneal fibroblasts: maintenance of the keratocyte phenotype in culture. Invest Ophthalmol Vis Sci 1999; **40**: (8): 1658-1663
272. Jester JV, Moller-Pedersen T, Huang J et al. The cellular basis of corneal transparency: evidence for 'corneal crystallins'. J Cell Sci 1999; **112 ( Pt 5)**: 613-622
273. King G, Holmes R. Human ocular aldehyde dehydrogenase isozymes: distribution and properties as major soluble proteins in cornea and lens. J Exp Zool 1998; **282**: (1-2): 12-17
274. Jester JV, Budge A, Fisher S et al. Corneal keratocytes: phenotypic and species differences in abundant protein expression and in vitro light-scattering. Invest Ophthalmol Vis Sci 2005; **46**: (7): 2369-2378

275. Jalbert I, Stapleton F, Papas E et al. In vivo confocal microscopy of the human cornea. Br J Ophthalmol 2003; **87**: (2): 225-236
276. Fitch JM, Mentzer A, Mayne R et al. Acquisition of type IX collagen by the developing avian primary corneal stroma and vitreous. Dev Biol 1988; **128**: (2): 396-405
277. Hendrix MJ, Hay ED, von der Mark K et al. Immunohistochemical localization of collagen types I and II in the developing chick cornea and tibia by electron microscopy. Invest Ophthalmol Vis Sci 1982; **22**: (3): 359-375
278. Creuzet S, Vincent C, Couly G. Neural crest derivatives in ocular and periocular structures. Int J Dev Biol 2005; **49**: (2-3): 161-171
279. Tripathi BJ, Tripathi RC, Livingston AM et al. The role of growth factors in the embryogenesis and differentiation of the eye. Am J Anat 1991; **192**: (4): 442-471
280. Azuma N, Hirakata A, Hida T et al. Histochemical and immunohistochemical studies on keratan sulfate in the anterior segment of the developing human eye. Exp Eye Res 1994; **58**: (3): 277-286
281. Funderburgh JL, Caterson B, Conrad GW. Keratan sulfate proteoglycan during embryonic development of the chicken cornea. Dev Biol 1986; **116**: (2): 267-277
282. Hart GW. Biosynthesis of glycosaminolgycans during corneal development. J Biol Chem 1976; **251**: (21): 6513-6521
283. Linsenmayer TF, Fitch JM, Schmid TM et al. Monoclonal antibodies against chicken type V collagen: production, specificity, and use for immunocytochemical localization in embryonic cornea and other organs. J Cell Biol 1983; **96**: (1): 124-132
284. Lwigale PY, Cressy PA, Bronner-Fraser M. Corneal keratocytes retain neural crest progenitor cell properties. Dev Biol 2005; **288**: (1): 284-293
285. Zieske JD. Corneal development associated with eyelid opening. Int J Dev Biol 2004; **48**: (8-9): 903-911
286. Cintron C, Covington H, Kublin CL. Morphogenesis of rabbit corneal stroma. Invest Ophthalmol Vis Sci 1983; **24**: (5): 543-556
287. Graw J. The genetic and molecular basis of congenital eye defects. Nat Rev Genet 2003; **4**: (11): 876-888
288. Alison MR, Poulsom R, Forbes S et al. An introduction to stem cells. J Pathol 2002; **197**: (4): 419-423
289. Parker GC, Anastassova-Kristeva M, Broxmeyer HE et al. Stem cells: shibboleths of development. Stem Cells Dev 2004; **13**: (6): 579-584
290. Cotsarelis G, Cheng SZ, Dong G et al. Existence of slow-cycling limbal epithelial basal cells that can be preferentially stimulated to proliferate: implications on epithelial stem cells. Cell 1989; **57**: (2): 201-209
291. Majo F, Rochat A, Nicolas M et al. Oligopotent stem cells are distributed throughout the mammalian ocular surface. Nature 2008; **456**: (7219): 250-254
292. Schermer A, Galvin S, Sun TT. Differentiation-related expression of a major 64K corneal keratin in vivo and in culture suggests limbal location of corneal epithelial stem cells. J Cell Biol 1986; **103**: (1): 49-62
293. Goldberg MF, Bron AJ. Limbal palisades of Vogt. Trans Am Ophthalmol Soc 1982; **80**: 155-171
294. Chee KY, Kicic A, Wiffen SJ. Limbal stem cells: the search for a marker. Clin Experiment Ophthalmol 2006; **34**: (1): 64-73
295. Chen Z, de Paiva CS, Luo L et al. Characterization of putative stem cell phenotype in human limbal epithelia. Stem Cells 2004; **22**: (3): 355-366
296. Townsend WM. The limbal palisades of Vogt. Trans Am Ophthalmol Soc 1991; **89**: 721-756
297. Dua HS, Shanmuganathan VA, Powell-Richards AO et al. Limbal epithelial crypts: a novel anatomical structure and a putative limbal stem cell niche. Br J Ophthalmol 2005; **89**: (5): 529-532

298. Shanmuganathan VA, Foster T, Kulkarni BB et al. Morphological characteristics of the limbal epithelial crypt. Br J Ophthalmol 2007; **91**: (4): 514-519
299. Boulton M, Albon J. Stem cells in the eye. Int J Biochem Cell Biol 2004; **36**: (4): 643-657
300. Dua HS, Azuara-Blanco A. Limbal stem cells of the corneal epithelium. Surv Ophthalmol 2000; **44**: (5): 415-425
301. Romano AC, Espana EM, Yoo SH et al. Different cell sizes in human limbal and central corneal basal epithelia measured by confocal microscopy and flow cytometry. Invest Ophthalmol Vis Sci 2003; **44**: (12): 5125-5129
302. Thoft RA, Friend J. The X, Y, Z hypothesis of corneal epithelial maintenance. Invest Ophthalmol Vis Sci 1983; **24**: (10): 1442-1443
303. Chang CY, Green CR, McGhee CN et al. Acute wound healing in the human central corneal epithelium appears to be independent of limbal stem cell influence. Invest Ophthalmol Vis Sci 2008; **49**: (12): 5279-5286
304. Takacs L, Toth E, Berta A et al. Stem cells of the adult cornea: from cytometric markers to therapeutic applications. Cytometry A 2009; **75**: (1): 54-66
305. Davies SB, Di Girolamo N. Corneal stem cells and their origins: significance in developmental biology. Stem Cells Dev **19**: (11): 1651-1662
306. Wagner W, Wein F, Seckinger A et al. Comparative characteristics of mesenchymal stem cells from human bone marrow, adipose tissue, and umbilical cord blood. Exp Hematol 2005; **33**: (11): 1402-1416
307. Kobayashi I, Ono H, Moritomo T et al. Comparative gene expression analysis of zebrafish and mammals identifies common regulators in hematopoietic stem cells. Blood **115**: (2): e1-9
308. Engelmann K, Bohnke M, Friedl P. Isolation and long-term cultivation of human corneal endothelial cells. Invest Ophthalmol Vis Sci 1988; **29**: (11): 1656-1662
309. Davison PF, Galbavy EJ. Connective tissue remodeling in corneal and scleral wounds. Invest Ophthalmol Vis Sci 1986; **27**: (10): 1478-1484
310. Ihanamaki T, Pelliniemi LJ, Vuorio E. Collagens and collagen-related matrix components in the human and mouse eye. Prog Retin Eye Res 2004; **23**: (4): 403-434
311. Fini ME. Keratocyte and fibroblast phenotypes in the repairing cornea. Prog Retin Eye Res 1999; **18**: (4): 529-551
312. Dua HS, Gomes JA, Singh A. Corneal epithelial wound healing. Br J Ophthalmol 1994; **78**: (5): 401-408
313. Wagoner MD. Chemical injuries of the eye: current concepts in pathophysiology and therapy. Surv Ophthalmol 1997; **41**: (4): 275-313
314. Crosson CE, Klyce SD, Beuerman RW. Epithelial wound closure in the rabbit cornea. A biphasic process. Invest Ophthalmol Vis Sci 1986; **27**: (4): 464-473
315. Maudgal P, Missotten L, *Monographs in ophthalmology 1*. Superficial keratitis. 1980, The Hague: Dr W Junk Publishers.
316. Pfister RR. The healing of corneal epithelial abrasions in the rabbit: a scanning electron microscope study. Invest Ophthalmol 1975; **14**: (9): 648-661
317. Robb RM, Kuwabara T. Corneal wound healing. I. The movement of polymorphonuclear leukocytes into corneal wounds. Arch Ophthalmol 1962; **68**: 636-642
318. Anderson RA. Actin filaments in normal and migrating corneal epithelial cells. Invest Ophthalmol Vis Sci 1977; **16**: (2): 161-166
319. Soong HK, Cintron C. Disparate effects of calmodulin inhibitors on corneal epithelial migration in rabbit and rat. Ophthalmic Res 1985; **17**: (1): 27-33
320. Ratkay-Traub I, Hopp B, Bor Z et al. Regeneration of rabbit cornea following excimer laser photorefractive keratectomy: a study on gap junctions, epithelial junctions and epidermal growth factor receptor expression in correlation with cell proliferation. Exp Eye Res 2001; **73**: (3): 291-302

321. Nagai N, Murao T, Ito Y et al. Enhancing effects of sericin on corneal wound healing in rat debrided corneal epithelium. Biol Pharm Bull 2009; **32**: (5): 933-936
322. Wilson SE, Netto M, Ambrosio R, Jr. Corneal cells: chatty in development, homeostasis, wound healing, and disease. Am J Ophthalmol 2003; **136**: (3): 530-536
323. Wilson SE, Mohan RR, Mohan RR et al. The corneal wound healing response: cytokine-mediated interaction of the epithelium, stroma, and inflammatory cells. Prog Retin Eye Res 2001; **20**: (5): 625-637
324. Weng J, Mohan RR, Li Q et al. IL-1 upregulates keratinocyte growth factor and hepatocyte growth factor mRNA and protein production by cultured stromal fibroblast cells: interleukin-1 beta expression in the cornea. Cornea 1997; **16**: (4): 465-471
325. Wilson SE, He YG, Weng J et al. Effect of epidermal growth factor, hepatocyte growth factor, and keratinocyte growth factor, on proliferation, motility and differentiation of human corneal epithelial cells. Exp Eye Res 1994; **59**: (6): 665-678
326. Tuominen IS, Tervo TM, Teppo AM et al. Human tear fluid PDGF-BB, TNF-alpha and TGF-beta1 vs corneal haze and regeneration of corneal epithelium and subbasal nerve plexus after PRK. Exp Eye Res 2001; **72**: (6): 631-641
327. Wilson SE, Liu JJ, Mohan RR. Stromal-epithelial interactions in the cornea. Prog Retin Eye Res 1999; **18**: (3): 293-309
328. Kitano S, Goldman JN. Cytologic and histochemical changes in corneal wound repair. Arch Ophthalmol 1966; **76**: (3): 345-354
329. Matsuda H, Smelser GK. Electron microscopy of corneal wound healing. Exp Eye Res 1973; **16**: (6): 427-442
330. Weimar V, *Healing processes in the cornea*. The Transparency of the Cornea, ed. S.P. Duke-Elder, E.S. 1960, Oxford: 111Blackwell Scienti®c Publications.
331. Wilson SE. Everett Kinsey Lecture. Keratocyte apoptosis in refractive surgery. Clao J 1998; **24**: (3): 181-185
332. Wilson SE, He YG, Weng J et al. Epithelial injury induces keratocyte apoptosis: hypothesized role for the interleukin-1 system in the modulation of corneal tissue organization and wound healing. Exp Eye Res 1996; **62**: (4): 325-327
333. West-Mays JA, Dwivedi DJ. The keratocyte: corneal stromal cell with variable repair phenotypes. Int J Biochem Cell Biol 2006; **38**: (10): 1625-1631
334. Gao J, Gelber-Schwalb TA, Addeo JV et al. Apoptosis in the rabbit cornea after photorefractive keratectomy. Cornea 1997; **16**: (2): 200-208
335. Mohan RR, Mohan RR, Wilson SE. Discoidin domain receptor (DDR) 1 and 2: collagen-activated tyrosine kinase receptors in the cornea. Exp Eye Res 2001; **72**: (1): 87-92
336. Fink SL, Cookson BT. Apoptosis, pyroptosis, and necrosis: mechanistic description of dead and dying eukaryotic cells. Infect Immun 2005; **73**: (4): 1907-1916
337. Jester JV, Petroll WM, Cavanagh HD. Corneal stromal wound healing in refractive surgery: the role of myofibroblasts. Prog Retin Eye Res 1999; **18**: (3): 311-356
338. Welch MP, Odland GF, Clark RA. Temporal relationships of F-actin bundle formation, collagen and fibronectin matrix assembly, and fibronectin receptor expression to wound contraction. J Cell Biol 1990; **110**: (1): 133-145
339. Zieske JD, Guimaraes SR, Hutcheon AE. Kinetics of keratocyte proliferation in response to epithelial debridement. Exp Eye Res 2001; **72**: (1): 33-39
340. Garana RM, Petroll WM, Chen WT et al. Radial keratotomy. II. Role of the myofibroblast in corneal wound contraction. Invest Ophthalmol Vis Sci 1992; **33**: (12): 3271-3282
341. Smelser G, *The Transparency of the Cornea*. Role of the epithelium in incorporation of sulfate in the corneal connective tissue, ed. S.P. Duke-Elder, E.S. 1960, Oxford: 125 Blackwell Scientic Publications.

342. Ross R, Everett NB, Tyler R. Wound healing and collagen formation. VI. The origin of the wound fibroblast studied in parabiosis. J Cell Biol 1970; **44**: (3): 645-654
343. Cintron C, Hong BS, Kublin CL. Quantitative analysis of collagen from normal developing corneas and corneal scars. Curr Eye Res 1981; **1**: (1): 1-8
344. Stramer BM, Zieske JD, Jung JC et al. Molecular mechanisms controlling the fibrotic repair phenotype in cornea: implications for surgical outcomes. Invest Ophthalmol Vis Sci 2003; **44**: (10): 4237-4246
345. Lakshman N, Kim A, Petroll WM. Characterization of corneal keratocyte morphology and mechanical activity within 3-D collagen matrices. Exp Eye Res 2010; **90**: (2): 350-359
346. Azar DT, Hahn TW, Jain S et al. Matrix metalloproteinases are expressed during wound healing after excimer laser keratectomy. Cornea 1996; **15**: (1): 18-24
347. Mulholland B, Tuft SJ, Khaw PT. Matrix metalloproteinase distribution during early corneal wound healing. Eye (Lond) 2005; **19**: (5): 584-588
348. Fini ME, Girard MT, Matsubara M. Collagenolytic/gelatinolytic enzymes in corneal wound healing. Acta Ophthalmol Suppl 1992; (202): 26-33
349. Girard MT, Matsubara M, Kublin C et al. Stromal fibroblasts synthesize collagenase and stromelysin during long-term tissue remodeling. J Cell Sci 1993; **104 ( Pt 4)**: 1001-1011
350. Matsubara M, Girard MT, Kublin CL et al. Differential roles for two gelatinolytic enzymes of the matrix metalloproteinase family in the remodelling cornea. Dev Biol 1991; **147**: (2): 425-439
351. Matsubara M, Zieske JD, Fini ME. Mechanism of basement membrane dissolution preceding corneal ulceration. Invest Ophthalmol Vis Sci 1991; **32**: (13): 3221-3237
352. Cionni RJ, Katakami C, Lavrich JB et al. Collagen metabolism following corneal laceration in rabbits. Curr Eye Res 1986; **5**: (8): 549-558
353. Cintron C, Hassinger LC, Kublin CL et al. Biochemical and ultrastructural changes in collagen during corneal wound healing. J Ultrastruct Res 1978; **65**: (1): 13-22
354. Cintron C, Kublin CL. Regeneration of corneal tissue. Dev Biol 1977; **61**: (2): 346-357
355. Maltseva O, Folger P, Zekaria D et al. Fibroblast growth factor reversal of the corneal myofibroblast phenotype. Invest Ophthalmol Vis Sci 2001; **42**: (11): 2490-2495
356. Jester JV, Petroll WM, Barry PA et al. Expression of alpha-smooth muscle (alpha-SM) actin during corneal stromal wound healing. Invest Ophthalmol Vis Sci 1995; **36**: (5): 809-819
357. Jester JV, Rodrigues MM, Herman IM. Characterization of avascular corneal wound healing fibroblasts. New insights into the myofibroblast. Am J Pathol 1987; **127**: (1): 140-148
358. Netto MV, Mohan RR, Sinha S et al. Stromal haze, myofibroblasts, and surface irregularity after PRK. Exp Eye Res 2006; **82**: (5): 788-797
359. Thomas S, Thomas M, Wincker P et al. Human neural crest cells display molecular and phenotypic hallmarks of stem cells. Hum Mol Genet 2008; **17**: (21): 3411-3425
360. El-Shabrawi Y, Kublin CL, Cintron C. mRNA levels of alpha1(VI) collagen, alpha1(XII) collagen, and beta ig in rabbit cornea during normal development and healing. Invest Ophthalmol Vis Sci 1998; **39**: (1): 36-44
361. Kaji Y, Obata H, Usui T et al. Three-dimensional organization of collagen fibrils during corneal stromal wound healing after excimer laser keratectomy. J Cataract Refract Surg 1998; **24**: (11): 1441-1446
362. Girard MT, Matsubara M, Fini ME. Transforming growth factor-beta and interleukin-1 modulate metalloproteinase expression by corneal stromal cells. Invest Ophthalmol Vis Sci 1991; **32**: (9): 2441-2454
363. Strissel KJ, Girard MT, West-Mays JA et al. Role of serum amyloid A as an intermediate in the IL-1 and PMA-stimulated signaling pathways regulating expression of rabbit fibroblast collagenase. Exp Cell Res 1997; **237**: (2): 275-287

364. Strissel KJ, Rinehart WB, Fini ME. Regulation of paracrine cytokine balance controlling collagenase synthesis by corneal cells. Invest Ophthalmol Vis Sci 1997; **38**: (2): 546-552
365. West-Mays JA, Strissel KJ, Sadow PM et al. Competence for collagenase gene expression by tissue fibroblasts requires activation of an interleukin 1 alpha autocrine loop. Proc Natl Acad Sci U S A 1995; **92**: (15): 6768-6772
366. Ye HQ, Azar DT. Expression of gelatinases A and B, and TIMPs 1 and 2 during corneal wound healing. Invest Ophthalmol Vis Sci 1998; **39**: (6): 913-921
367. Ye HQ, Maeda M, Yu FS et al. Differential expression of MT1-MMP (MMP-14) and collagenase III (MMP-13) genes in normal and wounded rat corneas. Invest Ophthalmol Vis Sci 2000; **41**: (10): 2894-2899
368. Wilson SE, Chaurasia SS, Medeiros FW. Apoptosis in the initiation, modulation and termination of the corneal wound healing response. Exp Eye Res 2007; **85**: (3): 305-311
369. Barbosa FL, Chaurasia SS, Kaur H et al. Stromal interleukin-1 expression in the cornea after haze-associated injury. Exp Eye Res 2010; **91**: (3): 456-461
370. Hoppenreijs VP, Pels E, Vrensen GF et al. Effects of human epidermal growth factor on endothelial wound healing of human corneas. Invest Ophthalmol Vis Sci 1992; **33**: (6): 1946-1957
371. Matsubara M, Tanishima T. Wound-healing of corneal endothelium in monkey: an autoradiographic study. Jpn J Ophthalmol 1983; **27**: (3): 444-450
372. Schultz G, Cipolla L, Whitehouse A et al. Growth factors and corneal endothelial cells: III. Stimulation of adult human corneal endothelial cell mitosis in vitro by defined mitogenic agents. Cornea 1992; **11**: (1): 20-27
373. Senoo T, Joyce NC. Cell cycle kinetics in corneal endothelium from old and young donors. Invest Ophthalmol Vis Sci 2000; **41**: (3): 660-667
374. Treffers WF. Human corneal endothelial wound repair. In vitro and in vivo. Ophthalmology 1982; **89**: (6): 605-613
375. Couch JM, Cullen P, Casey TA et al. Mitotic activity of corneal endothelial cells in organ culture with recombinant human epidermal growth factor. Ophthalmology 1987; **94**: (1): 1-6
376. Zhu C, Joyce NC. Proliferative response of corneal endothelial cells from young and older donors. Invest Ophthalmol Vis Sci 2004; **45**: (6): 1743-1751
377. Yokoo S, Yamagami S, Yanagi Y et al. Human corneal endothelial cell precursors isolated by sphere-forming assay. Invest Ophthalmol Vis Sci 2005; **46**: (5): 1626-1631
378. McGowan SL, Edelhauser HF, Pfister RR et al. Stem cell markers in the human posterior limbus and corneal endothelium of unwounded and wounded corneas. Mol Vis 2007; **13**: 1984-2000
379. Laing RA, Neubauer L, Oak SS et al. Evidence for mitosis in the adult corneal endothelium. Ophthalmology 1984; **91**: (10): 1129-1134
380. Olsen EG, Davanger M. The healing of human corneal endothelium. An in vitro study. Acta Ophthalmol (Copenh) 1984; **62**: (6): 885-892
381. O'Brien TP, Li Q, Ashraf MF et al. Inflammatory response in the early stages of wound healing after excimer laser keratectomy. Arch Ophthalmol 1998; **116**: (11): 1470-1474
382. Helena MC, Baerveldt F, Kim WJ et al. Keratocyte apoptosis after corneal surgery. Invest Ophthalmol Vis Sci 1998; **39**: (2): 276-283
383. Folkman J, *History of angiogenesis*. Angiogenesis: an Integrative Approach from Science to Medicine, ed. F.J. Figg WD. 2008: Springer. 1-14.
384. Penn JS, Madan A, Caldwell RB et al. Vascular endothelial growth factor in eye disease. Prog Retin Eye Res 2008; **27**: (4): 331-371
385. Cueni LN, Detmar M. The lymphatic system in health and disease. Lymphat Res Biol 2008; **6**: (3-4): 109-122

386. Ellenberg D, Azar DT, Hallak JA et al. Novel aspects of corneal angiogenic and lymphangiogenic privilege. Prog Retin Eye Res 2010; **29**: (3): 208-248
387. Redlitz A, Daum G, Sage EH. Angiostatin diminishes activation of the mitogen-activated protein kinases ERK-1 and ERK-2 in human dermal microvascular endothelial cells. J Vasc Res 1999; **36**: (1): 28-34
388. Azar DT. Corneal angiogenic privilege: angiogenic and antiangiogenic factors in corneal avascularity, vasculogenesis, and wound healing (an American Ophthalmological Society thesis). Trans Am Ophthalmol Soc 2006; **104**: 264-302
389. Chang JH, Gabison EE, Kato T et al. Corneal neovascularization. Curr Opin Ophthalmol 2001; **12**: (4): 242-249
390. Kenyon KR, Fogle JA, Stone DL et al. Regeneration of corneal epithelial basement membrane following thermal cauterization. Invest Ophthalmol Vis Sci 1977; **16**: (4): 292-301
391. Carmichael T, *Corneal angiogenesis*. Ocular Angiogenesis: Diseases, Mechanisms, and Therapeutics, ed. B.C. Tombran-Tink J. 2006: Humana Press. 50-71.
392. Awwad ST, Heilman M, Hogan RN et al. Severe reactive ischemic posterior segment inflammation in acanthamoeba keratitis: a new potentially blinding syndrome. Ophthalmology 2007; **114**: (2): 313-320
393. Cursiefen C, Maruyama K, Jackson DG et al. Time course of angiogenesis and lymphangiogenesis after brief corneal inflammation. Cornea 2006; **25**: (4): 443-447
394. Cursiefen C, Schlotzer-Schrehardt U, Kuchle M et al. Lymphatic vessels in vascularized human corneas: immunohistochemical investigation using LYVE-1 and podoplanin. Invest Ophthalmol Vis Sci 2002; **43**: (7): 2127-2135
395. Chang LK, Garcia-Cardena G, Farnebo F et al. Dose-dependent response of FGF-2 for lymphangiogenesis. Proc Natl Acad Sci U S A 2004; **101**: (32): 11658-11663
396. Ecoiffier T, Yuen D, Chen L. Differential distribution of blood and lymphatic vessels in the murine cornea. Invest Ophthalmol Vis Sci 2010; **51**: (5): 2436-2440
397. Maruyama K, Ii M, Cursiefen C et al. Inflammation-induced lymphangiogenesis in the cornea arises from CD11b-positive macrophages. J Clin Invest 2005; **115**: (9): 2363-2372
398. Pearce DJ, Ridler CM, Simpson C et al. Multiparameter analysis of murine bone marrow side population cells. Blood 2004; **103**: (7): 2541-2546
399. Rehman J, Li J, Orschell CM et al. Peripheral blood "endothelial progenitor cells" are derived from monocyte/macrophages and secrete angiogenic growth factors. Circulation 2003; **107**: (8): 1164-1169
400. Skobe M, Dana R. Blocking the path of lymphatic vessels. Nat Med 2009; **15**: (9): 993-994
401. Regenfuss B, Onderka J, Bock F et al. Genetic heterogeneity of lymphangiogenesis in different mouse strains. Am J Pathol 2010; **177**: (1): 501-510
402. Shi W, Ming C, Liu J et al. Features of corneal neovascularization and lymphangiogenesis induced by different etiological factors in mice. Graefes Arch Clin Exp Ophthalmol 2010; **249**: (1): 55-67
403. Du Y, Funderburgh ML, Mann MM et al. Multipotent stem cells in human corneal stroma. Stem Cells 2005; **23**: (9): 1266-1275
404. Funderburgh ML, Du Y, Mann MM et al. PAX6 expression identifies progenitor cells for corneal keratocytes. Faseb J 2005; **19**: (10): 1371-1373
405. Yoshida S, Shimmura S, Shimazaki J et al. Serum-free spheroid culture of mouse corneal keratocytes. Invest Ophthalmol Vis Sci 2005; **46**: (5): 1653-1658
406. Bez A, Corsini E, Curti D et al. Neurosphere and neurosphere-forming cells: morphological and ultrastructural characterization. Brain Res 2003; **993**: (1-2): 18-29
407. Jiang Y, Vaessen B, Lenvik T et al. Multipotent progenitor cells can be isolated from postnatal murine bone marrow, muscle, and brain. Exp Hematol 2002; **30**: (8): 896-904

408. Milward EA, Lundberg CG, Ge B et al. Isolation and transplantation of multipotential populations of epidermal growth factor-responsive, neural progenitor cells from the canine brain. J Neurosci Res 1997; **50**: (5): 862-871
409. Reynolds BA, Tetzlaff W, Weiss S. A multipotent EGF-responsive striatal embryonic progenitor cell produces neurons and astrocytes. J Neurosci 1992; **12**: (11): 4565-4574
410. Reynolds BA, Weiss S. Generation of neurons and astrocytes from isolated cells of the adult mammalian central nervous system. Science 1992; **255**: (5052): 1707-1710
411. Lanza RP, Cibelli JB, Blackwell C et al. Extension of cell life-span and telomere length in animals cloned from senescent somatic cells. Science 2000; **288**: (5466): 665-669
412. Orlando V. Polycomb, epigenomes, and control of cell identity. Cell 2003; **112**: (5): 599-606
413. Simon JA, Tamkun JW. Programming off and on states in chromatin: mechanisms of Polycomb and trithorax group complexes. Curr Opin Genet Dev 2002; **12**: (2): 210-218
414. Molofsky AV, Pardal R, Iwashita T et al. Bmi-1 dependence distinguishes neural stem cell self-renewal from progenitor proliferation. Nature 2003; **425**: (6961): 962-967
415. Park IK, Qian D, Kiel M et al. Bmi-1 is required for maintenance of adult self-renewing haematopoietic stem cells. Nature 2003; **423**: (6937): 302-305
416. Ema H, Sudo K, Seita J et al. Quantification of self-renewal capacity in single hematopoietic stem cells from normal and Lnk-deficient mice. Dev Cell 2005; **8**: (6): 907-914
417. McCulloch EA, Siminovitch L, Till JE. Spleen-Colony Formation in Anemic Mice of Genotype Ww. Science 1964; **144**: 844-846
418. Nobuhisa I, Takizawa M, Takaki S et al. Regulation of hematopoietic development in the aorta-gonad-mesonephros region mediated by Lnk adaptor protein. Mol Cell Biol 2003; **23**: (23): 8486-8494
419. Majumdar MK, Thiede MA, Haynesworth SE et al. Human marrow-derived mesenchymal stem cells (MSCs) express hematopoietic cytokines and support long-term hematopoiesis when differentiated toward stromal and osteogenic lineages. J Hematother Stem Cell Res 2000; **9**: (6): 841-848
420. Ramalho-Santos M, Yoon S, Matsuzaki Y et al. "Stemness": transcriptional profiling of embryonic and adult stem cells. Science 2002; **298**: (5593): 597-600
421. Tumbar T, Guasch G, Greco V et al. Defining the epithelial stem cell niche in skin. Science 2004; **303**: (5656): 359-363
422. Abbott BL. ABCG2 (BCRP) expression in normal and malignant hematopoietic cells. Hematol Oncol 2003; **21**: (3): 115-130
423. Scharenberg CW, Harkey MA, Torok-Storb B. The ABCG2 transporter is an efficient Hoechst 33342 efflux pump and is preferentially expressed by immature human hematopoietic progenitors. Blood 2002; **99**: (2): 507-512
424. Zhou S, Schuetz JD, Bunting KD et al. The ABC transporter Bcrp1/ABCG2 is expressed in a wide variety of stem cells and is a molecular determinant of the side-population phenotype. Nat Med 2001; **7**: (9): 1028-1034
425. Cai J, Cheng A, Luo Y et al. Membrane properties of rat embryonic multipotent neural stem cells. J Neurochem 2004; **88**: (1): 212-226
426. Jang YK, Park JJ, Lee MC et al. Retinoic acid-mediated induction of neurons and glial cells from human umbilical cord-derived hematopoietic stem cells. J Neurosci Res 2004; **75**: (4): 573-584
427. Martin CM, Meeson AP, Robertson SM et al. Persistent expression of the ATP-binding cassette transporter, Abcg2, identifies cardiac SP cells in the developing and adult heart. Dev Biol 2004; **265**: (1): 262-275
428. Lechner A, Leech CA, Abraham EJ et al. Nestin-positive progenitor cells derived from adult human pancreatic islets of Langerhans contain side population (SP) cells defined by

expression of the ABCG2 (BCRP1) ATP-binding cassette transporter. Biochem Biophys Res Commun 2002; **293**: (2): 670-674
429. Terunuma A, Jackson KL, Kapoor V et al. Side population keratinocytes resembling bone marrow side population stem cells are distinct from label-retaining keratinocyte stem cells. J Invest Dermatol 2003; **121**: (5): 1095-1103
430. Triel C, Vestergaard ME, Bolund L et al. Side population cells in human and mouse epidermis lack stem cell characteristics. Exp Cell Res 2004; **295**: (1): 79-90
431. Doyle LA, Yang W, Abruzzo LV et al. A multidrug resistance transporter from human MCF-7 breast cancer cells. Proc Natl Acad Sci U S A 1998; **95**: (26): 15665-15670
432. Sarkadi B, Homolya L, Szakacs G et al. Human multidrug resistance ABCB and ABCG transporters: participation in a chemoimmunity defense system. Physiol Rev 2006; **86**: (4): 1179-1236
433. Sarkadi B, Ozvegy-Laczka C, Nemet K et al. ABCG2 -- a transporter for all seasons. FEBS Lett 2004; **567**: (1): 116-120
434. de Paiva CS, Chen Z, Corrales RM et al. ABCG2 transporter identifies a population of clonogenic human limbal epithelial cells. Stem Cells 2005; **23**: (1): 63-73
435. Lee RH, Kim B, Choi I et al. Characterization and expression analysis of mesenchymal stem cells from human bone marrow and adipose tissue. Cell Physiol Biochem 2004; **14**: (4-6): 311-324
436. Zhang Y, Li C, Jiang X et al. Human placenta-derived mesenchymal progenitor cells support culture expansion of long-term culture-initiating cells from cord blood CD34+ cells. Exp Hematol 2004; **32**: (7): 657-664
437. Artavanis-Tsakonas S, Rand MD, Lake RJ. Notch signaling: cell fate control and signal integration in development. Science 1999; **284**: (5415): 770-776
438. Kadesch T. Notch signaling: a dance of proteins changing partners. Exp Cell Res 2000; **260**: (1): 1-8
439. Smith GH, Gallahan D, Diella F et al. Constitutive expression of a truncated INT3 gene in mouse mammary epithelium impairs differentiation and functional development. Cell Growth Differ 1995; **6**: (5): 563-577
440. Grindley JC, Davidson DR, Hill RE. The role of Pax-6 in eye and nasal development. Development 1995; **121**: (5): 1433-1442
441. Hitchcock PF, Macdonald RE, VanDeRyt JT et al. Antibodies against Pax6 immunostain amacrine and ganglion cells and neuronal progenitors, but not rod precursors, in the normal and regenerating retina of the goldfish. J Neurobiol 1996; **29**: (3): 399-413
442. Hill RE, Favor J, Hogan BL et al. Mouse small eye results from mutations in a paired-like homeobox-containing gene. Nature 1991; **354**: (6354): 522-525
443. Hogan BL, Horsburgh G, Cohen J et al. Small eyes (Sey): a homozygous lethal mutation on chromosome 2 which affects the differentiation of both lens and nasal placodes in the mouse. J Embryol Exp Morphol 1986; **97**: 95-110
444. Chow RL, Altmann CR, Lang RA et al. Pax6 induces ectopic eyes in a vertebrate. Development 1999; **126**: (19): 4213-4222
445. Halder G, Callaerts P, Gehring WJ. Induction of ectopic eyes by targeted expression of the eyeless gene in Drosophila. Science 1995; **267**: (5205): 1788-1792
446. Osumi N, Shinohara H, Numayama-Tsuruta K et al. Concise review: Pax6 transcription factor contributes to both embryonic and adult neurogenesis as a multifunctional regulator. Stem Cells 2008; **26**: (7): 1663-1672
447. Raymond PA, Barthel LK, Bernardos RL et al. Molecular characterization of retinal stem cells and their niches in adult zebrafish. BMC Dev Biol 2006; **6**: 36
448. Thummel R, Kassen SC, Enright JM et al. Characterization of Muller glia and neuronal progenitors during adult zebrafish retinal regeneration. Exp Eye Res 2008; **87**: (5): 433-444

449. Cheyette BN, Green PJ, Martin K et al. The Drosophila sine oculis locus encodes a homeodomain-containing protein required for the development of the entire visual system. Neuron 1994; **12**: (5): 977-996
450. Ghanbari H, Seo HC, Fjose A et al. Molecular cloning and embryonic expression of Xenopus Six homeobox genes. Mech Dev 2001; **101**: (1-2): 271-277
451. Kawakami K, Ohto H, Takizawa T et al. Identification and expression of six family genes in mouse retina. FEBS Lett 1996; **393**: (2-3): 259-263
452. Leppert GS, Yang JM, Sundin OH. Sequence and location of SIX3, a homeobox gene expressed in the human eye. Ophthalmic Genet 1999; **20**: (1): 7-21
453. Paulsson M, Heinegard D. Purification and structural characterization of a cartilage matrix protein. Biochem J 1981; **197**: (2): 367-375
454. Hascall V, Hascall G, *Cell Biology of Extracellular Matrix*, ed. H. E. 1981, New York: Plenum Publishing Corp. 39-63.
455. Lalonde R, Strazielle C. Neurobehavioral characteristics of mice with modified intermediate filament genes. Rev Neurosci 2003; **14**: (4): 369-385
456. Heald R, Nogales E. Microtubule dynamics. J Cell Sci 2002; **115**: (Pt 1): 3-4
457. Yoshida S, Shimmura S, Nagoshi N et al. Isolation of multipotent neural crest-derived stem cells from the adult mouse cornea. Stem Cells 2006; **24**: (12): 2714-2722
458. Du Y, Sundarraj N, Funderburgh ML et al. Secretion and organization of a cornea-like tissue in vitro by stem cells from human corneal stroma. Invest Ophthalmol Vis Sci 2007; **48**: (11): 5038-5045
459. Fishell G, Mason CA, Hatten ME. Dispersion of neural progenitors within the germinal zones of the forebrain. Nature 1993; **362**: (6421): 636-638
460. Michalczyk K, Ziman M. Nestin structure and predicted function in cellular cytoskeletal organisation. Histol Histopathol 2005; **20**: (2): 665-671
461. Cattaneo E, McKay R. Proliferation and differentiation of neuronal stem cells regulated by nerve growth factor. Nature 1990; **347**: (6295): 762-765
462. Reynolds BA, Weiss S. Clonal and population analyses demonstrate that an EGF-responsive mammalian embryonic CNS precursor is a stem cell. Dev Biol 1996; **175**: (1): 1-13
463. Lendahl U, Zimmerman LB, McKay RD. CNS stem cells express a new class of intermediate filament protein. Cell 1990; **60**: (4): 585-595
464. Chou YH, Khuon S, Herrmann H et al. Nestin promotes the phosphorylation-dependent disassembly of vimentin intermediate filaments during mitosis. Mol Biol Cell 2003; **14**: (4): 1468-1478
465. Namiki J, Tator CH. Cell proliferation and nestin expression in the ependyma of the adult rat spinal cord after injury. J Neuropathol Exp Neurol 1999; **58**: (5): 489-498
466. Vaittinen S, Lukka R, Sahlgren C et al. The expression of intermediate filament protein nestin as related to vimentin and desmin in regenerating skeletal muscle. J Neuropathol Exp Neurol 2001; **60**: (6): 588-597
467. Espana EM, Kawakita T, Di Pascuale MA et al. The heterogeneous murine corneal stromal cell populations in vitro. Invest Ophthalmol Vis Sci 2005; **46**: (12): 4528-4535
468. Nakamura M, Okano H, Blendy JA et al. Musashi, a neural RNA-binding protein required for Drosophila adult external sensory organ development. Neuron 1994; **13**: (1): 67-81
469. Kaneko Y, Sakakibara S, Imai T et al. Musashi1: an evolutionally conserved marker for CNS progenitor cells including neural stem cells. Dev Neurosci 2000; **22**: (1-2): 139-153
470. Maslov AY, Barone TA, Plunkett RJ et al. Neural stem cell detection, characterization, and age-related changes in the subventricular zone of mice. J Neurosci 2004; **24**: (7): 1726-1733
471. Imai T, Tokunaga A, Yoshida T et al. The neural RNA-binding protein Musashi1 translationally regulates mammalian numb gene expression by interacting with its mRNA. Mol Cell Biol 2001; **21**: (12): 3888-3900

472. Kawaguchi A, Miyata T, Sawamoto K et al. Nestin-EGFP transgenic mice: visualization of the self-renewal and multipotency of CNS stem cells. Mol Cell Neurosci 2001; **17**: (2): 259-273
473. Baddoo M, Hill K, Wilkinson R et al. Characterization of mesenchymal stem cells isolated from murine bone marrow by negative selection. J Cell Biochem 2003; **89**: (6): 1235-1249
474. Oh H, Bradfute SB, Gallardo TD et al. Cardiac progenitor cells from adult myocardium: homing, differentiation, and fusion after infarction. Proc Natl Acad Sci U S A 2003; **100**: (21): 12313-12318
475. Spangrude GJ, Heimfeld S, Weissman IL. Purification and characterization of mouse hematopoietic stem cells. Science 1988; **241**: (4861): 58-62
476. Welm BE, Tepera SB, Venezia T et al. Sca-1(pos) cells in the mouse mammary gland represent an enriched progenitor cell population. Dev Biol 2002; **245**: (1): 42-56
477. Ito CY, Li CY, Bernstein A et al. Hematopoietic stem cell and progenitor defects in Sca-1/Ly-6A-null mice. Blood 2003; **101**: (2): 517-523
478. Civin CI, Trischmann T, Kadan NS et al. Highly purified CD34-positive cells reconstitute hematopoiesis. J Clin Oncol 1996; **14**: (8): 2224-2233
479. Krause DS, Fackler MJ, Civin CI et al. CD34: structure, biology, and clinical utility. Blood 1996; **87**: (1): 1-13
480. Joseph A, Hossain P, Jham S et al. Expression of CD34 and L-selectin on human corneal keratocytes. Invest Ophthalmol Vis Sci 2003; **44**: (11): 4689-4692
481. Toti P, Tosi GM, Traversi C et al. CD-34 stromal expression pattern in normal and altered human corneas. Ophthalmology 2002; **109**: (6): 1167-1171
482. Espana EM, Kawakita T, Liu CY et al. CD-34 expression by cultured human keratocytes is downregulated during myofibroblast differentiation induced by TGF-beta1. Invest Ophthalmol Vis Sci 2004; **45**: (9): 2985-2991
483. Thomas ML. The leukocyte common antigen family. Annu Rev Immunol 1989; **7**: 339-369
484. Shivtiel S, Kollet O, Lapid K et al. CD45 regulates retention, motility, and numbers of hematopoietic progenitors, and affects osteoclast remodeling of metaphyseal trabecules. J Exp Med 2008; **205**: (10): 2381-2395
485. Bialek P, Kern B, Yang X et al. A twist code determines the onset of osteoblast differentiation. Dev Cell 2004; **6**: (3): 423-435
486. Fowlkes JL, Bunn RC, Liu L et al. Runt-related transcription factor 2 (RUNX2) and RUNX2-related osteogenic genes are down-regulated throughout osteogenesis in type 1 diabetes mellitus. Endocrinology 2008; **149**: (4): 1697-1704
487. Gong XQ, Li L. Dermo-1, a multifunctional basic helix-loop-helix protein, represses MyoD transactivation via the HLH domain, MEF2 interaction, and chromatin deacetylation. J Biol Chem 2002; **277**: (14): 12310-12317
488. Lee MS, Lowe G, Flanagan S et al. Human Dermo-1 has attributes similar to twist in early bone development. Bone 2000; **27**: (5): 591-602
489. Murakami M, Ohkuma M, Nakamura M. Molecular mechanism of transforming growth factor-beta-mediated inhibition of growth arrest and differentiation in a myoblast cell line. Dev Growth Differ 2008; **50**: (2): 121-130
490. Ota MS, Loebel DA, O'Rourke MP et al. Twist is required for patterning the cranial nerves and maintaining the viability of mesodermal cells. Dev Dyn 2004; **230**: (2): 216-228
491. Sharabi AB, Aldrich M, Sosic D et al. Twist-2 controls myeloid lineage development and function. PLoS Biol 2008; **6**: (12): e316
492. Shelton EL, Yutzey KE. Twist1 function in endocardial cushion cell proliferation, migration, and differentiation during heart valve development. Dev Biol 2008; **317**: (1): 282-295
493. Sosic D, Richardson JA, Yu K et al. Twist regulates cytokine gene expression through a negative feedback loop that represses NF-kappaB activity. Cell 2003; **112**: (2): 169-180

494. Isenmann S, Arthur A, Zannettino AC et al. TWIST family of basic helix-loop-helix transcription factors mediate human mesenchymal stem cell growth and commitment. Stem Cells 2009; **27**: (10): 2457-2468
495. Weaving L, Mihelec M, Storen R et al. Twist2: role in corneal stromal keratocyte proliferation and corneal thickness. Invest Ophthalmol Vis Sci 2010; **51**: (11): 5561-5570
496. Medina PP, Castillo SD, Blanco S et al. The SRY-HMG box gene, SOX4, is a target of gene amplification at chromosome 6p in lung cancer. Hum Mol Genet 2009; **18**: (7): 1343-1352
497. Cheung M, Chaboissier MC, Mynett A et al. The transcriptional control of trunk neural crest induction, survival, and delamination. Dev Cell 2005; **8**: (2): 179-192
498. O'Donnell M, Hong CS, Huang X et al. Functional analysis of Sox8 during neural crest development in Xenopus. Development 2006; **133**: (19): 3817-3826
499. Poche RA, Furuta Y, Chaboissier MC et al. Sox9 is expressed in mouse multipotent retinal progenitor cells and functions in Muller glial cell development. J Comp Neurol 2008; **510**: (3): 237-250
500. Come C, Arnoux V, Bibeau F et al. Roles of the transcription factors snail and slug during mammary morphogenesis and breast carcinoma progression. J Mammary Gland Biol Neoplasia 2004; **9**: (2): 183-193
501. Kavanagh DP, Kalia N. Hematopoietic Stem Cell Homing to Injured Tissues. Stem Cell Rev 2011;
502. Pontikoglou C, Deschaseaux F, Sensebe L et al. Bone Marrow Mesenchymal Stem Cells: Biological Properties and Their Role in Hematopoiesis and Hematopoietic Stem Cell Transplantation. Stem Cell Rev 2011;
503. Brissette-Storkus CS, Reynolds SM, Lepisto AJ et al. Identification of a novel macrophage population in the normal mouse corneal stroma. Invest Ophthalmol Vis Sci 2002; **43**: (7): 2264-2271
504. Hamrah P, Liu Y, Zhang Q et al. The corneal stroma is endowed with a significant number of resident dendritic cells. Invest Ophthalmol Vis Sci 2003; **44**: (2): 581-589
505. Hamrah P, Zhang Q, Liu Y et al. Novel characterization of MHC class II-negative population of resident corneal Langerhans cell-type dendritic cells. Invest Ophthalmol Vis Sci 2002; **43**: (3): 639-646
506. Banchereau J, Steinman RM. Dendritic cells and the control of immunity. Nature 1998; **392**: (6673): 245-252
507. Steinman RM, Cohn ZA. Identification of a novel cell type in peripheral lymphoid organs of mice. I. Morphology, quantitation, tissue distribution. J Exp Med 1973; **137**: (5): 1142-1162
508. Corbi AL, Lopez-Rodriguez C. CD11c integrin gene promoter activity during myeloid differentiation. Leuk Lymphoma 1997; **25**: (5-6): 415-425
509. Geissmann F, Manz MG, Jung S et al. Development of monocytes, macrophages, and dendritic cells. Science **327**: (5966): 656-661
510. Nakamura T, Ishikawa F, Sonoda KH et al. Characterization and distribution of bone marrow-derived cells in mouse cornea. Invest Ophthalmol Vis Sci 2005; **46**: (2): 497-503
511. Sosnova M, Bradl M, Forrester JV. CD34+ corneal stromal cells are bone marrow-derived and express hemopoietic stem cell markers. Stem Cells 2005; **23**: (4): 507-515
512. Barbosa FL, Chaurasia SS, Cutler A et al. Corneal myofibroblast generation from bone marrow-derived cells. Exp Eye Res 2010; **91**: (1): 92-96
513. Thill M, Schlagner K, Altenahr S et al. A novel population of repair cells identified in the stroma of the human cornea. Stem Cells Dev 2007; **16**: (5): 733-745
514. Miraglia S, Godfrey W, Yin AH et al. A novel five-transmembrane hematopoietic stem cell antigen: isolation, characterization, and molecular cloning. Blood 1997; **90**: (12): 5013-5021
515. Yin AH, Miraglia S, Zanjani ED et al. AC133, a novel marker for human hematopoietic stem and progenitor cells. Blood 1997; **90**: (12): 5002-5012

516. Corbeil D, Roper K, Hellwig A et al. The human AC133 hematopoietic stem cell antigen is also expressed in epithelial cells and targeted to plasma membrane protrusions. J Biol Chem 2000; **275**: (8): 5512-5520
517. Corbeil D, Fargeas CA, Huttner WB. Rat prominin, like its mouse and human orthologues, is a pentaspan membrane glycoprotein. Biochem Biophys Res Commun 2001; **285**: (4): 939-944
518. Shmelkov SV, St Clair R, Lyden D et al. AC133/CD133/Prominin-1. Int J Biochem Cell Biol 2005; **37**: (4): 715-719
519. Shmelkov SV, Jun L, St Clair R et al. Alternative promoters regulate transcription of the gene that encodes stem cell surface protein AC133. Blood 2004; **103**: (6): 2055-2061
520. Yu Y, Flint A, Dvorin EL et al. AC133-2, a novel isoform of human AC133 stem cell antigen. J Biol Chem 2002; **277**: (23): 20711-20716
521. Dua HS, Joseph A, Shanmuganathan VA et al. Stem cell differentiation and the effects of deficiency. Eye (Lond) 2003; **17**: (8): 877-885
522. Fernandez Pujol B, Lucibello FC, Gehling UM et al. Endothelial-like cells derived from human CD14 positive monocytes. Differentiation 2000; **65**: (5): 287-300
523. Zhao Y, Glesne D, Huberman E. A human peripheral blood monocyte-derived subset acts as pluripotent stem cells. Proc Natl Acad Sci U S A 2003; **100**: (5): 2426-2431
524. Carlson EC, Wang IJ, Liu CY et al. Altered KSPG expression by keratocytes following corneal injury. Mol Vis 2003; **9**: 615-623
525. Funderburgh JL. Keratan sulfate: structure, biosynthesis, and function. Glycobiology 2000; **10**: (10): 951-958
526. Chakravarti S, Magnuson T, Lass JH et al. Lumican regulates collagen fibril assembly: skin fragility and corneal opacity in the absence of lumican. J Cell Biol 1998; **141**: (5): 1277-1286
527. Du Y, Carlson EC, Funderburgh ML et al. Stem cell therapy restores transparency to defective murine corneas. Stem Cells 2009; **27**: (7): 1635-1642
528. Patel SA, Sherman L, Munoz J et al. Immunological properties of mesenchymal stem cells and clinical implications. Arch Immunol Ther Exp (Warsz) 2008; **56**: (1): 1-8
529. Arnalich-Montiel F, Pastor S, Blazquez-Martinez A et al. Adipose-derived stem cells are a source for cell therapy of the corneal stroma. Stem Cells 2008; **26**: (2): 570-579
530. Moseley TA, Zhu M, Hedrick MH. Adipose-derived stem and progenitor cells as fillers in plastic and reconstructive surgery. Plast Reconstr Surg 2006; **118**: (3 Suppl): 121S-128S
531. Kim M, Choi YS, Yang SH et al. Muscle regeneration by adipose tissue-derived adult stem cells attached to injectable PLGA spheres. Biochem Biophys Res Commun 2006; **348**: (2): 386-392
532. Conejero JA, Lee JA, Parrett BM et al. Repair of palatal bone defects using osteogenically differentiated fat-derived stem cells. Plast Reconstr Surg 2006; **117**: (3): 857-863
533. Miyahara Y, Nagaya N, Kataoka M et al. Monolayered mesenchymal stem cells repair scarred myocardium after myocardial infarction. Nat Med 2006; **12**: (4): 459-465
534. Fraser JK, Wulur I, Alfonso Z et al. Fat tissue: an underappreciated source of stem cells for biotechnology. Trends Biotechnol 2006; **24**: (4): 150-154
535. Liu H, Zhang J, Liu CY et al. Cell therapy of congenital corneal diseases with umbilical mesenchymal stem cells: lumican null mice. PLoS One 2010; **5**: (5): e10707
536. Mitalipova M, Calhoun J, Shin S et al. Human embryonic stem cell lines derived from discarded embryos. Stem Cells 2003; **21**: (5): 521-526
537. Reubinoff BE, Pera MF, Fong CY et al. Embryonic stem cell lines from human blastocysts: somatic differentiation in vitro. Nat Biotechnol 2000; **18**: (4): 399-404
538. Reyes M, Lund T, Lenvik T et al. Purification and ex vivo expansion of postnatal human marrow mesodermal progenitor cells. Blood 2001; **98**: (9): 2615-2625
539. Schwartz RE, Reyes M, Koodie L et al. Multipotent adult progenitor cells from bone marrow differentiate into functional hepatocyte-like cells. J Clin Invest 2002; **109**: (10): 1291-1302

540. Prusa AR, Marton E, Rosner M et al. Oct-4-expressing cells in human amniotic fluid: a new source for stem cell research? Hum Reprod 2003; **18**: (7): 1489-1493
541. Li H, Liu H, Heller S. Pluripotent stem cells from the adult mouse inner ear. Nat Med 2003; **9**: (10): 1293-1299
542. Alessandri G, Pagano S, Bez A et al. Isolation and culture of human muscle-derived stem cells able to differentiate into myogenic and neurogenic cell lineages. Lancet 2004; **364**: (9448): 1872-1883
543. Young HE, Duplaa C, Yost MJ et al. Clonogenic analysis reveals reserve stem cells in postnatal mammals. II. Pluripotent epiblastic-like stem cells. Anat Rec A Discov Mol Cell Evol Biol 2004; **277**: (1): 178-203
544. Sieber-Blum M, Grim M, Hu YF et al. Pluripotent neural crest stem cells in the adult hair follicle. Dev Dyn 2004; **231**: (2): 258-269
545. Dvash T, Mayshar Y, Darr H et al. Temporal gene expression during differentiation of human embryonic stem cells and embryoid bodies. Hum Reprod 2004; **19**: (12): 2875-2883
546. Itskovitz-Eldor J, Schuldiner M, Karsenti D et al. Differentiation of human embryonic stem cells into embryoid bodies compromising the three embryonic germ layers. Mol Med 2000; **6**: (2): 88-95
547. Alison M, Sarraf C. Hepatic stem cells. J Hepatol 1998; **29**: (4): 676-682
548. Gage FH. Mammalian neural stem cells. Science 2000; **287**: (5457): 1433-1438
549. Jiang Y, Jahagirdar BN, Reinhardt RL et al. Pluripotency of mesenchymal stem cells derived from adult marrow. Nature 2002; **418**: (6893): 41-49
550. Potten CS. Stem cells in gastrointestinal epithelium: numbers, characteristics and death. Philos Trans R Soc Lond B Biol Sci 1998; **353**: (1370): 821-830
551. Watt FM. Epidermal stem cells: markers, patterning and the control of stem cell fate. Philos Trans R Soc Lond B Biol Sci 1998; **353**: (1370): 831-837
552. Weissman IL. Translating stem and progenitor cell biology to the clinic: barriers and opportunities. Science 2000; **287**: (5457): 1442-1446
553. Avilion AA, Nicolis SK, Pevny LH et al. Multipotent cell lineages in early mouse development depend on SOX2 function. Genes Dev 2003; **17**: (1): 126-140
554. Boyer LA, Lee TI, Cole MF et al. Core transcriptional regulatory circuitry in human embryonic stem cells. Cell 2005; **122**: (6): 947-956
555. Chambers I, Colby D, Robertson M et al. Functional expression cloning of Nanog, a pluripotency sustaining factor in embryonic stem cells. Cell 2003; **113**: (5): 643-655
556. Muller T, Fleischmann G, Eildermann K et al. A novel embryonic stem cell line derived from the common marmoset monkey (Callithrix jacchus) exhibiting germ cell-like characteristics. Hum Reprod 2009; **24**: (6): 1359-1372
557. Niwa H, Miyazaki J, Smith AG. Quantitative expression of Oct-3/4 defines differentiation, dedifferentiation or self-renewal of ES cells. Nat Genet 2000; **24**: (4): 372-376
558. Ferri AL, Cavallaro M, Braida D et al. Sox2 deficiency causes neurodegeneration and impaired neurogenesis in the adult mouse brain. Development 2004; **131**: (15): 3805-3819
559. Gubbay J, Collignon J, Koopman P et al. A gene mapping to the sex-determining region of the mouse Y chromosome is a member of a novel family of embryonically expressed genes. Nature 1990; **346**: (6281): 245-250
560. Sasai Y. Roles of Sox factors in neural determination: conserved signaling in evolution? Int J Dev Biol 2001; **45**: (1): 321-326
561. Furuta Y, Hogan BL. BMP4 is essential for lens induction in the mouse embryo. Genes Dev 1998; **12**: (23): 3764-3775
562. Kamachi Y, Uchikawa M, Collignon J et al. Involvement of Sox1, 2 and 3 in the early and subsequent molecular events of lens induction. Development 1998; **125**: (13): 2521-2532

563. Kamachi Y, Uchikawa M, Tanouchi A et al. Pax6 and SOX2 form a co-DNA-binding partner complex that regulates initiation of lens development. Genes Dev 2001; **15**: (10): 1272-1286
564. Kondoh H, Uchikawa M, Kamachi Y. Interplay of Pax6 and SOX2 in lens development as a paradigm of genetic switch mechanisms for cell differentiation. Int J Dev Biol 2004; **48**: (8-9): 819-827
565. Kim JH, Jee MK, Lee SY et al. Regulation of adipose tissue stromal cells behaviors by endogenic Oct4 expression control. PLoS One 2009; **4**: (9): e7166
566. Nayernia K, Lee JH, Drusenheimer N et al. Derivation of male germ cells from bone marrow stem cells. Lab Invest 2006; **86**: (7): 654-663
567. Pallante BA, Duignan I, Okin D et al. Bone marrow Oct3/4+ cells differentiate into cardiac myocytes via age-dependent paracrine mechanisms. Circ Res 2007; **100**: (1): e1-11
568. Zhang S, Jia Z, Ge J et al. Purified human bone marrow multipotent mesenchymal stem cells regenerate infarcted myocardium in experimental rats. Cell Transplant 2005; **14**: (10): 787-798
569. Hart AH, Hartley L, Ibrahim M et al. Identification, cloning and expression analysis of the pluripotency promoting Nanog genes in mouse and human. Dev Dyn 2004; **230**: (1): 187-198
570. Santagata S, Hornick JL, Ligon KL. Comparative analysis of germ cell transcription factors in CNS germinoma reveals diagnostic utility of NANOG. Am J Surg Pathol 2006; **30**: (12): 1613-1618
571. Becskei A, Serrano L. Engineering stability in gene networks by autoregulation. Nature 2000; **405**: (6786): 590-593
572. Rodda DJ, Chew JL, Lim LH et al. Transcriptional regulation of nanog by OCT4 and SOX2. J Biol Chem 2005; **280**: (26): 24731-24737
573. Yu J, Vodyanik MA, Smuga-Otto K et al. Induced pluripotent stem cell lines derived from human somatic cells. Science 2007; **318**: (5858): 1917-1920
574. Le Lievre CS, Le Douarin NM. Mesenchymal derivatives of the neural crest: analysis of chimaeric quail and chick embryos. J Embryol Exp Morphol 1975; **34**: (1): 125-154
575. Kruger GM, Mosher JT, Bixby S et al. Neural crest stem cells persist in the adult gut but undergo changes in self-renewal, neuronal subtype potential, and factor responsiveness. Neuron 2002; **35**: (4): 657-669
576. Li HY, Say EH, Zhou XF. Isolation and characterization of neural crest progenitors from adult dorsal root ganglia. Stem Cells 2007; **25**: (8): 2053-2065
577. Fernandes KJ, McKenzie IA, Mill P et al. A dermal niche for multipotent adult skin-derived precursor cells. Nat Cell Biol 2004; **6**: (11): 1082-1093
578. Wong CE, Paratore C, Dours-Zimmermann MT et al. Neural crest-derived cells with stem cell features can be traced back to multiple lineages in the adult skin. J Cell Biol 2006; **175**: (6): 1005-1015
579. Miura M, Gronthos S, Zhao M et al. SHED: stem cells from human exfoliated deciduous teeth. Proc Natl Acad Sci U S A 2003; **100**: (10): 5807-5812
580. Motohashi T, Aoki H, Chiba K et al. Multipotent cell fate of neural crest-like cells derived from embryonic stem cells. Stem Cells 2007; **25**: (2): 402-410
581. Takashima Y, Era T, Nakao K et al. Neuroepithelial cells supply an initial transient wave of MSC differentiation. Cell 2007; **129**: (7): 1377-1388
582. Henion PD, Weston JA. Timing and pattern of cell fate restrictions in the neural crest lineage. Development 1997; **124**: (21): 4351-4359
583. Pacini S, Carnicelli V, Trombi L et al. Constitutive expression of pluripotency-associated genes in mesodermal progenitor cells (MPCs). PLoS One 2010; **5**: (3): e9861
584. Greco SJ, Liu K, Rameshwar P. Functional similarities among genes regulated by OCT4 in human mesenchymal and embryonic stem cells. Stem Cells 2007; **25**: (12): 3143-3154

585. Thummel R, Enright JM, Kassen SC et al. Pax6a and Pax6b are required at different points in neuronal progenitor cell proliferation during zebrafish photoreceptor regeneration. Exp Eye Res 2010; **90**: (5): 572-582
586. Yamamoto S, Nagao M, Sugimori M et al. Transcription factor expression and Notch-dependent regulation of neural progenitors in the adult rat spinal cord. J Neurosci 2001; **21**: (24): 9814-9823
587. Millimaki BB, Sweet EM, Riley BB. Sox2 is required for maintenance and regeneration, but not initial development, of hair cells in the zebrafish inner ear. Dev Biol 2010; **338**: (2): 262-269
588. Song N, Jia XS, Jia LL et al. Expression and role of Oct3/4, Nanog and Sox2 in regeneration of rat tracheal epithelium. Cell Prolif 2010; **43**: (1): 49-55
589. Cvekl A, Tamm ER. Anterior eye development and ocular mesenchyme: new insights from mouse models and human diseases. Bioessays 2004; **26**: (4): 374-386
590. Amit M, Carpenter MK, Inokuma MS et al. Clonally derived human embryonic stem cell lines maintain pluripotency and proliferative potential for prolonged periods of culture. Dev Biol 2000; **227**: (2): 271-278
591. Hiyama E, Hiyama K. Telomere and telomerase in stem cells. Br J Cancer 2007; **96**: (7): 1020-1024
592. Mohan RR, Hutcheon AE, Choi R et al. Apoptosis, necrosis, proliferation, and myofibroblast generation in the stroma following LASIK and PRK. Exp Eye Res 2003; **76**: (1): 71-87
593. Netto MV, Mohan RR, Sinha S et al. Effect of prophylactic and therapeutic mitomycin C on corneal apoptosis, cellular proliferation, haze, and long-term keratocyte density in rabbits. J Refract Surg 2006; **22**: (6): 562-574
594. Wilson SE, Mohan RR, Hutcheon AE et al. Effect of ectopic epithelial tissue within the stroma on keratocyte apoptosis, mitosis, and myofibroblast transformation. Exp Eye Res 2003; **76**: (2): 193-201
595. Power WJ, Kaufman AH, Merayo-Lloves J et al. Expression of collagens I, III, IV and V mRNA in excimer wounded rat cornea: analysis by semi-quantitative PCR. Curr Eye Res 1995; **14**: (10): 879-886
596. Martinez-Garcia MC, Merayo-Lloves J, Blanco-Mezquita T et al. Wound healing following refractive surgery in hens. Exp Eye Res 2006; **83**: (4): 728-735
597. Del Pero RA, Gigstad JE, Roberts AD et al. A refractive and histopathologic study of excimer laser keratectomy in primates. Am J Ophthalmol 1990; **109**: (4): 419-429
598. Malley DS, Steinert RF, Puliafito CA et al. Immunofluorescence study of corneal wound healing after excimer laser anterior keratectomy in the monkey eye. Arch Ophthalmol 1990; **108**: (9): 1316-1322
599. Mohan RR, Stapleton WM, Sinha S et al. A novel method for generating corneal haze in anterior stroma of the mouse eye with the excimer laser. Exp Eye Res 2008; **86**: (2): 235-240
600. Matsuda A, Yoshiki A, Tagawa Y et al. Corneal wound healing in tenascin knockout mouse. Invest Ophthalmol Vis Sci 1999; **40**: (6): 1071-1080
601. Miyazaki K, Okada Y, Yamanaka O et al. Corneal wound healing in an osteopontin-deficient mouse. Invest Ophthalmol Vis Sci 2008; **49**: (4): 1367-1375
602. Fantes FE, Hanna KD, Waring GO, 3rd et al. Wound healing after excimer laser keratomileusis (photorefractive keratectomy) in monkeys. Arch Ophthalmol 1990; **108**: (5): 665-675
603. Galiacy SD, Fournie P, Massoudi D et al. Matrix metalloproteinase 14 overexpression reduces corneal scarring. Gene Ther 2010;
604. Vandesompele J, De Preter K, Pattyn F et al. Accurate normalization of real-time quantitative RT-PCR data by geometric averaging of multiple internal control genes. Genome Biol 2002; **3**: (7): RESEARCH0034

605. Pfaffl MW, Horgan GW, Dempfle L. Relative expression software tool (REST) for group-wise comparison and statistical analysis of relative expression results in real-time PCR. Nucleic Acids Res 2002; **30**: (9): e36
606. Livak KJ, Schmittgen TD. Analysis of relative gene expression data using real-time quantitative PCR and the 2(-Delta Delta C(T)) Method. Methods 2001; **25**: (4): 402-408
607. Beyne-Rauzy O, Recher C, Dastugue N et al. Tumor necrosis factor alpha induces senescence and chromosomal instability in human leukemic cells. Oncogene 2004; **23**: (45): 7507-7516
608. Manders EM, Stap J, Brakenhoff GJ et al. Dynamics of three-dimensional replication patterns during the S-phase, analysed by double labelling of DNA and confocal microscopy. J Cell Sci 1992; **103 ( Pt 3)**: 857-862
609. Fathke C, Wilson L, Hutter J et al. Contribution of bone marrow-derived cells to skin: collagen deposition and wound repair. Stem Cells 2004; **22**: (5): 812-822
610. Gibson MC, Schultz E. Age-related differences in absolute numbers of skeletal muscle satellite cells. Muscle Nerve 1983; **6**: (8): 574-580
611. Ishii G, Sangai T, Sugiyama K et al. In vivo characterization of bone marrow-derived fibroblasts recruited into fibrotic lesions. Stem Cells 2005; **23**: (5): 699-706
612. Rouger K, Fornasari B, Armengol V et al. Progenitor cell isolation from muscle-derived cells based on adhesion properties. J Histochem Cytochem 2007; **55**: (6): 607-618
613. Schultz E, Jaryszak DL. Effects of skeletal muscle regeneration on the proliferation potential of satellite cells. Mech Ageing Dev 1985; **30**: (1): 63-72
614. Schnapp E, Kragl M, Rubin L et al. Hedgehog signaling controls dorsoventral patterning, blastema cell proliferation and cartilage induction during axolotl tail regeneration. Development 2005; **132**: (14): 3243-3253
615. Aisner DL, Wright WE, Shay JW. Telomerase regulation: not just flipping the switch. Curr Opin Genet Dev 2002; **12**: (1): 80-85
616. Tichon A, Gowda BK, Slavin S et al. Telomerase activity and expression in adult human mesenchymal stem cells derived from amyotrophic lateral sclerosis individuals. Cytotherapy 2009; **11**: (7): 837-848
617. Gotte M, Wolf M, Staebler A et al. Increased expression of the adult stem cell marker Musashi-1 in endometriosis and endometrial carcinoma. J Pathol 2008; **215**: (3): 317-329
618. Fu W, Killen M, Culmsee C et al. The catalytic subunit of telomerase is expressed in developing brain neurons and serves a cell survival-promoting function. J Mol Neurosci 2000; **14**: (1-2): 3-15
619. Mattson MP, Fu W, Zhang P. Emerging roles for telomerase in regulating cell differentiation and survival: a neuroscientist's perspective. Mech Ageing Dev 2001; **122**: (7): 659-671
620. Jagadeesh S, Kyo S, Banerjee PP. Genistein represses telomerase activity via both transcriptional and posttranslational mechanisms in human prostate cancer cells. Cancer Res 2006; **66**: (4): 2107-2115
621. Zhou SY, Zhang C, Baradaran E et al. Human corneal basal epithelial cells express an embryonic stem cell marker OCT4. Curr Eye Res 2010; **35**: (11): 978-985
622. Racila D, Winter M, Said M et al. Transient expression of OCT4 is sufficient to allow human keratinocytes to change their differentiation pathway. Gene Ther 2010;
623. Christen B, Robles V, Raya M et al. Regeneration and reprogramming compared. BMC Biol 2010; **8**: 5
624. Kragl M, Knapp D, Nacu E et al. Cells keep a memory of their tissue origin during axolotl limb regeneration. Nature 2009; **460**: (7251): 60-65
625. Kuroda T, Tada M, Kubota H et al. Octamer and Sox elements are required for transcriptional cis regulation of Nanog gene expression. Mol Cell Biol 2005; **25**: (6): 2475-2485
626. Ecoiffier T, Yuen D, Chen L. Differential distribution of blood and lymphatic vessels in the murine cornea. Invest Ophthalmol Vis Sci **51**: (5): 2436-2440

627. Gruntzig J, Nolte S, Schad P et al. [Lymph drainage of the cornea, limbus and conjunctiva]. Klin Monbl Augenheilkd 1987; **190**: (6): 491-495
628. Dravida S, Pal R, Khanna A et al. The transdifferentiation potential of limbal fibroblast-like cells. Brain Res Dev Brain Res 2005; **160**: (2): 239-251
629. Gang EJ, Bosnakovski D, Figueiredo CA et al. SSEA-4 identifies mesenchymal stem cells from bone marrow. Blood 2007; **109**: (4): 1743-1751
630. Polisetty N, Fatima A, Madhira SL et al. Mesenchymal cells from limbal stroma of human eye. Mol Vis 2008; **14**: 431-442
631. Brandl C, Florian C, Driemel O et al. Identification of neural crest-derived stem cell-like cells from the corneal limbus of juvenile mice. Exp Eye Res 2009; **89**: (2): 209-217
632. Chen WY, Tseng SC. Differential intrastromal invasion by normal ocular surface epithelia is mediated by different fibroblasts. Exp Eye Res 1995; **61**: (5): 521-534
633. Kato N, Shimmura S, Kawakita T et al. Beta-catenin activation and epithelial-mesenchymal transition in the pathogenesis of pterygium. Invest Ophthalmol Vis Sci 2007; **48**: (4): 1511-1517
634. Kawakita T, Espana EM, He H et al. Intrastromal invasion by limbal epithelial cells is mediated by epithelial-mesenchymal transition activated by air exposure. Am J Pathol 2005; **167**: (2): 381-393
635. Kawashima M, Kawakita T, Higa K et al. Subepithelial corneal fibrosis partially due to epithelial-mesenchymal transition of ocular surface epithelium. Mol Vis **16**: 2727-2732
636. Thill M, Berna M, Schlagner K et al. *Expression of the Putative Stem Cell Marker CD133 in the Human Eye*. 2005 [cited; Conference panel abstract retrieved online. Invest Ophthalmol Vis Sci. 46: E-Abstract 3090. http://abstracts.iovs.org/cgi/content/abstract/3046/3095/3090].
637. Reneker LW, Bloch A, Xie L et al. Induction of corneal myofibroblasts by lens-derived transforming growth factor beta1 (TGFbeta1): a transgenic mouse model. Brain Res Bull **81**: (2-3): 287-296
638. Wu Y, Zhao RC, Tredget EE. Concise review: bone marrow-derived stem/progenitor cells in cutaneous repair and regeneration. Stem Cells 2010; **28**: (5): 905-915
639. Chen L, Tredget EE, Wu PY et al. Paracrine factors of mesenchymal stem cells recruit macrophages and endothelial lineage cells and enhance wound healing. PLoS One 2008; **3**: (4): e1886
640. Kinnaird T, Stabile E, Burnett MS et al. Local delivery of marrow-derived stromal cells augments collateral perfusion through paracrine mechanisms. Circulation 2004; **109**: (12): 1543-1549
641. Mayer H, Bertram H, Lindenmaier W et al. Vascular endothelial growth factor (VEGF-A) expression in human mesenchymal stem cells: autocrine and paracrine role on osteoblastic and endothelial differentiation. J Cell Biochem 2005; **95**: (4): 827-839
642. Aggarwal S, Pittenger MF. Human mesenchymal stem cells modulate allogeneic immune cell responses. Blood 2005; **105**: (4): 1815-1822
643. Nemeth K, Leelahavanichkul A, Yuen PS et al. Bone marrow stromal cells attenuate sepsis via prostaglandin E(2)-dependent reprogramming of host macrophages to increase their interleukin-10 production. Nat Med 2009; **15**: (1): 42-49
644. Stappenbeck TS, Miyoshi H. The role of stromal stem cells in tissue regeneration and wound repair. Science 2009; **324**: (5935): 1666-1669
645. Wen Z, Zheng S, Zhou C et al. Repair mechanisms of bone marrow mesenchymal stem cells in myocardial infarction. J Cell Mol Med
646. Penna C, Raimondo S, Ronchi G et al. Early homing of adult mesenchymal stem cells in normal and infarcted isolated beating hearts. J Cell Mol Med 2008; **12**: (2): 507-521
647. Duan X, Kang E, Liu CY et al. Development of neural stem cell in the adult brain. Curr Opin Neurobiol 2008; **18**: (1): 108-115

648. Alvarez-Buylla A, Lim DA. For the long run: maintaining germinal niches in the adult brain. Neuron 2004; **41**: (5): 683-686
649. Lie DC, Song H, Colamarino SA et al. Neurogenesis in the adult brain: new strategies for central nervous system diseases. Annu Rev Pharmacol Toxicol 2004; **44**: 399-421
650. Brundin L, Brismar H, Danilov AI et al. Neural stem cells: a potential source for remyelination in neuroinflammatory disease. Brain Pathol 2003; **13**: (3): 322-328
651. Picard-Riera N, Decker L, Delarasse C et al. Experimental autoimmune encephalomyelitis mobilizes neural progenitors from the subventricular zone to undergo oligodendrogenesis in adult mice. Proc Natl Acad Sci U S A 2002; **99**: (20): 13211-13216
652. Li L, Xie T. Stem cell niche: structure and function. Annu Rev Cell Dev Biol 2005; **21**: 605-631
653. Martino G, Pluchino S. The therapeutic potential of neural stem cells. Nat Rev Neurosci 2006; **7**: (5): 395-406
654. Kataoka K, Medina RJ, Kageyama T et al. Participation of adult mouse bone marrow cells in reconstitution of skin. Am J Pathol 2003; **163**: (4): 1227-1231
655. Han M, Yang X, Taylor G et al. Limb regeneration in higher vertebrates: developing a roadmap. Anat Rec B New Anat 2005; **287**: (1): 14-24
656. Babaie Y, Herwig R, Greber B et al. Analysis of Oct4-dependent transcriptional networks regulating self-renewal and pluripotency in human embryonic stem cells. Stem Cells 2007; **25**: (2): 500-510
657. Wakamatsu Y, Endo Y, Osumi N et al. Multiple roles of Sox2, an HMG-box transcription factor in avian neural crest development. Dev Dyn 2004; **229**: (1): 74-86
658. Duncan AW, Rattis FM, DiMascio LN et al. Integration of Notch and Wnt signaling in hematopoietic stem cell maintenance. Nat Immunol 2005; **6**: (3): 314-322
659. Fre S, Huyghe M, Mourikis P et al. Notch signals control the fate of immature progenitor cells in the intestine. Nature 2005; **435**: (7044): 964-968
660. Jensen J, Pedersen EE, Galante P et al. Control of endodermal endocrine development by Hes-1. Nat Genet 2000; **24**: (1): 36-44
661. Raetzman LT, Cai JX, Camper SA. Hes1 is required for pituitary growth and melanotrope specification. Dev Biol 2007; **304**: (2): 455-466
662. Tang H, Brennan J, Karl J et al. Notch signaling maintains Leydig progenitor cells in the mouse testis. Development 2008; **135**: (22): 3745-3753
663. Livesey FJ, Cepko CL. Vertebrate neural cell-fate determination: lessons from the retina. Nat Rev Neurosci 2001; **2**: (2): 109-118
664. Zhang L, Yang X, Yang S et al. The Wnt /beta-catenin signaling pathway in the adult neurogenesis. Eur J Neurosci 2011; **33**: (1): 1-8
665. Feijoo CG, Onate MG, Milla LA et al. Sonic hedgehog (Shh)-Gli signaling controls neural progenitor cell division in the developing tectum in zebrafish. Eur J Neurosci 2011;
666. Haycraft CJ, Zhang Q, Song B et al. Intraflagellar transport is essential for endochondral bone formation. Development 2007; **134**: (2): 307-316
667. Machold R, Hayashi S, Rutlin M et al. Sonic hedgehog is required for progenitor cell maintenance in telencephalic stem cell niches. Neuron 2003; **39**: (6): 937-950
668. Bernard F, Krejci A, Housden B et al. Specificity of Notch pathway activation: twist controls the transcriptional output in adult muscle progenitors. Development **137**: (16): 2633-2642
669. Jung KM, Bae IH, Kim BH et al. Comparison of flow cytometry and immunohistochemistry in non-radioisotopic murine lymph node assay using bromodeoxyuridine. Toxicol Lett 2010; **192**: (2): 229-237
670. Ezhkova E, Fuchs E. Regenerative medicine: An eye to treating blindness. Nature **466**: (7306): 567-568
671. Jiang TS, Cai L, Ji WY et al. Reconstruction of the corneal epithelium with induced marrow mesenchymal stem cells in rats. Mol Vis **16**: 1304-1316

672. Takahashi K, Yamanaka S. Induction of pluripotent stem cells from mouse embryonic and adult fibroblast cultures by defined factors. Cell 2006; **126**: (4): 663-676
673. Hanna J, Wernig M, Markoulaki S et al. Treatment of sickle cell anemia mouse model with iPS cells generated from autologous skin. Science 2007; **318**: (5858): 1920-1923
674. Lako M, Armstrong L, Stojkovic M. Induced pluripotent stem cells : it looks simple but can looks deceive? Stem Cells **28**: (5): 845-850

# Index: Internet Image Bibliography

**Project 1**

**A.** http://www.britannica.com/EBchecked/topic-art/69390/100407/A-diagram-of-the-structure-of-the-human-eye-showing

**B.** http://education.vetmed.vt.edu/Curriculum/VM8054/EYE/EMBYEYE.HTM

**C.** http://snpcenter.grcf.jhmi.edu/downloads/genomewide_snp6_datasheet.pdf

**D.** http://www.charite.de/molbiol/bioinf/tumbiol/Microarrayanalysis/Introduction/index.html

**E.** http://www.ihatemyglasses.com/bladeless_epiLASIK.html

**F.** http://www.pennopto.com/images/surgery10.jpg

**G.** http://emedicine.medscape.com/article/1222586-overview

**H.** http://www.lazereyeblog.com/

**I.** http://www.lasikcomplications.com/largepupils.htm

**J.** http://emedicine.medscape.com/article/1202284-treatment

**K.** http://www.cleveland.com/healthfit/index.ssf/2010/06/stem_cells_reverse_blindness_c.html

**Project 2**

**A.** http://chefcalvin.files.wordpress.com/2010/01/orth_cornea.jpg

**TITLE: Visual Disorders: From Genetics to Cell Biology**


**SUMMARY**

High myopia is a severe ametropia. A new genome-wide study was designed to identify the genes underlying the high myopia phenotype in the French Caucasian population. A new cohort was recruited but not sufficiently completed, thus requiring a mutli-step replication analysis that is still underway today. The identification of genes involved in myopia development is important for the understanding of the physiopathology of the disease.

Myopia can be treated by refractive error surgery that remodels the cornea. An average of 1.75% of patients operated develop corneal stromal opacities. The mechanisms underlying the normal corneal stromal wound response are still elusive. We investigated the phenotype of cells involved in stromal wound repair using a mouse model of full thickness corneal incision wounding. For the first time *in vivo* we suggest the localisation of a stromal progenitor pool that expands in response to corneal wounding. We also demonstrate that adult keratocyte cells in the *in vivo* wounded stroma could revert back to their embryonic cell phenotype, indicating that these cells could be relatively plastic. These results give insights into novel cell phenotypes in the wounded stroma with potential roles in stromal repair and opacity formation that require further investigation.

**AUTEUR : Jacqueline BUTTERWORTH**

**TITRE : Les troubles visuels: De la génétique à la biologie cellulaire**

**DIRECTEUR DE THESE : Pr Patrick CALVAS/ Pr François MALECAZE**

**LIEU ET DATE DE SOUTENANCE : Toulouse, 22 avril 2011**

---


**RESUME en français**

La myopie forte est une amétropie sévère. Une nouvelle étude de génotypage pangénomique visant à identifier de gènes de susceptibilité à la myopie forte dans la population française caucasienne a été développée. Une nouvelle cohorte a été constituée. Sa taille modeste, nécessite une analyse de réplication en plusieurs étapes qui est en cours. L'identification des gènes impliqués est importante pour la compréhension de la physiopathologie de la maladie.

Un des traitements courant de la myopie est la chirurgie réfractive. En moyenne, 1,75% de patients opérés développent des opacités stromales. Les mécanismes de la réponse cicatricielle normale du stroma restent méconnus. A la suite d'une blessure transfixiante de la cornée, nous avons analysé les phénotypes des cellules dans le stroma cornéen blessé chez un modèle murin. Pour la première fois *in vivo,* nous avons identifié des progéniteurs du stroma qui se multiplient à la suite d'une blessure. Nous montrons ainsi que les cellules stromales adultes semblent acquérir un phénotype identique à celui de leurs précurseurs embryonnaires dans le stroma blessé. Ceci suggère la plasticité de ces cellules. Nos résultats mettent en évidence de nouveaux phénotypes cellulaires dont les rôles potentiels dans la réparation du stroma et dans la formation des opacités doivent être évalués.


---


*TITRE et résumé en anglais au recto de la dernière page*


---


**MOTS-CLES**

Myopie forte, gène, cornée, biologie cellulaire, réparation stromale, cellules progénitrices

**DISCIPLINE ADMINISTRATIVE**

Biologie-Santé-Biotechnologies


---


**INTITULE ET ADRESSE DE L'U.F.R. OU DU LABORATOIRE :**
INSERM U563
CHU Purpan
31024 Toulouse, France